CUKUROVA UNIVERSITY

INSTITUTE OF NATURAL AND APPLIED SCIENCES

PhD THESIS

Development and Characterization of Bioresin Based Composites from Vegetable Oils for Automotive Applications

Berkay KARAÇOR

Department of Automotive Engineering

April, 2025

CUKUROVA UNIVERSITY

INSTITUTE OF NATURAL AND APPLIED SCIENCES

PhD THESIS APPROVAL

Development and Characterization of Bioresin-Based Composites from Vegetable Oils for Automotive Applications

---

Berkay KARAÇOR

Department of Automotive Engineering

This Doctorate Thesis was evaluated by the following Jury Members on 14/04/2025 and was approved by unanimity / majority of votes.

Jury : Prof. Dr. Mustafa ÖZCANLI (Advisor) ……

: Assoc. Prof. Dr. Hasan SERİN ……

: Prof. Dr. Ahmet ÇALIK ……

: Prof. Dr. Abdulkadir YAŞAR ……

: Prof. Dr. Erinç ULUDAMAR ……

This Thesis was written in the Department of Automotive Engineering Institute of Natural and Applied Sciences.

Thesis Number:

Prof. Dr. Sadık DİNÇER
Director
Institute of Natural and Applied Sciences

This work was supported by the Çukurova University Scientific Research and Project Unit.
Project ID: FDK2023-15823

CONTENTS

CUKUROVA UNIVERSITY
INSTITUTE OF NATURAL AND APPLIED SCIENCES

PhD THESIS

Development and Characterization of Bioresin-Based Composites from Vegetable Oils for Automotive Applications

Berkay KARAÇOR

Advisor: Prof. Dr. Mustafa ÖZCANLI

Department of Automotive Engineering

ABSTRACT

In this study, while using bio-based resin by adding five different vegetable oils to the epoxy resin in certain proportions as a matrix, the mechanical, thermal, physical, and morphological characterization of the bio-composites formed by reinforcing this bio-based resin with flax/jute intraply woven fabric was investigated. The production of the materials was carried out by vacuum assisted resin transfer molding method. Bio-based resin was created by adding cottonseed oil, rapeseed oil, linseed oil, palm oil, and soybean oil to 10%, 20%, 30% and 40% to epoxy resin. Composite products were produced in 21 different combinations, including samples prepared with pure epoxy resin. As a result of mechanical tests such as tensile, three-point bending, hardness and Charpy impact, it was determined that adding 10% to 20% vegetable oil to the epoxy resin increased the flexibility of the sample while reducing its strength to a certain extent. As the oil content increased towards 40%, significant decreases were observed in mechanical properties compared to samples prepared with pure epoxy resin. This situation was also confirmed in the morphological image analysis of the samples. In the physical test such as water test, the addition of canola, palm and soybean oil to the resin at 10% and 20% decreased the water absorption rates. In thermal tests, TGA analysis reveals that as the oil content increases, the initial decomposition temperature decreases compared to the pure epoxy resin sample and also a decrease in thermal stability is observed. DSC analysis shows that at 10% oil content, the glass transition temperature increases significantly compared to the pure epoxy resin sample, and significant increases are reflected in the reaction temperature. When the results are evaluated as a whole, it is predicted that adding 10% to 20% vegetable oil to epoxy resin, which is a petroleum-based source, will be an environmentally friendly bioresin and will increase material properties such as toughness, although it reduces some mechanical properties, and can be used in areas exposed to external forces in vehicles. It is also predicted that it can be preferred in the interior of vehicles due to its physical and thermal properties.

Keywords: Composites, Biocomposites, Bio-based matrix, Vegetable oils, Flax/Jute fabric.

ÇUKUROVA ÜNİVERSİTESİ
FEN BİLİMLERİ ENSTİTÜSÜ

DOKTORA TEZİ

Otomotiv Uygulamaları için Bitkisel Yağlardan Biyoreçine Bazlı Kompozitlerin Geliştirilmesi ve Karakterizasyonu

Berkay KARAÇOR

Danışman: Prof. Dr. Mustafa ÖZCANLI

Otomotiv Mühendisliği Anabilim Dalı

ÖZ

Bu çalışmada, matriks olarak epoksi reçineye beş farklı bitkisel yağın belirli oranlarda ilave edilmesiyle biyo bazlı reçine kullanılırken, bu biyo bazlı reçinenin keten/jüt dokuma kumaşı ile takviye edilmesiyle oluşan biyokompozitlerin mekanik, termal, fiziksel ve morfolojik karakterizasyonları incelenmiştir. Malzemelerin üretimi vakum destekli reçine transfer kalıplama yöntemi ile gerçekleştirilmiştir. Epoksi reçineye %10, %20, %30 ve %40 oranlarında pamuk yağı, kanola yağı, keten tohumu yağı, palm yağı ve soya fasulyesi yağı eklenerek biyo bazlı reçine oluşturulmuştur. Saf epoksi reçine ile hazırlanan numuneler de dahil olmak üzere 21 farklı kombinasyonda kompozit ürünler üretilmiştir. Yapılan çekme, üç nokta eğme, sertlik ve Charpy darbe gibi mekanik testler sonucunda epoksi reçineye %10 ile %20 oranında bitkisel yağ eklemenin numunenin esnekliğini arttırırken mukavemetlerini belirli bir ölçüde azalttığı tespit edilmiştir. Yağ oranı %40 a doğru arttıkça mekanik özelliklerde saf epoksi reçine ile hazırlanan numunelere göre önemli düşüşler görülmüştür. Bu durum numunelerin morfolojik görüntü analizlerinde de doğrulanmıştır. Su testi gibi fiziksel testte ise kanola, palm ve soya yağının %10 ve %20 oranında reçineye eklenmesi su emilim oranlarını düşürmüştür. Termal testlerde ise TGA analizi yağ oranı arttıkça numunelerde saf epoksi reçineli numuneye göre ilk bozunma sıcaklığının azaldığını ayrıca termal kararlılığında da azalma görüldüğünü ortaya çıkarır. DSC analizleri ise %10 yağ oranlarında camsı geçiş sıcaklığının saf epoksi reçineli numuneye göre iyi derecede arttığını, reaksiyon ısısında kayda değer artışlar yansıdığını gösterir. Sonuçlar bütünüyle değerlendirildiğinde petrole bağlı bir kaynak olan epoksi reçineye %10 ile %20 oranında bitkisel yağ eklenmesinin hem çevre dostu bir biyoreçine olması hem de mekanik bazı özellikleri azaltsa da tokluk gibi malzeme özelliklerini arttırmasıyla araçlarda dış kuvvete maruz kalan alanlarda kullanılabileceği, ayrıca fiziksel ve termal özellikleriyle de araçlarda iç mekân da tercih edilebileceği öngörülmektedir.

Anahtar Kelimeler: Kompozitler, Biyokompozitler, Biyo bazlı matris, Bitkisel yağlar, Keten/Jüt kumaş.

GENİŞLETİLMİŞ ÖZET

Mühendislik malzemeleri temelde metaller, seramikler, polimerler ve kompozitler olarak dört ayrı alanda incelenir. Bu dört temel sınıftan kompozit malzemeler, ilk üç kategorinin bir kombinasyonu olup en az iki ayrı bileşen içeren malzeme tipleridir. İnsanlar tarafından eski çağlardan beri kerpiçten ev yapımı, tekerlek yapımı gibi temel ihtiyaçların karşılanmasında yararlanılan malzeme türüdür. Genelde farklı özellikleri bulunan en az iki farklı malzemenin makroskobik olarak bir araya gelmesiyle oluşurlar. Kompozitlerde içerdikleri malzemenin özelliklerini korumakla beraber tamamen yeni bir yapı oluşumu gerçekleşmektedir.

Teknolojinin gelişmesiyle beraber geleneksel malzemelerin yerini alternatif malzemeler almaya başlamış yeni malzeme arayışı hızlanmıştır. Ayrıca günümüzde artan küresel çevre sorunları ile birlikte çevre dostu, geri dönüştürülebilir ve sürdürülebilir malzemeye olan ilgi kompozitler sayesinde daha da artmaktadır. Çünkü kompozitleri oluşturan takviye elemanı ve matris yapı yeşil kompozit diye adlandırılan yapıya dönüşüme oldukça uygundur. Matris veya takviye elemanının doğadan elde edilen üründen olması durumu yapıyı kısmi yeşil kompozit yapmakta hem matris hem de takviye elemanı doğal kaynaklardan elde edilmişse bu kompozit yapı tamamen yeşil kompozit olarak adlandırılmaktadır.

Günümüzde uygun maliyetle geri dönüştürülebilen, biyolojik olarak parçalanabilen, yenilenebilir kaynaklardan elde edilen biyo malzemeler giderek artan oranda bir kullanım oranına sahip olmaktadır. Kullanım ömrü bitiminde doğada çözülmeyen yani yenilenemeyen hammaddelerden üretilen kompozit malzemelerin çevresel açıdan önemli bir probleme neden olmasıyla, biyo kompozitlerin önemi daha da anlaşılmıştır. Yenilenebilir malzemelerden polimerleri dönüştürme süreci, bozunma için tasarım, kirliliğin önlenmesi, enerji verimliliği ve yenilenebilir hammaddelerin kullanımı gibi yeşil kimyanın ilkelerini de kapsar. Özellikle, bu, günlük yaşam ürünleri için kalıcı olarak bir hammadde temeli sağlayabilir ve CO_2 emisyonlarını en aza indirerek sera etkilerine daha fazla katkıda bulunmayı önleyebilir. Ayrıca, doğanın sentetik potansiyelinden yararlanan yenilenebilir hammaddelerin kullanımı, bozunma için yerleşik bir tasarım veya ortaya çıkan ürünlerin beklenen daha düşük toksisitesi gibi diğer yeşil kimya ilkelerini de karşılayabilir. Özellikle kompozitlerin yaygın olarak tercih edildiği inşaat, havacılık ve otomotiv gibi sektörlerde biyo kompozitlere yönelim bu alanın giderek gelişmesine neden olmuştur. Araştırmacılar da bu ihtiyaca yönelik, doğal liflerle ve doğal matrislerle oluşturulan biyo-kompozitlerin geliştirilmesine odaklanmıştır. Doğal lifler olarak jüt, keten, rami, kenevir, ısırgan otu, sisal, abaka, muz, kenaf, ananas, bambu, pamuk, hindistan cevizi lif, kapok ve pirinç kabuğu gibi materyaller tercih edilirken matris malzemeleri termoset reçinelere soya fasulyesi yağı, pamuk tohumu yağı, keten tohumu yağı, kanola yağı, palmiye yağı, hindistan cevizi yağı, hint yağı, aspir yağı, karanja, sarı kantaron, yer fıstığı, kuşburnu tohumu, safran, üzüm çekirdeği, ve perilla yağının reçineyle karıştırılmasıyla oluşturulmaktadır. Petrol bazlı ürünlerin sahip olduğu bazı dezavantajlar ve yenilenebilir çözümler

bulma ihtiyacı nedeniyle bu oluşturulan yeni tip biyo kompozit malzemelerde doğal elyafların maliyeti, ağırlık azaltma, geri dönüşümle önemli avantajlara sahip olacaktır.

Otomotiv endüstrisi de biyo kompozitlere en fazla ihtiyaç duyan sektör olarak biyokompozitlerin kullanımında ön sıralarda yer almaktadır. Endüstride düşük yakıt tüketen ve mümkün olduğunca az emisyon yayan araçlar üretme zorunluluğu, ürünlerin daha hafif hale getirmede biyo katkılı malzeme ihtiyacını öne çıkarmaktadır. Doğal, ağırlıklı olarak bitki kaynaklı bileşenlere dayalı takviyeli kompozitler, artık ihtiyaç duyulmadığında çevreye geri dönen ve bu yüzyılda devrim niteliğinde olabilecek makul derecede uzun ömürlü malzemeler giderek revaçta olmaktadır.

Mevcut çalışmada da otomotiv sektöründe kullanılan petrol bazlı plastiklere alternatif olarak yeni tip bir biyokompozit geliştirilmesi hedeflenmiştir. Bunun için takviye elemanı olarak doğal liflerden keten/jüt intraply dokuma kumaşı seçilmiş ayrıca matris yapısı için ise epoksi reçine içerisine pamuk yağı, kanola yağı, keten tohumu yağı, palm yağı ve soya fasulyesi yağı kullanılmıştır. Keten/jüt intraply kumaşı hem ham jüt hem de keten kumaşın özelliklerini taşımaktadır. Mukavemet özellikleri jüt kumaşa göre yüksek olup, yüksek modül, iyi termal ve elektriksel yalıtım özellikleri korunmuştur. Termoset reçineler; iyi sertlik ve yüksek elektriksel direnç, kimyasal ve çözücülere karşı dayanım, termal ve boyutsal kararlılıklarıyla elyaf takviyeli kompozitlerde matris sistemini için önemli bir kombinasyon sağlar. Epoksi de termoset reçine sınıfında elyaf takviyeli kompozitlerde, matris malzemesi olarak sıklıkla tercih edilen bir tür reçinedir. Beş farklı bitkisel yağ epoksi reçine içerisine %10, %20, %30 ve %40 gibi dört farklı oranda eklenerek hem optimum bitkisel yağ oranı bulmak hem de mekanik, termal ve fiziksel olarak en uygun bitkisel yağ reçine kombinasyonu ortaya çıkarılmak istenmiştir.

Çalışmada 21 farklı kombinasyon oluşturulmuş, parçalar vakum infüzyon tekniği ile üretilmiştir. Bitkisel yağlar önce reçine içerisine eklenerek oda sıcaklığı koşullarında manyetik karıştırıcıda ortalama 4 saat 750 rpm de karıştırılmıştır. Ardından hazırlanan biyoreçine kumaşa emdirilerek biyo kompozit numuneler oluşturulmuş, bu numuneler 24 saat kürleme işleminden sonra etüv fırınında post kürleme işlemine tabi tutulmuştur. Numunelere çekme, üç nokta eğme, charpy darbe, sertlik, su emilim, termal ve morfolojik testler uygulanmıştır. Böylece numunelerin mekanik, termal ve fiziksel karakteristikleri ortaya konulacak otomotiv sektöründe kullanılabilirliği yorumlanacaktır. Bununla birlikte tüm numuneler için maliyet-özellik verimi analizi gerçekleştirilerek sektöre yönelik bir fikir oluşturulmak hedeflenmiştir.

Çekme mukavemeti sonuçlarında saf epoksi reçine ile hazırlanan numunede çekme mukavemetinin 39,942 MPa, elastik modülün 370 MPa, yüzde uzamanın ise %24,72 olduğu görüldü. Pamuk yağı, palm yağı, kanola yağı, soya fasulyesi yağı ve keten tohumu yağının eklendiği reçinelerle üretilen numunelerde sırasıyla ortalama çekme mukavemeti değerleri, 32,592 MPa ile 40,722 MPa, 32,812 MPa ile 38,584 MPa, 31,496 ile 41,288 MPa, 30,626 MPa ile 39,254 MPa çıkmıştır.

Üç nokta eğme testi sonuçları saf epoksi reçine ile hazırlanan numunede eğme stresinin 56,33 MPa, maksimum kırılma kuvvetinin 156,21 N olduğunu ortaya çıkardı. Pamuk yağı, palm yağı, kanola yağı, soya fasulyesi yağı ve keten tohumu yağının eklendiği reçinelerle üretilen numunelerde eğme stresi değerleri sırasıyla, 23,14 MPa ile 42,25 MPa, 18,19 MPa ile 44,5 MPa, 20,28 MPa ile 37,63 MPa, 21,1 MPa ile 34,88 MPa,23,39 MPa ile 46,4 MPa bulunmuştur.

Charpy darbe test sonuçları saf epoksi reçine ile hazırlanan numunede 12,5 J lük bir absorbe enerjisi göstermiştir. Pamuk yağı, palm yağı, kanola yağı, soya fasulyesi yağı ve keten tohumu yağının eklendiği reçinelerle üretilen numunelerde sırasıyla absorbe edilen enerji değerleri 9,5-33,75 J,11,25-39 J,11,5-17,25 J,12-43 J ve 16-35,5 J olmuştur.

Sertlik test sonuçlarında saf epoksi reçine ile hazırlanan numunede 119 HV değerine ulaşılmıştır. Pamuk yağı, palm yağı, kanola yağı, soya fasulyesi yağı ve keten tohumu yağının reçinelere eklentisi ile üretilen numunelerde sırasıyla sertlik değerleri ortalama 94,84-149,17 HV, 125,37-171,19 HV, 151,21-168,52 HV, 150,77-156,88 HV ve 120,8-149,73 HV dir.

Su emilimi test sonuçları saf epoksi reçine ile hazırlanan numunede test öncesi ve test sonu ağırlık arasında 2,345 g lık fark bulunduğunu göstermiştir. Bu fark pamuk yağı, palm yağı, kanola yağı, soya fasulyesi yağı ve keten tohumu yağının reçinelere eklentisi ile üretilen numunelerde sırasıyla 3,403-6,247 g, 2,585-5,32 g, 2,705-6,39 g, 2,242-6,656 g ve 4,328-6,144 g değerlerinde hesaplanmıştır.

Termogravimetrik analizde saf epoksi reçine ile hazırlanan numunede %81 lik bir ağırlık kaybı bulunurken bu oranlar pamuk yağı, palm yağı, kanola yağı, soya fasulyesi yağı ve keten tohumu yağının reçinelere eklentisi ile üretilen numunelerde sırasıyla %82-85, %76,9-83,1, %81,9-84,1, %82,1-83,9, %81,5-83,8 değerlerinde bulunmuştur. Bozunma sıcaklıkları bakımından, saf epoksi reçine ile hazırlanan numunede ilk bozunma sıcaklığı 302 °C olurken, bu sıcaklıklar pamuk yağı, palm yağı, kanola yağı, soya fasulyesi yağı ve keten tohumu yağının reçinelere eklentisi ile üretilen numunelerde sırasıyla 282-287 °C, 279-283 °C, 282-291 °C, 278-286 °C, 276-279 °C değerlerinde bulunmuştur.

DSC analizi sonuçları saf epoksi' nin camsı geçiş sıcaklığı 72,77 °C iken, büyük tepe sıcaklık değerini ise 351,42 °C olduğunu göstermiştir. Pamuk yağı, palm yağı, kanola yağı, soya fasulyesi yağı ve keten tohumu yağının reçinelere eklentisi ile üretilen numunelerde sırasıyla camsı geçiş sıcaklığı 75,77-90,52 °C, 73,57-88,52 °C, 73,37-91,37 °C ,72,4-87,86 °C ,74,15-82,66 °C değerlerinde bulunmuştur. Büyük tepe sıcaklıklarında ise pamuk yağı, palm yağı, kanola yağı, soya fasulyesi yağı ve keten tohumu yağının eklendiği reçinelerle üretilen numunelerde sırasıyla ortalama sıcaklık değerleri, 348,94-356,1 °C, 345,97-355,62 °C, 351,67-355,3 °C ,351,05-366,51 °C ,349,61-358,84 °C çıkmıştır. DSC analizi sonuçlarından biri de ısıl değerdir. Saf epoksi' nin ısıl reaksiyon değeri 74,16 J/g olarak bulunmuştur. Pamuk yağı, palm yağı, kanola yağı, soya fasulyesi yağı ve keten tohumu yağının reçinelere eklentisi ile üretilen numunelerde sırasıyla ısıl reaksiyon değeri 65,42-82,5 J/g, 60,99-88,1 J/g, 58,3-94,42 J/g ,72,56-79,51 J/g ,57,24-93,78 J/g olarak verilmiştir.

Morfolojik analizlerde de mekanik sonuçlar doğrulanmış olup, saf epoksi' nin boşluk oranı değeri %32,06 olarak hesaplanmıştır. Pamuk yağı, palm yağı, kanola yağı, soya fasulyesi yağı ve keten tohumu yağının reçinelere eklentisi ile üretilen numunelerde ise sırasıyla boşluk oranı değeri %29,88- 33,71, %28,29-36,97, %27,1-32,05, %24,36-37,35, ve %27,57-33,33 olarak hesaplanmıştır.

Birim ağırlık başına düşen maliyet kıyaslamasında saf epoksiye değer olarak (1,22 kat) en yakın olan numune %30 keten tohumu yağının eklendiği biyo kompozit malzeme iken, en fazla fark olan (1,73 kat) numune ise %10 soya fasulyesi yağı eklenen biyo kompozit numunedir.

Analizler bütünüyle değerlendirildiğinde petrol bazlı epoksi reçineye soya fasulyesi yağının %20 oranında eklenmesi en optimum sonucu vermektedir. Pamuk yağının %40 oranında epoksi reçineye eklenmesi de hemen arkasında sıralanmaktadır. Yağ oranları kıyaslamasında da en ideal oranlar %10 ile %20 bitkisel yağ oranları olduğu analizlerden ortaya çıkmıştır. Yağ oranlarının %20 den fazla artışının numunelerde mekanik, termal ve fiziksel olarak olumlu bir etki yaratmamıştır. Üretilen biyokompozitler sünek bir davranış gösterirken elastik özellikleri saf epoksi reçine ile hazırlanan numuneye göre yüksektir. Bu durum da başta otomotiv sektöründe araç tamponları olmak üzere inşaat ve havacılık gibi alanlarda malzemeden esneklik beklenen şartlarda bu biyokompozitlerin kullanılabileceği öngörülmektedir.

ACKNOWLEDGEMENTS

First of all, I would like to express my sincere gratitude to my advisor Prof. Dr. Mustafa ÖZCANLI for his continuous support, patience, motivation and wisdom. Thanks to his mentoring skills and guidance, I was able to complete the research and writing of this thesis. I am grateful to him not only for being a great advisor but also for being a lifelong mentor.

In addition to my advisor Prof. Dr. Mustafa ÖZCANLI, I would like to thank Assoc. Prof. Dr. Hasan SERİN and Assistant Professor Şafak YILDIZHAN for their help and valuable advice throughout my study. I would also like to thank the other jury members Prof. Dr. Ahmet Çalık, Prof. Dr. Abdulkadir YAŞAR and Prof. Dr. Erinç Uludamar who evaluated my thesis.

I would like to thank Prof. Dr. Ali KESKİN, Prof. Dr. Mustafa Atakan AKAR, Assoc. Prof. Dr. Tayfun ÖZGÜR, Asst. Prof. Dr. Erdi TOSUN, Asst. Prof. Dr. Sinan KEİYİNCİ for their endless support. I would also like to thank Dean of Ceyhan Faculty of Engineering Prof. Dr. Abdulkadir YAŞAR, Asst. Prof. Dr. Arif Emre AKTAŞ, Distinguished Research Assistant Dr. Ali Cem YAKARYILMAZ, who are working in our department, and also Dr. Banu ÖZKESER and Koluman Otomotiv Endüstri A.Ş. for their support during the tests.

I would especially like to thank my valuable colleagues, Research Assistant Umut KUMLU and Research Assistant Ömer HÜKÜMDAR, who are always with me, for their valuable help and invaluable advice. I would also like to thank Research Assistant Mustafa İlteriş BIÇAK. I would also like to thank Çukurova University Scientific Research Projects Unit for their financial support (Project ID: FDK-2023-15823).

I would also like to thank my mother, father, and sister for their trust and support throughout this process.

Finally, I would like to thank the valuable and hardworking, selfless students of the Automotive Engineering composite laboratory who graduated and are currently continuing their undergraduate education. Without their support and collective work, the production and testing processes would not be completed.

LIST OF TABLES

LIST OF FIGURES

SYMBOLS AND ABBREVIATIONS

$: Dollar
µm : Micrometer
AECO : Acrylated epoxidized canola oil
AEFO : Acrylated epoxidized flaxseed oil
AESO : Acrylate epoxidized soybean oil
Al_2O_3 : Aluminum oxide
ASTM : American society for testing and materials
B : Boron
BC : Before christ
C : Carbon
C/C : Carbon/carbon
cm : Centimeter
cm^3 : Centimeter cubic
CO_2 : Carbon dioxide
CUMERLAB : Çukurova University Faculty of Engineering Automotive Engineering Laboratory
DGEBA : Diglycidyl ether of bisphenol A
DMA : Dynamic mechanical analysis
DSC : Differential scanning calorimetry analysis
DVB : Divinylbenzene
EHO : Epoxidized hemp oil
ELO : Epoxidized linseed oil
EMS : Epoxidized methyl soyate
ESO : Epoxidized soybean oil
ETO : Triolein
EVO : Epoxidized vegetable oils
g : Gram
Gpa : Gigapascal
HDPE : High density polyethylene
J : Joule
J/F : Jute/Flax intraply fabric
Kg : Kilogram
kg-f : kilogram-force
kJ/m^2 : Kilojoule/meter square
L/d : Length/diameter

LCM : Liquid composite molding

LDPE : Low density polyethylene

m : Meter

m^3 : Meter cubic

MAECO : Maleinized acrylated epoxidized canola oil

ME : Methacrylated eugenol

$Mg_2B_2O_5$: Magnesium borate

mgr KOH/g :Milligram potassium hydroxide/gram

mm : Millimeter

mm^2/s : millimeter square/second

MMSO : Methacrylic anhydride modified soybean oil

Mpa : Megapascal

mPas : Millipascal seconds

MSO : Methacrylated soybean oil

OH : Hydroxyl molecule

PALF : Pineapple leaf fibers

PAN : Polyacrylonitrile

PE : Polyethylene

PEEK : Polyether ether ketone

PET : Polyethylene terephthalate

PP : Polypropylene

ppm/°C : Parts per million/Celsius

PS : Polystyrene

PU : Polyurethane

PVC : Polyvinyl chloride

RRIM : Reinforced reaction injection molding

RTM : Resin transfer molding

SAc : Sebacic acid

SEM : Scanning electron microscopy

SiC : Silicon carbide

SMC : Sheet molding compounds

SRIM : Structural reaction injection molding process

T_g : Glass transition temperature

TGA : Thermogravimetric analysis

UPE : Unsaturated polyester

USD : United states dollar

VARTM : Vacuum assisted resin transfer molding

1. INTRODUCTION

Material selection in engineering design performs a crucial role in the emergence of a successful sustainable product. In the selection of materials, besides the mechanical characteristics, the physical and metaphysical characteristics of the products and the satisfaction of the requester have an important share on the material (Al-Oqla and Sapuan, 2014). The essential element in any manufacturing industry is materials. Pure metals, alloys, and composites are the types of materials commonly used in the manufacturing industry. Due to the fact that the metals and alloys used since ancient times could not meet some engineering expectations in the modern age, there have been some incomplete points. Since the metals and alloys used since ancient times could not meet the expectations in some engineering structures in the modern age, areas where these materials are lacking have emerged. Composite materials have been the materials that filled this deficiency. Composite materials have replaced them in areas where conventional materials are insufficient, owing to their good damping capabilities, high specific strength and specific coefficients (Kerni et al., 2020). They come to the fore as a substitute for traditional materials in many application areas with their lightening processes, advanced chemical, mechanical, and physical features (Seabra et al., 2020). The macroscopic combination of at minimum two dissimilar materials with divergent characteristics is defined as a composite material. The idea of composite materials has not emerged recently and has been used by humanity since ancient times. Composite materials consisting of a combination of straw/clay, bamboo fibers/laminated wood were used extensively as building materials in ancient times (Kaw, 2006). The majority of composites are materials made by humans, but there are examples of composite materials in nature, such as the trunk of a tree or bones. Although the use of composites has decreased in relative importance with the introduction of metals and polymers in the early 20th century, it has recently been the subject of more research by researchers. When producing a composite material, the basic idea is to adapt the material characteristic to the design requirements of the product or systems. The use of the components that make up a composite material alone represent character traits that are notably different from the composite material. For example, the matrix element, which is one of the basic components, cannot have a high strength without the reinforcement element in the composite material, and the reinforcement element cannot distribute the applied load to the entire structure (Yildizhan, 2020).With a great deal of work being done in the transportation, aerospace and maritime fields, there are many unexplored potentially applicable areas for composite materials (Djunaedi, 2007). It is stated that the interest in the global composite market will continue to grow in the future, from transportation to construction, from wind energy to maritime, from consumer goods to electricity and electronics and aviation (Almaguer et al., 2011). The increasing use of composite materials is a major factor in the automotive industry's efforts to reduce the weight of components used in cars and to increase their efficiency (Muthu, 2019). It is understood that many companies in the automotive industry are using new materials to

develop advanced vehicle and powertrain systems to gain additional efficiency, reduce emissions, improve fuel economy and lighten their vehicles without sacrificing safety (Taub, 2006). However, the current climate crisis in the world and the increase in environmental problems day by day have proven that a difficult process has begun for the resources in the world. In this case, sustainability and recycling processes have become a necessity in all sectors, including the automotive sector (Sarikaya et al., 2019). In particular, the composite industry, where petroleum-based resins and reinforcement materials are predominantly used, has also been directly affected by this situation. Manufacturers seeking a solution to this problem have begun to explore different biomaterials to increase the use of natural materials in the fabrication of composites and to produce bio-composites (Roy et al., 2020).

With the increasing awareness of the exhaustion of environmental resources and the decline in fossil fuel reserves, it has become essential to develop new sustainable materials to be used in different areas called biocomposites. Biocomposites are composite materials produced by combining one or more phases from a biological source. In biocomposites, plant fibers such as hemp, cotton, jute, kenaf, sisal, flax, waste paper fibers or recycled wood , by-products from food crops can be used as reinforcing elements, while polymers made from renewable resources such as vegetable oils, recycled thermoplastics and starches can be used as matrix elements (Fowler et al., 2006; Muthu, 2019). The term biocomposite is generally referred to composites in which one of the matrix or reinforcing material with partially natural components is from natural materials, while a combination in which the matrix and reinforcing material components are both natural is defined as green composites (Ozkur, 2021).

Natural fibers as a reinforcing element in composite materials have recently been preferred over synthetic fibers due to their low density, low cost, biodegradability and non-corrosive structural advantages. Composites are produced by combining natural fibers such as, jute, hemp, bamboo, flax agave, banana, pineapple and rubber tree with both thermoset and thermoplastic resin structures. However, since these resin structures are petroleum-based resin structures, it is expected that resins based on natural renewable resources will be used in addition to natural fibers in the production of biocomposite materials (Morye and Wool, 2005). The fact that non-biodegradable products consist of petroleum-based products, waste disposal and increasing costs become a major problem, leading the scientific community to bio-based resins. Interest in vegetable oils is growing due to the many advantages they offer for existing bio-based polymers, such as availability, cost-effectiveness, biodegradability and renewability. Vegetable oils also have low viscosity, non-volatile and non-toxic properties. This makes these biopolymers a valuable alternative chemical. They are preferred as efficient renewable starting materials for the fabrication of a wide variety of monomers and polymers (Narewska et al., 2014; Wu and Li, 2018). Vegetable oils, including edible oils and drying oils, can be modified to display a variety of functionality, allowing for the fabrication of new materials with a wide range of functionality from structural to functional (Mosiewicki and Aranguren, 2013).

Among these vegetable oils, oils such as cottonseed oil, soybean oil, castor oil, and linseed oil have been encouraging points for researchers in the creation of resins and prepolymers that can be shown as alternatives to petroleum-based sources. In addition, the low mechanical and thermophysical characteristics of crosslinked functionalized oils can be enhanced by strengthening renewable biofibers. Thus, the dependence of both resin and fibers on fossil resources can be further reduced and their negative environmental impacts can be minimized (Muthu, 2019). Due to the interest in the versatility of vegetable oil components, several studies exist for the full use of soybean, linseed, safflower oils and castor oil in oleoresin. In these studies, researchers tried to polymerize vegetable oils by epoxidation process. Epoxy resins, which are inherently brittle, have been hardened by incorporating the relatively inexpensive and easily biodegradable epoxidized vegetable oils (EVO) into the epoxy system (Tan and Chow, 2010a). Acrylate epoxidized soybean oil (AESO) is also a frequently preferred type of bioresin for use in fiber-reinforced composites. Nevertheless, due to its high viscosity and insufficient reactive groups compared to petroleum-based resins, it is not possible to use pure AESO as a matrix material in compounds. For this reason, studies are continuing on different types of resins that can be used with AESO (Ozkur et al., 2021). There are several studies in the literature with the epoxidation process of vegetable oils and AESO-epoxy hybrid resin systems. However, there is no hybrid bioresin study created by adding vegetable oils to epoxy resin without any chemical treatment. The lack of such a study that can be used instead of epoxy resin is the main objective of this study.

Within the scope of this study, it was aimed to create a hybrid bioresin by adding five different vegetable oils (soybean oil, palm oil, rapeseed oil, cottonseed oil, flaxseed oil) to the epoxy resin at the rates of 10%, 20%, 30% and 40%. In the experimental study, the mechanical, thermal, physical and morphological effects of the increased oil ratio in bioresins formed by adding 10%, 20%, 30% and 40% vegetable oil and in biocomposites formed with pure epoxy resin without oil additives were investigated. The composite formed by using flax/jute intraply woven fabric as a reinforcing element is intended to be a partial biocomposite, thus it is aimed to produce a product that causes minimal damage to the environment, can participate in the environmental cycle ecologically, and will not cause environmental waste problems. It is thought that this product will be produced in a way that will reduce the use of metal materials as an energy absorber in the front and rear bumper sections of automobiles. Thus, it will both contribute to fuel economy by reducing vehicle weight and contribute to vehicle projects consisting of green materials that have emerged recently. Apart from the automobile sector, it can be preferred as an important alternative in other sectors that require energy absorption. Vacuum infusion assisted resin transfer molding technique was used to produce the samples. Tests were carried out in order to use the biocomposites formed as a result of 21 different combinations in different areas and to determine the optimum vegetable oil ratio. Materials produced within the scope of the study were subjected to tensile test, three-point bending test, impact test, hardness test, thermogravimetric, differential scanning calorimetry, water

absorption test, and Scanning Electron Microscopy (SEM) analysis. Thus, the products produced were examined in terms of mechanical, thermal, physical and morphological and comparisons will be made.

2. COMPOSITE MATERIALS

Composites are structures that combine two or more components with important properties to create a material with unique properties. Composite materials have a material structure developed to meet the needs of strong and light materials in many areas (Ramamoorthy, 2015). The most significant developments in the increasing use of composites can be remarked in the automotive sector as producers try to augment the efficiency of the car by reducing the weight of the parts used in the car. Polymer-based composite materials arouse increasing interest and curiosity, as they have various advantages such as customization flexibility, high strength/weight ratio, corrosion and chemical resistance properties, high hardness/weight ratio, tribological properties, and ease of manufacture for a specific application (Muthu, 2019).

Composites have discrete properties and are usually fabricated by reinforcement of a matrix structure. The most common matrix materials used are thermoplastics or thermoset such as vinylester, polyester, and, epoxy while the most prevalent reinforcements are aramid, glass and carbon fibers. Composite materials exhibit anisotropic features, and the material, whose properties change with the direction of the applied load, has different features from the conventional materials used for production. It may also contain additives, core materials or fillers (Yıldızhan et al., 2018). Composite materials have some disadvantages and advantages over conventional materials. It has advantages such as reduced cost, improved strength, hardness, fatigue and impact resistance, thermal conductivity due to the use of fewer parts, and disadvantages with its high production cost, repair cost and anisotropic properties (Kaw, 2006).Table 2.1 displays the pros and cons of composite materials.

Table 2.1. Pros and cons of composite materials (Campbell, 2010)

Advantages	**Disadvantages**
Lighter weight	High raw material costs
Improved fatigue life	High fabrication and assembly costs
Corrosion resistance	Susceptibility to impact damage and delamination
Reduced assembly costs	Adverse effects of both temperature and moisture
-	Greater difficulty in repairing

It is predicted that the market share will gradually increase as the use of composites becomes more widespread and used in new sectors. According to the researches, it is stated that the global composite market size is 105.75 billion USD (United States dollar) in 2022, and it is expected that the market will reach approximately 191.36 billion USD in 2032. From 2023 to 2032, a remarkable growth of 6.1% is foreseen in the market. The distribution of this estimated growth by years is indicated in Figure 2.1.

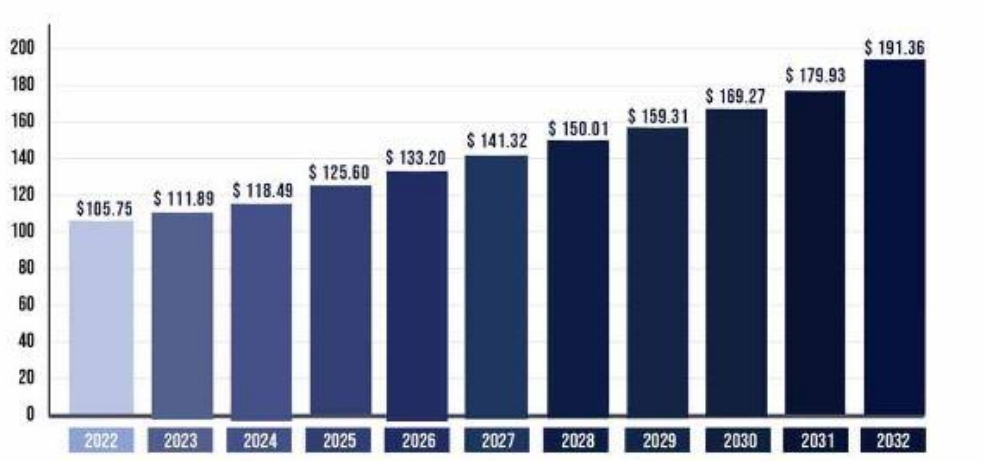

Figure 2.1. The global composites market size predictions from 2023 to 2032 (Precedence research, 2023)

Composite materials find application in many areas such as construction, automotive, defense industry, biomedical, maritime, and energy sectors. Especially since the emission standards implemented in the automotive field contain serious restrictions, automobile manufacturers tend towards composite materials and see composites as a serious solution. Manufacturers prefer to use composites in parts such as dashboard, door panel, carpeting, rear shelf, floor, headliner, tunnel, bonnet, head restraint, lower shield, structural parts, wheelhouse, engine compartment, gasket lining, clutch linings, brake pads, springs, and bumper (Kaw, 2006; PinettePei Engineering and Machinery, 2023).

2.1. Reinforcement Elements

Composite structures consist of two main components as matrix material and reinforcement material. In composites, reinforcing materials determine the hardness and strength characteristics of the composites they form (Ozkur, 2021). Reinforcements basically provide matrix materials with special characteristics such as temperature resistance, hardness, high strength, electrical and thermal conductivity (Yim et al., 2017). Often in composite materials, reinforcement elements are distributed as geometrically different elements. Composites according to the reinforcement structure; particle-reinforced composites having one or more components dispersed in the matrix; fiber-reinforced composites and laminated composites consisting of layers with at least two different components joined together to form a laminate (Thakur et al., 2017). Composite types according to the reinforcement element are given in Figure 2.2.

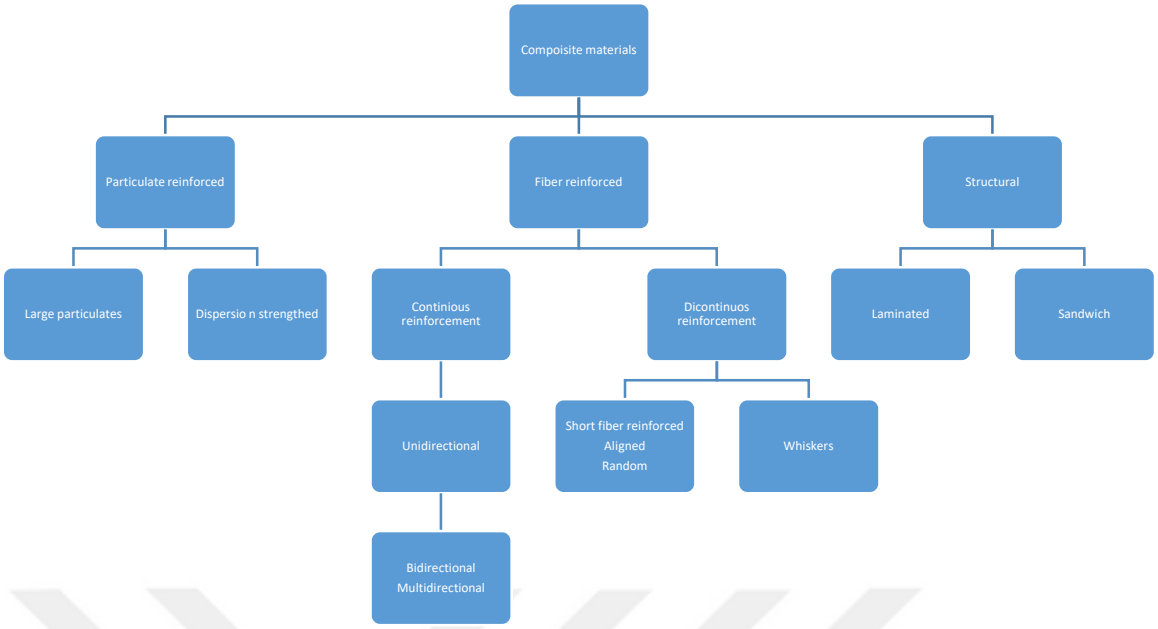

Figure 2.2. The classifications of composites according of reinforcement types

It is stated that composites are born from biomaterials that use plant fibers as reinforcement. There are also examples of linen and hemp fabrics being used as reinforcement of ceramics in 6500 BC (Before Christ). It shows that the Egyptians used grass and straw as reinforcement fibers in mud and clay bricks when they were building walls 3000 years ago, and plant fibers have a very old history (D. U. Shah, 2013). Fibers are usually categorized into two classes; these are synthetic fibers and natural fibers. The advantages of natural fibers are that they are sustainable, renewable, abundant in nature and biodegradable. In addition, its potential to solve the waste management problem and its strength and mechanical properties encourage researchers to increase the number of natural fibers used as reinforcement elements in composite materials (Boquillon, 2006; Muthu, 2019). The classification of natural fibers is displayed in Figure 2.3.

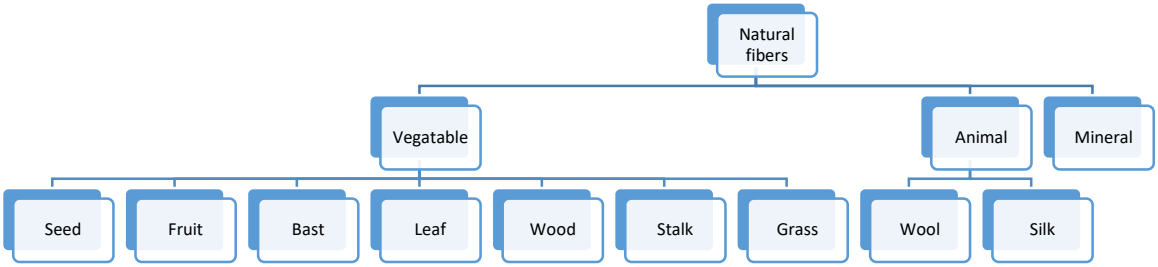

Figure 2.3. The classifications of natural fibers (Amar K. Mohanty et al., 2005)

Within this category, another classification is made according to plant origin. These are cotton and kapok for seed; coconut for fruit; kenaf, flax, jute and hemp as bast; sisal, banana, and palm as leaves; hardwood and softwood for wood fiber; bamboo and wheat types for stalk. Generally, natural fibers do not show the same mechanical characteristics as carbon fibers from synthetic fibers, but some behave similarly to glass fibers. Compared to E-glass, natural fibers such as sisal, jute, flax, hemp, and kenaf have significant economic and ecological advantages i.e., being renewable, available in large quantities, low fossil fuel energy requirements. The increasing importance of issues such as environmental safety and recyclability brings to the fore the preference of natural fibers as reinforcement elements in engineering polymeric materials instead of glass fibers, which are synthetic fibers (Anonymous, 2012; George et al., 2001; Jabbar et al., 2016). In the absence of fiber density, synthetic fibers exhibit unsurpassed mechanical features compared to natural fibers. However, the fact that the cost of natural fibers is quite low compared to synthetic fibers and the specific strength and modulus of natural fibers are similar to synthetic fibers as seen in Table 2.2, revealing that natural fibers can compete with synthetic fibers (Väisänen et al., 2017).

Table 2.2. Mechanical characteristics of synthetic and natural fibers (John and Sabu, 2012)

Fiber	**Density (g/cm^3)**	**Specific strength (MPa cm^3/g)**	**Specific modulus (GPa cm^3/g)**	**Tensile strength (MPa)**	**Elastic modulus (GPa)**
Carbon	1.4-1.8	1710	164-171	3000-4000	250-500
Glass	2.6	850-1300	27	2200-3600	65
Flax	1.4-1.5	250-650	18	350-1040	28-70
Jute	1.3-1.5	310-625	2-37	200-770	20-55
Hemp	1.4-1.6	630	25	690	630
Coir	1.2-1.5	146	3-5	180	4-6
Sisal	1.5	335-430	6-15	100-800	9-22
Cotton	1.5-1.6	191-310	3-8	290-490	5-12
Bamboo	0.6-1.1	600	48-89	140-230	11-17
Kenaf	1.4-1.5	641	36	930	53
Wool	1.3	38-242	1.8-3.8	50-315	2.3-5
Wood	1.4	64-130	7-50	90-180	10-70
Silk	1.3-1.4	100-1500	4-20	100-1500	5-25
Feather	0.9	112-226	3.3-11	100-203	3-10

Natural fibers are usually lignocellulosic and comprise of helically wrapped cellulose microfibrils in the matrix structure of lignin and hemicellulose. Cellulose is naturally occurring, renewable, biodegradable, abundant on earth and can be obtained from numerous sources. It is also seen as an limitless resource of raw materials for biocompatible products and environmentally friendly (Jabbar et al., 2017). Cellulose found in natural fibers contains different natural substances. The most important among them are lignin and various waxes. In tough natural fiber, different cells are connected by lignin and lignin acts as a cementing material. While factors such as harvest stage, plant type, and extraction method determine the quality of natural fibers, the chemical composition, morphology, mechanical strength and polymer matrix reinforcing capacity of the fibers also indirectly depend on the factors affecting this quality. Mechanical characteristics are specified by microfibril angle and cellulose content. Low microfibril angle and high cellulose content are expected from fiber as a reinforcing element in polymer composites (Bledzki et al., 1996; W. Liu et al., 2019; Williams and Wool, 2000). Table 2.3 displays chemical compositions of natural fibers. Table 2.4 also indicates the physical features of some natural fibers.

Table 2.3. Chemical compositions of natural fibers (Lalit et al., 2018)

Fiber	**Lignin (%)**	**Cellulose (%)**	**Hemicellulose (%)**	**Pectin (%)**	**Ash (%)**	**Wax (%)**
Pineapple	4.4-10.1	57.5-74.3	80.7	1.1	0.9-4.7	3.3
Ramie	0.6	68.6	13.1	1.9	-	0.3
Flax	2	64.1	16.7	1.8	13.1	1.5
Jute	0.2	64.4	12	11.8	0.5-2.1	0.5
Hemp	2.6-13	55-80.2	12-22.4	0.9-3.0	0.5-0.8	0.2
Coir	32.7-53.3	19.9-36.7	11.9-15.4	4.7-7.0	-	-
Sisal	9.9	65.8	12	0.8	4.2	0.3
Cotton	28.2	82.7	5.7	5.7	-	0.6
Bamboo	10.2-21.4	48.2-73.8	12.5-73.3	0.37	2.3	-
Kenaf	15-21	37-49	18-24	8.9	2.4-5.1	0.5
Banana	14.4-21.6	28.3-55	10.2-15.9	2.1-4.1	2.1	3-5
Bagasse	21.2-24	28.3-55	20-36.3	-	1-4	0.9
Sea grass	5	57	38	10	-	-
Rice husk	-	38-45	12-20	-	20	-

Table 2.4. Physical properties of natural fibers (Torres et al., 2019)

Fiber	**Length (mm)**	**Diameter (μm)**	**Aspect ratio (L/d)**
Pineapple	8	20	400
Ramie	120	50	2400
Flax	33	19	1700
Jute	2	20	100
Hemp	25	25	1000
Coir	0.3-1.2	10-24	45
Sisal	3	20	150
Cotton	20	20	1000
Bamboo	2.7	14	190
Kenaf	5	21	240
Banana	0.9-5.5	11-81	75
Abaca	2-12	20	350
Curaua	-	60	-
Kapok	19	19	1000

Natural fibers have superiorities such as good acoustic insulation and thermal properties, non-corrosive effect on screws and other metal parts, non-harmful processing, tool wear and no skin irritation. Nevertheless, it has disadvantages such as its tendency to absorb moisture, formation of odor due to the decomposition process, limited maximum processing temperatures, and relatively low durability due to weather conditions (Faruk et al., 2014).

Natural fibers

Natural fibers are observed in three groups as vegetable, animal and mineral fibers, as mentioned in Figure 1.3. While plant fibers are cellulose-based, animal-derived fibers consist of proteins; silk and wool are examples of animal-derived fibers. Mineral fibers are known for examples of asbestos, which are used in very small amounts during extraction due to factors affecting human health, and basalt which obtained from basalt rocks (Ozkur, 2021).

Jute fiber

Jute fiber is one of the most important plant fibers used in a variety of applications and is known for its appearance as a long, soft and shiny fiber as seen Figure 2.4 that can be spun into coarse, strong threads. Jute is referred to as the cheapest lignocellulosic, easily available, long plant bast fibre. Jute plant is a plant that grows in hot and humid climates and is grown only for its fibers. The production of this plant, which grows for four to six months in tropical and subtropical climates, is carried out in a wide geography from South America to the Far East. Besides being grown in the delta formed by the Ganges River and Bramhaputra River in India and Bangladesh, Brazil, Thailand and China are also important producers are counted among them. Since jute fiber has properties such as low extensibility, acoustic insulation, low thermal conductivity and high tensile strength, it is also used by hybridizing it with other synthetic or natural fibers (Anonymous, 2012; Holbery and Houston, 2006; John and Sabu, 2012; Amar K. Mohanty et al., 2005; Muthu, 2019; Torres et al., 2019). Jute plant is an herbaceous plant that can reach 2 to 3.5 m in height and has a stem of 2 to 3 cm in diameter. Although the structure of jute fibers has a polygonal cross-sectional structure, the dimensions of the cell walls are various. Jute fibers are sensitive to photochemical and chemical effects, but are resistant to microorganisms. Although jute fibers are strong, they are brittle and have low elongation at break due to their high lignin content. The low density, specific hardness and strength of jute fiber are competitive with the corresponding amounts of glass fiber. Jute fiber shows superior characteristics than glass fiber in terms of module on specific module and cost basis. In addition, jute fiber is close to glass fiber in terms of specific strength/unit cost ratio (A. K. Mohanty et al., 2000; Amar K. Mohanty et al., 2005). Jute is a durable, biodegradable, easily available, cost-effective, environmentally friendly and anti-static fiber. In addition, its high specific strength, good thermal and electrical insulation properties and high modulus make jute fiber stand out for use in luggage, carpets and various floor coverings. Besides, jute fiber has the highest priority among natural reinforcement materials in the use of composites in structures such as panels, suspended ceilings and furniture (Ozkur, 2021).

Figure 2.4. Jute fiber (Anonymous, 2012; Muthu, 2019)

Flax fiber

Flax, one of the oldest natural fibers thoroughly used in modern textile production, is a plant type grown for the aim of obtaining fiber and seed oil. Figure 2.5 displays the flax fiber. Flax is one of the bast fibers cultivated in temperate regions, and textile flax is primarily grown in Europe, China, India, Argentina, and Russia. Flax fiber has been used as textile products since early Mesopotamian times. Linen fibers are known for being very strong yet flexible. Linen is a particularly inextensible fibre, stretching only lightly as tension rises. Even with a small degree of elongation, flax is referred to as an elastic fibre. The characteristics of flax fiber are controlled by its molecular fine structure, and the molecular structure is also affected by the growing conditions of the fibers and the applied retting process. Flax fibers stand out as a suitable reinforcement material in polymeric matrix composites with their low density, low price, superior mechanical features and biodegradability. With developing technology, production costs can be kept at the optimum level with fibers that are more uniform in terms of color, durability, length and fineness and therefore more suitable for composites. By choosing flax fibers instead of glass fibers in composite materials, material separation and recycling have been improved, and the opportunity for the reuse of production waste has emerged. Flax fibers have been preferred by many European vehicle manufacturers because they are a green product, can be produced in consistent quality, and use minimum pesticides in their production, and have become the guide of the composite industry in vehicles. It is stated that the use of flax reinforced composites in both vehicle exterior parts (such as underbody panel) and vehicle interior areas (such as door panel) is becoming increasingly widespread (Z. Liu et al., 2006; Marsh, 2003; Amar K. Mohanty et al., 2005; Muthu, 2019; Torres et al., 2019). Linen is a strong fibre; its strength increases under wet conditions and it has the capacity to absorb 20% moisture without feeling wet. Flax fibers are resistant to abrasion with good thermal conductivity properties. This

allows flax to be used in the production of rope and sacks. Flax fibers gradually lose their strength if exposed to sunlight. Flax has good resistance to alkaline solutions and can resist dilute weak acids, but is vulnerable to attack by hot dilute acids or cold concentrated acids (John and Sabu, 2012).

Figure 2.5. Flax fiber (Melelli et al., 2022; Shebaz Ahmed et al., 2023)

Hemp fiber

Hemp fiber is known as soft but durable fibers grown from plants of the hemp genus. Hemp is a type of bast fiber that is domestic to Central Asia and has been grown for more than 12,000 years and does not require any herbicides, insecticides, fungicides or fertilizers. Hemp plants as seen in Figure 2.6 have impressive growth rates and quickly cover the soil, suppressing some soil-borne pathogens. They also increase the yield of the next crop by returning nutrients to the soil. Hemp fibers have high strength but low breaking elongation, have outstanding moisture durability and rot very slowly in water. Hemp fiber finds application by mixing it with polypropylene in a non-woven mat that turns into a three-dimensional part through the compression molding technique. It is stated that hemp has a much lower density, an equivalent Young's modulus, and less cost and molding time when compared to synthetic fibers glass fiber. Due to its properties, it is used in areas such as musical instruments, construction materials, food, composites and plastics, special paper, medicine, textiles, fuel, automotive industry and sports equipment production (Anonymous, 2012; Amar K. Mohanty et al., 2005; Muthu, 2019).

Figure 2.6. Hemp fiber (Anonymous, 2012)

Kenaf fiber

Kenaf fiber is an annual herbaceous plant that has the potential to grow more than 3 m in a period of 3 months under ambient conditions and can be grown in a wide variety of weather conditions. Kenaf is a yearly crop that grows in Africa and Asia and draws attention with its resemblance to read. In addition, it is known as a valuable plant structure in preventing global warming with its highest carbon dioxide absorption among all plants. Kenaf is a pale fiber as seen in Figure 2.7 that contains less non-cellulosic material than jute. It has a tensile strength similar to low grade jute and weaken only slightly when wet. Kenaf has low density, high specific mechanical properties, biodegradability, non-corrosive during processing. In addition to being used instead of glass fiber or other synthetic fibers in the automotive industry, it is also used in automobile instrument panels, in the production of rope, twine, carpet backing and burlap, and in the production of carpet padding (Anonymous, 2012; Amar K. Mohanty et al., 2005; Torres et al., 2019).

Figure 2.7. Kenaf fiber (Anonymous, 2012)

Ramie fiber

Ramie fiber is known as the longest and strongest textile fiber among fibers and is mostly grown in China, Malaysia and Japan as seen in Figure 2.8. Ramie fibers are white in color and are obtained from the trunk bark. These fibers have interesting characteristics such as long fiber length, smooth texture, and excellent tensile strength, as well as the ability to resist the effects of chemicals and absorb moisture better than other fibers. The fibers are distinguished by their exceptional strength, which increases slightly even when wet. With its superior fiber characteristics, ramie fibers have a high potential to be preferred as reinforcement elements in polymer composites. The usage areas of fibers obtained from ramie include twines, cords, clothing fabrics, vehicle interiors, industrial packaging and canvases (John and Sabu, 2012; Amar K. Mohanty et al., 2005; Muthu, 2019; Torres et al., 2019).

Figure 2.8. Ramie fiber (Debnath, 2017)

Sisal fiber

Sisal fiber, a tough fiber obtained from the leaves of the sisal plant, is among the four most commonly used plant fibers. A sisal plant has approximately 200-250 leaves, and each of them contains 1000-1200 fiber bundles consisting of 4% fiber, 0.75% cuticle, 8% dry matter and 87.25% water. They have a very long lifespan of 7 to 10 years. These fibers as seen in Figure 2.9 are durable and strong, with high resistance to moisture and heat. Although sisal is a plant domestic to Mexico and Central America, it is now thoroughly cultivated in tropical countries in the West Indies, Africa, and the Far East. Almost half of the total production of vegetable fibers is sisal fibre. The approximate annual production of sisal fiber worldwide is 4.5 million tons. The structure of sisal fibers is smooth, straight and yellow, and it does not break down quickly under the influence of salt water. The tensile characteristics of sisal fiber are not the same along its length. In fibers extracted from the root or the lower part of the leaf, the tensile strength and modulus are lower, but the breaking stress is higher. While the fibers become stronger and harder in the middle span, the fibers removed from the end have intermediate properties. The toughness, tensile strength and modulus characteristics of sisal fibers decline with the increase in temperature. Sisal leaves obtained from the mother plant are found in the form of sisal fibers in mats, ropes, cords, and handicraft products (John and Sabu, 2012; Amar K. Mohanty et al., 2005; Muthu, 2019; Sahoo et al., 2018c; Sahoo et al., 2018; Torres et al., 2019).

Figure 2.9. Sisal fiber (Puttegowda et al., 2018)

Abaca fiber

Abaca is a plant closely attached to banana. Although the abaca plant has an akin aspect, unlike bananas, its fruit is not convenient for human consumption and is also not appropriate for economically. Abaca fibers can grow up to 3-4 m. It is known to be native to the Philippines and is

also grown in Central and South America and Indonesia. Abaca fibers are a hard fiber that is separated from the plant in a similar way to sisal fiber. Abaca fiber is recognized as the strongest of all plant fibers. In terms of tensile strength, it has three times the strength of cotton and twice the strength of sisal, and is much more robust to deterioration in salt water than most other plant fibers. Abaca is a yellowish white and shiny fiber as seen in Figure 2.10. Abaca fibers are used in the production of handicraft products such as mats, ropes, bags, place mats and slippers (Amar K. Mohanty et al., 2005; Muthu, 2019; Peças et al., 2018; Torres et al., 2019).

Figure 2.10. Abaca fiber (Simbaña et al., 2020)

Pineapple leaf fiber

Pineapple fibers, obtained as a by-product from the cultivation of pineapple fruit grown mostly in tropical climates, attract attention due to their higher tensile strength along with their relatively low price. Pineapple leaf fibers (PALF) as seen in Figure 2.11 are of good quality and have a webless structure compared to jute. The excellent mechanical characteristics of PALF are also due to its high cellulose content and relatively low microfibrillar angle. It has mechanical properties very similar to jute fiber. Due to its nature, its ability to absorb moisture is quite high, and in the textile industry, it is generally combined with silk to create fabric. Pineapple fiber leaves are approximately 91 cm long and 5 to 7.5 cm wide, sword-shaped, dark green in color. While strong, white and silky fibers can be separated from these leaves, these fibers are mostly seen as waste until today. Pineapple leaf fiber has bending and torsional stiffness comparable to jute fibers. Pineapple leaf fiber differs from others by showing a different characteristic as the fiber bundle strength declines by 50% when wet, while the yarn strength rises by approximately 13%. The existence of high amounts of lignin and other waxy substances and the high coarseness of PALF make it difficult for the dye to penetrate and cause the dyes to fade faster compared to cotton. Pineapple leaf threads were generally used in the production of mats, carpets, fabrics and curtains (Amar K. Mohanty et al., 2005; Muthu, 2019; Peças et al., 2018; Torres et al., 2019).

Figure 2.11. Pineapple leaf fiber (Asim et al., 2015)

Banana fiber

Banana plants have a stem structure with a length of 2.7-6.7 m and a width of 10-20 cm at the base. It has a sheath structure before expanding, and its length is 2–4 m and width is 13−20 cm. Banana fibers are produced from the stem of the banana plant, which contains high amounts of potassium and carbohydrates. The fibers as seen in Figure 2.12 are spread longitudinally in the sheaths, and the sheaths also vary in width, length, and color. The main countries producing banana are the Philippines, Indonesia and India. Banana fibers have been preferred as textile fibers since ancient times. Although the cellulose and structure of banana fibers are similar to sisal fiber, they have higher tensile properties than sisal fiber due to the lower spiral angle in the fiber's structure (Amar K. Mohanty et al., 2005; Muthu, 2019; Torres et al., 2019).

Figure 2.12. Banana fiber (Onlineclothingstudy, 2020)

Bamboo fiber

Bamboo is known as one of the largest plants in the grass family, with a very high growth rate and short growth cycle, grown mainly in the Asian region. Bamboo plant has a high strength/weight ratio and is one of the fastest growing plants. Additionally, features such as not using pesticides or herbicides, having low water requirement, and keeping the roots intact while harvesting from the base make these plants stand out. Its fibers as can be seen in Figure 2.13 can be obtained from the pulp of the bamboo plant. The fiber surface is round and smooth, and the length/diameter ratio is high. It is lighter, harder and stronger than fiberglass. It is also stated that the energy consumption required to produce bamboo fiber mat covers a small part (17%) of the energy required to produce glass fiber of the same structure. Fibers are often used in the construction, furniture, paper and textile industries. In addition, bamboo is used in kitchens and sports equipment, especially in Japanese culture, and it is stated that Thomas Edison made better light bulbs by making filaments from bamboo (Amar K. Mohanty et al., 2005; Muthu, 2019; Peças et al., 2018).

Figure 2.13. Bambu fiber (Karahan et al., 2006)

Coir fiber

Coconut fiber is a fiber located geometrically between the outer shell and the hard inner shell of the coconut. When the fiber is not mature, it shows a pale color, then hardens and turns yellow as a lignin layer. There are two types of coconut fiber: brown coconut and white coconut. Brown coconuts are harvested from fully mature coconuts. They are strong, thick, and have high wear robust. It is generally preferred in the production of sacks, trousers and mops. White coconut fibers, on the other hand, are white or light brown in color, collected from the coconut before it matures. These fibers are smoother, thinner and generally have weaker characteristics than brown coconut fiber. Mature brown coconut fiber contains more lignin and less cellulose than fibers such as flax and cotton, and is therefore less flexible but stronger. Coconut fibers as seen in Figure 2.14 have large production areas in the coastal regions of the India, Indonesia, Philippines, Malaysia and Sri Lanka in the wet tropical regions of Asia. Coconut is one of the most durable plant fibers available and is pill-free and highly resistant to abrasion and rotting. In addition, coconut fiber has naturally insulated and sound-absorbing properties, is antistatic and is not easy to ignite. Coconut fibers have many applications, including horticulture and geotextiles, due to their ability to remain intact without disintegrating even when immersed in water for a long period of time. Coconut fibers are used to make a diversity of products, such as nets, brooms and brushes, ropes and threads for mats and bags,

as well as padding for mattresses. Having high moisture absorption rates allows these fibers to be widely used as seat cushions in the automotive industry (Anonymous, 2012; Amar K. Mohanty et al., 2005; Monteiro et al., 2005; Suardana et al., 2011; Torres et al., 2019).

Figure 2.14. Coir fiber (Ru et al., 2022)

Cotton fiber

Representing 46% of the world's natural and chemical fiber production, cotton is the most widely used seed fiber and is widely preferred in textiles all over the world. Cotton fibers as seen in Figure 2.15 are a plant that has been used in textile production since the first societies and is of tropical origin but is grown most successfully in temperate climates where rainfall is well distributed. Cotton is hydrophilic and its fibers swell significantly in water, and it also dries slowly. Cotton releases a significant amount of heat while absorbing moisture, but soil and oil absorption and release rates are also high. Cotton fibers show stable behavior in water, and their wet strength is higher than their dry strength. Although cotton has lower toughness and initial modulus compared to hemp fibers, its breaking elongation, flexibility and elasticity recovery are higher. It is also used by mixing with other natural fibers to produce stronger textile products. While cotton fibers form the backbone of the world textile trade, this plant is found in the production of numerous products, especially textile and yarn products, rope and automobile tire cords (John and Sabu, 2012; Amar K. Mohanty et al., 2005; Muthu, 2019; Peças et al., 2018).

Figure 2.15. Cotton fiber (learn.genetics.utah.edu, 2023)

Synthetic fibers

Synthetic fibers are fibers obtained artificially from polymers that do not occur in nature, and their main source of energy and the energy required to process these fibers are obtained from petrochemicals. These fibers, which are mostly obtained from petroleum-based by-products and refined in laboratories and on an industrial scale, are obtained by combining various chemicals. They show high thermal, mechanical, and physical characteristics. These characteristics of fibers can be greatly varied by using different combinations of chemicals and production processes, e.g. polyester, nylon, polyurethane, acrylic. Synthetic fibers are in three main groups: carbon, aramid (Kevlar) and glass fibers. Kevlar, carbon and glass fibers are used in sports, automotive, aviation, marine, defense, construction, etc. due to their specific mechanical strength, light weight and the possibility of producing parts of different sizes in special designs. They are the three most preferred synthetic fibers in composite materials in many different sectors. Figure 2.16 displays the carbon, aramid and glass fiber (Hidalgo-Salazar and Correa, 2018; Muthu, 2019).

Figure 2.16. Synthetic fiber a) Carbon fiber b) Aramid fiber c) Glass fiber (Muthu, 2019)

Carbon fibers

Carbon fibers have very high specific strength and hardness, as well as extremely high chemical robust and thermal characteristics. These unique characteristics are due to their flawless structure and the improvement of highly anisotropic graphic crystallites that are aligned along the fiber axis during the manufacturing process. The main source from which approximately 90% of carbon fiber is produced is Polyacrylonitrile (PAN), with the remainder being rayon and petroleum pitch. Rayon and PAN are organic polymers and contain long strings of molecules connected to each other by carbon atoms. Although the very high cost of carbon fibers limits their use in composites in areas other than aviation applications, much research is being conducted on how to extract carbon from natural resources to produce carbon fibers and how to reduce the production costs of these carbon fibers. Thus, the preference rate of these fibers in the production of high-end luxury and sports cars, satellites, aviation structures and rockets are increasing (Amar K. Mohanty et al., 2005; Muthu, 2019). Figure 2.17 indicates the different types of carbon fiber.

Figure 2.17. Different types of carbon fiber (zoltek.com, 2023)

Aramid fibers

Aramid fiber was the first type of organic fiber used as reinforcement in advanced composites with sufficiently high tensile modulus and strength that it has much better mechanical characteristics than steel and glass fibers on an equal weight basis. Aramid fibers are also called kevlar fibers. Kevlar fiber ribbons are created by combining para-phenylenediamine with terephthaloyl chloride, which forms aromatic polyamide threads. Due to the structure of aramid fibers, it has high resistance to heat and flame and maintains these properties at high temperatures. Because they are considered high-performance fibers, they have relatively high prices. There are different types of fibers such as Kevlar, Kevlar 49 and Kevlar 29, and these fibers are generally used in the production of armor. Also, kevlar is highly preferred in areas such as defense, aerospace, automobile and biomedical industries, especially studies are carried out on ballistic applications of kevlar fiber reinforced composites (Ertekin, 2017; Karacor and Ozcanli, 2022a; Muthu, 2019; Yang, 2017). Figure 2.18 displays the diverse types of aramid fibers.

Figure 2.18. Different types of aramid fiber (Ertekin, 2017)

Glass fibers

The most commonly used synthetic fibers for many applications in the composite industry are glass fibers (Figure 2.19). Compared to kevlar and carbon fibers, glass fibers are affordable and have a wide variety of fibers. The production cost of these fibers, which are produced by drawing liquefied glass with 50% silica and other mineral oxides, is also affordable. The main advantages of glass fiber are high chemical resistance, low cost, high tensile strength and excellent insulating properties. Disadvantages include susceptibility to wear during processing, relatively low tensile modulus and high density for commercial fibers, somewhat high hardness and low fatigue resistance. There are glass fiber grades based on various chemical combinations to meet the specific requirements of different markets, such as A glass, C glass, E-glass, S glass. Although the strength of e-glass is quite high, its density is very low and Young's modulus is not very high. For this reason, while the modulus-to-weight ratio of glass fibers is moderate, the strength-to-weight ratio is quite high. These fibers are generally preferred in fuel tanks, automotive body construction, bulletproof glass, energy sector, construction industry, sports and aviation (John and Sabu, 2012; Karacor and Ozcanli, 2023a; Karacor and Ozcanli, 2020; Muthu, 2019).

Figure 2.19. Different types of glass fiber (neg.co.jp, 2023)

Mineral fibers

Naturally occurring or slightly modified fibers produced from minerals are called mineral fibers. Asbestos and ceramics are widely known mineral fibres. Mineral fibers can function in high temperature conditions. A new type of mineral-based fiber with very high thermal, chemical and mechanical characteristics has emerged, known as basalt fiber. Researchers are working to use this fiber as a potential replacement for synthetic fibers. While animal and mineral-based fibers are not often preferred in composite fabrication; It is preferred in the production of areas such as clothing, paper and handicrafts (Lalit et al., 2018; Muthu, 2019).

Asbestos

Asbestos is one of the naturally occurring mineral fibers of a group of mineral silicate fibers that include the serpentine and amphibole series. In this mineral group, there are five amphibole minerals such as the serpentine mineral chrysotile (white asbestos) and actinolite, amosite (brown asbestos), anthophyllite, crocidolite (blue asbestos) and tremolite. Asbestos fibers (Figure 2.20) are short, discontinuous fibers with high surface area and a high length/diameter ratio (John and Sabu, 2012). Asbestos is used as a loose fibrous mixture combined with plastics and resins or other materials woven into textiles. Applications where asbestos is used include roofing, cement pipes and sheets, textiles, gaskets, thermal and electrical insulation, coatings and compounds, friction materials (e.g., brake pads and shoes), flooring plastics, paper, yarn, mastics, fiber bonding and milling board (International Agency for Research on Cancer (IARC), 2012).

Figure 2.20. Asbestos fiber (textileblog.com, 2021)

Basalt fiber

With increasing interest in recent years, basalt fibers are at the forefront of replacing traditional glass fibers due to their advantages such as environmental cost and chemical-physical properties. Although mineral fibers extracted from basalt rocks are not new, their suitability as reinforcement in polymer composites is relatively new. Basalt fiber production is carried out by melting the by-product of basalt rocks obtained from quarries. Extrusion through a small nozzle at 1500 °C typically results in a fiber with a diameter of approximately 20 µm. Mechanically continuous basalt fibers are comparable to glass fibers. The elastic modulus of basalt fibers is highly dependent on the chemical composition. However, their modulus is comparable to or slightly higher than glass fibres, and both tensile strength and elongation at break are higher than glass fibres. It has very high thermal and chemical resistance and its characteristics are comparable to carbon fibers. Although it has all the properties similar to synthetic fibers, it is obtained naturally. These characteristics found in basalt fibers (Figure 2.21) not only lead to increased environmental sustainability in the formation

of composite materials, but also have enabled them to emerge as an alternative to glass fibers as improving impact resistance in composite laminates (Muthu, 2019; Sarasini et al., 2014).

Figure 2.21. Basalt fiber (Basaltex.com, 2023)

2.2. Matrix Elements

The matrix structure surrounds the reinforcement elements and protects them from chemical and environmental effects. The matrix structure has basic functions such as holding the fibers together, distributing or transferring the loads, protecting the fibers both in the structure and during production, and controlling the electrical and chemical properties of the composite it forms the structure of. Depending on the intended use of the composite structure, it should minimize moisture absorption from the matrix, have a low coefficient of thermal expansion, low shrinkage rate, have sufficient strength, modulus and elongation (the elongation value should be greater than the fiber), have excellent chemical resistance and dimensional stability, transfer the load to the fibers. It is expected to be sufficiently elastic to be able to transfer, and to completely penetrate or bond to the fiber (Peters, 1998; Sezgin et al., 2020).

Composite materials are divided into classes according to their matrix structures, as shown in Figure 2.22. As seen in Figure 2.22, this classification is made in three groups: metal matrix composites, ceramic matrix composites and polymer matrix composites.

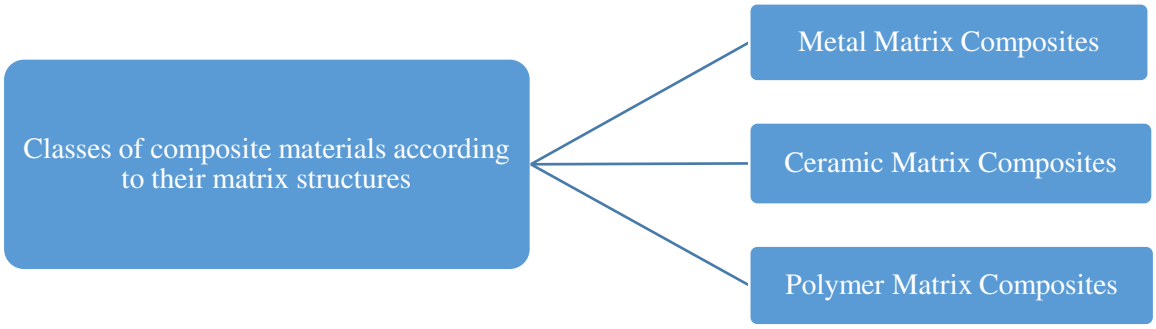

Figure 2.22. General classification of composite materials according to matrix types

In metal matrix composites, matrix materials are generally magnesium, aluminum, copper, titanium, and super alloys. Metal matrices are reinforced with particles, continuous or discontinuous fibers, or bristles. Ceramic or polymer-based fibers are generally preferred as reinforcement materials. Metal matrix composites find use in areas that require very high strength and hardness, low density, and some specific characteristics such as thermal stability, tribological properties and thermal expansion. These areas include the production of brake pads, brake discs, calipers, piston walls, turbine blades, cylinder liners, bearings and missiles (Mohan Kumar et al., 2018; Yildizhan, 2020).

It is stated that the most common metal matrix composite material is aluminum-based matrix composites, which have improved strength and stiffness, relatively low density, improved high wear resistance and temperature characteristics. While superior strength and stiffness are achieved by reinforcing an aluminum-based matrix, the most common reinforcement materials in aluminum-based metal matrix composites include non-metallic ceramics such as silicon carbide (SiC), aluminum oxide (Al_2O_3), carbon (C) and boron (B) (Kumar and Venkatesh, 2019).

Magnesium-based metal matrix composite materials are considered one of the most important types of metal matrix composite materials. They are produced using magnesium or magnesium alloys as matrix material. Although magnesium-based metal matrix composite materials are low-cost, magnesium is high-cost despite its low density and good mechanical properties. Reinforcements mostly used in the manufacturing of metal matrix composite materials are magnesium borate ($Mg_2B_2O_5$), SiC, Al_2O_3 and fly ash (J and Satish, 2018).

Copper-based metal matrix composite materials are used in certain areas where good wear, corrosion resistance, high heat and electrical conductivity are required. So that, copper-based metal matrix composite materials are often preferred in electronic devices and integrated circuits. Reinforcements such as alumina and graphite are used in the production of copper-based metal matrix composite materials. However, in conditions where high temperatures are required, titanium and some super alloys are chosen for the matrix material in metal matrix production (Somani et al, 2019; Wilzer et al., 2015).

Ceramic materials are materials that find a wide range of applications in engineering with their high thermal and resistance, high strength and hardness properties. Examples of these areas are generally found in aviation and space applications, such as rocket engine nozzles that require high service temperatures. In addition to its positive properties, it also has negative aspects such as low satiety characteristics. Monolithic ceramic materials are significantly prone to brittleness and can often cause major problems upon impact. Due to this disadvantage in ceramic matrix composite materials, it is aimed to improve the toughness properties of monolithic ceramics by using continuous or discontinuous reinforcement. While these reinforcing elements in ceramic matrices appear as particles, hairs or continuous fibers, the most common reinforcing material in ceramic matrix composite production is SiC, and different fibers and hairs such as carbon and Al_2O_3 are also used (Griffith and Halloran, 1996; Z. Lu et al., 2019). Ceramic matrix composite materials show different mechanical properties compared to other types of composites. Compared to polymer and metal matrix composites, the ceramic matrix composite material fails to meet the initial load. Ceramic matrix composite materials can be produced by powder dispersion, reactive melt infiltration, liquid precursors, polymer infiltration and pyrolysis or gas infiltration methods. Glass matrix composites and carbon glass composites are also referred to as ceramic matrix composite materials. In recent years, carbon/carbon (C/C) composites, especially C/C composites, are increasingly in demand due to their superior temperature resistance and are offered as materials used in missiles and space shuttles (Naslain, 2004; Windhorst and Blount, 1997).

Polymer matrix composites are basically classified as thermosets, thermoplastics and elastomers. Polymer matrix composite materials are the most widely used composite type in the sector and are known for being produced with more affordable costs and simpler production methods compared to metal matrix composites and ceramic matrix composite materials. High breaking strength, high specific strength and hardness, advanced wear and corrosion resistance characteristics make polymer matrix materials preferred in many different areas (Campbell, 2010).

Thermoplastic materials are known for their meltability, being able to flow when heated repeatedly and solidify when cooled. This curing process is completely reversible, making these types of polymers remoldable and recyclable. These polymers have high strength and shrinkage resistance because the remolding process is carried out without a major impact on the physical properties of the polymers. These types of materials are preferred in many structural applications in

the presence of lower forces and stresses. In addition, this type of polymer has high impact resistance, resistance to chemicals, and a higher recyclability rate with environmentally friendly production. Among the most negative aspects of this type of polymers, it can be said that their cost is expensive and their temperature resistance is lower compared to thermosets. Polyvinyl chloride (PVC), polyethylene (PE), polystyrene (PS), polypropylene (PP), high density polyethylene (HDPE), low density polyethylene (LDPE), nylon 6, polyethylene terephthalate, and polyether ether ketone (PEEK) are examples of thermoplastic materials. can be given (Jafferjı, 2011; Amar K. Mohanty et al., 2005; Muthu, 2019; Nickels, 2019).Table 2.5 indicates also the some thermoplastic material characteristics.

Table 2.5. Some thermoplastic polymer properties (Anonymous, 2012)

Property	**PP**	**PS**	**Nylon 6**	**Nylon 6,6**	**HDPE**	**LDPE**
Tensile strength (MPa)	26-41.4	25-69	43-79	12.4-94	14.5-38	40-78
Elongation (%)	15-700	1-2.5	20-150	35->300	2.0-130	90-800
Elastic modulus (GPa)	0.95-1.77	4-5	2.9	2.5-3.9	0.4-1.5	0.055-0.38
Izod impact strength	21.4-267	1.1	42.7-160	16-554	26.7-1.068	>854
Water absorption (24h-20°C)	0.01-0.02	0.03-0.1	1.3-1.8	1.0-1.6	0.01-0.2	<0.015
Heat deflection temperature (°C)	50-63	Max.220	56-80	75-90	43-60	32-50
Melting temperature (°C)	160-176	110-135	215	250-269	120-140	105-116
Glass transition temperature (°C)	-10 to -23	-	48	80	-133 to -100	-125
Coefficient of thermal expansion (mm/mm/°C*10^5)	6.8-13.5	6-8	8-8.6	7.2-9	12-13	10
Density (g/cm^3)	0.889-0.92	1.04-1.06	1.12-1.14	1.13-1.15	0.94-0.96	0.91-0.925

Thermoset materials consist of a three-dimensional network structure held together by cross-links that cure irreversibly to form a fusible material. These cross-linked structures are strong, creep resistant and highly resistant to solvents. Thermoset polymers also have structural integrity and high hardness, chemical and temperature resistance, high mechanical strength, and these properties

contain the basic characteristics required for industrial design. Flexibility in design, good aesthetic appearance and cost effectiveness are among the advantages offered by thermosets. The disadvantages of thermoset polymers include their inability to be remolded, not recycled, and difficulty in surface treatment. However, these thermosets have lower impact resistance or impact strength properties. Examples of thermosetting polymers or resins include polyester, epoxy, phenolic resin, cyanate ester, furan vinylester, polycarbonate, silicone, bismaleimide, polyimides, and urethane (Auvergne et al., 2014; Jafferjı, 2011; Jakobsen et al., 2014; Muthu, 2019; Saheb and Jog, 1999). The most commonly used matrix among thermosetting materials is epoxy resin. Its high strength, effective electrical insulation, excellent adhesion to various substrates, low shrinkage, and higher chemical and thermal resistance characteristics make it an important candidate for use in many areas (Pawar et al., 2016; Sezgin et al., 2022; Wen et al., 2013). Application areas of thermosetting resins and examples of their precursors are given in Table 2.6.

Table 2.6. Thermoset materials and their precursors and applications (Jafferjı, 2011)

Resin	**Precursor**	**Applications**
Epoxy	Bisphenols and epichlorohydrin	Fiber composites for automotive, aerospace applications electrical laminates, marine construction, surface coating, engineering adhesives, paints
Unsaturated polyester	Diols, dicarboxylic acids, and reactive diluents e.g. styrene	Fiber composites for mechanical equipment, electrical and lighting industries, building construction, and surface coating
Phenolic resin	Formaldehyde and phenol	Casting and fiber composites for household appliances, electrical and lighting industries, electrical laminates, molding compounds, laminate moldings, ablative coating aircraft construction and accessories, automotive, foundry binders, and wood adhesive
Melamine	Formaldehyde and melamine	Textile auxiliaries, wood materials processing, friction linings, coatings, and molding compounds
Vinylester	Acrylic or methacrylic acid and epoxy resin	Building construction, marine construction, electrical industries and fiber composites for mechanical equipment
Urea	Formaldehyde and urea	Foams, textile auxiliaries, molding compounds, foundry binder, and wood materials

Polyurethane (PU)	Hydroxylfunctionalised oligomer [polyol) and diisocyanate	Adhesives, foams, coating, acid-resistant cements, and encapsulating materials
Cyanate ester	Alcohol or phenol and cyanogen halide	Fiber composites for re-entry vehicles, missiles rocket, and aircraft
Furan	Furfuryl alcohol	Molding compounds, acid-resistant cements refractory materials processing, wheels, fiber composites, and grinding
Bismaleimide	Amine and bismaleic acid	Fiber composites for re-entry vehicles, missiles rockets, and aircraft
Polyimide	Dianhydride and diamines	Composite and coating and for high temperature applications

2.3. Biocomposites

Recently, researchers have been striving to reduce the carbon footprint of existing materials by combining bioplastics and synthetic plastics or reinforcing them with natural or synthetic fibers. From an economic and environmental perspective, this substitution of petroleum-based raw materials with renewable resources has become a necessity as nature offers a wide range of bio-transformed products such as carbohydrates, fats and oils, fermentation derivatives or products of microbial activity (Gandini, 2008; Pilla, 2011; Juan C. Ronda et al., 2013). With the latest developments in natural fiber development and composite science, materials produced from renewable resources, especially biocomposites, are becoming more popular to further support global sustainability (Drzal et al., 2001; Holser, 2008; La Mantia and Morreale, 2011). Biocomposites are defined as composite materials consisting of one or more phases derived from a biological origin. They are types of structures containing different fiber/resin combinations such as natural fiber/synthetic resin, synthetic fiber/bioresin and natural fiber/bioresin. Natural fiber-reinforced matrix structures of these types began to be used approximately 3,000 years ago, when house walls were built using straw-reinforced clay. Although animals and plants continue their natural development, many biological materials such as wood, shell, bone, teeth, horn and skin have been preferred in composites where high mechanical strength/hardness and low weight materials are advantageous. At the beginning of the 20th century, Ford created the first automobile prototype from hemp fibers and wanted to use natural fibers that exhibit high specific strength in automobiles, but the economic conditions at the time did not allow the development of this idea (Fowler et al., 2006; Jiang, 2015). However, with developing technology and conditions, the potential use of biocomposites in the preparation of environmentally friendly composites is taking an increasing share in various industrial applications. These sectors include automobiles and rail vehicles, aviation, sports, furniture and entertainment

sectors (Johnson et al., 2017; Nickel and Riedel, 2003). Figure 2.23 indicates the examples of different sector applications.

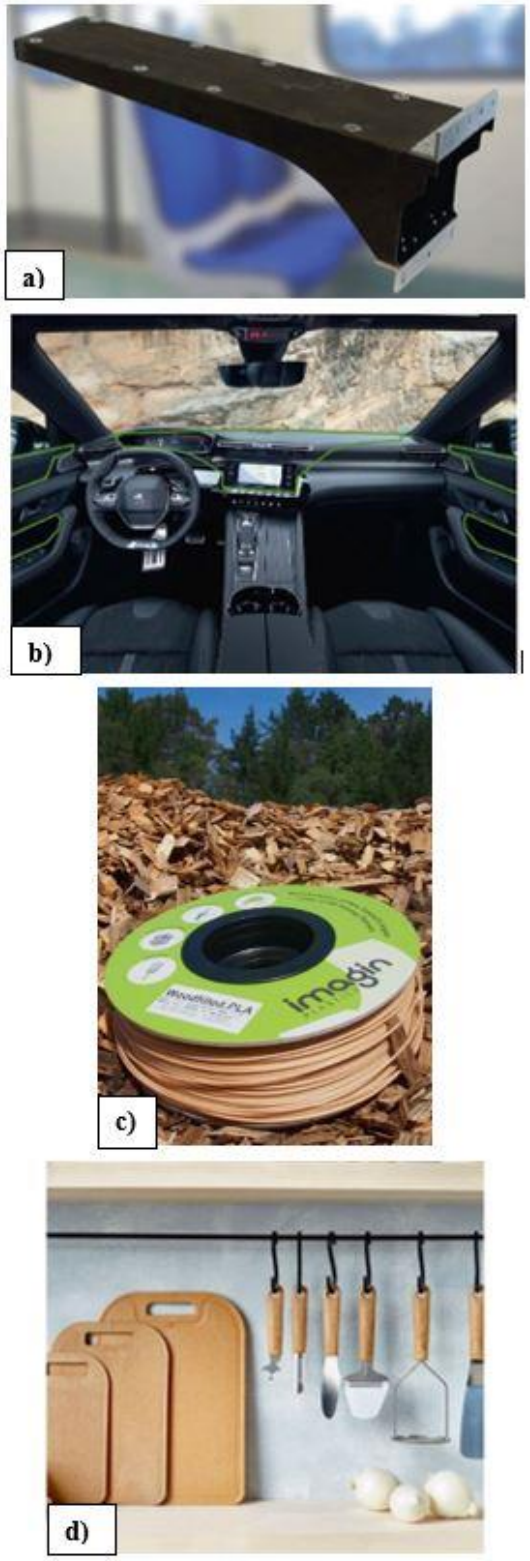

Figure 2.23. Different sector applications of biocomposite a) railway b) automobile c) plastic d) kitchen utensil (Holmes, 2019)

Apart from biological, economic and political factors, health is also an important issue for manufacturers. That is why manufacturers are working to replace petroleum-based materials with bio-based ones to encourage safer polymer production methods (Lutton et al., 2017).

Moreover, biocomposites are divided into two classes, fully biodegradable and partially biodegradable, and can also be divided into structural and non-structural classes according to the application area. Biodegradability also varies depending on the type of matrix or filler used (Izran et al., 2014).

2.4. Biobased Resins

The rapid depletion of fossil resources and increasing concerns about environmental sustainability have led researchers to look for renewable and bio-based raw materials as alternatives to petroleum-based materials. Epoxy resins are generally obtained from non-renewable petroleum-based resources. They have superior fatigue strength, outstanding adhesion, excellent chemical resistance, electrical insulation features, and high tensile and compressive strengths. Although epoxy resins have a wide range of uses with their many advantages, their high cross-linking density causes their impact resistance to be low. This situation causes a limitation in its use in the field of materials requiring high impact resistance. This has accelerated the processes and studies of obtaining bio-based epoxy resins from vegetable oils such as soybean oil, cottonseed oil, linseed oil, canola oil, palm oil and coconut oil. In this context, such vegetable oils are increasingly coming to the fore with their environmental friendliness, abundance in nature, biodegradability and ability to form pre-polymers (Khandelwal et al., 2018; Miyagawa et al., 2005; Omonov and Curtis, 2016; Woo and Kim, 2021). Especially recently, various new polymeric materials have been produced from vegetable oils and their derivatives, with thermophysical and mechanical characteristics that meet the demands of the industry and can find many possible application areas such as biomedical, construction, sport and automobile (Bao et al., 2014; Biermann et al., 2005; Y. Lu and Larock, 2009; Meier et al., 2007). However, historically the use of vegetable oils as a chemical product has not emerged recently. Vegetable oils are widely used in painting paints, other paints, varnishes and as a component of linoleum due to their film-forming properties. The use of these vegetable oils in coatings has survived to this day, and vegetable oils have also spread into the structural composites, surfactants, car shampoos, detergents, lubricants, and biofuels sectors (Paramarta, 2016; Can et al., 2001; Madbouly et al., 2016; Uosukainen et al.,1998). In addition to the advantages of the polymer synthesis process in vegetable oils, the biggest disadvantage is that vegetable oils, except castor oil, cannot be converted into their original polymer structure. The hydroxyl groups that castor oil has distinguishes it from others by being able to take part in the polymerization reactions of its triglycerides (Mercangöz et al., 2004). Vegetable oils are tri-esters of glycerol with various fatty acids and are liquid at room temperature. They are structuring whose physical and chemical properties are determined by the degree of unsaturation and changes in the length of the carbon chain. In general,

vegetable oils with higher melting points have fewer carbon-carbon double bonds, more carbon in the fatty acid chain, and an E (trans) configuration and conjugation of carbon-carbon double bonds (Montero de Espinosa and Meier, 2011; Sivasubramanian, 2010; Xia and Larock, 2010). Epoxides are a type of compounds that can be extracted from vegetable oils and form epoxy resins. These resins are obtained simply from unsaturated vegetable oils through the process known as epoxidation (Espinoza-Perez, 2009). Epoxidized oils can be shown to be good alternatives to renewable substitute resins as epoxy precursors. However, it is also stated that biobased thermoset resins have poor mechanical characteristics. This situation is caused by the low reactivity of epoxy groups and their tendency to intramolecular bonding. Any epoxidized oil exhibits limited mechanical and thermal characteristics and poorly cross-linked materials are obtained (Ahn, 2011; Marrot et al., 2014; Petrović, 2010). With these epoxidized vegetable oils, bioresins that are relatively low-cost, capable of minimizing carbon dioxide (CO_2) gas emissions that will cause global warming, are permanently renewable, and have a superior biodegradability effect can be produced (Lligadas et al., 2013; Tan and Chow, 2010b).

Epoxidation of alkenes and other unsaturated hydrocarbon chains is one of the most useful reactions in organic synthesis. Because the epoxide group formed is an active intermediate that provides the necessary functionality. The product can thus be used for further chemical transformations. Additionally, epoxidation can be used to reach the most economical state of a product (Dinda et al., 2008; Petrović et al., 2002). Thermosetting resins obtained by the epoxidation process, which involves the introduction of a single oxygen atom into each unsaturated bond, have improved durability and environmentally friendly character (Thakur and Thakur, 2018). Epoxy, alkyd, polyurethane and acrylate resins are types of resins produced from vegetable oils. Epoxidized vegetable oils are customarily preferred as plasticizers and stabilizers for PVC and also in painting and coating formulations (Cheong et al., 2009; Gerbase et al., 2002). Unsaturated fatty compounds are subjected to conversion into epoxidized vegetable oils by an on-site performic acid procedure in the industrial area. Nevertheless, it has been found that the use of strong mineral acids produces undesirable by-products such as ring-forming epoxides that are far from distinctive. The use of various catalysts such as ion exchange resins, transition metal complexes, Ventello catalyst, enzymes and crown ethers emerges in this context. AESO is one of the common vegetable oil thermosetting resins that is commercially affordable and easy to obtain. Acrylated epoxidized oils are obtained by synthesis processes from the reaction of acrylic acid with epoxidized triglycerides. The chemical modification of soybean oil for the production of AESO takes place in two steps. Soybean oil is first epoxidized to form epoxidized soybean oil (ESO) and then functionalized with acrylate groups to form AESO. Different processes can be performed on ESO to obtain methacrylated soybean oil (MSO) or methacrylic anhydride modified soybean oil (MMSO). In addition to soybean oil, it has also been stated that thermoset materials can be created from radish, linseed, canola, olive, cottonseed, peanut, corn and castor oils (Anastas and Zimmerman, 2013; Ramamoorthy, 2015;

Raquez et al., 2010; Sahoo et al., 2015a). However, the very high viscosity of AESO at room temperature causes some problems in the fabrication of fiber reinforced composites. Studies on this have shown that mixing a reactive diluent such as styrene with AESO positively affects the mechanical characteristics and processability of composites (Ozkur et al., 2022).

Natural oils have a triglyceride structure consisting of a high percentage of unsaturated fatty acid side chains. Due to their multiple C-bonds, they are ideal monomers of natural origin for the production of biopolymers. Although more than 1000 fatty acids have been identified, only about 20 are found in significant quantities in vegetable oils. The composition of fatty acids also varies depending on the crop, plant type, growing conditions and season (Abbasov et al., 2020; Amar K. Mohanty et al., 2005; Patil and Waghmare, 2013; Juan Carlos Ronda et al., 2011). Vegetable oils generally require conversion reactions to increase their reactivity towards polymerization reactions. After the product has finished its use, it is in the form of waste and can re-join the ecological cycle as a part of biomass through biodegradation. Figure 2.24 indicates the life cycles of triglyceride oil-based polymers vegetable oils can be used as dye and polymer additives, binders, lubricants, polymers and surfactants in the cosmetic industry, pharmaceutical industry, detergent industry, packaging and plastic industry (Altuncu, 2015).

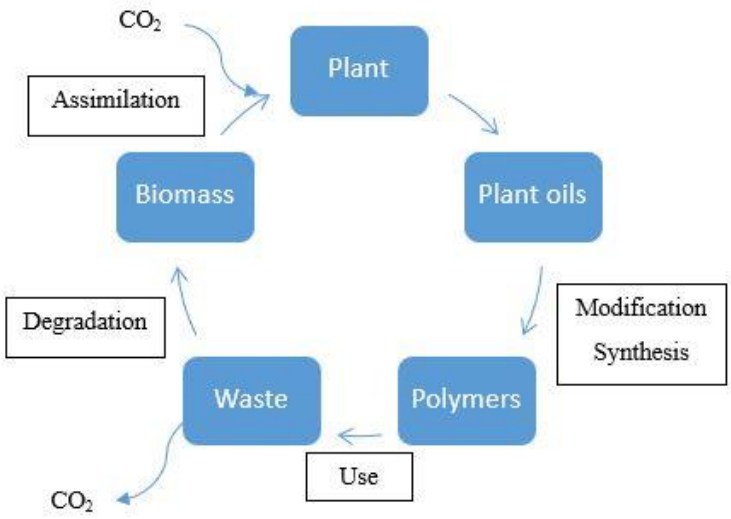

Figure 2.24. Life cycle of triglyceride oil-based polymers (Güner et al., 2006)

2.5. Production Techniques

Due to the different physical and mechanical characteristics of the materials, the production technique used in creating the final state of the material is important. In each production technique, various material components, various processing conditions and equipment required for part manufacturing are different. In composite production, a wide variety of types and characteristic materials are used, including resin, prepreg, fiber, particle and fabric, and different production

methods are used according to these types. is used (Ozkur, 2021). Figure 2.25 reflects the production techniques generally used for the production of composite materials.

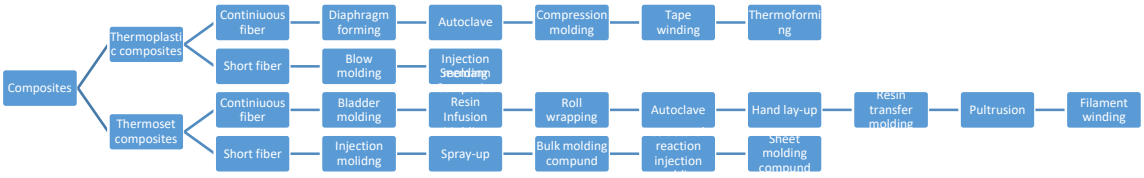

Figure 2.25. Composite processing technique (Mazumdar, 2002)

There are two classes of production techniques for composite production: open mold and closed mold techniques. The open mold technique is a technique in which the laminates and the top layer of the matrix are exposed to the atmosphere and an uncontrolled surface condition occurs. This technical tool manufacturing process is known for the possibility of implementing a simple, low-cost, rapid product development cycle. Closed molding, also called liquid composite molding, involves placing fibers inside a vacuum bag or on a two-sided mold. The gaps in the laminates are filled by introducing a liquid resin into the mold cavity. In this technique, the need for special equipment and suitability for automation enable large piece and high-volume production (Sas et al., 2015; Sevkat and Brahimi, 2011; Yildizhan, 2020). Table 2.7 indicates the open and closed mold techniques examples. Table 2.8 shows which manufacturing method is more suitable according to the production amount.

Table 2.7. Closed and open mold techniques (Zin et al., 2016)

Closed Mold Techniques	**Open Mold Techniques**
Pultrusion	Spray-up
Vacuum Bag Molding	Filament Winding
Compression molding	Hand Lay-Up
Resin Transfer Molding (RTM)	-
Vacuum Infusion Processing	-

Table 2.8. Manufacturing method suitability according to volume production (Zin et al., 2016)

Low Volume	Medium Volume	High Volume
Vacuum Infusion Processing	Wet Lay Up Compression Molding	Reinforced Reaction Injection Molding (RRIM)
Vacuum Bagging	Resin Transfer Molding	Continuous Lamination
Hand Lay-Up	Centrifugal Casting	Pultrusion
Spray Up	Filament Winding	Compression Molding

2.5.1. Hand Lay-Up

The hand lay-up production technique is one of the simplest, cost-effective production methods widely preferred for combining resin and fabric components as seen in Figure 2.26. In this process, the fiber reinforcement is manually placed in a single-sided mold and the principle of impregnating the resin on the reinforcement through cylinder brushes is applied. The main advantage of the hand lay-up technique is the ability to produce complex, very large parts in a practical way. Furthermore, the cost of equipment and tools is very affordable compared to other methods. The premier disadvantage of hand layup is that the process is labor intensive, resulting in long cycle times and low volume part output. However, the nature of the hand-laying process is that parts with inconsistent fiber orientations can result. Another disadvantage due to the structure of production is the formation of laminates of variable thickness. Thus, parts with fiber volume and mechanical strength where dimensional tolerances are not constant can be produced. Besides health and safety issues of the resins used and the high styrene content of the resins are also the demerit of the method (Kim et al., 2014; Kozlowski et al., 2004; Sevkat and Brahimi, 2011; Zin et al., 2016). With this method, it is possible to produce various aircraft and automotive parts such as non-structural parts, aircraft seats, car instrument panels and interior cabin parts (Zin et al., 2016).

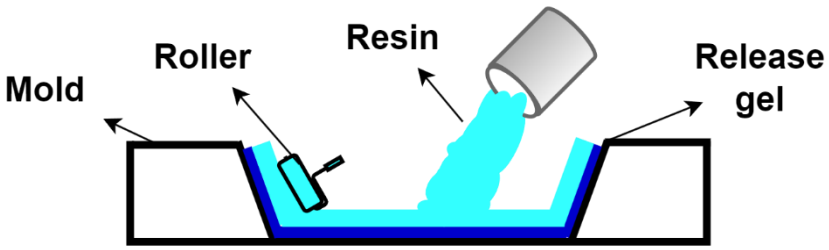

Figure 2.26. The schematic view of hand lay-up method (Zin et al., 2016)

2.5.2. Filament Winding

Filament winding technique involves first soaking the fiber tows in a resin bath and then winding them on a mandrel in different directions (Figure 2.27). The control of the winding process is done by the rotation speed of the mandrel and the fiber feeding mechanism. Filament winding mainly produces open-ended structures such as cylinders or closed-ended structures such as pressure

vessels and tanks. This is due to high hardness/weight ratios. Composite overwound pressure vessels are one of the well-known applications of this technique, which is of critical importance in the propulsion of spacecraft, attitude control systems and life support applications in the filament winding process. The design of these vessels requires a combination between liner analysis and fiber overwrap. While kevlar, glass, and carbon fibers are used as reinforcement elements in the filament winding process, epoxy, vinylester and polyester are used as matrix elements. However, glass fibers and polyester resins are more common due to their low cost. The advantages of this technique are that it is the only method that can be used to make cost-effective and high-performance composite parts. It uses low-cost raw material systems and low-cost tooling, and can automate filament winding for the production of high-volume composite parts. Its disadvantages are that it is limited to the production of closed and convex structures, that not all fiber angles can be easily produced, that the maximum fiber volume ratio that can be achieved is limited to 60%, and that it is difficult to obtain an equal fiber distribution and resin content throughout the thickness of the laminate (Mazumdar, 2002; Amar K. Mohanty et al., 2005; Zin et al., 2016).

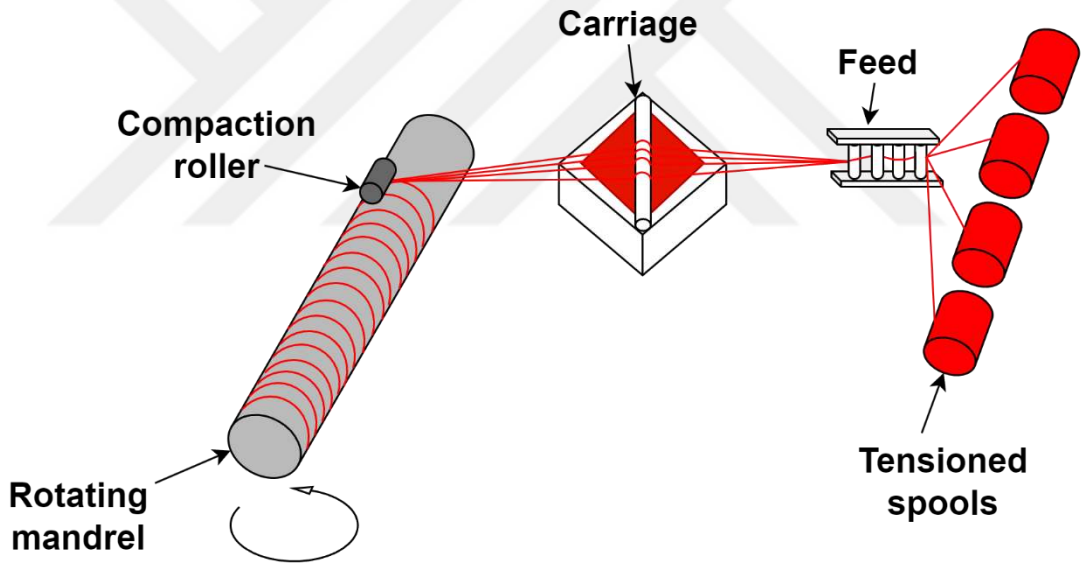

Figure 2.27. The schematic view of filament winding method (Boon et al., 2021)

2.5.3. Spray Up

The spraying method is the process of manufacturing by spraying the resin and fiber onto an open mold with the pressurized air provided by the spray gun as indicated in Figure 2.28. The spray gun functions by simultaneously cutting continuous fiber rovings to a predetermined length and spraying them onto the mold through a resin spray. The presence of air between the layers in the mold is eliminated by applying a roller onto the sprayed material. The curing process takes place at room temperature, depending on the resin used. Aramid fiber, glass fiber, and carbon fiber are used as reinforcement elements, and these elements are embedded in the mold in the form of continuous strand mat, fabric and various core materials. Polyurethane resin, epoxy, unsaturated polyester,

polyvinyl ester, polyester, and phenolic resin are used as matrix elements. It is possible to repeat the process for the desired part thickness, and the quality of the composite part produced with this technique is largely related to the skill of the worker. Due to the structure of the process, the manufacturing method is efficient and flexibility in production can be achieved by changing the design. In addition to being suitable for various part sizes, the spraying method is a method that provides high volume reinforcement fraction economically with cost-effective equipment. It is a technique that finds application in the production of lower load-bearing parts such as boat, duct and air handling equipment, storage tanks and truck bodies. Its disadvantages are that it is not appropriate for the production of parts with high structural requirements, it is difficult to control the volume fraction and thickness of the fiber, it releases styrene emissions due to the open mold structure, the surface quality cannot be the same on both surfaces, that it is not a convenient method for parts where dimensional accuracy and process repeatability are required (Mazumdar, 2002; Zin et al., 2016).

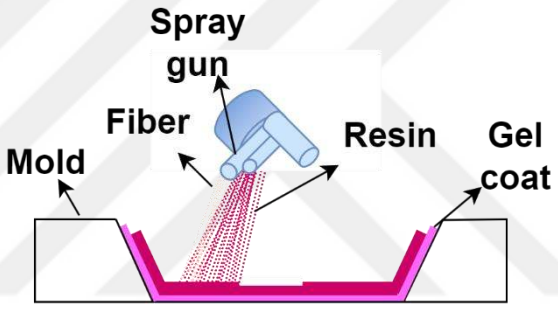

Figure 2.28. The schematic view of spray up method (Shukla and Garg, 2023)

2.5.4. Pultrusion

Pultrusion is a production technique that produces continuous profiles with a fixed cross-section in hybrid composites. For thermoplastic pultrusion molding, as the reinforcing fibers and resin are drawn through a heat mold, when heat and pressure are introduced, the resin begins to melt and penetrate the reinforcing fibers as shown in Figure 2.29. Carbon, E-glass, aramid fibers and S-glass are used as reinforcement, and vinylester, epoxy, phenolic resins and polyester are used as matrix elements. Various variables such as preheating method, mold temperature, and drawing speed are determining factors for a potential industrial application. Although this technique is similar to the metal extrusion process, the point of difference is that the material is pushed from the mold in the metal extrusion process and pulled from the mold in the pultrusion process. The pultrusion process is low cost, simple, high volume, automatic and continuous. Pultrusion is generally preferred for specific field applications where finished, smooth parts that do not require finishing are desired. Its most common applications include railings, tubes, stairs, beams, walkways and bridges, electrical enclosures, flooring and equipment support, conduits, and light poles. The advantages of this process include that it is a continuous process, can be fully automated to obtain the finished part, and enables

the production of low-cost commercial products using low-cost fiber and resin systems. Among its disadvantages are that the fiber angles in the produced parts are limited to 0°, it is suitable for parts with fixed sections along their length but cannot produce conical and complex shapes, parts with very high tolerances cannot be manufactured in internal and external dimensions, thin wall parts cannot be produced, it is limited to the axial direction, structures requiring complex loading cannot be produced (Mazumdar, 2002; Amar K. Mohanty et al., 2005; Wiedmer and Manolesos, 2006; Zin et al., 2016).

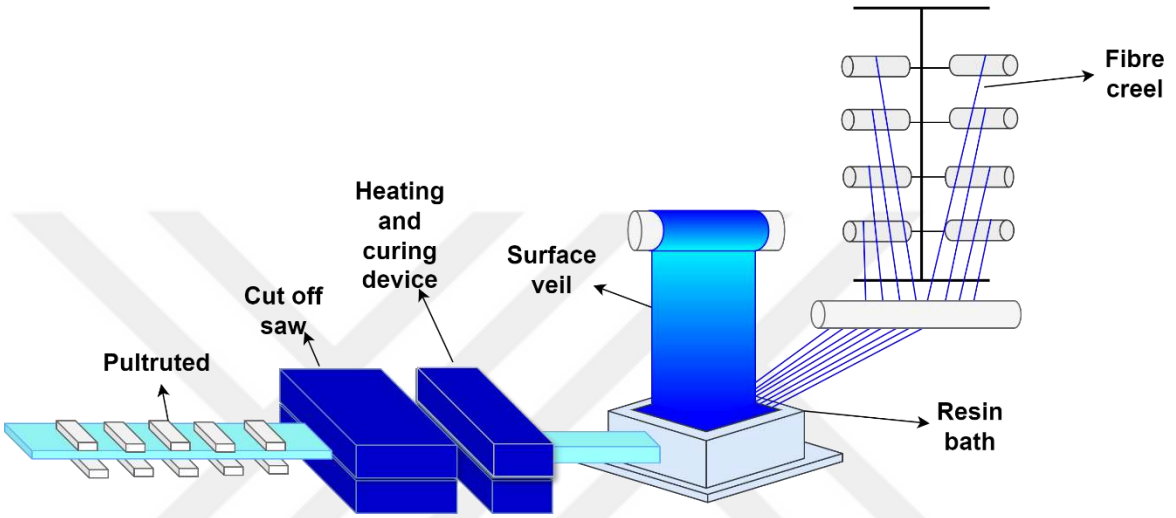

Figure 2.29. The schematic view of pultrusion method (Haghani and Yang, 2016)

2.5.5. Roll Wrapping

Roll wrapping is a similar process to pre-impregnation insertion, except that a cylindrical or round-taper mandrel tool is used (Figure 2.30). The technique is convenient for high-volume production of tubular components and has a cost-effective initial investment. In the roll wrapping process, carbon/epoxy unidirectional prepregs are generally preferred in part production. In this method, first the prepreg is rolled on a removable mandrel, followed by shrink tape wrapping for reinforcement. Finally, the solidification process in the entire assembly is carried out by mass curing. The roll-winding process is common for making bicycle frames, fishing rods, golf shafts, and other tubular shapes. The roll winding process enters into rivalry with filament winding and pultrusion techniques in tube manufacturing in the composite industry. The advantages of roll wrapping over others are that the initial investment cost and prototyping cost are reasonable, it provides a high fiber volume ratio, the desired fiber orientation can be easily achieved, and thin and conical sections can be produced easily. Disadvantages include factors such as the inability to produce complex parts, the inability to manufacture thick composite parts due to limitations in applying pressure, the difficulty of obtaining consistent fiber orientation during production, and the formation of pores and gaps between layers (Mazumdar, 2002).

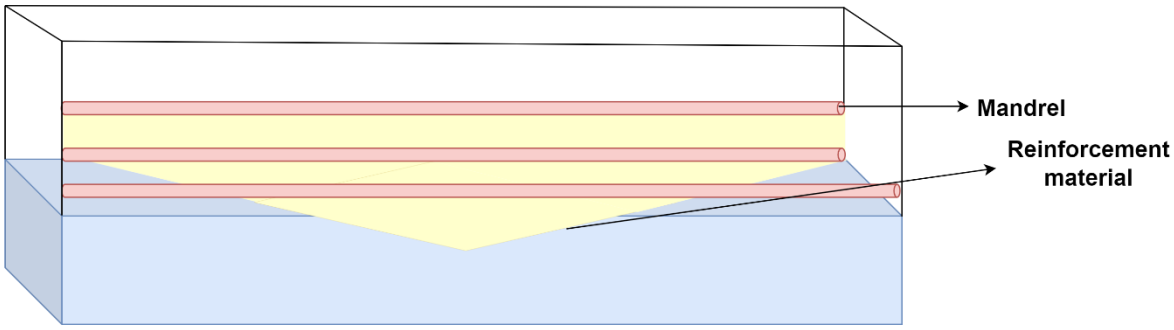

Figure 2.30. The schematic view of roll wrapping method

2.5.6. Compression Molding

Compression molding is the process of hardening the part by placing composite materials between two matching molds under high pressure and heat as seen in Figure 2.31. There are molding types such as sheet molding compound, bulk molding compound, thick molding compound, and wet lay compression molding, which are defined according to the type of molded materials. Compression molding provides flexibility in part design, as well as features such as protrusions, inserts, attachments, and ribs. This technique allows rapid curing of large quantities of fiber-reinforced complex polymer parts. Curing time is related to the size, thickness and shape of the part. Compression molding is one of the fastest methods in the fabrication of thermoset matrix composite parts. Sheet molding compounds (SMC) are thus the most widely accepted form of material in fiber-reinforced composites in the automotive industry, accounting for 70% of composites by mass. SMC compression molding is used in the automotive industry to produce roof panels, doors, hoods, cover panels such as quarter panels, deck lids, ground effect packages, fenders and add-ons such as spoilers, and limited access panels. In the compression molding method, phenolic resin, epoxy, bismaleimides, vinylester and polyester are used as matrix materials, and carbon, glass, aramid, sisal, jute, hemp, bagasse, kenaf, banana, cotton and stitched materials are used as reinforcement elements. SMC compression molding has many advantages, such as the possibility of high-volume production, the possibility of producing low-cost components in high volume, high surface quality and good shaping possibilities, and the ability to combine multiple parts into a single molded part. This technique also has disadvantages such as the high initial investment cost of the process due to high equipment and mold costs, not being suitable for the production of a small number of parts or prototype applications, and the production of non-structural parts (Kandar and Akil, 2016; Mazumdar, 2002; Amar K. Mohanty et al., 2005; Zin et al., 2016).

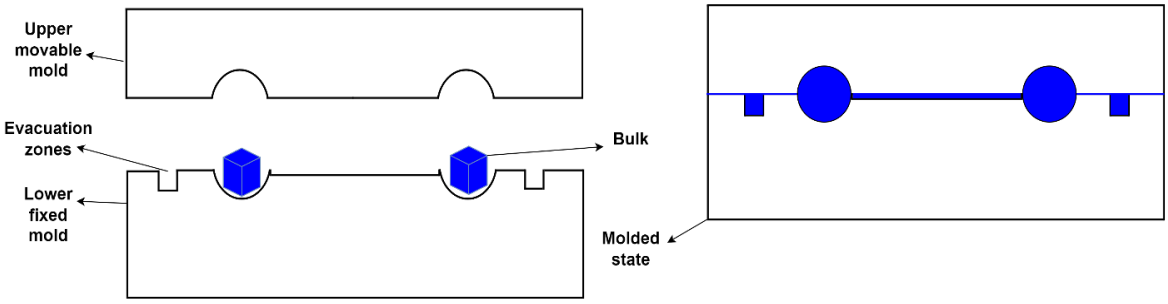

Figure 2.31. The schematic view of compression molding method (Shukla and Garg, 2023)

2.5.7. Injection Molding

Injection molding is the most common production process in the production of finished forms of thermoplastics, the use of which is increasing day by day in fiber-filled thermoplastics as indicated in Figure 2.32. It is a high-volume production process and is ideal for producing parts for automotive, consumer, and recreational applications. The injection molding process follows the process of injecting a fixed amount of material into heated mold cavities and then, after crosslinking is completed, the mold is opened and the part is deposited into a collection bin. Processing time is approximately 20 to 60 seconds, in this respect injection molding is known for having the highest production rate in the shortest process cycle time compared to other molding processes. Production speed can be improved by using a multi-cavity mold. Although this method is generally used in the production of small-sized parts, it also offers the opportunity to be used in the construction of large structures. Sink waste, sewing machine parts, small electrical appliances, small appliance motors, electrical plug fuses, household items such as mugs, buckets, soap containers, toys, housings and housings of various units, equipment housing, gears, computer parts, automotive parts produced by the injection molding method. It has advantages such as production of complex shapes in one time, high part repeatability, tight dimensional control, enabling the production of low-cost parts, good surface coating quality, and very low scrap loss. It has disadvantages high initial investment cost; not suitable for prototype part production; not suitable for manufacturing low volume parts due to high tooling costs, it involves a longer delivery time due to situations such as mold design, mold making, computer simulation of the production process; too many process variables such as back pressure, injection pressure, mold temperature, melt temperature, shot size create difficulty in determining the quality of the part (Mazumdar, 2002; Amar K. Mohanty et al., 2005).

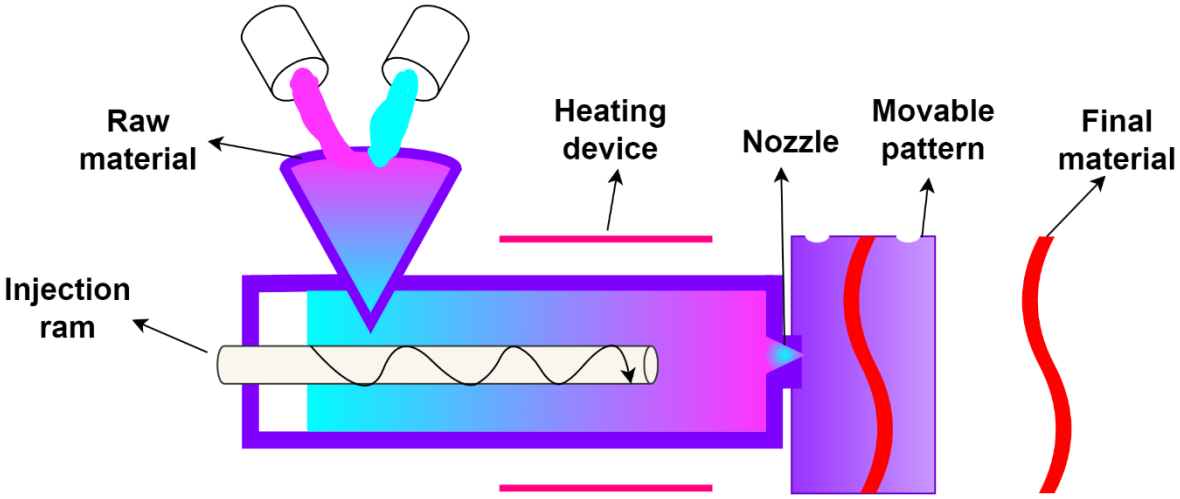

Figure 2.32. The schematic view of injection molding method (Mazumdar, 2002)

2.5.8. Autoclave

In this technique, prepregs are laid on a tool in a predetermined order and spot welded to restrict movement relative to each other in the stacked layers as displayed in Figure 2.33. Welding is not applied to thermosets. Then, the prepared part is placed in a vacuum bag and placed in an autoclave, then heat and pressure are then applied to cure and strengthen the part and waited to complete the process cycle. While this process is similar to the hot press method, it differs from that method by the method of applying pressure and heat. The autoclave process is used in the aerospace industry to make harder composite parts. Prepregs made of unidirectional fibers, mostly PEEK carbon fiber and PPS carbon are the materials used in this method. Along with glass and kevlar fibers, PP, nylon and other plastic types of polymers are used as part raw materials. Its advantages are that it enables the production of structural composite components with a high fiber volume ratio, that it allows the production of any fiber orientation, that it is suitable for the construction of prototype parts, and that it can be made in a simple way for the design of vehicle parts. Its disadvantages include requiring a high capital investment, operator labor intensity, and labor costs (Mazumdar, 2002).

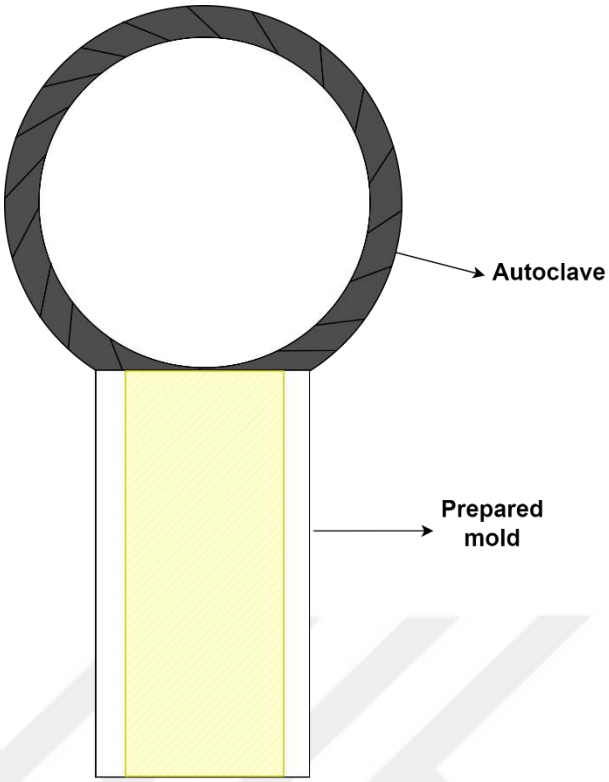

Figure 2.33. The schematic view of autoclave method (Kaw, 2006)

2.5.9. Diaphragm Forming

The diaphragm forming process differs from thermoplastic filament winding, autoclave and pultrusion processes because it is not compatible with thermoset technology (Figure 2.34). This method has been developed specifically to work with thermoplastic prepregs, and in this technique, pre-impregnated layers in the form of composite sheets are placed between two flexible diaphragms and formed under heat and pressure against a female mold. The prepreg layers thus move freely between two restricted diaphragms. In this technique, the composite sheet is formed by stacking unidirectional pre-impregnated materials in the desired order and direction, while composite sheets consist of carbon/PEEK, carbon/PPS, carbon/nylon and glass/nylon prepregs. This technique is superior to other methods by using continuous fibers in the production of parts, providing excellent structural properties and creating acceptable complex shapes with equal thickness, with an acceptable high production efficiency. The limitations of this method are that it is limited to the production of parts with constant thickness and the production of complex parts is shown by the difficulty of maintaining uniform fiber distribution (Mazumdar, 2002).

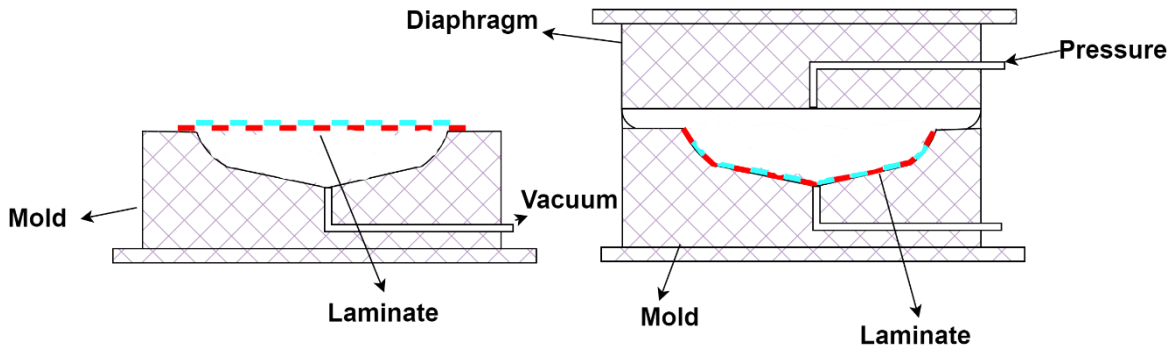

Figure 2.34. The schematic view of diaphragm method (Mazumdar, 2002)

2.5.10. Resin Transfer Molding

The resin transfer molding method, which produces complex parts with smooth surfaces on all exposed surfaces, is a closed molding technique by placing the reinforcement material in a closed mold under pressure as indicated in Figure 2.35. Placing the materials in the dry mold allows the combination of different materials and orientations. Achieving a fast cycle time in the process depends on temperature-controlled tooling, in which the tool cavity volume can be adjusted for the desired part thickness. Vacuum can be used to improve resin flow within the mold cavity, and a wide variety of tooling opportunities are available for this technique, including low-cost composite and temperature-controlled metal machining. Before placing the reinforcement into the mold, a mold release agent is applied to the surface, then, while the mold is closed and compressed, the resin is injected under pressure through the mixing injection equipment, allowing the part to cure in the mold. The compression process can be in the form of environmental compression or press compression. While RTM can be applied at room temperature, heated molds are required to achieve product consistency as well as fast cycle times. RTM is commonly used in aerospace, automotive, sporting goods and consumer product applications such as doors, helmets, bicycle frames, hockey sticks, windmill blades, aircraft parts, sports car bodies, and automotive panels. In the RTM process, fiber preforms or fabrics are preferred as reinforcement, while a wide variety of resin systems, including, epoxy, vinylester, polyester, phenolic and methylmethacrylate, are preferred as matrix. It has positive aspects such as compared to pressure molding and injection molding, the initial investment cost is low, the molds can be produced close to dimensional tolerances, parts with good surface quality can be produced on both sides, a wide variety of reinforcement materials can be used, low volatile emissions are created, and material waste and processing costs are reduced. The negative aspects of this technique include the need for a high rate of experimentation in the manufacture of complex parts, the fact that the tool design is not simple, and the cost of tools and equipment is higher compared to manual laying and spraying processes (Mazumdar, 2002; Pearce et al., 2000; Zin et al., 2016).

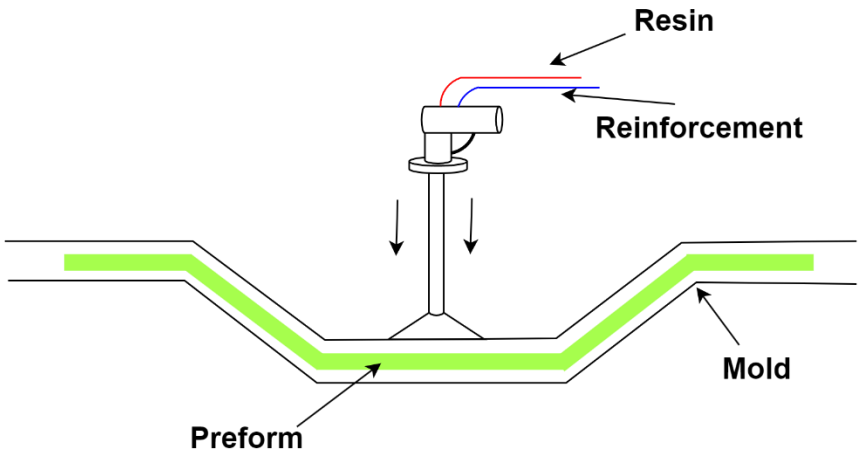

Figure 2.35. The schematic view of resin transfer molding method (Trofimov et al., 2023)

2.5.11. Structural Reaction Injection Molding Process

The SRIM process is similar to the RTM process except for the resin used and the mixing of resins before injection as seen in Figure 2.36. In this process, the two resins are mixed at a very high speed in a mixing chamber before being injected into the mold. Low pressure is used to prevent the fibers from washing at the injection port. Glass fiber is the most commonly preferred fiber type in this technique. The resin used in this process has very low viscosity and the most common resin is polyisocyanurate. This mixed resin is integrated into the mold with fiber preforms. The preform used here can consist of short or long fibers. Automotive parts such as bumper beams, fascia, pickup truck boxes and body panels are produced with SRIM. In the production of automotive parts, the possibility of producing high-volume structural parts at low cost and the possibility of producing small to large parts with complex configurations are among the advantageous aspects of this technique. The high initial investment cost and tooling cost, and the inability to obtain a high fiber volume ratio are the disadvantages of this technique (Mazumdar, 2002).

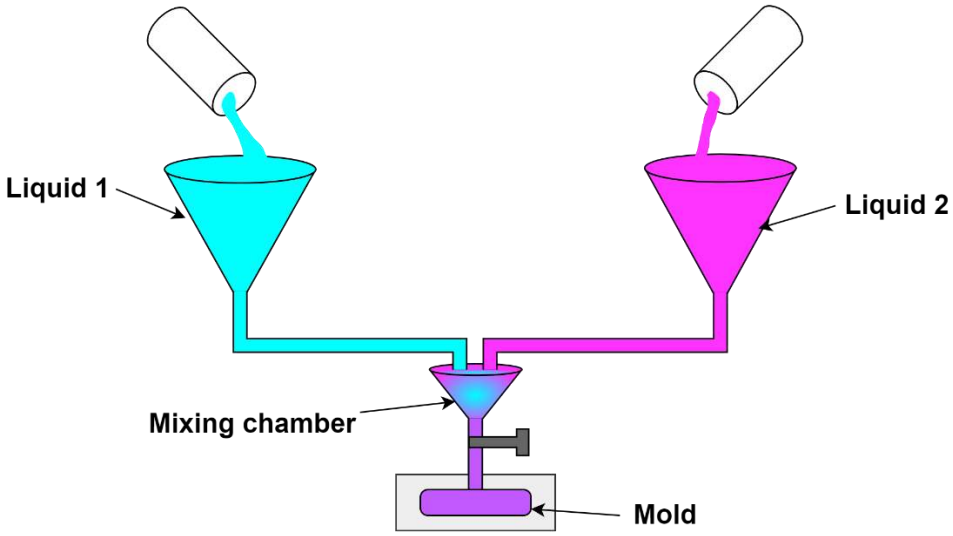

Figure 2.36. The schematic view of structural reaction injection molding method (Mazumdar, 2002)

2.5.12. Vacuum Bag Molding

The vacuum bagging method is a slightly more advanced version of the hand lay-up method and is known as a process that applies mechanical pressure to the laminate during the curing process as displayed in Figure 2.37. This technique has a great impact on removing air trapped between laminates, maintaining the position of fiber orientation during curing, reducing moisture and optimizing the fiber/resin ratio in the composite part. In a vacuum bagging process, a peeling fabric is placed on the mold as the first layer, followed by a composite plate, perforated nylon, vacuum blanket and vacuum nylon. The vacuum pump is operated to create 1 atm pressure and vacuum force is applied to the prepared mold. Carbon, glass, aramid, kenaf, jute, hemp, cotton, sisal, bagasse and banana, stitched materials are also used as reinforcement elements in this technique. Vehicle body parts, helmet and door panels, are the products of this technique. While lower void content, reduced volatile emission amount, and higher fiber content laminates constitute the positive aspects of this technique, the disadvantages are the high level of skill expectation of the operator, the use of resin being largely dependent on the skill of the operator, and the additional costs incurred for bagging the material (Zin et al., 2016).

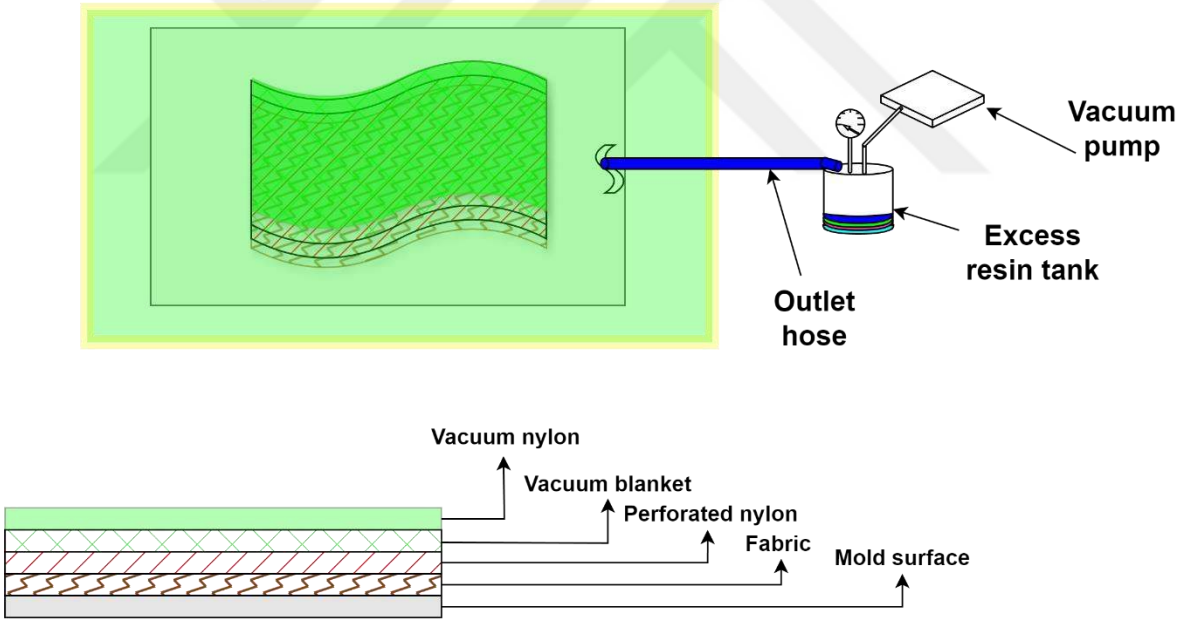

Figure 2.37. The schematic view of vacuum bag molding method

2.5.13. Vacuum Assisted Resin Transfer Molding Method (VARTM)

Vacuum Assisted Resin Transfer Molding (VARTM) is a widely preferred LCM (Liquid composite molding) technique due to its ability to produce large-scale, low-cost composites (Figure 2.38). In this process, the preform is placed on a one-sided processing surface, and the other part is disconnected from the outside with a vacuum bag. Air in the system is removed from the mold cavity by applying vacuum to the system, which causes the fiber to compress under atmospheric pressure, drawing the resin into the mold cavity through the flow line. When the resin reaches the exit section,

the resin flow is stopped, while vacuum is applied until the resin cures and the final composite part leaves the mold (Acheson et al., 2004). The advantages of VARTM include much lower cycle times, although they have their limits, organic compound evaporation occurs only during the resin mixing process and the ability to produce higher volumes and produce parts with a higher degree of repeatability. Besides, with this process, it is possible to reduce the percentage of voids encountered in other large part production processes such as hand play up and to increase the mechanical characteristics and fiber content of the produced part. Flexibility of one of the mold faces causes the thickness of the molded part to be partially related to the compressibility and vacuum negative pressure of the fiber-resin composite before it hardens. VARTM helps reduce tooling costs in processes with matching tools found in RTM, autoclave or compression molding and in higher performance composites. Compared to hand lay-up, which is the most basic of production methods, hand lay-up requires minimum necessary equipment such as a single-sided mold, resin impregnation brush rollers and resin, while VARTM requires additional equipment and tooling materials and is more costly. Another disadvantage found in VARTM is the difficulty of predicting resin flow, as the resin flow through the junctions cannot be predicted and the mold filling behavior can vary greatly due to high fiber volumes in these regions and changes in temperature, pressure, and resin flow during the process initiate void formation, leading to a decrease in the strength and modulus of the produced composites and premature damage behavior under load (Bodaghi et al., 2020; Dhimole et al., 2021; O'Donnell et al., 2004; Sevkat and Brahimi, 2011). For this reason, VARTM is seen as the most cost-optimal production method for large composite parts such as turbine blades, windmill components and ship hulls (M. Shah and Chaudhary, 2020).

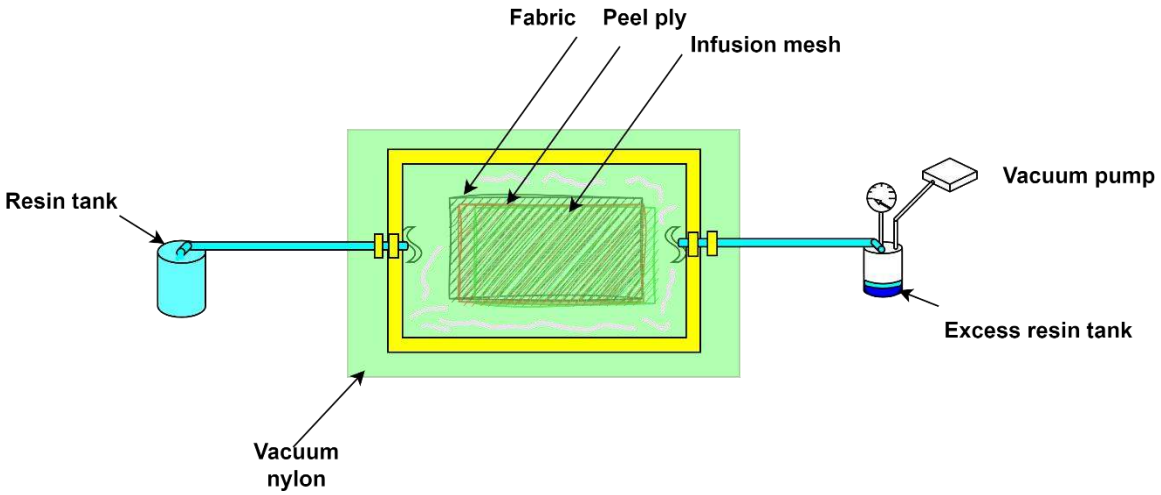

Figure 2.38. The schematic view of vacuum assisted resin transfer molding method

3. PRELIMINARY WORK

The continuous development of technology, the requirements of the industry, and the advancement of material science make researchers focus more on researching composite materials. Composite materials are a subject of extensive research with the various matrices, reinforcement elements, additives, fillers they use, as well as production parameters and different production methods. There are still missing points in the studies on this subject. The flexible adaptability of composite materials opens up the possibility of producing composites with different properties in a wide variety of composite materials.

When the studies in which the reinforcement elements are biomaterial are examined, Zhan (Zhan, 2010) aimed to design a bio-based printed circuit board using E-glass fibers, chicken feather fibers and soybean-based resin. The thermal properties, mechanical properties, flammability, electrical properties, and copper-composite adhesion status of the designed material were examined. It has been stated that chicken feather fiber or hybrid fiber reinforced soybean oil-based resin composites show very good chemical resistance against the chemicals used during printed circuit board manufacturing, and can provide advantages in terms of energy consumption, greenhouse gas emissions and toxicity compared to designs made with traditional epoxy and glass fiber composites. Nevertheless, it has been understood that it is essential to improve some properties of biocomposite materials, such as peel strength, in order to be preferred as an alternative to printed circuit boards. De Lemos et al. (de Lemos et al., 2017) produced composite materials using sugarcane, wood, babassu, bamboo, kenaf and coconut fiber as reinforcing elements, with or without using binders. By examining the morphological, thermal and mechanical properties of these materials, they investigated which parts of the automotive parts they are suitable for. In applications where impact resistance is important, composites containing coconut wood fiber, babassu fiber and coconut fiber are more suitable to use as they perform better than others. The composite consisting of polypropylene, coupling agent and wood flour, such as the reference glass fiber reinforced sample, has shown to be a good option in applications where thermal resistance is desired. Density generally stands out as an advantage in the use of natural fibers as reinforcement in composites in reducing weight and less fuel consumption for vehicles. Depending on the required properties desired in automotive, the possibility of using these materials in various applications has been demonstrated.

Oztemur et al. (Oztemur et al., 2022) aimed to design a composite shock absorber with bioresin by using denim wastes in different layers. They tested the physical and mechanical features of reinforcement elements formed from single, two and three different layers. They found that the density of the produced composite samples did not differ much according to the number of layers and was 0.115 g/cm^3. Based on the results of the falling weight test, they discovered that the amount of energy absorbed in parallel with the rise in the number of layers from one to three was 0.91 J, 4.67 J and 6.99 J, respectively. Considering the impact resistance of the three-layer composite panel, it

has been revealed that an environmentally friendly, biodegradable and green composite can be produced as an alternative to impact absorbing panels in construction and automobile structures. In the production of composite panels with the vacuum infusion technique, Oztemur et al. (Oztemur et al., 2021) used fiber and fabric forms from denim waste as reinforcement elements, and epoxy and acrylate AESO-based hybrid resins in the matrix structure. They applied physical tests to their samples with impact resistance against falling and dynamic mechanical analysis. They combined a matrix structure consisting of 70% epoxy and 30% AESO hybrid resins and 100% epoxy resin with a structure of two-layer, three-layer and fiber web between two layers and three-layer fiber web reinforcement elements. Regardless of the resin type, weight drop impact test results revealed that three-layer fabric and fabric/fiber reinforced panels absorbed more energy than other samples. While AESO-added fiber/fabric sandwich structured samples are seen as a good alternative option as impact absorbing panels in various usage areas such as construction and automotive, with their good impact resistance properties, it is thought that the use of denim waste and the use of bio-resin in the matrix will also provide environmental benefits in terms of utilization of solid wastes.

Rana and Evitts (Rana and Evitts, 2015) performed tensile, three-point bending and hardness tests on the composite material they created by adding different amounts of styrene to the AEFO (Acrylated epoxidized flaxseed oil) resin and changing the amount of flax fiber. While they changed the amount of styrene by 10%, 20%, 30%, 40% and 50%, the amount of flax fiber was changed by 2%, 5% and 10%. The augment in flax fiber content caused an arise in hardness, Young's modulus, flexural strength, flexural modulus, and tensile strength of AEFO biocomposite. By hybridizing glass fiber with hemp and linen fabrics, Khot et al.(Khot et al., 2001) created asymmetric and symmetric composite materials with AESO resin. In symmetrical composites, as the flax ratio increases by 20% from 0% to 100% and the glass fiber ratio decreases at the same rate, the tensile strength increases from 128.8 MPa to 26.1 MPa. In the asymmetric composite, as the flax content increases from 20% to 60% by 20%, the tensile strength value decreases from 111.7 MPa to 68.9 MPa. It was observed that as the flax ratio increased by 20% from 0% to 100% and the glass fiber ratio decreased at the same rate, the bending strength value decreased from 205.5 MPa to 61 MPa. Hong and Wool (Hong and Wool, 2005) aimed to develop a bio-based material for use in electronics, automotive, electronics and aerospace applications using soybean oils and keratin feather fibers. In terms of the amount of fracture energy, it was determined that as the keratin fiber ratio increased from 0% to 20% in composites using AESO cured at room conditions, the fracture energy increased from 1,420 kJ/m^2 to 1,820 kJ/m^2, and the flexural yield strength increased from 34.807 MPa to 38.782 MPa. At the end of the study, it was stated that keratin fiber and AESO resin are hydrophobic, the density of the composites decreases below 1 g/cm^3 with the increment in keratin fiber content, and the thermal expansion coefficient is low enough (67.4 ppm/°C), resulting in an innovative bio-based material. In their study, Kocaman and Ahmetli (Kocaman and Ahmetli, 2016) used banana peel and seashell as filling materials, and epoxy and AESO resin as a hybrid matrix material. They examined the effect

on mechanical properties by adding 30% and 50% sebacic acid (SAc) to the resin. While the tensile strength value is found to be lower in samples with 50% SAc added than in those with 30% Sac added, the percentage elongation increases in samples with 30% compared to 50%. Hardness, percent elongation and tensile strength values were found to be higher in samples made with seashell reinforcement than in samples reinforced with banana peel. In elastic modulus values, banana peel reinforced samples reached higher values at 30% and 40% filler reinforcement.

Lee et al. (Lee et al., 2013) examined how the interaction between the AESO resin and the fiber changed by applying different surface chemicals onto the ramie fiber. The applied silane and peroxide chemical modifications decreased the hydrophilicity of ramie fiber and increased the adhesion between the fiber and AESO resin. Additionally, chemical treatments reduced the presence of foreign substances on the surface along with the detection of morphological changes such as microcracks and micro pits on the surface. The interfacial shear strength between ramie fibers and AESO resin was improved with chemical modification. In the study of Ramamoorthy et al. (Ramamoorthy et al., 2012), the changes in water absorption and mechanical characteristics were investigated by creating hybrid composites using non-woven and woven jute, non-woven regenerated cellulose mat and woven glass fiber. It has been determined that the samples containing only glass fibers are the ones that absorb the least water, applying alkaline treatment to the lyocell sample does not reduce water absorption, and the water absorption rate decreases in hybrid samples where the glass fiber ratio increases and the natural fiber content decreases. While the bending strength results were parallel to the tensile strength results, Lyocell samples treated with alkali showed lower bending strength values than the untreated ones. In the impact test results, lyocell and glass fiber reinforced samples gave the highest value. It was found that as the use of lyocell and glass fiber fabric in hybrid composites increased, the impact strength value also increased.

Haq et al. (Haq et al., 2008) created a composite by combining unsaturated polyester resin and soybean oil with hemp and nanoclay. In the composites they created, the percentages were unsaturated polyester: epoxidized soybean oil 100:0, 90:10, and 80:20. The nanoclay addition was unsaturated polyester: epoxidized soybean oil: nanoclay 100:0:1.5 and 90:10:1.5. While the tensile strength and tensile modulus of the specimens decreased with the addition of bio-resin, an advance in the tensile modulus was examined with the addition of nanoclay, but the tensile strength decreased. Higher elongation and higher impact strength were found in biocomposites with the addition of epoxidized soybean oil. Samples made with resin mixtures adding nanoclay are more brittle, and their ductility, impact strength and elongation at break have decreased. Sahoo et al. (Sahoo et al. ,2017) wanted to examine the effect of sisal fiber on the composites they created by adding sisal fiber to bio resin at rates of 5%, 10% and 15%. While there was a 1.58-times decrease in tensile strength in the sample with 15% sisal fiber added compared to pure epoxy, a 2.43-times increase in impact strength was found. In the thermal analysis results, it was determined that the glass transition temperature decreased by 12 °C in the sample with 15% sisal fiber added compared to the pure epoxy

sample, and the first temperature at which it started burning decreased to 115 °C lower. The study reflects an increase in the hydrophilic nature of the surfaces in composites reinforced with sisal fiber, and also reveals that they have mechanical strength, durability and modulus suitable for use in the automotive and construction fields. In addition, the composite elements formed from fibers have a better storage modulus and damping factor, and are also lighter, which is expected to reduce the fuel consumption of vehicles. In the study, Quirino (Quirino, 2011) created a composite material by reinforcing conjugated linseed and soybean oil-based thermoset resins with wood flour and wood fibers. It was found that when 60%-85% wood floor was added to the resin, the tensile strength value increased with the augment in the filler ratio. It has been stated that the maple/oak flour mixture has 1.025 times better tensile strength than the pine flour mixture at the same particle size. When hardwood fiber was used as reinforcement, a composite material with 7.07 times higher mechanical characteristics than the composite reinforced with pine wood flour emerged. In the study, air laid flax, coarse hemp, air laid flax-PET (Polyethylene Terephthalate) hybrid and dissolving pulp sheet were used together with AESO resin as reinforcement materials to produce a structural composite. While the tensile strength of the composite using air laid flax reached the highest value with 78 MPa, the composite using coarse hemp showed the lowest value with 41 MPa. According to the bending test results, the composite material using dissolving pulp sheet had the highest bending strength with 140 MPa. The outcomes of the study are that the glass fiber composites taken as reference samples give higher values, especially in terms of impact resistance, in comparison to the natural fiber composites, the bending characteristics of the natural fiber composites are not much lower than the glass fiber composites. In natural fiber composites, the sensitivity of the hydrophilic structure of the fibers to moisture was also revealed in the aging test, and it was stated that it would be more reasonable to apply this type of natural reinforcement materials in interior products (Åkesson et al., 2009).

Considering the studies in the literature where different matrix components are used in the formation of bioresins, Ozkur et al. (Ozkur et al., 2019) investigated the impact resistance of composite materials they produced by combining jute fabric with bioresin to which soybean oil was added at different rates. They found that when 30%, 60% and 90% soybean oil was added to the epoxy resin, the absorbed energy increased compared to the sample with pure epoxy resin. Sudha et al. (Sudha et al., 2017) studied the effect of changing the ratio of ECO samples on the mechanical properties by creating biobased resin blends from epoxidized castor oil and diglycidyl ether of bisphenol A (DGEBA). While the addition of 20% by weight ECO to the bioresin gave the most ideal result for impact resistance, the glass transition temperature also declined with the arise of ECO content from 10% to 50%. Additionally, increased thermal stability of pure epoxy at high temperatures was detected in thermal analyses. An increasing energy absorption capability with the increase in ECO content was revealed in dynamic mechanics analysis. It was stated that the increase in ECO content in bioresin caused less crack area on the impact fractured surface in micrographs. It

has been said that high amounts of ECO added to the epoxy resin led to increased toughness in the mixtures by reducing the crosslink density in the epoxy network. Espinoza-Perez et al. (Espinoza-Perez et al., 2011) added ECO and ESO bioresins to the epoxidized vegetable oil resins they created and examined their mechanical and thermal performance. In the study where glass fiber was used as a reinforcement element, a decrease of 19.49% and 36.2% in the glass transition temperature was observed in the comparison of two different curing agents in the samples with the addition of ECO and EVO to 30% epoxidized vegetable oil. In the bending strength, 30% ECO and ESO addition caused a decrease of 13.88% and 36.11% in the comparison of two different curing agents. They stated that ECO and ESO added samples exhibited slightly lower thermal and mechanical characteristics than composites containing 0% EVO, suggesting that ECO and ESO can be used in composite applications.

In the study of Enis and Sezgin (Enis and Sezgin, 2021), they used epoxy resin and acrylated epoxidized soybean oil as matrix structure, while jute fabric was preferred as reinforcement element. Bio-resin ratio was from 0 to 100% and samples were subjected to three different curing temperatures as 20, 90 and 120 °C after production. Water absorption, wettability, thermal and morphological properties of the samples were investigated according to the increase in bio resin and the change in curing temperature. While the glass transition temperatures in the produced samples were observed to decrease with the increase in the bioresin ratio, post-curing temperatures were not found to have a clear effect on the glass transition temperatures. In terms of water absorption, the increase in bioresin ratio from 0% to 100% caused the increase in water absorption in the samples to be quite high. It has been determined that the water contact angle decreases significantly with the effect of increasing the hydrophilicity of the material with the increment in the bioresin ratio, and the augment in the bioresin ratio also eliminates the brittle structure of the matrix phase in the morphological structure. Ozkur et al. (Ozkur et al., 2020) aimed to create a bioresin by using AESO resin instead of epoxy for the production of an environmentally friendly material. They investigated the mechanical, thermal, physical and morphological effects of the increase in the amount of AESO resin on the samples they produced. In the results, it was specified that the optimum ratio in tensile and flexural strength was in composites containing 30% AESO resin, while the impact strength increased more in composites with 50% and more AESO content. While an accelerated increase in water absorption was also found in composites with 50% and more AESO content, it was observed that the sample containing 100% AESO absorbed 2.83 times more energy in the falling weight impact test than the sample containing no AESO. The produced biocomposite materials are considered to be potential materials in various end-use areas such as the construction industry, sports equipment and the automotive industry, where human health and environmental factors are taken into account.

Abu Bakar et al. (Abu Bakar et al., 2018) wanted to investigate the mechanical and thermal effects of ESO by combining DGBEA resin with ESO in different proportions. As the ESO content rises from 10% to 40%, the tensile and bending strength values decrease, and conversely, in impact

strength values, the augment in ESO leads to an increase in ductility and therefore to an arise in the absorption of impact energy. From the thermal analysis results, they determined that the initial temperature at which it starts burning drops by 12 °C when the ESO ratio is 40%. Miyagawa et al. (Miyagawa et al., 2007) combined unsaturated polyester with EMS to create a new bio-based material. They found that heat distortion temperature and glass transition temperature declined as the EMS amount raised from 0% to 25%. Since 25% EMS addition gives approximately the same value as 0% EMS addition in Izod impact strength value, it seems possible to replace UPE with EMS. Liu (Liu, 2014) created a new bio renewable thermoset resin based on AESO and methacrylated eugenol (ME) and analyzed it by dynamic mechanical analysis (DMA), compression testing, and TGA (Thermogravimetric Analysis). A decrease of 26.8 °C was found in the glass transition temperature with the AESO increasing from 0% to 40%, and the temperature at which the initial combustion started also decreased by 41 °C. In the compression test, it was stated that with the decrease of AESO content, the overall hardness will decrease in copolymers obtained by incorporating flexible triglyceride molecules, thus increasing the compression modulus. Sahoo et al. (Sahoo et al., 2019) aimed to create a new type of bioresin by epoxidizing linseed and castor oil and to reinforce this resin with sisal fiber to create an environmentally friendly product compared to petroleum-based derived materials. They investigated whether the samples subjected to mechanical, thermal, morphological and dynamic mechanical tests could be a renewable material. The void fractions in hybrid samples decreased by 1.68-1.75 times in individual samples to which ECO and ELO (Epoxidized linseed oil) were added at 30% compared to the pure epoxy sisal fiber combination. It was determined that the elongation amounts in bio resin samples containing ECO and ELO increased by 1.06-1.51 times compared to samples containing pure epoxy sisal fiber. It is shown that the incorporation of 30% ELO and ECO causes the epoxy matrix to be extremely plasticized and dissipates a higher amount of energy, and that these types of materials can be preferred in automotive, construction, and constructive structures with their reduced noise and vibration regulation and energy absorption ability. Fu et al. (Fu et al., 2010) examined the changes in mechanical and thermal properties by changing the AESO resin content and iodine value in the resin. It was found that as the mass fraction of AESO ascended, the high temperature glass transition temperature decreased from 43.6 °C to 36.4 °C, while the low temperature glass transition temperature declined from 8.1 °C to 1.6 °C. As the mass ratio of AESO increased from 30% to 80%, the tensile strength declined, and the degradation rate raised with the increase in AESO content in the resin.

In another vegetable oil-based bioresin study (Jin and Park, 2008), a new biobased resin was obtained by mixing DGEBA resin with ESO or ECO at ratios ranging from 20% to 80% by weight. In the thermal analysis results, the peak temperature in the DGEBA/ESO sample is higher than the DGEBA/ECO sample under the same conditions, and the enthalpy reaction value of the DGEBA/ESO sample is also higher than the enthalpy reaction value of the DGEBA/ECO system. In resins containing ECO samples, both the initial combustion temperature and the maximum

temperature reached are lower than in samples containing EVO, with a very small difference. Manthey et al. (Manthey et al., 2013) studied a new bioresin material by adding EHO and ESO to a resin at the rates of 10%, 20%, 30% and 40% and reinforcing the new bioresin with jute fiber. In the charpy impact strength test, 1.68 times higher values were found in the specimen containing 40% ESO and 1.59 times higher values were reached in the specimen containing 40% EHO compared to the pure epoxy jute reinforced sample. In the three-point bending test, the value was found to be 1.36 times lower in the specimen containing 10% ESO and 1.03 times lower in the specimen containing 10% EHO compared to the pure epoxy jute reinforced specimen, and the samples with 40% of both bioresins had very low bending strength values. Moisture absorption in epoxy bioresin mixtures and jute fiber reinforced biocomposite samples is parallel to the increase in ESO and EHO amounts. The results of this study revealed that the incorporation of EHO-based bioresins to jute fiber reinforced biocomposites provided dynamic mechanical properties, water absorption ability, and mechanical performance that were competitive with the addition of ESO. In their two studies, Miyagawa et al. (Miyagawa et al., 2004b, 2004a) aimed to create a new bioresin by mixing ELO with DGEBF resin in different proportions. In the study conducted with bioresin to which ELO was added at 20% increasing rates from 0% to 100%, the storage modulus, glass transition temperature and heat distortion temperature decreased inversely with the increase in ELO amount. In the study conducted with bioresin to which ELO was added at 5% increasing rates from 0% to 30%, the storage modulus, glass transition temperature and crosslink density showed a significant decrease with increasing amounts of ELO. In the former mentioned ELO study, izod impact strength did not alter with changing the amount of ELO added, whereas in the later mentioned study, izod impact strength raised remarkably with increasing the amount of ELO added. In both studies, no phase separation was detected from the morphological images. Di Mauro et al. (Di Mauro et al., 2020) compared the thermal, thermo-mechanical and mechanical performance of 11 different vegetable oils by determining ELO and ESO as the reference vegetable oil-based resins. Epoxidized perilla oil had the highest glass transition temperature of 91 °C, while epoxidized St John's wort oil and epoxidized karanja oil gave the lowest glass transition temperature of 17 °C. DSC (Differential Scanning Calorimetry Analysis) analyses also reveal that epoxidized perilla oil gives the highest enthalpy of reaction value. Epoxidized camelina oil gives the highest young modulus value of 830.6 MPa, while epoxidized grapeseed oil gives the highest fracture stress with 12.7 MPa. Also, epoxidized karanja oil gave the lowest young modulus value and the lowest fracture stress value. Epoxidized karanja oil was the type that exhibited the highest thermal stability because epoxidized vegetable oil resins with low epoxy content exhibited higher thermal stability, and increasing epoxy content decreased thermal stability. Moreover, epoxidized perilla oil is the type that exhibits the lowest thermal stability behavior. The fact that the obtained materials have a bio-based carbon content of more than 80%, can exhibit soft, plastic, hard and rigid properties depending on the type of oil they contain, and also have recyclable, reusable and repairable characteristics reflects that they can be functionally

preferred in various areas such as protective coatings, structural matrices and composites. In their study, Fahimian et al. (Fahimian et al., 2008) created bioresin using Acrylated Epoxidized Canola Oil (AECO) and Maleinized Acrylated Epoxidized Canola Oil (MAECO). They used hemp and flax fiber as pure and hybrid reinforcement elements. It was used as AECLO in the production of composites by mixing with epoxidized linseed oil and AECO. Storage modulus values in samples using polyester resin showed better results than the other two bioresins. Also, although the situation was similar in glass transition temperatures, samples using AECLO gave competitive results. Gerbase et al. (Gerbase et al., 2002) combined ESO with different anhydrides and studied their thermal characteristics. The results showed that decreasing the anhydride/epoxy ratio decreased T_g (glass transition temperature). When the effect of the epoxidation degree of soybean oil on mechanical characteristics and T_g was examined, it was found that the higher the amount of epoxy groups, the higher the T_g and hardness. Espinoza Perez et al. (Espinoza Pérez et al., 2009) prepared bio resins with soybean oil and canola oil and investigated the thermal and physical properties of these bio resins. Apparent viscosities were found to be between 140-152 mPas for ECO and 155-160.5 mPas for ESO. When the temperatures at which it started burning were examined, it was found that the temperature for the ECO sample was 8.2-8.7 C, while the temperature for the ESO sample was -27.3 C. While the enthalpy values of the ECO sample were 8.3-9.6 J/g, the values of the ESO sample were 12.8-15.3 J/g. They stated that the epoxidized canola oil they prepared offers a greener alternative to the production of petroleum-based resins for application in composite materials.

In literature studies, soybean oil is mainly used for bioresin material production. Vegetable oils such as castor oil, canola oil, linseed oil and rapeseed oil have also been used in many different applications. Different fiber types such as cotton, hemp, jute, and flax have also been preferred as reinforcement materials in biocomposite material production. Table 3.1 presents the different bioresin and biocomposite types obtained as a result of literature research.

Table 3.1. Different types of bioresin or biocomposites with vegetable oil

Fiber type	**Matrix**	**Vegetable oil**	**Tensile strength (MPa)**	**Young Modulus (MPa)**	**Tensile modulus (GPa)**	**Flexural strength**	**Impact energy(J)**	**References**
-	Epoxidized soybean oil	Soybean oil	15	-	-	-	-	(Tsujimoto et al., 2016)
	Epoxidized linseed oil	Linseed oil	40					
Jute	Wheat gluten using water	-	28.6-68.6	434-2928	-	10-4-20.2	-	(Reddy and Yang, 2011a)
	Polypropylene		31.3-35.2	495-500		10.6		
Kenaf	Epoxidized soybean oil+ Maleated soybean oil+ Hexamethylene diamine+ maleated methyl soyate	Soybean oil	2-12	-	-	-	-	(Tran et al., 2006)
Kayocell								
Protein grits								
Solka-floc								
Jute	Soy protein	-	49-64	558-4074	4.2-6.1	11.3-24.1	-	(Reddy and Yang, 2011b)

	Polypropylene		31.3-35.2	495-500	2.4-3.2	10.6		
Hemp	AESO	Soybean oil	51.2-84.2	-	1.79-2.92	66.3-116.6	15.84-25.12	(W. Liu et al., 2018)
-	ESO	Soybean oil	36-59	2434-3145	-	79-106	-	(Zhu et al., 2004)
	Epoxidized methyl soyate and		31-54	2621-2952		89-112		
	Epoxidized allyl soyate		41-60	2972-3193		70-107		
Keratin feather fibers	AESO	Soybean oil	-	-	-	34.807-57.791	-	(Hong and Wool, 2005)
Post-consumer denim fabric and jute	Epoxy	Soybean oil	30-55	450-810	-	58-90	-	(Temmink et al., 2018)
	AESO		12-36	100-420		20-42	-	
	Polyester		18-20	200-500		32-41	-	
-	Epoxy	Linseed oil+ Castor oil	49.04	-	1841.41	-	-	(Sahoo et al., 2018a)
	ELO		5.25		53.58			
	ECO		0.258		1.49			

-	Epoxy ELO	Linseed oil	55.05 20.3-42.29	-	1379.5 709.12-1270.04		66.4 72.7-95.05	(Sahoo et al., 2018b)
-	Epoxy ESO	Soybean oil	47.77-77.61	2.22-2.66	-	78.23-94.87	-	(Peter Niedermann et al., 2014)
	ESO Tri glycidyl ether of glycerol Tetra glycidyl ether of pentaerythritol Diglycidyl ether of bisphenol A	Soybean oil	70.89 96.73 93.68 100.42	7280 9070 9190 9220	-	92.28 129.71 120.82 131.66	-	(Péter Niedermann et al., 2017)
-	AESO	Soybean oil	0.6-1.0	2.0-4.4	-	-	-	(Wang et al., 2016)
Hemp+ Glass	Vinylester Soy based resin	-	15-170 10-140	-	7-15 8-11	-	-	(Flanigan et al., 2006)
-	ESO ELO Triolein (ETO)	Soybean oil +Linseed oil+ High oleic algal oil	3.3 14 1.9	34 350 35	-	-	-	(Radojčić et al., 2022)

-	Vinylester AESO	Soybean oil	-	-	-	123 15-112	-	(Grishchuk and Karger-Kocsis, 2011)
-	Styrene and DVB	Olive, peanut, sesame, canola, corn, soybean, grapeseed, sunflower, low saturation soy, safflower, walnut and linseed oils	1-2-10.9	13-125.6	-	-	-	(Andjelkovic et al., 2005)
Kenaf	AESO Styrene	Soybean oil	60 105	-	4000 4500	85 130	-	(Wu and Li, 2016)

4. MATERIAL AND METHOD

4.1. Material

4.1.1. Flax/Jute Fabric

In the study, upholstery flax/jute fabric was selected as the reinforcement element. The flax/jute fabric seen in Figure 4.1 is woven from first quality jute and flax yarn with a weight of 265 g per meter square (m^2). This fabric, used for upholstery and decorative purposes, was supplied by kumascı.com company in Istanbul. Both flax and jute fabrics are natural fibers and stand out in terms of being both cost-effective and environmentally friendly. Weaving the two fabrics together with an intraply weave strengthens the relatively low mechanical properties of jute and also creates a natural, recyclable and sustainable product. With this fabric type used, it will contribute to the biocomposite production targeted in the study. Table 4.1 indicates the flax/jute fabric properties.

Figure 4.1. The cutting pieces of flax/jute fabric

Table 4.1. Fabric properties (Karaçor and Ozcanli, in press)

Fabric	Thickness (mm)	Density (g/cm^3)	Tensile strength (MPa)	Elastic modulus (GPa)	Elongation at failure (%)
Flax/Jute	0.7	1.3-1.5	320-2000	27.6-103	1-3.3

4.1.2. Epoxy and Hardener

Epoxy resins are resins containing a wide variety of polymer networks characterized by the presence of more than one 1,2-epoxy group per molecule (Ernault et al., 2017; Unnikrishnan and Thachil, 2006). There are many types of epoxy resins used, the non-epoxy part of the molecule can be aliphatic, cyclo-aliphatic or aromatic hydrocarbon, as well as non-hydrocarbon and polar. Epoxy resins can be cured by a wide variety of curing agents through curing reactions, and their characteristics vary depending on the particular combination of epoxy resins and curing agents used.

Epoxy resins are used functionally in many different areas today as fiber-reinforced materials, general-purpose adhesives, high-performance coatings and encapsulation materials due to their superior mechanical properties, high adhesion to many surfaces, and good heat and chemical resistance (Jin et al., 2015; Unnikrishnan and Thachil, 2006). Epoxy resins are generally cured by adding 1 or 2 times more hardener to the resin-hardener ratio, unlike polyester or vinyl ester resins, which are catalyzed by adding a small amount of catalyst to the resin, such as 1-3%. Similar to other thermoset resins, cured epoxy resins may have inherently low impact strength, low fracture toughness, lack of shape retention after cure/polymerization, and reduced resistance to crack initiation and propagation. The advantages and limitations of epoxy resins can be determined by the degree of intensity of pre-crosslinking curing kinetics and chemical compositions, by the chemical structure of the resin and hardener, and by the network obtained after curing (Saba et al.,2016).

In the study, L160 epoxy resin and H160 hardener was used. They were purchased from Kompozitshop company, which is located in Istanbul. It has been stated that lamination epoxy resin is used in advanced composite part manufacturing, marine, defense, space, sports equipment, automotive, aviation sectors and wind turbines. The manufacturer states that the resin has a very high level of compatibility, very good mechanical and thermal properties and a working time of 45 minutes to 4-5 hours. Table 4.2 displays the epoxy and hardener characteristics.

Table 4.2. Epoxy and hardener characteristics (Kompozitshop,2024)

	HEXION MGS Lamination Epoxy resin L160	**HEXION MGS Lamination Epoxy hardener H160**
Viscosity (mPas)	700-900	10-50
Refractor index	1.548-1.553	1.520-1.521
Amine value (mgr KOH/g)	-	550-650
Density (g/cm³)	1.13-1.17	0.96-1.00
Operating temperature	-60 °C / +80 °C with heat treatment -60 °C / +50 °C without heat treatment	-
Process temperature	+10 °C / +50 °C	-
Measurement conditions	25 °C	25 °C

4.1.3. Vegetable Oils

In this study, the aim was to obtain bioresin using vegetable oils such as soybean oil, palm oil, rapeseed (canola) oil, cottonseed oil and flax oil. Each type of oil was added to the epoxy at 10%, 20%, 30%, and 40% by weight to form bioresin. Cottonseed oil was supplied by a group called Toroslar in Istanbul, palm oil was supplied by a company called Kimyacınız in Istanbul, canola oil,

linseed oil and soybean oil were supplied by a company called TOS organic spices in Antalya. Figure 4.2 indicates the used vegetable oils.

Figure 4.2. Vegetable oil used in this study

Cottonseed oils

Cotton seeds are seeds used both as animal feed and as edible oil and lubricant. The second largest producer of cotton seeds in the world is India, which is also known as an agricultural country. It is stated that cottonseed oil is preferred in India as a cost-effective and useful oil type during resin production in surface coating applications. The ratio of saturated (26-35%) fatty acids to unsaturated (65-75%) fatty acids in cottonseed oil is 1:2. Cottonseed oil containing double bonds and ester bonds is becoming a potential raw material for the production of vegetable oil-based resins. With this high degree of unsaturation in cottonseed oil, it can produce different solutions in terms of chemical transformation for the production of polyurethanes with various properties. Although cotton is grown primarily for cotton fiber production, it is also the world's sixth largest source of vegetable oil. A relatively small amount of the oil produced is used in the formulation of cosmetics and other industrial uses, including the manufacture of pesticides, explosives and rubber (Karacor and Ozcanli, 2024).

Canola oils

Canada is the world's second largest producer and largest exporter of canola oil. The presence of approximately 60% oleic acid in canola oil puts this oil in the first position for epoxidation among others. With the amount of oleic acid it contains, canola oil reflects a difference in terms of fatty acid profile compared to the content of polyunsaturated linoleic acid found in soybean oil (53%). Another notable difference between these oils is the lower saturated fatty acid content in canola oil (6%) than in soybean oil (15%), which is reflected in both the levels of unsaturation and saturation characteristic of canola oil-based resins. This fatty acid form of canola oil is why it is suitable for use with epoxy

resins, since saturated fatty acids cannot be epoxidized and therefore cannot accompany the formation of polymers (Karacor and Ozcanli, 2024).

Flaxseed oils

Natural oils obtained from agricultural sources have the potential to provide useful raw materials for polymer synthesis. Unsaturated fatty acids such as flaxseed oil are commonly used in coatings and printing inks, and epoxidized oils are used as reinforcements in thermoplastics to increase flexibility and stability. Among non-edible oils, the distinctive structure of flaxseed oil makes it a priority in reducing the inherent brittleness of epoxy. Flaxseed oil is known as a drying oil due to its high iodine values. The high iodine value in the oil is a degree of the high number of double bonds in the oil. This gives flaxseed oil a good chemical reaction opportunity with many double C bonds. It also allows the use of this oil with higher performance bio-based or sustainable polymers with highly unsaturated or reactive sites. Flaxseed oil is also utilized for its drying properties in commercial applications such as varnishes, oil-based paints, linoleum, putty, etc. Epoxidized flaxseed oil is commonly used as a plasticizer in epoxy resins, polyvinyl chlorides for flexibility, and in coatings and adhesive applications (Karacor and Ozcanli, 2024).

Palm oils

Palm oil is a commodity of particular importance in the Asia-Pacific region, with Malaysia and Indonesia being the main producers. Apart from these countries, Thailand also has the capacity to produce large quantities of palm oil for both domestic consumption and export. In addition, palm trees are the species that provide the highest vegetable oil yield at affordable costs, with a production of 3.8 tons per hectare per year, compared to castor oil and coconut production sources. Palm oil can be used as a reinforcement in polyester resins by providing porous surface morphology, toughness, hardness and better mechanical bonding in composite production. Palm oil biomass is also increasingly prominent due to its availability in some tropical countries and its demand in composite industries. Apart from food, the use of palm oil products in pharmaceutical products, soap and detergent production and cosmetic products is increasing. Palm oil is seen as a promising potential as a renewable raw material that can be used instead of industrial chemicals. Palm oil-based products in coatings that can be cured under ultraviolet light mostly contain epoxidized palm oil (Karacor and Ozcanli, 2024).

Soybean oils

Soybean oil is considered the most attractive type of vegetable oil because it is very affordable and abundant. Soybean oil differs from other vegetable oils as an effective reactive thinner or hardener by its different composition and oxidation process as given in Table 4.3. Soybean oil is

a type of vegetable oil consisting of triglyceride molecules derived from unsaturated acids. Unsaturated acids need to be functionalized by adding epoxy, carboxyl or hydroxyl groups to be used in the formation of polymeric materials. For paints and coatings, they have double bonds that are reactive sites. Resins and plastics are important areas where industrial soybean oil is used. With modifications that facilitate the polymerization of soybean oil, solid films and composite materials used in infrastructure, aviation, military, automotive, marine, sports and industrial areas can be manufactured (Karacor and Ozcanli, 2024). Table 4.3 reflects the chemical compositions of the vegetable oils in the study. The characteristic properties of the oils used are given in Table 4.4.

Table 4.3. Chemical compositions of used vegetable oils (Karacor and Ozcanli, 2024)

Natural oils	**Fatty acids (%)**						
	Linoleic	**Stearic**	**Palmitic**	**Oleic**	**Linolenic**	**Gadoleic**	**Arachidic**
Cottonseed oil	54.4	2.6	21.6	18.6	0.7	0.12	0.21
Canola oil	18.4	2.0	4.3	4.3	7.2	1.1	0.6
Flaxseed oil	15.3	3.5	5.5	19.1	56.6	0.12	0.5
Palm oil	10.1	4.2	42.8	40.5	-	-	-
Soybean oil	53.3	4.0	11.0	23.4	7.8	0.37	0.5

Table 4.4. Characteristics of used vegetable oils (Karak, 2012; Y. Lu and Larock, 2009; Petrović, 2010)

	Density (g/cm^3)	**Iodine value (mg/100 g)**	**Viscosity (mm^2/s)**
Cottonseed oil	0.93	90-119	40
Canola oil	0.917	110-126	35.14
Flaxseed oil	0.932	>177	53
Palm oil	0.893	50-55	40.19
Soybean oil	0.924	123-139	42

Table 4.5 shows the code names given for the produced biocomposite materials. In the study, epoxy resin was considered as a fixed sample and the proportions of other five different oils were increased from 10% to 40% to form bioresin.

Table 4.5. Code names of produced biocomposite samples

Code names	Explanation of codes
EPOXY	Sample with only epoxy resin without any oil
ECO10	Bio resin sample containing epoxy and cottonseed oil at 10% of epoxy weight
ECO20	Bio resin sample containing epoxy and cottonseed oil at 20% of epoxy weight
ECO30	Bio resin sample containing epoxy and cottonseed oil at 30% of epoxy weight
ECO40	Bio resin sample containing epoxy and cottonseed oil at 40% of epoxy weight
ECAO10	Bio resin sample containing epoxy and canola oil at 10% of epoxy weight
ECAO20	Bio resin sample containing epoxy and canola oil at 20% of epoxy weight
ECAO30	Bio resin sample containing epoxy and canola oil at 30% of epoxy weight
ECAO40	Bio resin sample containing epoxy and canola oil at 40% of epoxy weight
EFO10	Bio resin sample containing epoxy and flaxseed oil at 10% of epoxy weight
EFO20	Bio resin sample containing epoxy and flaxseed oil at 20% of epoxy weight
EFO30	Bio resin sample containing epoxy and flaxseed oil at 30% of epoxy weight
EFO40	Bio resin sample containing epoxy and flaxseed oil at 40% of epoxy weight
EPO10	Bio resin sample containing epoxy and palm oil at 10% of epoxy weight
EPO20	Bio resin sample containing epoxy and palm oil at 20% of epoxy weight
EPO30	Bio resin sample containing epoxy and palm oil at 30% of epoxy weight
EPO40	Bio resin sample containing epoxy and palm oil at 40% of epoxy weight
ESO10	Bio resin sample containing epoxy and soybean oil at 10% of epoxy weight
ESO20	Bio resin sample containing epoxy and soybean oil at 20% of epoxy weight
ESO30	Bio resin sample containing epoxy and soybean oil at 30% of epoxy weight
ESO40	Bio resin sample containing epoxy and soybean oil at 40% of epoxy weight

4.2. Method

Intraply jute/flax fabrics were cut according to the dimensions of each test sample and prepared for composite material production. Figure 4.3 indicates the fabric samples cut according to standard test sizes. The cutting of fabrics and biocomposite material production processes were carried out in the Materials Laboratory of Çukurova University Automotive Engineering Department.

Figure 4.3. Flax/jute fabrics cut according to test standards

Vacuum assisted resin transfer molding method (VARTM) was used as the production method. Vacuum nylon, vacuum sealing tape, peeling fabric, infusion net and vacuum hoses required for the production of composite materials were also supplied and made ready for production. Figure 4.4 displays the required equipments for composite production.

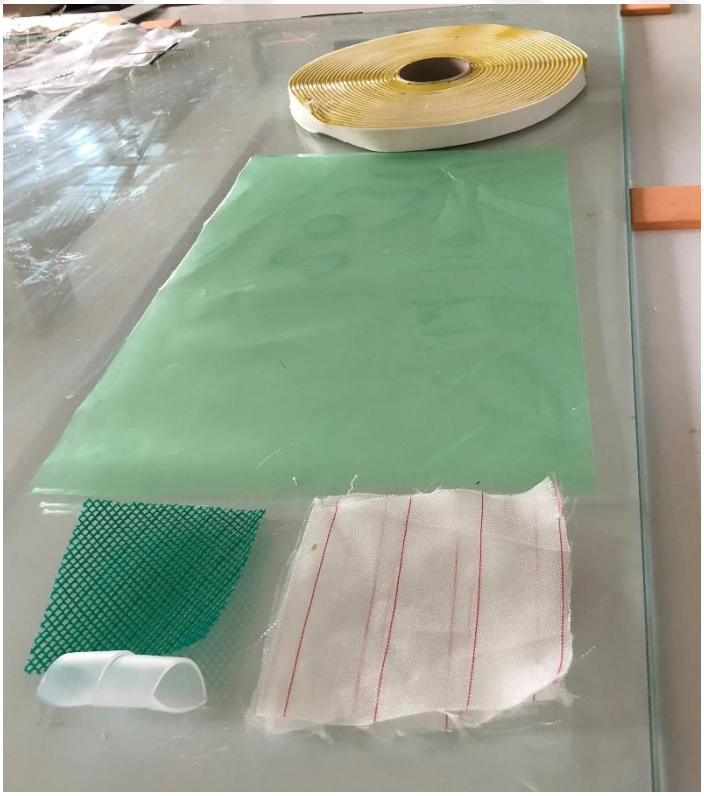

Figure 4.4. Required equipments for VARTM method

Bio composite samples were produced by adding 10%, 20%, 30% and 40% vegetable oil by weight to the epoxy resin. In hardener, 25% by weight of epoxy was added to the mixture as specified by the supplier company. In the production of biocomposite materials, bioresin production was primarily carried out. For this, the preparation of the epoxy resin and vegetable oil mixture was carried out in the Çukurova University Automotive Engineering Department Laboratories. As shown in Figure 4.5, the epoxy resin was placed in the glass container in a predetermined amount. Then, vegetable oil was added to the resin according to the oil percentages given in Figure 4.6 and Table 4.5. Figure 4.7 represents the first mixture of vegetable oil and resin. To mix the vegetable oil and epoxy resin, they were placed in a magnetic stirrer and the mixing process was continued with 750 rpm for 4 hours until they were mixed homogeneously. Figure 4.8 indicates the first version placed on the magnetic stirrer, and Figure 4.9 shows the images taken while the mixing process was continuing. Figure 4.10 indicates the schematic view of bioresin preparing and integration of the system.

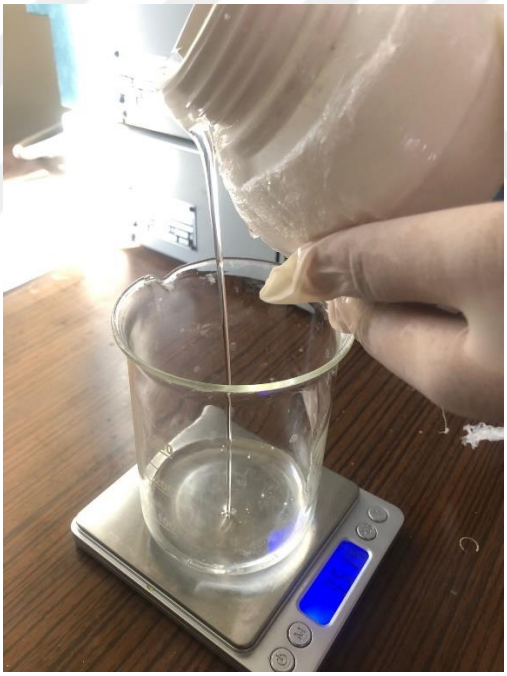

Figure 4.5. Epoxy resin preparation

Figure 4.6. Vegetable oil addition to epoxy

Figure 4.7. Mixture of vegetable oil and resin

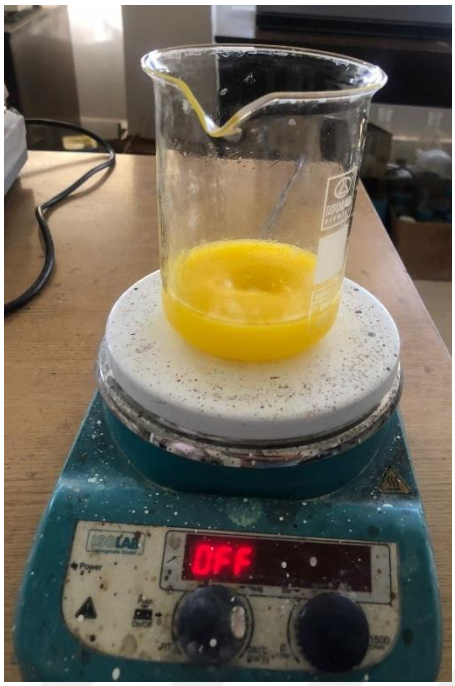

Figure 4.8. Before mixing

Figure 4.9. Mixing process

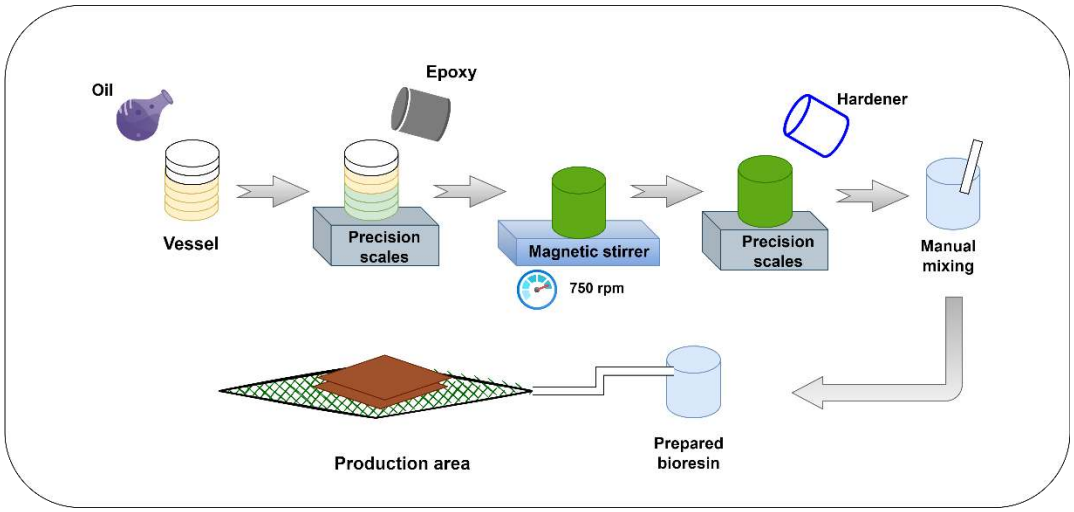

Figure 4.10. Preparation bioresin and integration to system

Figure 4.11 to Figure 4.17 represent the preparation stages for material production. First, after the surface to be produced was cleaned, the area to be produced was determined with vacuum sealing tapes as shown in Figure 4.11. Then, mold release wax was applied to the surface as shown in Figure 4.12, which allows the part to be easily separated from the surface after production. Inlet and out vacuum hoses were attached to system.

Figure 4.11. Specified area for production

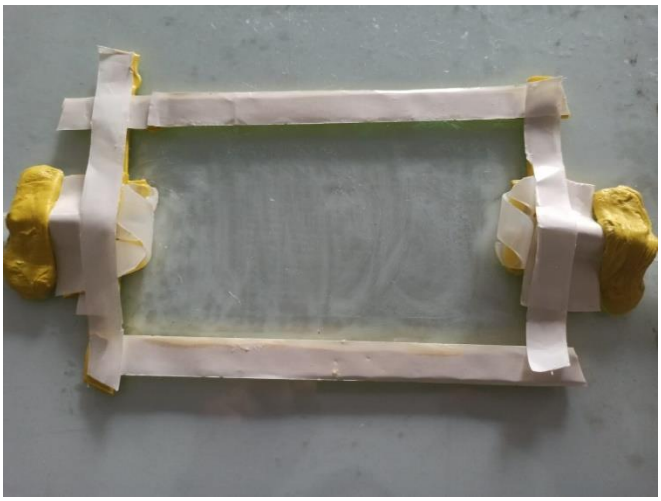

Figure 4.12. Release wax applied surface

As seen in Figure 4.13, a predetermined number of fabric samples for which test will be produced were arranged in the production area. After that, first peel ply was laid on the fabric as in Figure 4.14, then infusion mesh was laid on the fabric as in Figure 4.15.

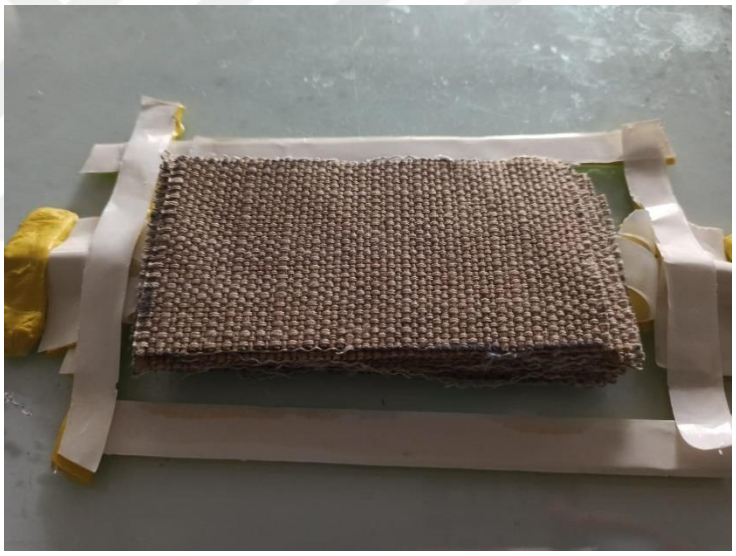

Figure 4.13. Fabrics laid

Figure 4.14. Peel ply addition

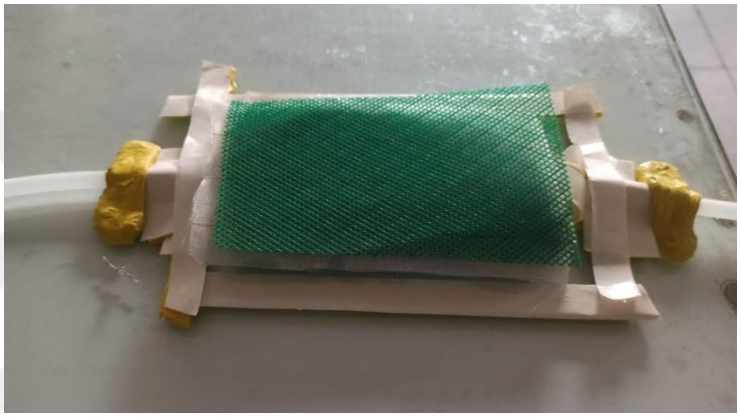

Figure 4.15. Infusion mesh laid

Finally, air tightness of the sample was ensured by laying vacuum nylon as shown in Figure 4.16. As seen in Figure 4.17, air tightness control of the system was carried out by operating the vacuum pump. The prepared bioresin was integrated into the system with the help of vacuum force. The inlet hose was kept open until the resin was absorbed by the entire sample. When absorption was completed, the inlet hose was closed and the excess resin was collected in a container to exit the system. The sample was left in this state for approximately 2 hours with the vacuum pump running at 1 atm pressure. When the excess resin flow ended after 2 hours, the vacuum pump was turned off and the sample was left to cure. The schematic representation of the production method is given in Figure 4.18. After 24 hours, the part was removed from the surface and placed in the drying oven as shown in Figure 4.19.

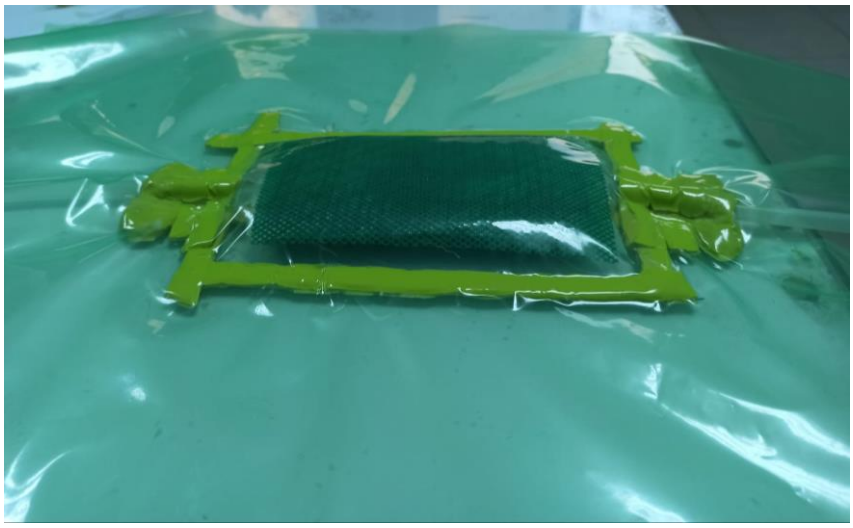

Figure 4.16. System attached with vacuum nylon

Figure 4.17. Sample under vacuum force

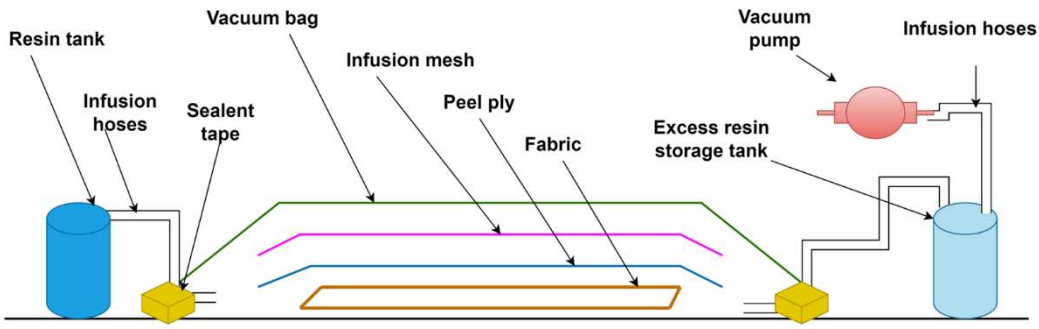

Figure 4.18. Schematic view of production method (Karaçor et al., 2024)

Figure 4.19. Sample placed in drying oven

Samples subjected to post-curing at 60 °C for 1 hour are made ready for tests. Figure 4.20 displays the samples for the hardness test, Figure 4.21 exhibits the samples for the water absorption test, Figure 4.22 presents the samples for the 3-point bending test, Figure 4.23 shows the samples for the Charpy impact test, and Figure 4.24 demonstrates the samples prepared for the tensile test.

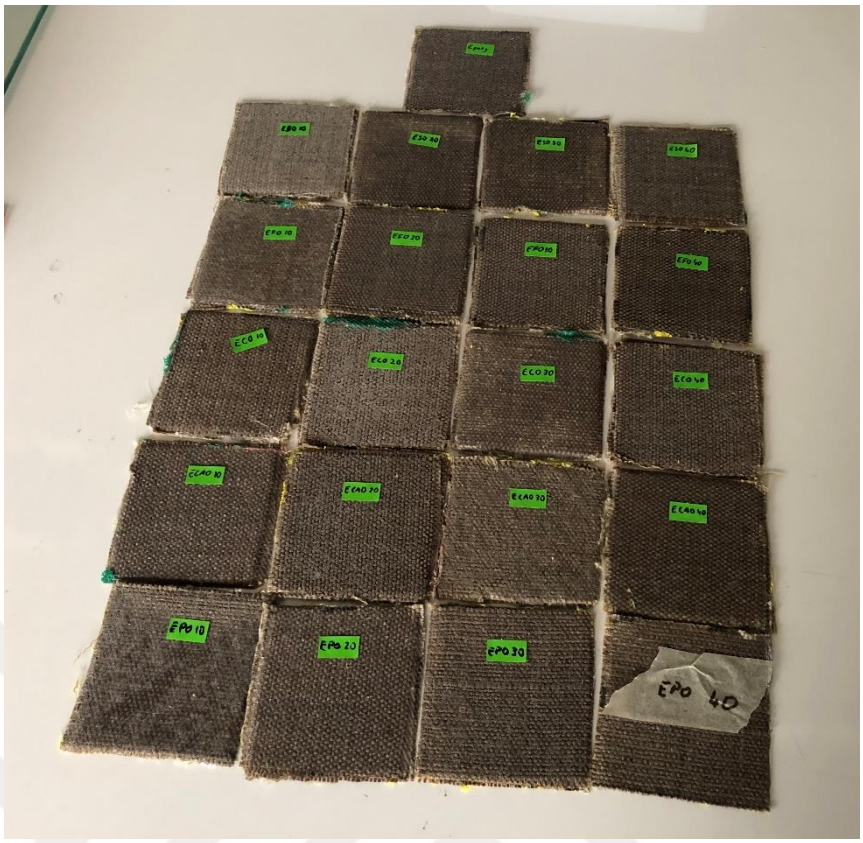

Figure 4.20. Hardness test samples

Figure 4.21. Water absorption test samples

Figure 4.22. Flexural test samples

Figure 4.23. Impact test samples

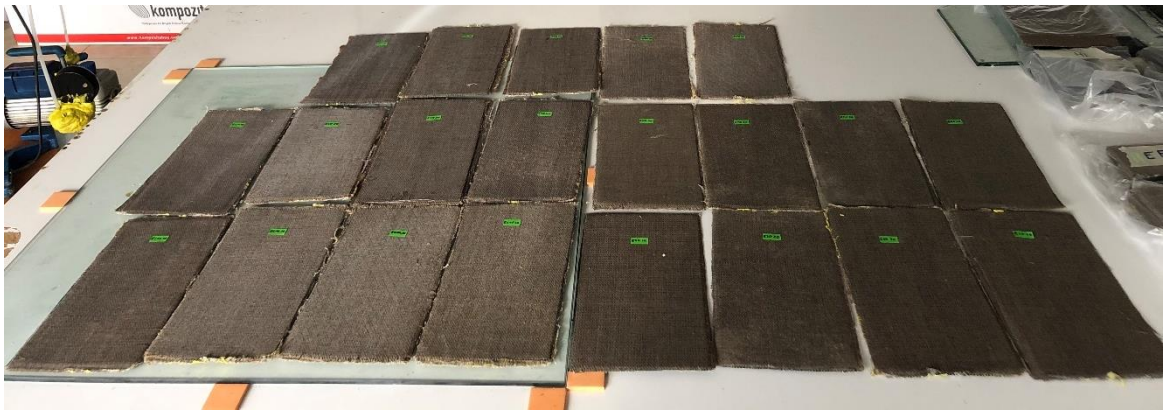

Figure 4.24. Tensile test samples

4.2.1. Specimen Cutting

As seen in Figures 4.22 to 4.24, the produced biocomposite samples must be cut according to standard test dimensions for testing. A laser cutting machine was used for this cutting process as seen in Figure 4.25.

Figure 4.25. Laser cutting machine

The flexural test mold sample dimensions seen in Figure 4.22 are 135 mm x 100 mm x 3.5 mm, while the Charpy impact test molds seen in Figure 4.23 are 135 mm x 72.5 mm x 100 mm. The tensile test mold sample dimensions shown in Figure 4.24 are 275 mm x 135 mmx 2.5 mm.

4.2.2. Weight and Volume Fractions

Volume

$$V_f = \frac{v_f}{v_c} \tag{4.1}$$

$$V_m = \frac{v_m}{v_c} \tag{4.2}$$

$$V_f + V_m = 1 \tag{4.3}$$

$$v_f + v_m = v_c \tag{4.4}$$

Weight

$$W_f = \frac{w_f}{w_c} \tag{4.5}$$

$$W_m = \frac{w_m}{w_c} \tag{4.6}$$

$$W_f + W_m = 1 \tag{4.7}$$

$$w_f = \rho_f v_f \tag{4.8}$$

$$w_m = \rho_m v_m \tag{4.9}$$

$$w_c = \rho_c v_c \tag{4.10}$$

$$w_f + w_m = w_c \tag{4.11}$$

Density

$$\rho_c v_c = \rho_f v_f + \rho_m v_m \tag{4.12}$$

$$\rho_c = \rho_f \frac{v_f}{v_c} + \rho_m \frac{v_m}{v_c} \tag{4.13}$$

$$\rho_c v_c = \rho_f V_f + \rho_m V_m \tag{4.14}$$

$$v_c = v_f + v_m \tag{4.15}$$

$$\frac{1}{\rho_c} = \frac{w_f}{\rho_f} + \frac{w_m}{\rho_m} \tag{4.16}$$

Void

$$V_v = \frac{v_v}{v_c} \tag{4.17}$$

Total volume of composite with void

$$v_c = v_f + v_m + v_v \tag{4.18}$$

Experimental density (ρ_{exp}) of composite

$$v_c = \frac{w_c}{\rho_{exp}} \tag{4.19}$$

Theoretical density (ρ_{theo}) of composite

$$v_f + v_m = \frac{w_c}{\rho_{theo}} \tag{4.20}$$

$$\frac{w_c}{\rho_{exp}} = \frac{w_c}{\rho_{theo}} + v_v \tag{4.21}$$

$$v_v = \frac{w_c}{\rho_{exp}} \left[\frac{\rho_{theo} - \rho_{exp}}{\rho_{theo}}\right] \tag{4.22}$$

The equations from 4.1 to 4.22 were modified from the book Mechanics of Composite Materials written by Autar K. Kaw (Kaw, 2006).

where,

w_f, w_m, w_c indicate weights of fiber, matrix, composite, respectively,

v_f, v_m, v_v indicate volumes of fiber, matrix, composite, respectively,

W_f, W_m indicate weight fractions of fiber rand matrix, respectively,

V_f, V_m indicate volume fractions of fiber rand matrix, respectively.

4.3. Tensile Test

Tensile testing is known as an important mechanical test used to determine the tensile characteristics of materials. With tensile testing, mechanical characteristics such as young modulus, tensile strength, elastic modulus and poisson ratio of the tested materials are obtained (Karaçor et al., 2023). After preparing the biocomposite sample molds for the tensile test, cuts were made on the laser cutting machine with 250 mm length, 25 mm width and 2.5 mm thickness in accordance with the dimensions specified in the ASTM D3039 standard (ASTM D3039/D3039-M, 2000). Technical drawings of sample dimensions are given in Figure 4.26. Five samples were cut from a mold and 5 samples were tested for each combination and the data obtained from these samples were averaged. Tensile test was performed with ALŞA hydraulic testing device in Koluman Automotive Industry Quality Laboratory. A photograph of the test device is presented in Figure 4.27. The load capacity of the device is 60 tons and tests were carried out at 2 mm/min cross head speed as specified in the ASTM standard. Sample dimensions were recorded in the interface program connected to the device before the test started, and the tests were carried out at room temperature (Karaçor et al., 2024). When the device completed the test, the data obtained as a result of the test was recorded graphically in the computer program and the data was obtained. In the samples prepared for tensile testing, flax/jute fabrics were laid in 4 layers. This resulted in a tolerance of 2.5 ± 0.25 mm for the samples produced with the VARTM method.

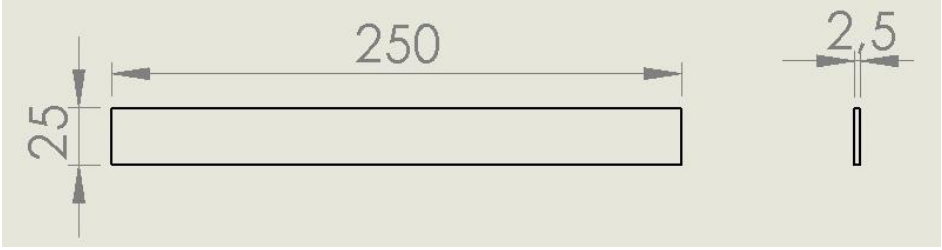

Figure 4.26. Technical drawing of produced tensile test samples (dimensions in mm)

Figure 4.27. Tensile test machine

4.4. Flexural Test

The bending tests were carried out at Dokuz Eylül University Engineering Laboratories according to ASTM D790 standards using the Instron 5985 250 kN testing machine given in Figure 4.28. As a result of the bending test, the bending stress that the materials show against the bending force, the bending modulus and the maximum force that the material will withstand until it breaks are obtained. Depending on the dimensions recommended for the bending properties of biocomposite materials produced according to the ASTM standard, samples of 125 mm length, 20 mm width and 3.5 mm thickness were obtained from the cutting process and tested (ASTM D790-03, 2003). Technical drawings of the flexural test samples are given in Figure 4.29. In the tests, each specimen was supported in a fixture with a span length of 112 mm such that the span-to-thickness ratio equaled 32:1 depending on the specimen thickness (Karacor and Ozcanli, 2023a).

Figure 4.28. Flexural test machine

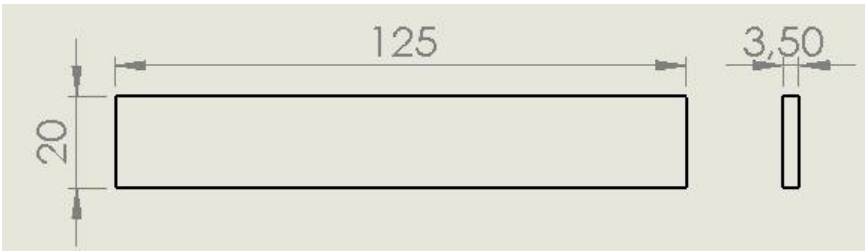

Figure 4.29. Technical drawing of flexural test samples (dimensions in mm)

The test was started by setting the machine speed to 5.9 mm/min. The test speed there was calculated according to the formulas given in 4.23 and 4.24 of the ASTM standards.

$$R = \frac{ZL^2}{6d} \tag{4.23}$$

$$D = \frac{rL^2}{6d} \tag{4.24}$$

Where R is the rate of crosshead motion, Z indicates rate of straining of the outer fiber and Z will be equal to 0.01, L shows support span length, d displays the depth of the material. Also, D is

the midspan deflection of material and r is the strain and the stress value can be calculated by setting r equal to 0.05 (ASTM D790-03, 2003).

The tests were carried out at room temperature. When the device completed the test, the data obtained the data obtained from the 5 samples as a result of the test were recorded graphically in the computer program and the data was created. In the samples prepared for the bending test, flax/jute fabrics were prepared in 5 layers. This resulted in a tolerance of 3.5 ± 0.3 mm in the samples produced for the test.

4.5. Impact Test

Impact testing is a test used to evaluate the toughness, brittleness, notch sensitivity and impact resistance of materials under sudden loading. The Charpy impact test measures the amount of energy absorbed by a sample under impact load. In addition, the impact resistance of the materials is determined as in the comparative impact strength equation 4.25.

$$Impact\ strength = \frac{E}{A} \tag{4.25}$$

where E displays the energy absorbed (J) and A shows the area (mm^2) which is calculated by multiplying the thickness and the width of the specimen (Çelik et al., 2023).

Charpy impact test was performed in accordance with ASTM D-6110 standard in Çukurova University Ceyhan Faculty of Engineering Laboratories. The visual of the test device is presented in Figure 4.30. The produced samples were tested by cutting them into 125 mm length, 12.5 mm width and 10 mm thickness according to the test standard (ASTM D6110-10, 2010). Technical drawings of the samples are given in Figure 4.31. Five samples were tested for each configuration and the results were recorded. In the samples prepared for the impact test, flax/jute fabrics were prepared and laid in 14 layers. The samples produced for this test were produced with a tolerance of 10 ± 0.2 mm.

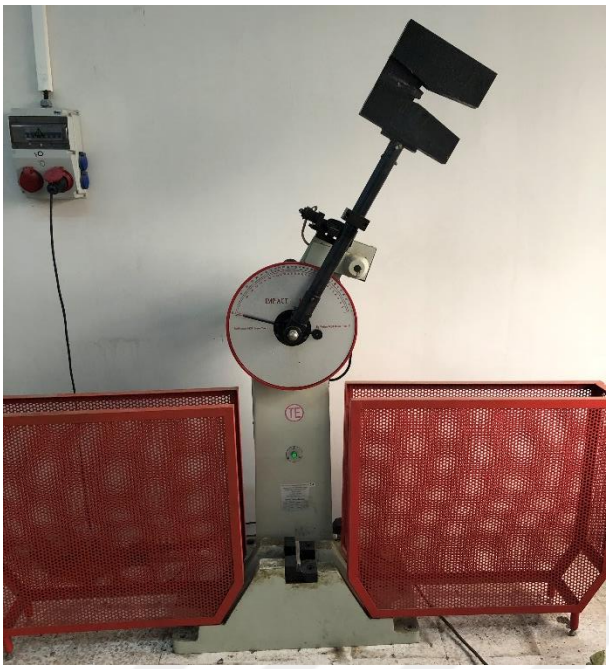

Figure 4.30. Charpy impact test machine

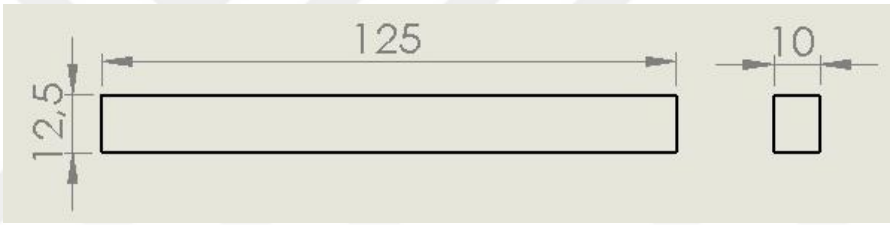

Figure 4.31. Technical drawing of Charpy impact test samples (dimensions in mm)

4.6. Hardness Test

The microhardness values of the produced composite samples were obtained by the Vickers hardness test. In the field of materials, hardness is defined as the resistance to permanent deformations depending on the bond strength of the atoms within the material. As a result of the force applied to the material, an indentation occurs in the material. This indentation varies according to the hardness method and measuring tip used, but in the Vickers hardness test, it is the shape of a 136° square diamond pyramid tip. The appearance of this indentation is approximately similar to the shape of a regular diamond slice (Çelik et al., 2023; Karacor and Ozcanli, 2022b). Hardness test was carried out at Çukurova University Faculty of Engineering Automotive Engineering Laboratory in AOB Lab product machine in accordance with ASTM E92-17 standard (ASTM E92-17, 2017). The sample dimensions were subjected to a hardness test as 70 mm x 70 mm x 1.5 mm. 15 hardness measurements were made on the prepared samples in each configuration and the average of these 15 values was written as the Vickers hardness value of the produced composites. 0.2 kgf was selected as the force applied on the sample. Figure 4.32 indicates the view of Vickers hardness test machine. In the samples prepared for the hardness test, flax/jute fabrics were prepared in 2 layers and the

spreading process was carried out. The samples produced for this test were produced with a tolerance of 1.5 ± 0.1 mm.

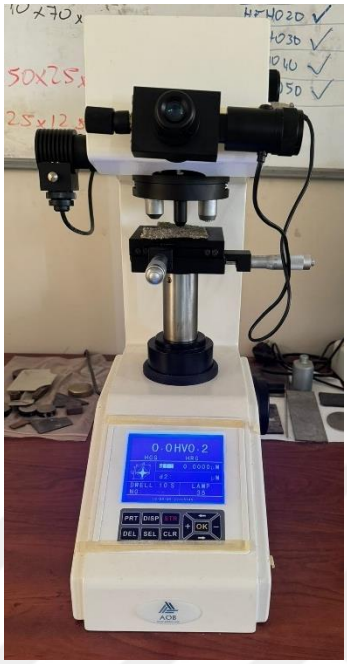

Figure 4.32. Vickers hardness test machine

4.7. Water Absorption Analysis

The purpose of water absorption analysis is to measure the water absorption capacity of the produced samples in water, taking into account ASTM D-5229 standards (ASTM International D5229, 2004). Water absorption test was carried out in Çukurova University Faculty of Engineering Automotive Engineering Laboratory (CUMERLAB). By observing the water absorption capacity of the samples in a certain period of time with the water absorption test, the water resistance capacity of the produced samples will be measured and learned (Karacor and Ozcanli, 2022b). For the water absorption test, the samples were produced with 100 mm length, 100 mm width and 2 mm thickness and made ready for the test. The 21 composite samples produced were subjected to water absorption test in water as in Figure 4.33 during their stay in the container. First, the dry weights of the products produced were measured on a digital scale as in Figure 4.34, then the samples were left in water for 336 hours. The samples were weighed at regular intervals and the amount of absorbed water was noted periodically. In the samples prepared for the water absorption test, flax/jute fabrics were laid in 3 layers and the samples were prepared. The samples produced for this test were produced with a tolerance of 2 ± 0.2 mm. The tests were carried out at room temperature. Tap water was used in the containers where the samples were placed. The reason for choosing tap water is that there are studies using tap water in the literature and these studies give results close to the real results.

Figure 4.33. Samples in water

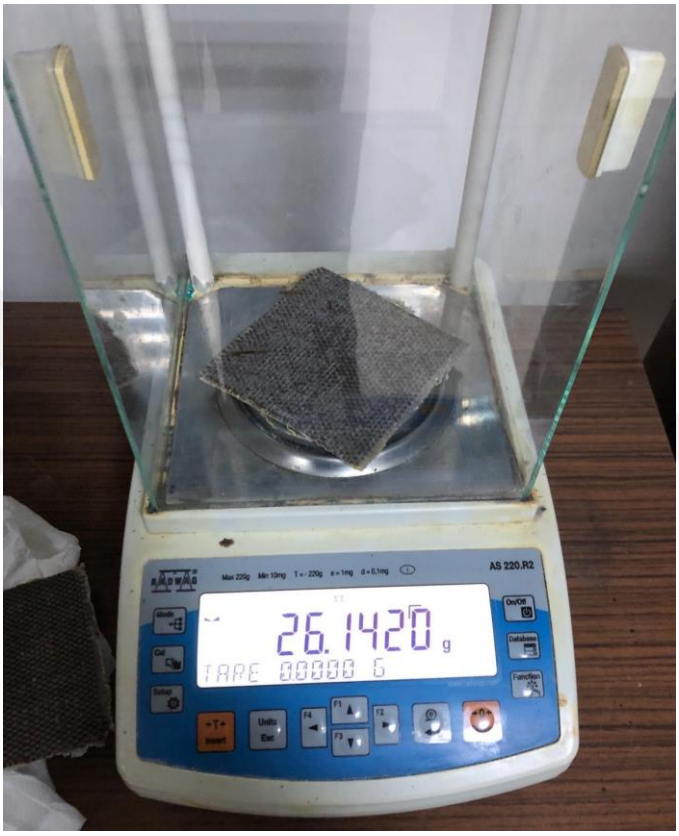

Figure 4.34. Samples weighed on digital scales

4.8. Thermogravimetric Analysis (TGA)

Thermal characteristics of biocomposite structures were determined by TGA and DSC analysis. TGA analyses were carried out at CUMERLAB. Thermal analysis, which is an ideal analytical method for a good understanding of the industrial production technology of different polymeric materials, is a guide in explaining the structure-property relationship and molecular design, especially when fiber-reinforced composites are considered. It also provides important data for determining the thermal stability of the material. With TGA analysis, the temperature at which the sample first begins to decompose and the temperatures until thermal equilibrium is reached are

determined (Karacor and Ozcanli, 2022a; Karacor and Ozcanli, 2020). In addition, the weight of the material before and after the test is learned and how much resistance the material has to heat is measured. TGA was performed with the Mettler Toledo TGA 3+ instrument at CUMERLAB. Figure 4.35 shows the visual of the TGA analyzer. Biocomposite samples were cut to fit into the instrument as shown in Figure 4.36 and their weights were recorded between 8.38 and 27.45 mg before being placed into the instrument. Then, the sample containers were placed into the instrument and the experiment was started. The samples were subjected to heating from 25 °C to 800 °C at a heating rate of 10 °C per minute in nitrogen atmosphere. When the test was completed, the data of the samples were recorded in the computer environment and the data were collected.

Figure 4.35. TGA analysis device

Figure 4.36. Samples prepared for TGA and DSC

4.9. Differential Scanning Calorimetry Analysis (DSC)

DSC analyses, like TGA analysis, were carried out at CUMERLAB. DSC is a thermal analysis method used to record the temperature required to create a zero-temperature difference between a material and a reference material when subjected to the same temperature conditions at controlled temperature or in a cooled environment. Heat flow provides information about the thermal characteristics of the material by recording the amount of energy absorbed or released during a particular physical or chemical transformation, such as glass transition, melting or crystallization

temperatures. DSC's ability to measure the heat flow rate in a thermal event as a function of time and temperature allows numerical data on melting and phase transitions in a composite system to be obtained in this way. DSC analysis first begins with the preparation of aluminum crucibles with lids (Karacor and Ozcanli, 2022a; Karacor and Ozcanli, 2020). As in Figure 4.36, the cut pieces are weighed with a precision scale and the sample weights between 14-22 mg are recorded. Then, the pieces are placed in the aluminum crucible with tweezers and the lid is placed on it. The sample pieces are closed in these small containers using a crucible press. The samples are then placed in the DSC device. The analysis was performed under standard conditions in a dynamic case on the Mettler Toledo DSC 3+ instrument at CUMERLAB as shown in Figure 4.37, which also gives the amount of energy absorbed or released when cooling and heating the material, while keeping the material at a constant isothermal temperature. Analyses were performed using the following standard procedures. Composite products weighing approximately 14-22 mg were heated from 20°C to 500°C at a heating rate of 10°C/min. The data obtained were then recorded on the computer and the results were graphed.

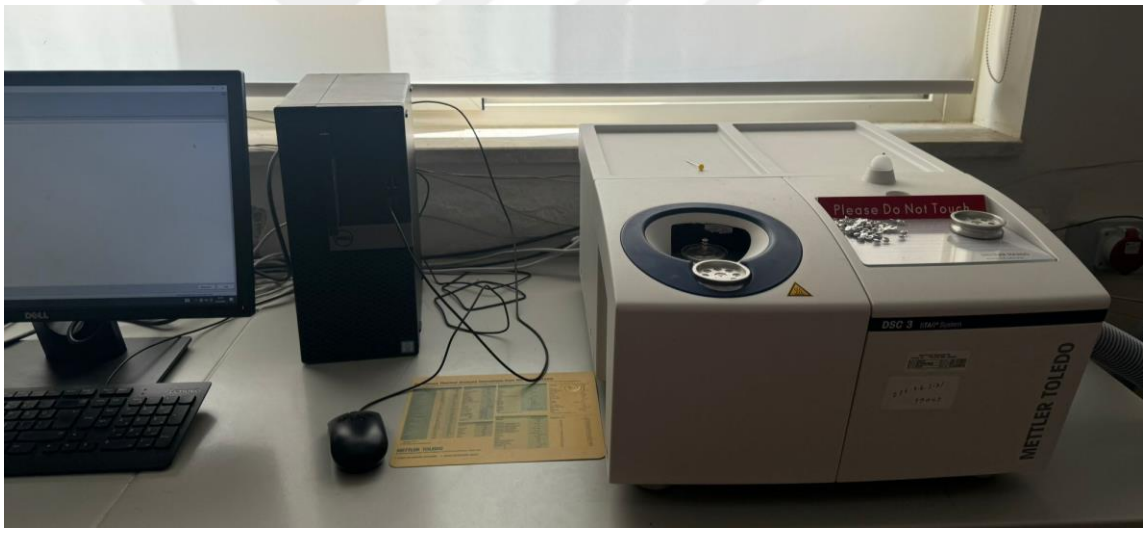

Figure 4.37. DSC analysis device

4.10. Morphological Analysis

Scanning Electron Microscope (SEM) analysis was used to examine and analyze the surface morphology of the produced composite products. SEM analyses were carried out at the Çukurova University Central Laboratory. The image of the device is given in Figure 4.38. SEM analyses were performed using the FEI Quanta 650 Field Emission device. The SEM device has a magnification capacity of 6-1,000,000 x while operating at an acceleration voltage of 100V-30kV. Before the samples were placed in the SEM analyzer, the surface conductivity was increased and the surface coating process was carried out by applying the gold sputtering method with the help of the device in Figure 4.39. Morphological examinations such as examination of the fracture surface of the

samples after the test, matrix cracks formed in the material, oil-epoxy interaction, fiber-matrix interactions, fiber-matrix bond dissociation and fiber breakage are carried out via SEM (Karacor and Ozcanli, 2022b, 2023b).

Figure 4.38. SEM analysis device

Figure 4.39. Gold powder spray device

5. RESULTS AND DISCUSSIONS

5.1. Theoretical Calculations

Taking the density of epoxy as 1.15 g/cm³ and the density of hardener as 0.98 g/cm³, the calculated total mass, volume and density of bioresins during the formation phase are given in Table 5.1. The densities of cottonseed oil, canola oil, flaxseed oil, palm oil and soybean oil are 0.93 g/cm³, 0.917 g/cm³, 0.932 g/cm³, 0.893 g/cm³ and 0.924 g/cm³, respectively.

Table 5.1. Theoretical calculations of prepared bioresin

Bioresins	Calculated bioresin weight (g)	Calculated bioresin volume (cm³)	Calculated bioresin density (g/cm³)
ECO10	62.1	56.681	1.094
ECO20	62.35	57.608	1.082
ECO30	60.45	56.443	1.063
ECO40	61.2	57.68	1.061
ECAO10	62.1	56.751	1.094
ECAO20	60.9	56.396	1.08
ECAO30	60.45	56.623	1.067
ECAO40	59.4	56.191	1.057
EFO10	62.21	56.768	1.096
EFO20	61.1	56.423	1.083
EFO30	62	57.862	1.071
EFO40	60.72	57.182	1.062
EPO10	63.99	58.617	1.092
EPO20	65.25	60.687	1.075
EPO30	60.45	56.964	1.061
EPO40	62.06	58.951	1.053
ESO10	62.1	56.713	1.095
ESO20	61.22	56.628	1.081
ESO30	60.45	56.524	1.069
ESO40	59.4	56.072	1.059

Table 5.2 displays the experimental weights, theoretical and experimental density calculations and void fraction ratios of the bio composite samples. The density calculated assuming that there is no resin loss in the system and that all of the resin is absorbed into the fabric without

vacuum or space is the theoretical density. Experimental density is the density calculated by measuring the mass and volume of the bio composite sample after production and removing the excess resin from the system, including vacuum and space. For the EPOXY sample, the measured weight was calculated to be 11.57 g the theoretical density was found to be 1.341g/cm³, the experimental density was 0.911g/cm³ and the void content was 32.06%.

Table 5.2. Theoretical calculations of biocomposite samples

Biocomposite samples	Measured weight (g)	Theoretical density (g/cm³)	Experimental density (g/cm³)	Void fractions (%)
ECO10	11.338	1.329	0.921	30.7
ECO20	10.901	1.324	0.894	32.47
ECO30	11.034	1.309	0.868	33.71
ECO40	10.205	1.305	0.915	29.88
ECAO10	10.544	1.358	0.991	27.1
ECAO20	10.412	1.332	0.968	27.32
ECAO30	10.642	1.323	0.95	28.2
ECAO40	10.413	1.348	0.916	32.05
EFO10	11.488	1.344	0.954	29.02
EFO20	10.663	1.331	0.964	27.57
EFO30	10.934	1.306	0.879	32.69
EFO40	10.46	1.32	0.88	33.33
EPO10	11.733	1.313	0.905	31.07
EPO20	10.58	1.329	0.953	28.29
EPO30	10.249	1.318	0.902	31.56
EPO40	10.162	1.301	0.82	36.97
ESO10	12.167	1.289	0.839	34.91
ESO20	11.798	1.338	1.012	24.36
ESO30	11.131	1.305	0.922	29.35
ESO40	10.953	1.32	0.827	37.35

The results in Table 5.2 display that the densities of the samples are comparatively low and that low density is of significant importance for a material in engineering applications. In addition, increasing the oil content in the bioresin, usually up to 30%, decreases the void fractions. Adding 40% oil to bio resin generally increases the number of voids in the produced biocomposite samples.

Table 5.3 displays the fiber weight fraction, matrix weight fraction, fiber volume fraction and matrix volume fraction. By obtaining these data, the weight of the 2-layer fabric was taken as 1.46

g, the height of the 2-layer fabric was taken as 0.182 cm, and the other weight and volume data were taken from Table 5.1 and the calculation was made.

Table 5.3. Fractions of biocomposite samples

Biocomposite samples	Fiber weight fraction (W_f)	Matrix weight fraction (W_m)	Fiber volume fraction (V_f)	Matrix volume fraction (V_m)
ECO10	0.0229	0.9770	0.1489	0.851
ECO20	0.0228	0.9771	0.1439	0.856
ECO30	0.0235	0.9764	0.1432	0.8567
ECO40	0.0233	0.9766	0.1375	0.8624
ECAO10	0.0229	0.977	0.1396	0.8603
ECAO20	0.0234	0.9765	0.1406	0.8593
ECAO30	0.0235	0.9764	0.1398	0.8601
ECAO40	0.0239	0.976	0.1432	0.8567
EFO10	0.0229	0.977	0.1497	0.8502
EFO20	0.0233	0.9766	0.1394	0.8605
EFO30	0.023	0.9769	0.1378	0.8621
EFO40	0.0234	0.9765	0.137	0.8629
EPO10	0.0223	0.9776	0.1466	0.8533
EPO20	0.0218	0.9781	0.1327	0.8672
EPO30	0.0235	0.9764	0.1392	0.8607
EPO40	0.0229	0.977	0.1333	0.8666
ESO10	0.0229	0.977	0.1449	0.855
ESO20	0.0232	0.9767	0.1484	0.8515
ESO30	0.0233	0.9767	0.1465	0.8534
ESO40	0.0239	0.976	0.1477	0.8522

5.2. Tensile Test Results

Table 5.4 indicates the tensile strength, elastic modulus and elongation results for EPOXY. Tensile strength results for ECO, ECAO, EFO, EPO, and ESO are given in Figure 5.1 to Figure 5.5, respectively. The results were created by testing 5 samples and determining the average and presenting them in graphs. Tensile strength values for ECO10, ECO20, ECO30, and ECO40 were reached as 39.138±3.13 MPa, 34.142±1.77 MPa, 32.592±1.79 MPa, 40.722±1.48 MPa, respectively. Tensile strength values for ECAO10, ECAO20, ECAO30, and ECAO40 are 41.288±3.1 MPa, 35.218±1.99 MPa, 33.57±2.97 MPa, 31.496±3.11 MPa, respectively. Tensile strength values of EFO10, EFO20, EFO30, and EFO40 samples were found to be 32.33±1.53 MPa, 35.412±1.96 MPa,

29.278±3.37 MPa, 28.002±1.33 MPa, respectively. Tensile strength values in EPO10, EPO20, EPO30, and EPO40 samples were determined as 38.508±2.17 MPa, 33.83±2.04 MPa, 38.584±1.32 MPa, 32.812±0.88 MPa, respectively. The tensile strength values of ESO10, ESO20, ESO30, and ESO40 samples were found as 32.448±2.72 MPa, 39.254±1.39 MPa, 30.626±2.27 MPa, 35.446±2.79 MPa, respectively.

Table 5.4. Tensile strength results of EPOXY samples

Sample	Tensile strength (MPa)	Elastic modulus (MPa)	Elongation (%)
EPOXY	39.942±4	370±75.13	24.72±1.78

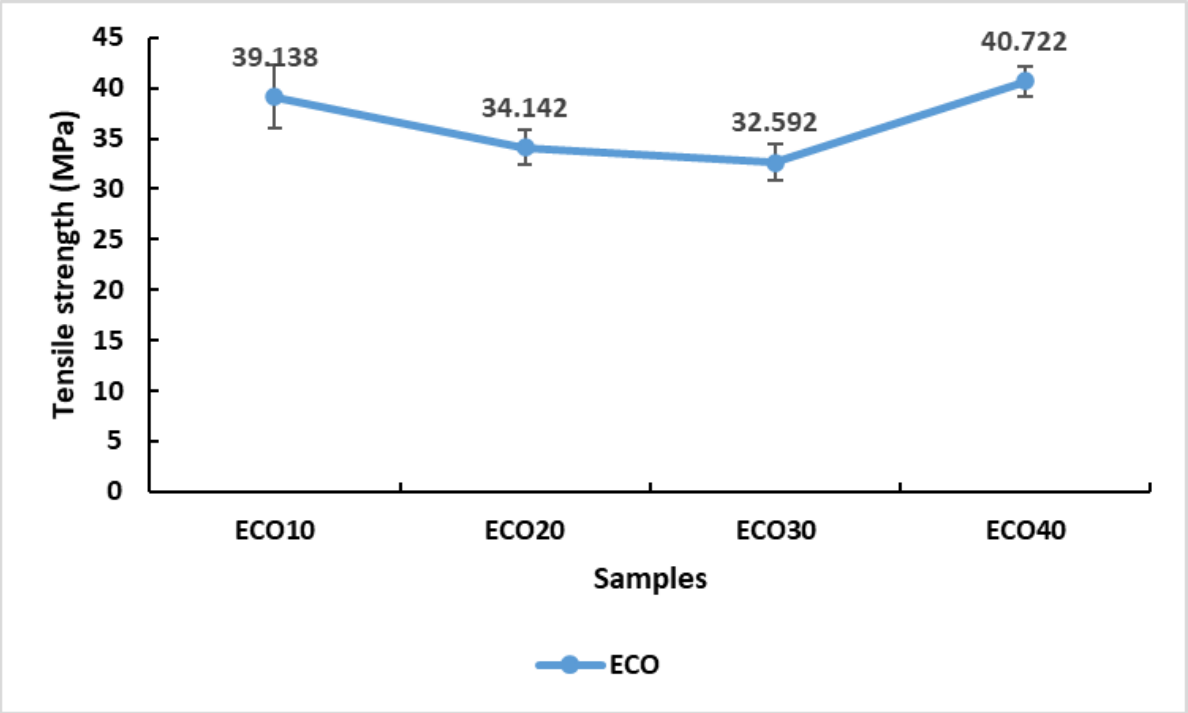

Figure 5.1. Tensile strength results of ECO samples

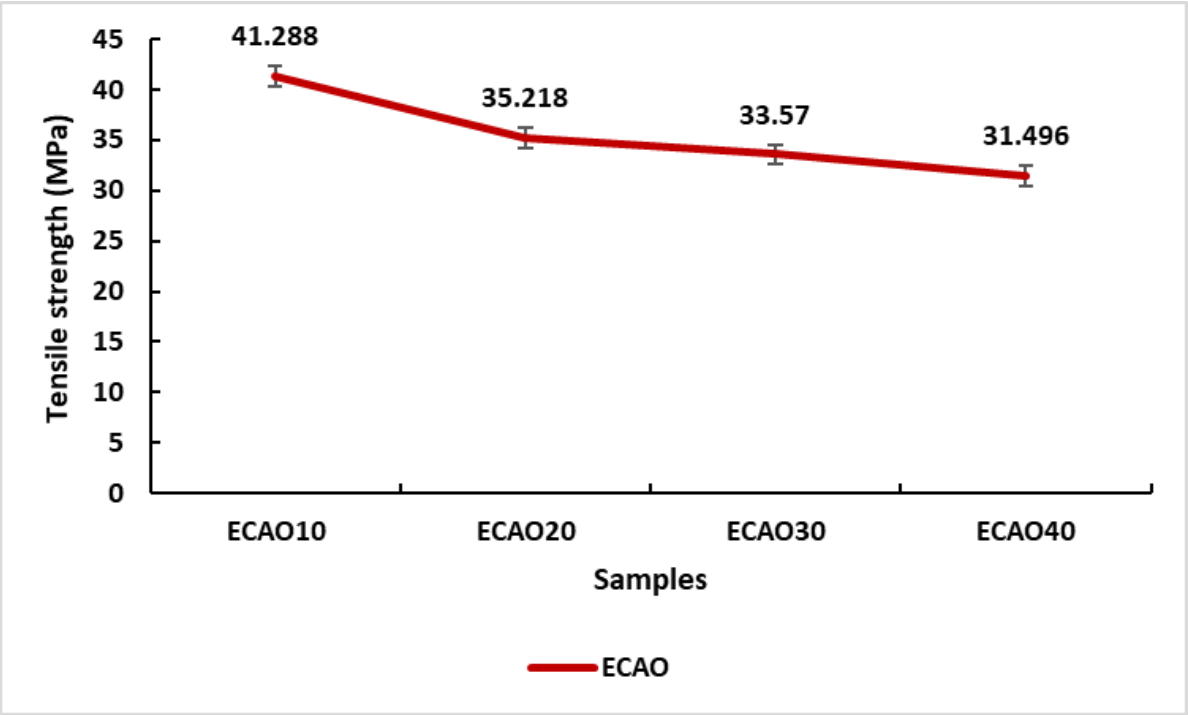

Figure 5.2. Tensile strength results of ECAO samples

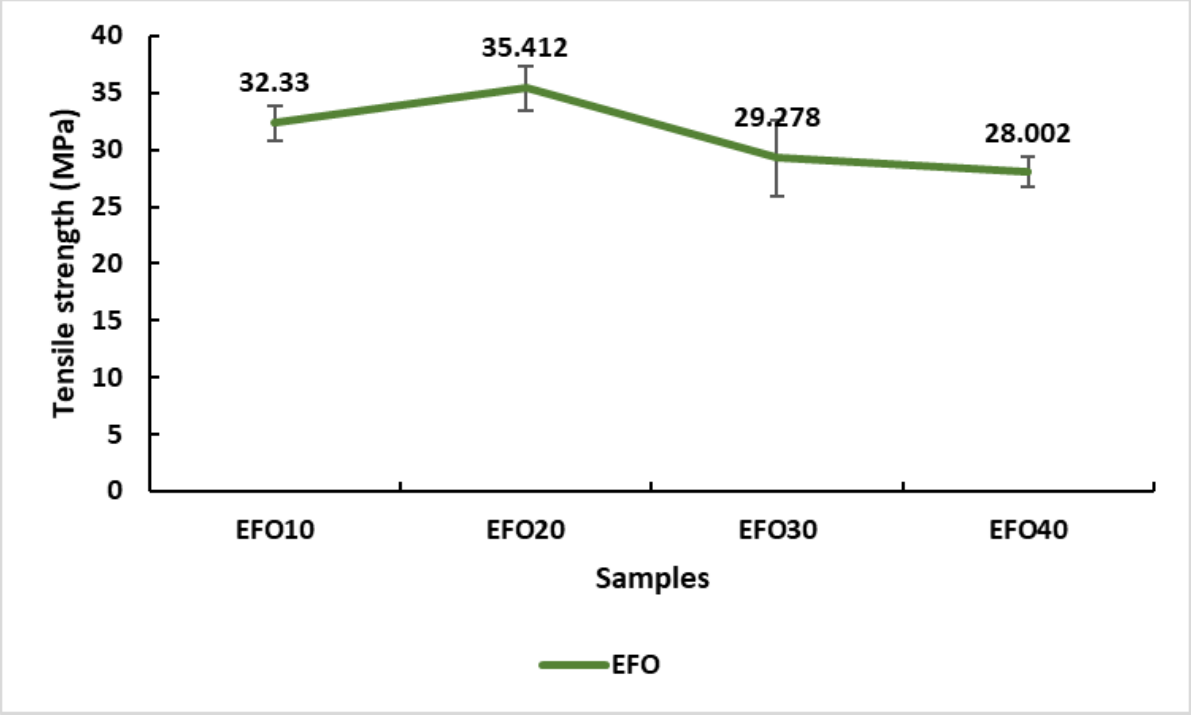

Figure 5.3. Tensile strength results of EFO samples

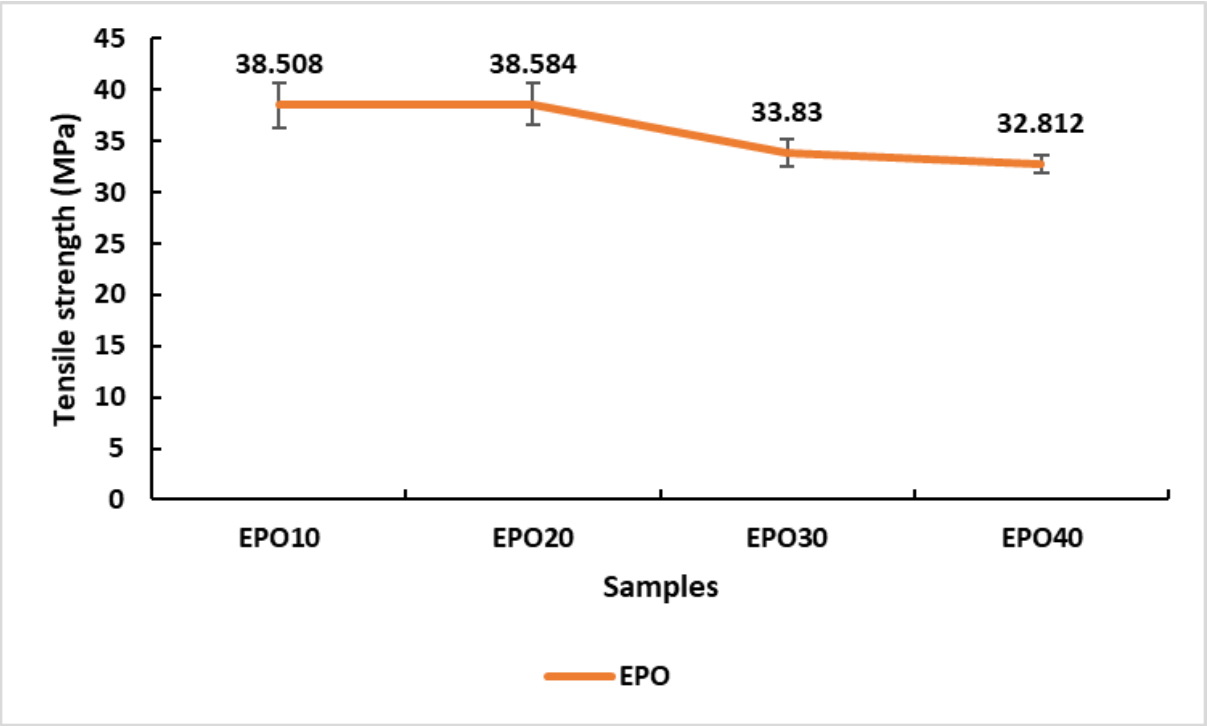

Figure 5.4. Tensile strength results of EPO samples

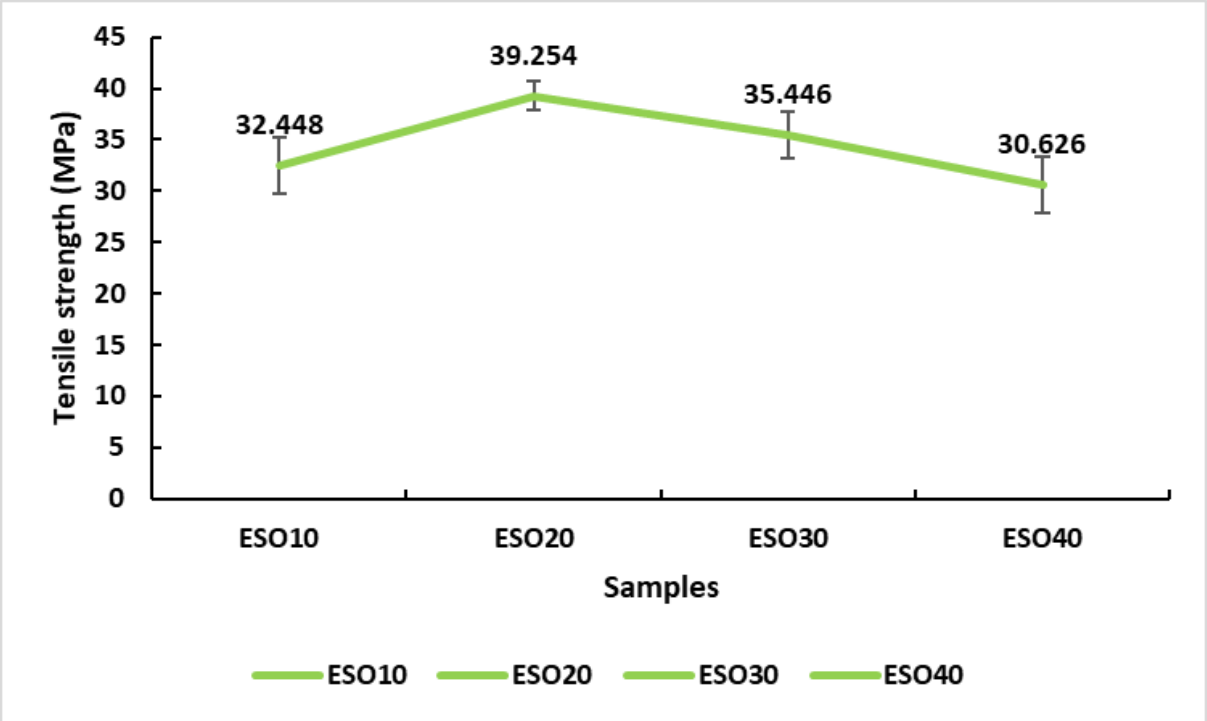

Figure 5.5. Tensile strength results of ESO samples

Elastic modulus values for ECO, ECAO, EFO, EPO, and ESO are given in Figure 5.6 to Figure 5.10, respectively. Modulus of elasticity values for ECO10, ECO20, ECO30, and ECO40 were reached as 116.6±25.89 MPa, 82.6±6.58 MPa, 74.8±3.27 MPa, 92.2±2.49 MPa, respectively. Modulus of elasticity values for ECAO10, ECAO20, ECAO30, and ECAO40 are 117.2±10.43 MPa,

91.2±2.96 MPa, 81.8±3.94 MPa, 81.6±3.21 MPa, respectively. Modulus of elasticity values of EFO10, EFO20, EFO30, and EFO40 samples were found to be 108.2±11.76 MPa, 112. 2±21.71 MPa, 97.6±8.68 MPa, 70.6±1.67 MPa, respectively. Modulus of elasticity values in EPO10, EPO20, EPO30, and EPO40 samples were determined as 120.8±12.32 MPa, 87.6±4.77 MPa, 86.6±3.78 MPa, 63.4±1.52 MPa, respectively. The modulus of elasticity values of ESO10, ESO20, ESO30, and ESO40 samples were found as 129.4±13.70 MPa, 137.2±26.39 MPa, 108±12.67 MPa, 102.6±8.5 MPa, respectively.

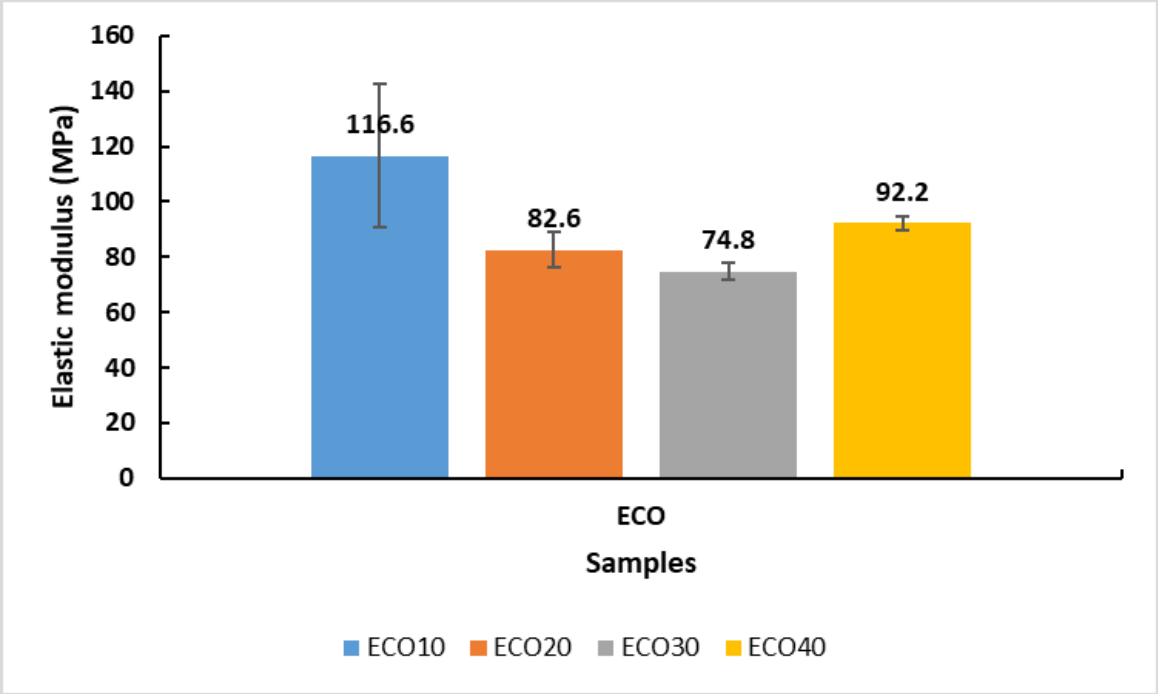

Figure 5.6. Modulus of elasticity results of ECO samples

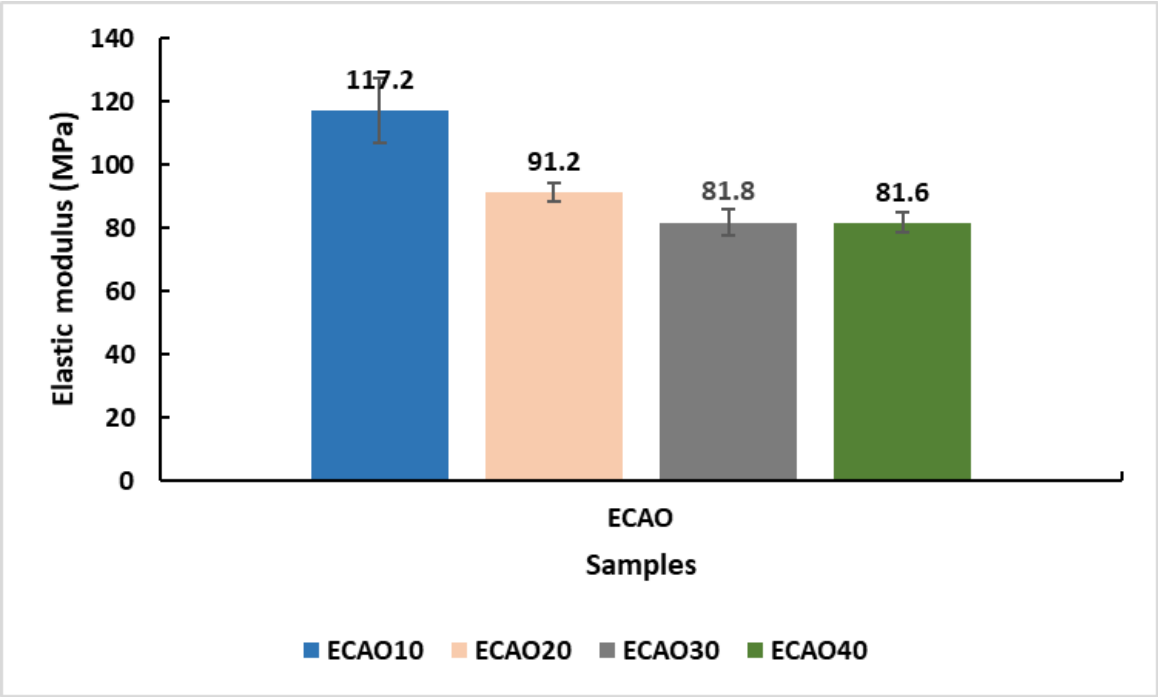

Figure 5.7. Modulus of elasticity results of ECAO samples

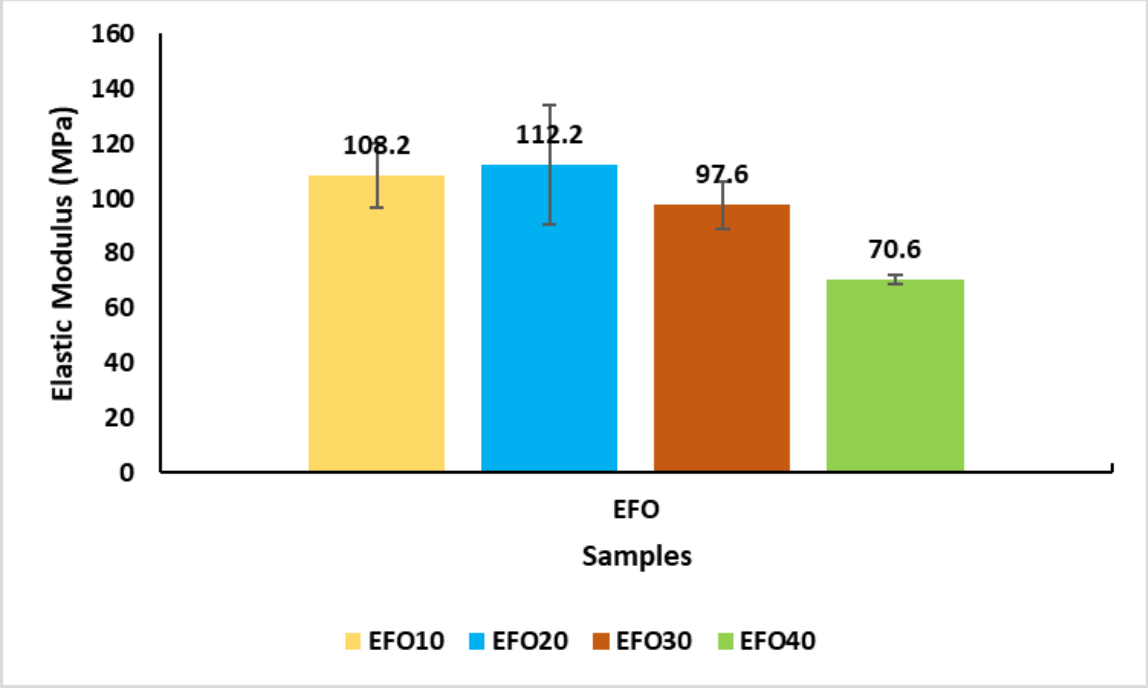

Figure 5.8. Modulus of elasticity results of EFO samples

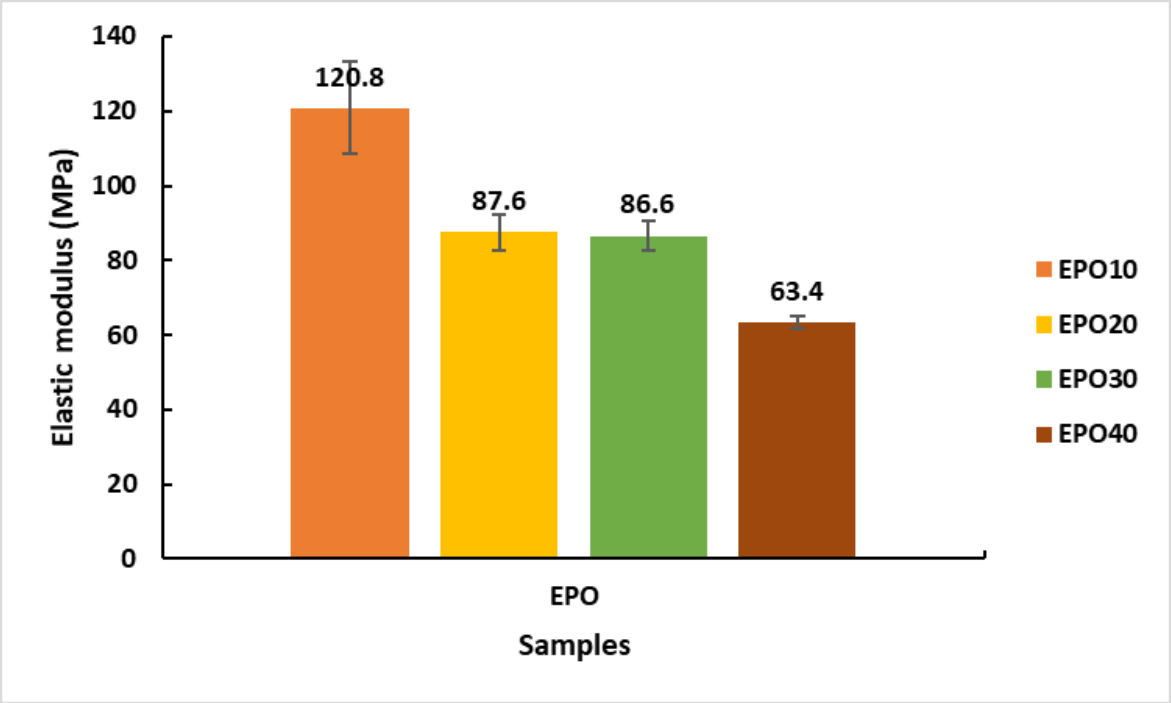

Figure 5.9. Modulus of elasticity results of EPO samples

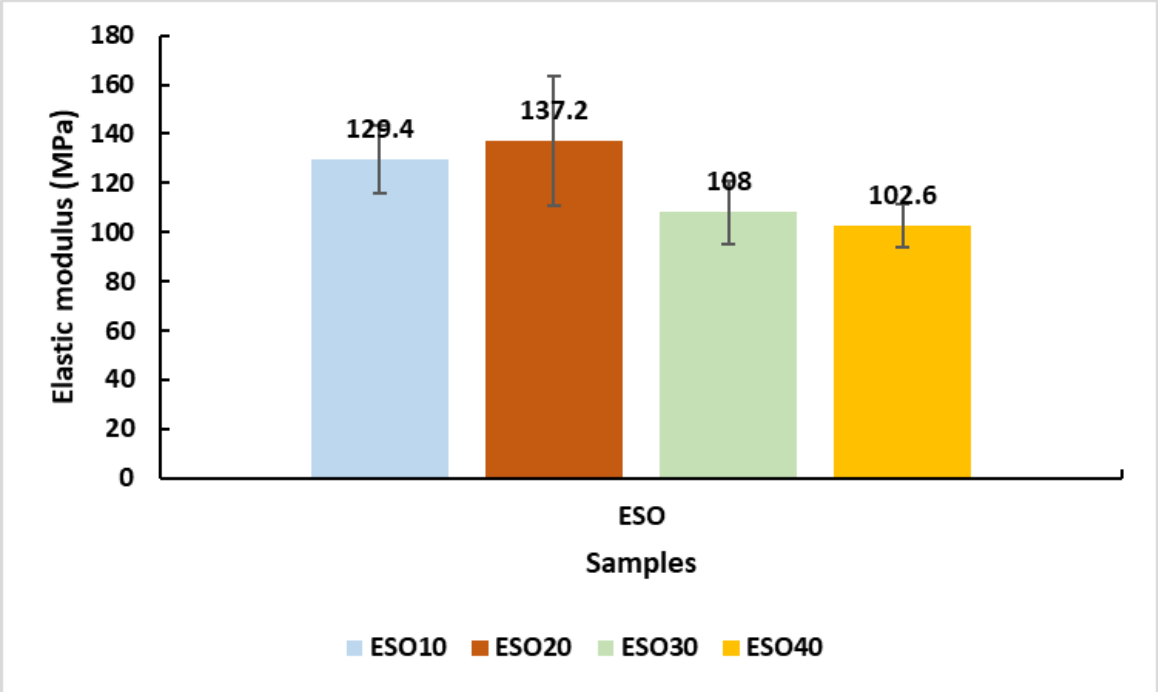

Figure 5.10. Modulus of elasticity results of ESO samples

Percentage elongation values for ECO, ECAO, EFO, EPO and ESO are presented in Figure 5.11 to Figure 5.15, respectively. Elongation values for ECO10, ECO20, ECO30, and ECO40 were reached as %31.42±2.0, %36.22±1.04, %37.7±2.12, %38.22±2.19, respectively. Elongation values for ECAO10, ECAO20, ECAO30, and ECAO40 are %31.74±2.3, %34.38±1.58, %36.34±1.83,

%34.52±2.52, respectively. Elongation values of EFO10, EFO20, EFO30, and EFO40 samples were found to be %28.94±2.67, %29. 6±2.84, %29.98±2.46, %34.18±2.1, respectively. Elongation values in EPO10, EPO20, EPO30, and EPO40 samples were determined as %30.82±0.91, %34.76±0.68, %37.2±0.83, %42.78±1.88, respectively. The elongation values of ESO10, ESO20, ESO30, and ESO40 samples were found as % 26.12±1.85, %26.72±1.7, %27.5±2.22, %30.76±2.22, respectively.

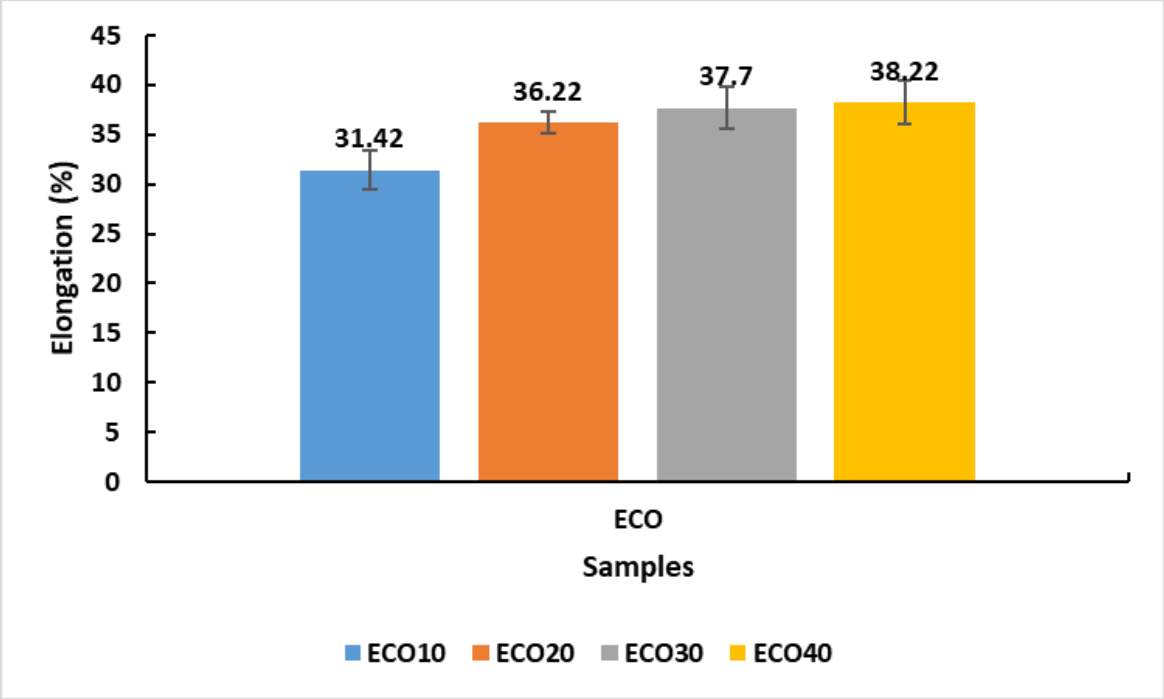

Figure 5.11. Elongation results of ECO samples

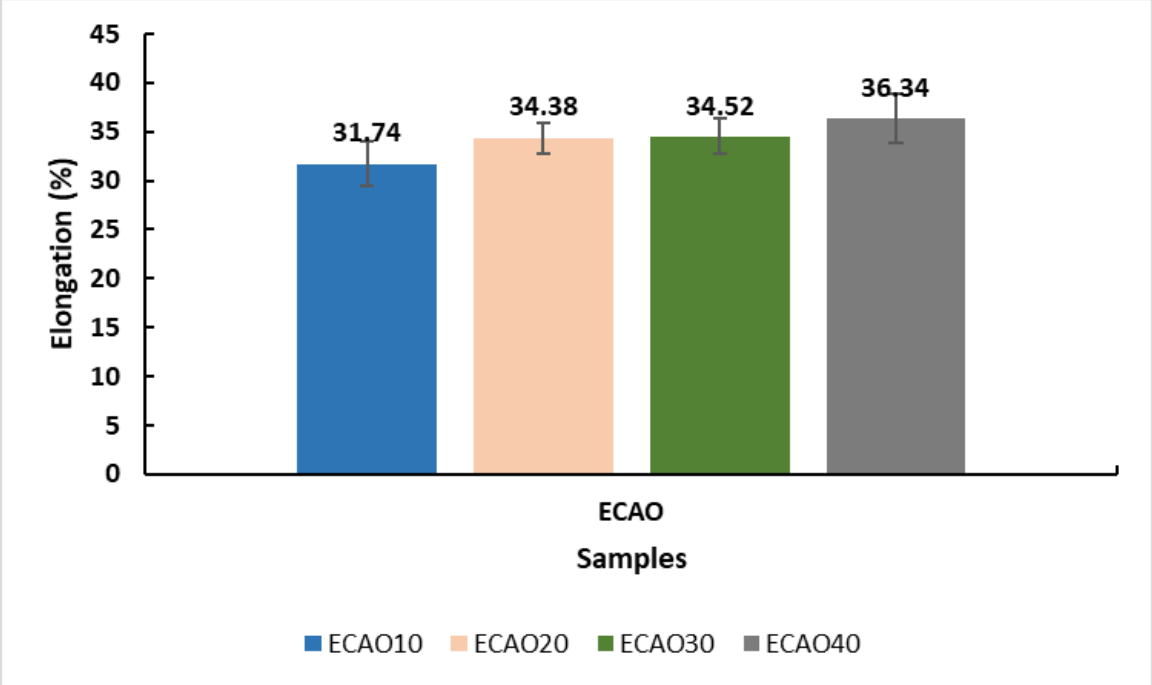

Figure 5.12. Elongation results of ECAO samples

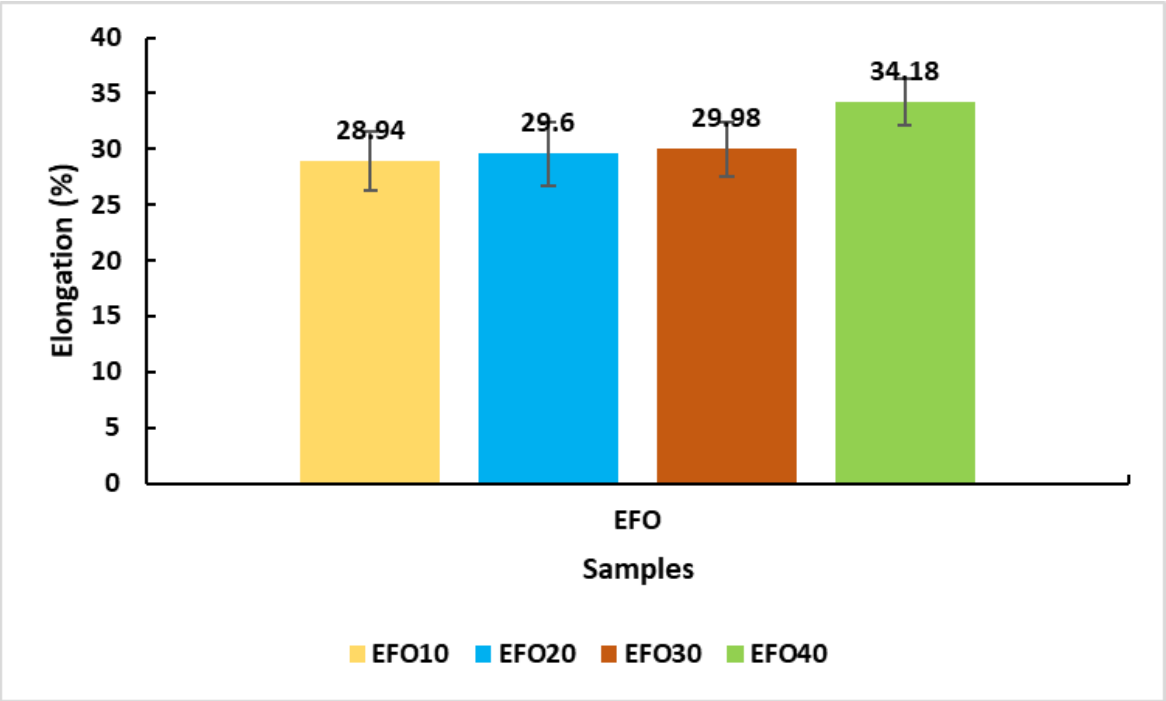

Figure 5.13. Elongation results of EFO samples

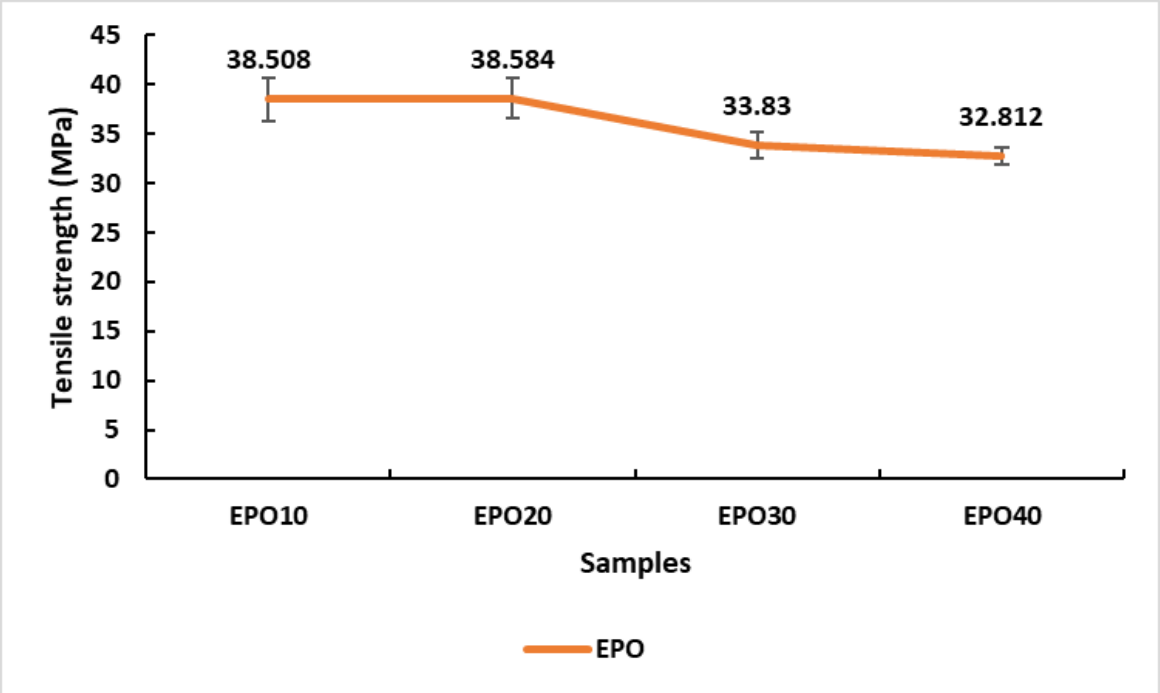

Figure 5.14. Elongation results of EPO samples

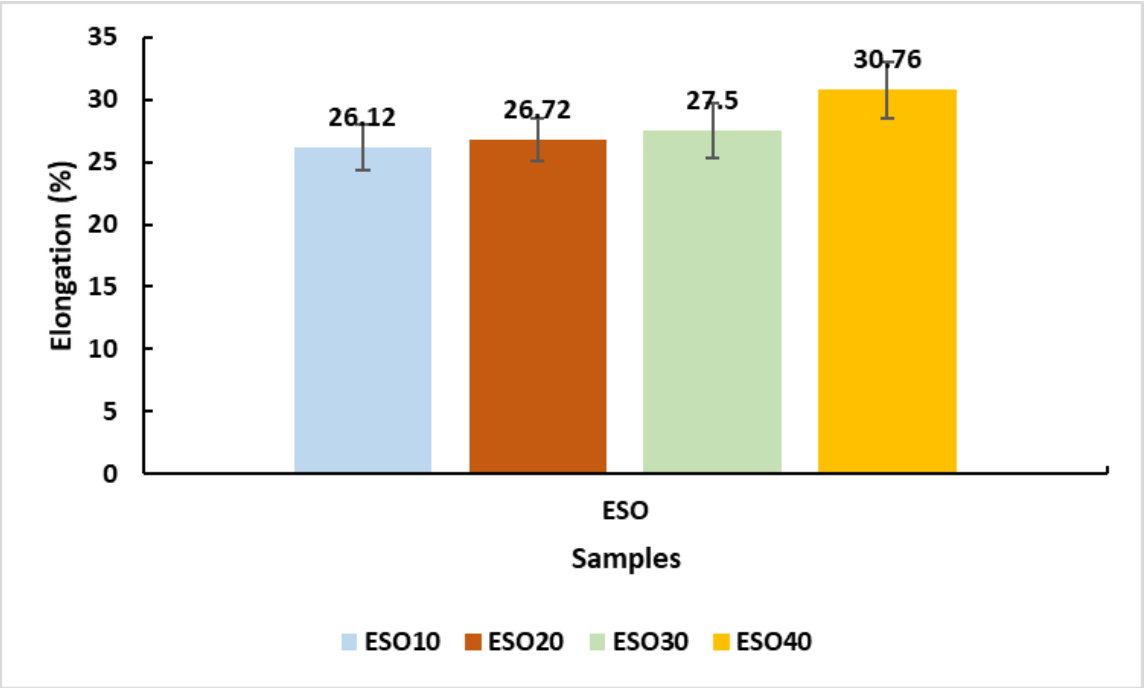

Figure 5.15. Elongation results of ESO samples

Table 5.5 presents the difference in values of the produced biocomposite samples compared to the homogeneous EPOXY sample. When the tensile strength values were examined, the tensile value of the EPOXY sample was found to be higher in samples other than ECO 40 and ECAO10. All bio composite samples produced had lower elastic modulus values than the EPOXY sample. In terms of percentage elongation, all produced biocomposite samples showed greater elongation than the EPOXY sample. As the oil ratio increased from 10% to 40%, the interphase bonds between the matrix and the fiber weakened and the tensile strength values decreased compared to the EPOXY sample. Achieving high tensile strength depends on strong interfacial bonding and good adhesion between the matrix and the fiber. The high strength value obtained in ECO40 and ECAO10 compared to EPOXY can be explained by the good interfacial bonding.

The positive effect of adding vegetable oil to the resin is seen in the elongation value results. It has been stated in previous studies that another factor caused by the plasticizing effect of vegetable oils added to this situation is crosslink density (Sudha et al., 2017). In a previous study, Ozkur (Ozkur, 2021) stated that adding a certain amount of AESO (30%) to the epoxy resin rises the tensile strength and this can be explained by the strong interfacial adhesion. In addition, in another study, Temmink et al.(Temmink et al., 2018) found lower tensile strength and higher elongation values in composites containing AESO compared to composites containing epoxy. The reason for this was shown to be the free movement ability of the polymer chains in the AESO resin when it was not fully cured and the flexibility of the composite structure with AESO resin.

The results in Table 5.5 are also parallel to the findings from these studies. The results also show that low oil content and high epoxy content cause the samples to reflect brittle material

properties, while an increment in oil content and a decrement in epoxy content causes the samples to exhibit ductile material characteristics.

Table 5.5. Differences in tensile strength, elastic modulus and elongation values

Biocomposite samples	**Difference of tensile strength compared to EPOXY sample (%)**	**Difference of elastic modulus compared to EPOXY sample (%)**	**Difference of elongation compared to EPOXY sample (%)**
ECO10	-2.013	-68.486	+27.104
ECO20	-14.521	-77.676	+46.521
ECO30	-18.402	-79.784	+52.508
ECO40	+1.953	-75.081	+54.612
ECAO10	+3.370	-68.324	+28.398
ECAO20	-11.827	-75.351	+39.078
ECAO30	-15.953	-77.892	+39.644
ECAO40	-21.146	-77.946	+47.006
EFO10	-19.058	-70.757	+17.071
EFO20	-11.341	-69.676	+19.741
EFO30	-26.699	-73.622	+21.278
EFO40	-29.893	-80.919	+38.269
EPO10	-3.590	-67.351	+24.676
EPO20	-3.400	-76.595	+50.485
EPO30	-15.302	-76.324	+40.615
EPO40	-17.851	-82.865	+73.058
ESO10	-18.762	-65.027	+5.663
ESO20	-1.722	-62.919	+8.091
ESO30	-11.256	-72.270	+24.434
ESO40	-23.324	-70.811	+11.246

When comparing 5 different vegetable oils, the values closest to the EPOXY sample in terms of average tensile strength value were found in the ECO specimens, and the most different values were observed in the EFO samples. In terms of percentage elongation values, the EPO samples had the highest difference compared to EPOXY, while the closest values were found in ESO samples. ECO samples are ranked behind EPO samples in terms of percentage elongation difference. Elastic modulus is considered an indicator of hardness in the material. While EPO samples were the samples with the highest negative difference compared to EPOXY in terms of elastic modulus value average,

ESO samples were the samples with the closest positive elastic modulus value average to EPOXY sample.

Figures 5.16 and 5.17 contain graphs showing the specific strength and specific modulus values of the samples, respectively. In the specific strength values of the samples, ECO40, ECAO10, EPO20 and ESO20 samples have higher specific strength values than the EPOXY sample. While it is supposed that the specific strength of ECO40 and ECAO10 samples is higher than the EPOXY sample, the fact that EPO20 and ESO20 samples are higher than the EPOXY sample is related to their low density. Other samples have lower specific strength values than the EPOXY sample. In the specific modulus graph data, it is expected that the EPOXY sample will reach the highest value as it has the highest elastic modulus value.

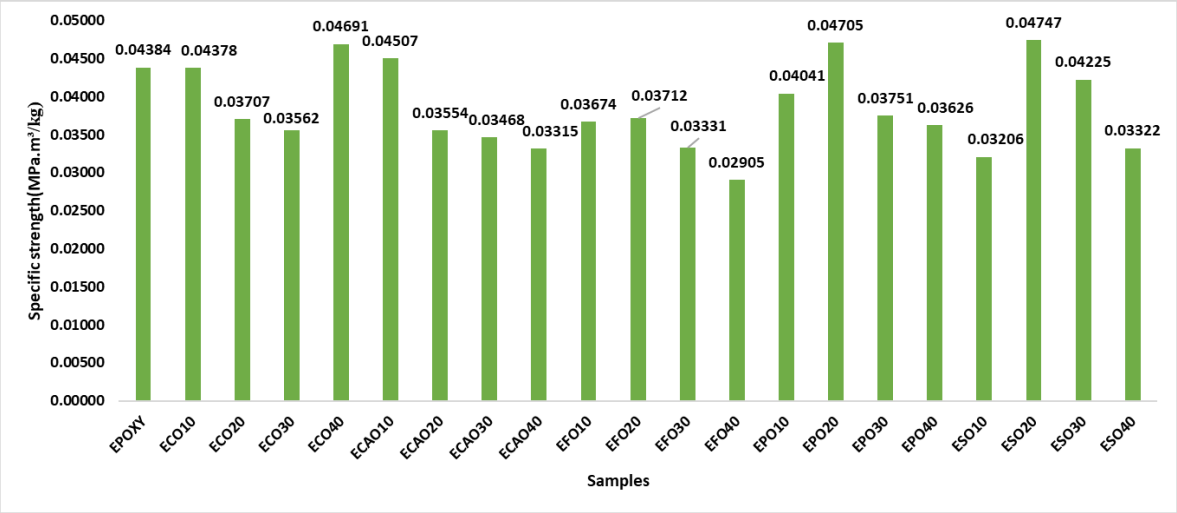

Figure 5.16. Specific strength results of samples

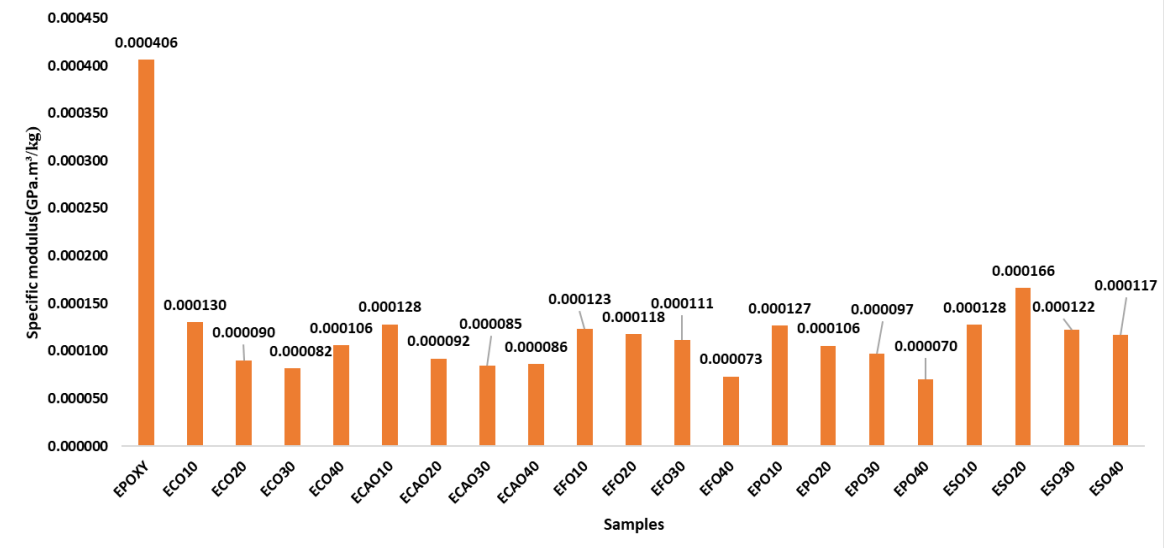

Figure 5.17. Specific modulus results of samples

Tensile test results also reveal that while an increment in the vegetable oil content in the epoxy resin up to 20% has a positive effect on tensile strength and elastic modulus, the addition of 30% and 40% vegetable oil into the resin causes these values to decrease. In terms of percentage elongation, the increase in the amount of vegetable oil in the epoxy causes the material to elongate more. Adding cottonseed oil to epoxy resin is more advantageous than other oils used in terms of increasing tensile strength and percentage elongation. Adding flaxseed oil to the resin did not create an advantage, as it was the oil type that reduced the tensile strength the most and also increased the percentage elongation the least after the ESO sample. Soybean oil, when added to the resin compared to other oil types, gave the closest values to the values of the EPOXY sample in terms of elastic modulus and percentage elongation. The reason for the difference between these vegetable oil types may be that they do not mix completely with the resin, cannot be homogenized, and cannot bond well enough with the fiber. When the vegetable oil percentages are examined, it is revealed that 10% to 20% vegetable oil ratio in tensile strength, 10% in elastic modulus and 40% vegetable oil ratio in percentage elongation are the most optimum ratios.

5.3. Flexural Test Results

Flexural stress results for EPOXY, ECO, ECAO, EFO, EPO, and ESO specimens are given in Figure 5.18 to Figure 5.42, respectively. The results were produced by testing 5 specimens, taking the average and presenting them as graphs. The proportional values of percent elongation for ECO10, ECO20, ECO30 and ECO40 were found to be 4.997±0.361 times, 5.151±0.2 times, 5.643±0.251 times, 5.129±0.55 times, respectively. The proportional values of percent elongation for ECAO10, ECAO20, ECAO30 and ECAO40 were found to be 6.23±0.31 times, 6.234±0.563 times, 6.23±0.475 times, 6.991±0.611 times, respectively. The percentage elongations of samples EFO10, EFO20, EFO30 and EFO40 were found to be 4.827±0.358 times, 5.233±0.156 times, 5.801±0.55 times, 5.824±0.241 times, respectively. The percentage elongations of samples EPO10, EPO20, EPO30 and EPO40 were found to be 4.455±0.494 times, 4.428±0.333 times, 4.564±0.528 times, 4.953±0.257 times, respectively. The percentage elongations of ESO10, ESO20, ESO30 and ESO40 samples were found to be 3.467±1.876 times, 5.143±0.247 times, 2.891±1.019 times, 5.522±0.847 times, respectively. The percentage elongation ratio for EPOXY was found to be 6.807±0.589.

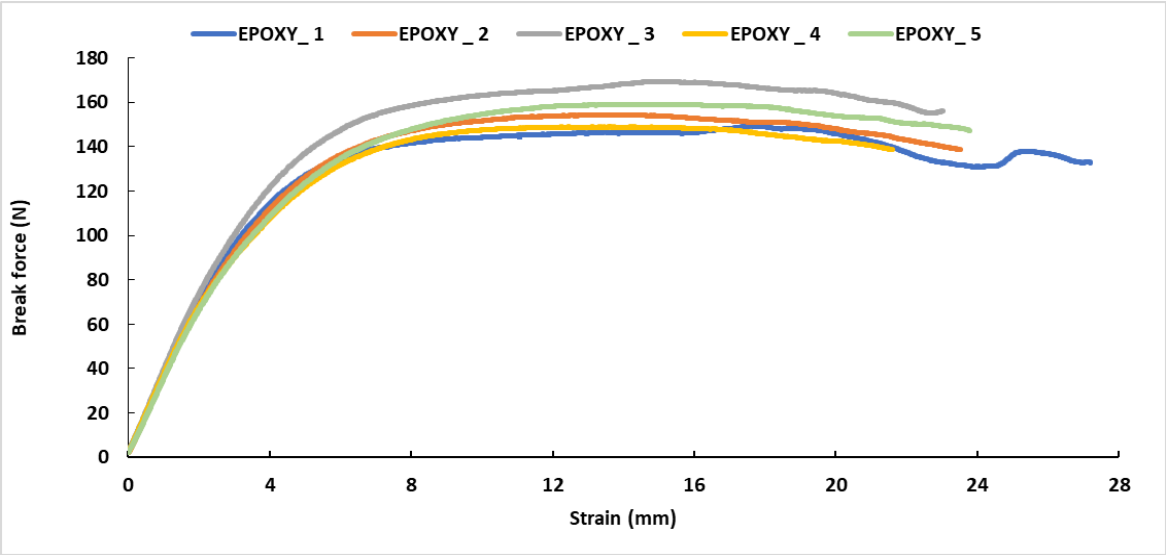

Figure 5.18. Flexural strength results of EPOXY samples

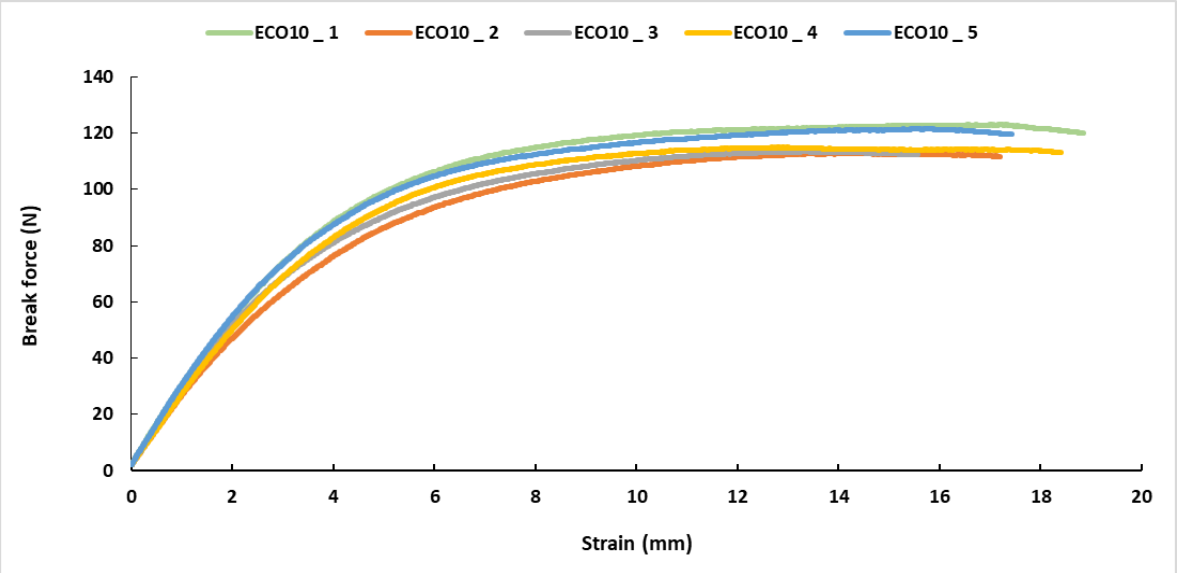

Figure 5.19. Flexural strength results of ECO10 samples

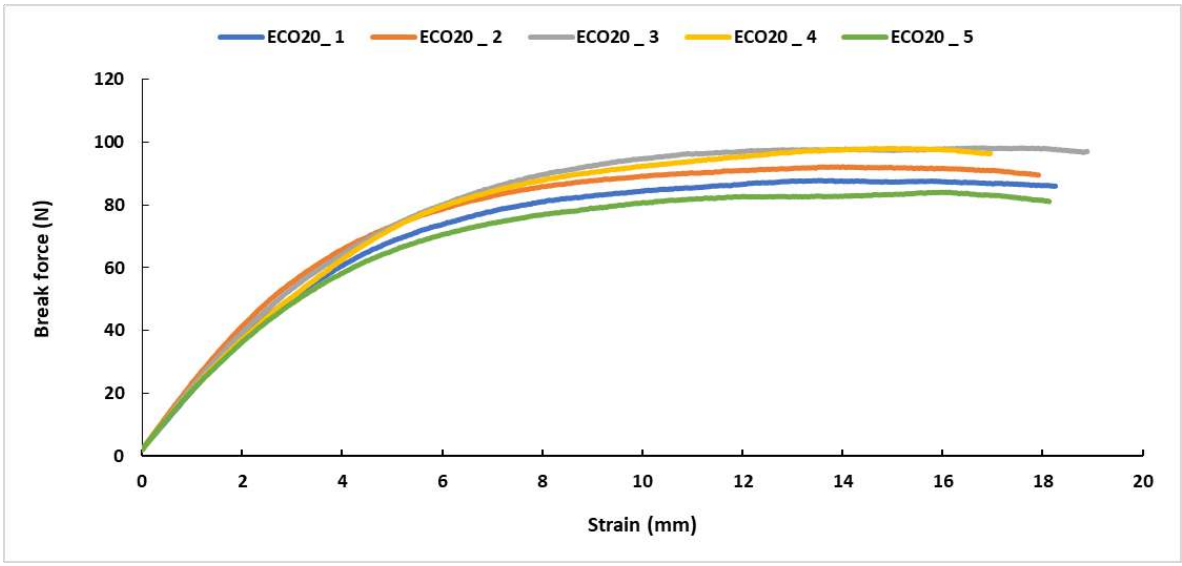

Figure 5.20. Flexural strength results of ECO20 samples

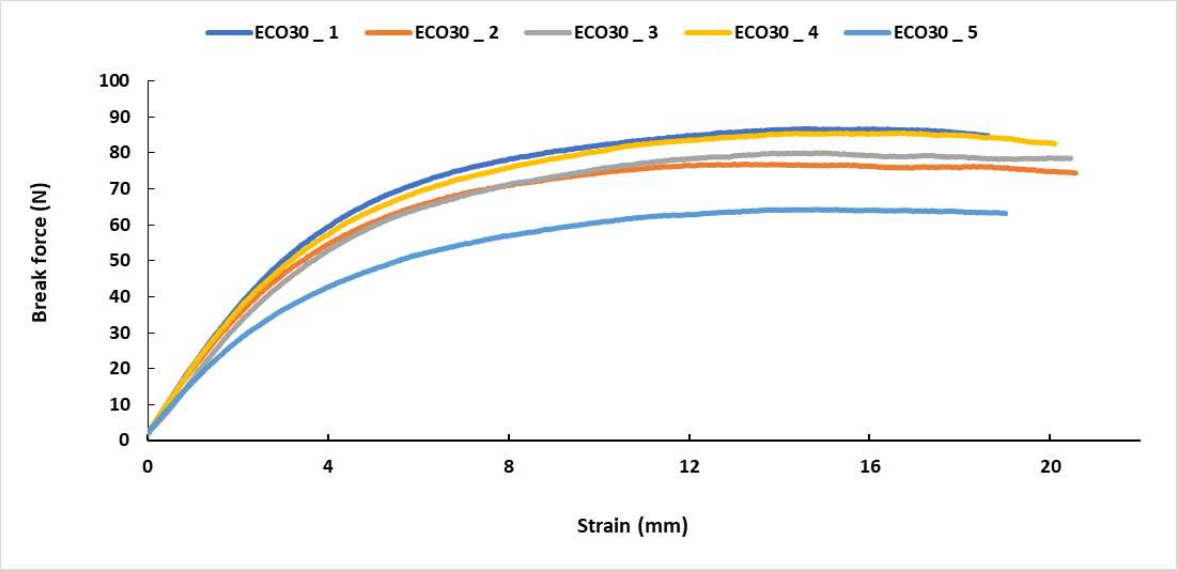

Figure 5.21. Flexural strength results of ECO30 samples

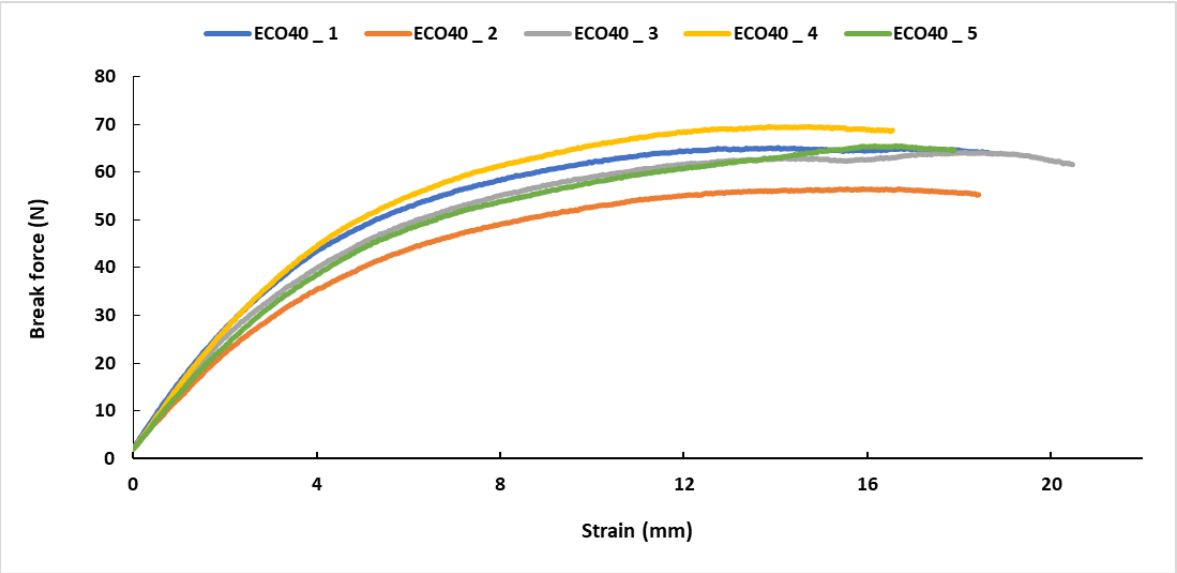

Figure 5.22. Flexural strength results of ECO40 samples

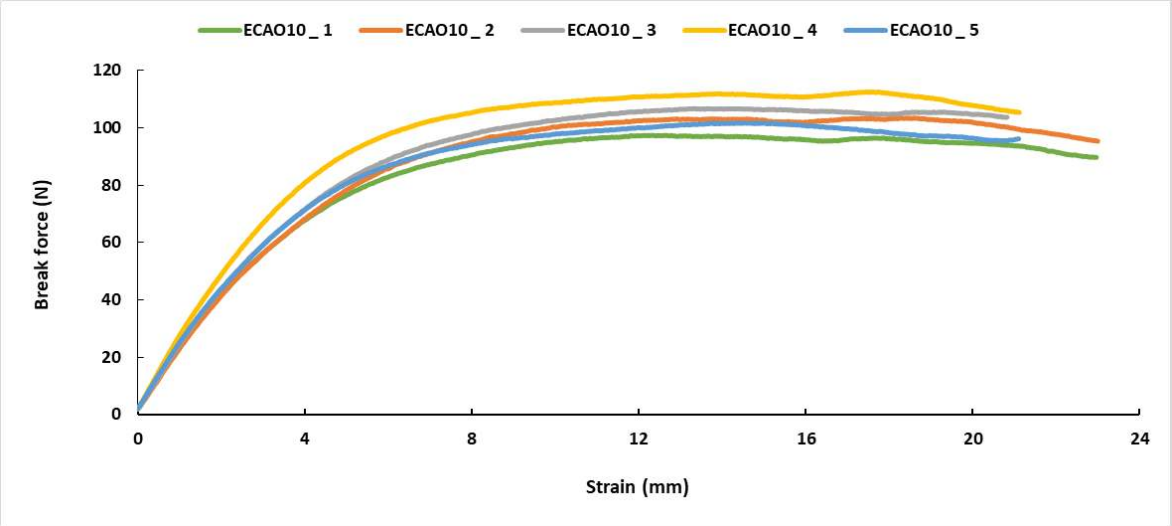

Figure 5.23. Flexural strength results of ECAO10 samples

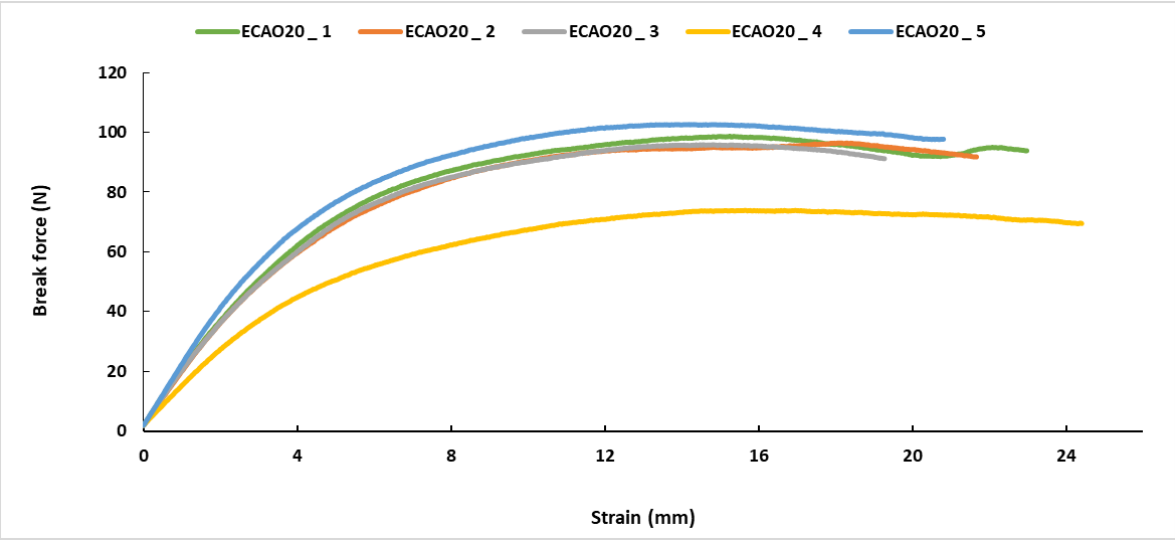

Figure 5.24. Flexural strength results of ECAO20 samples

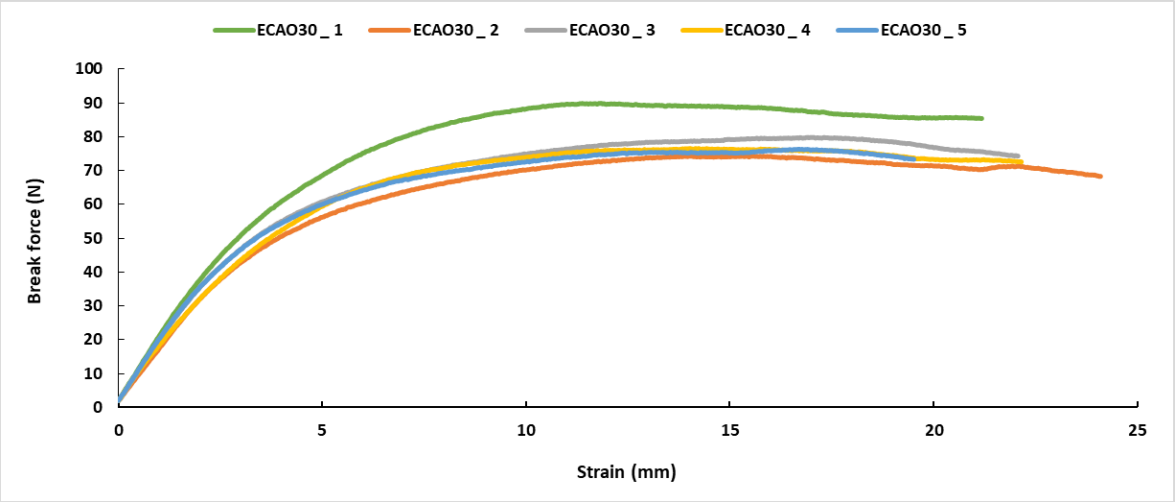

Figure 5.25. Flexural strength results of ECAO30 samples

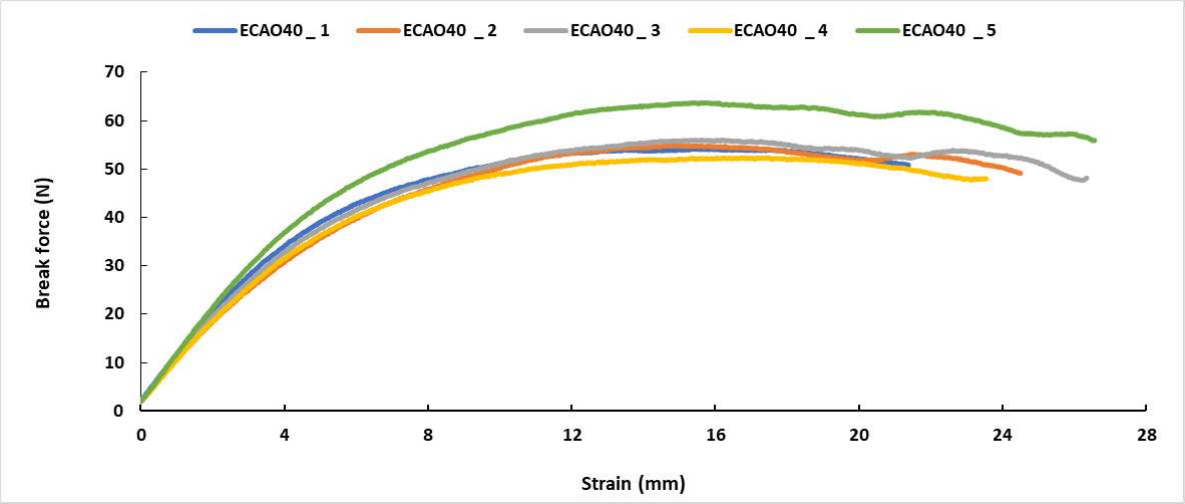

Figure 5.26. Flexural strength results of ECAO40 samples

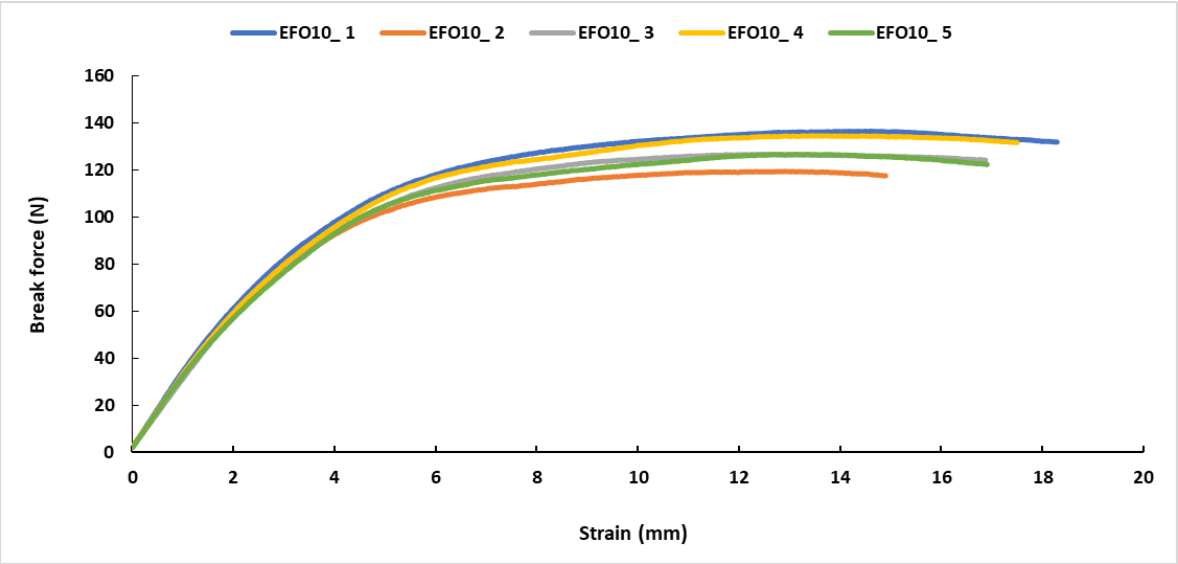

Figure 5.27. Flexural strength results of EFO10 samples

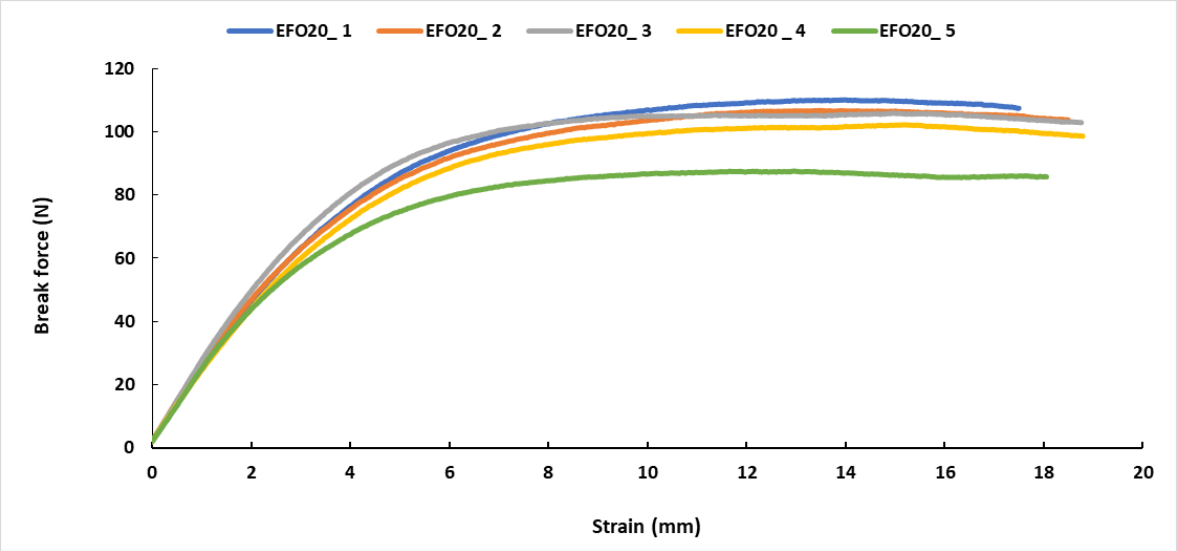

Figure 5.28. Flexural strength results of EFO20 samples

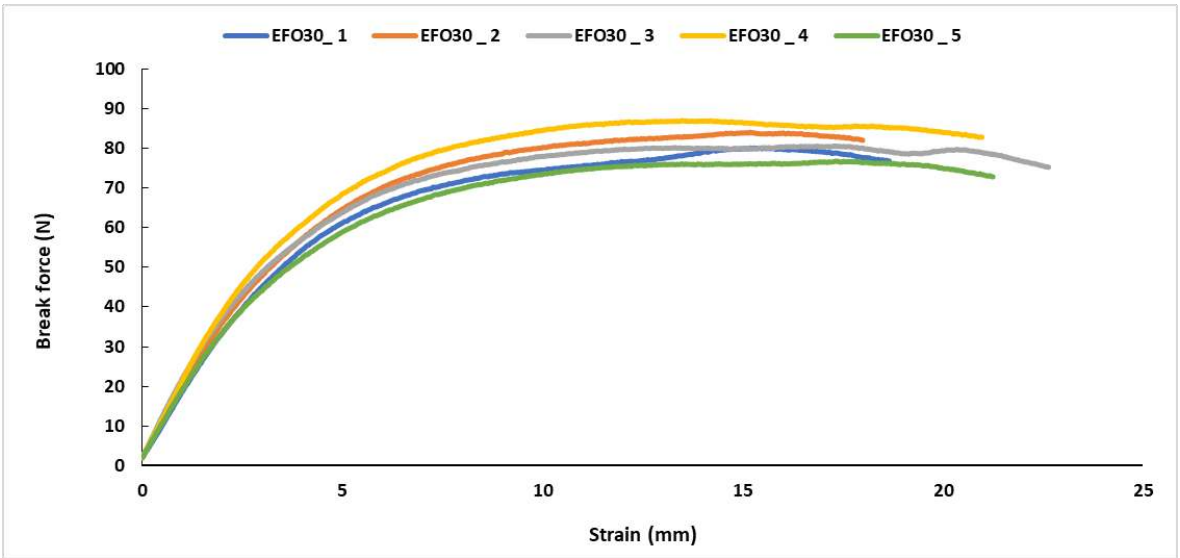

Figure 5.29. Flexural strength results of EFO30 samples

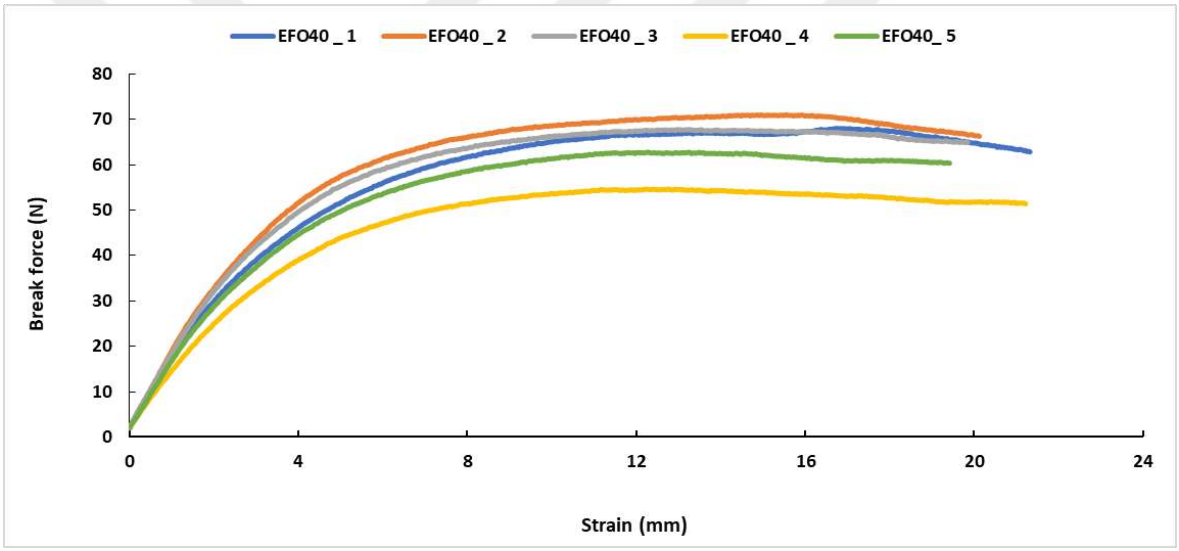

Figure 5.30. Flexural strength results of EFO40 samples

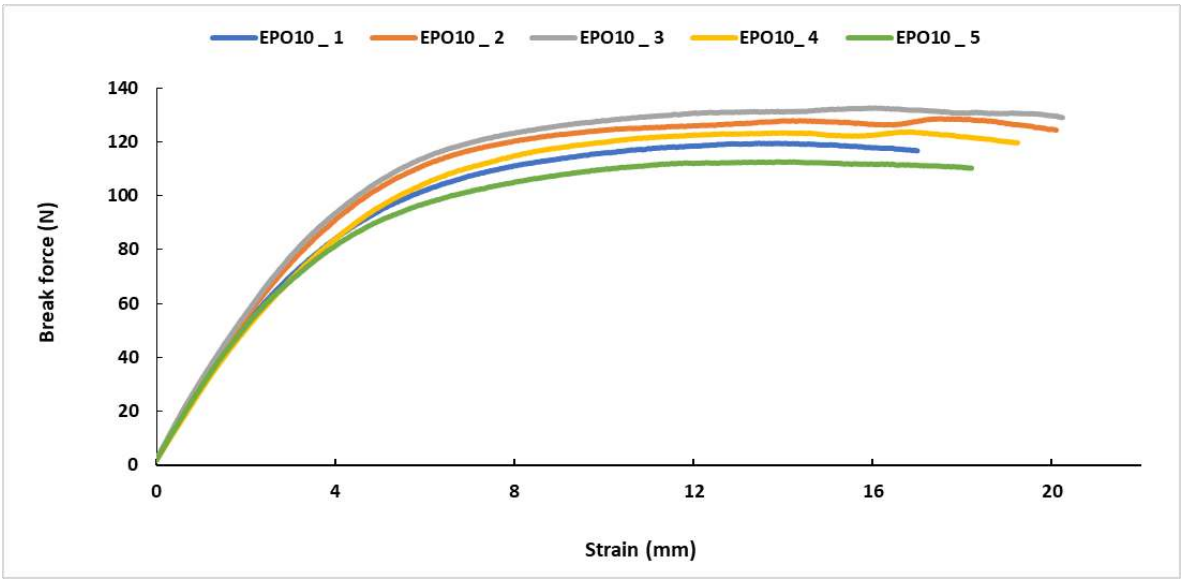

Figure 5.31. Flexural strength results of EPO10 samples

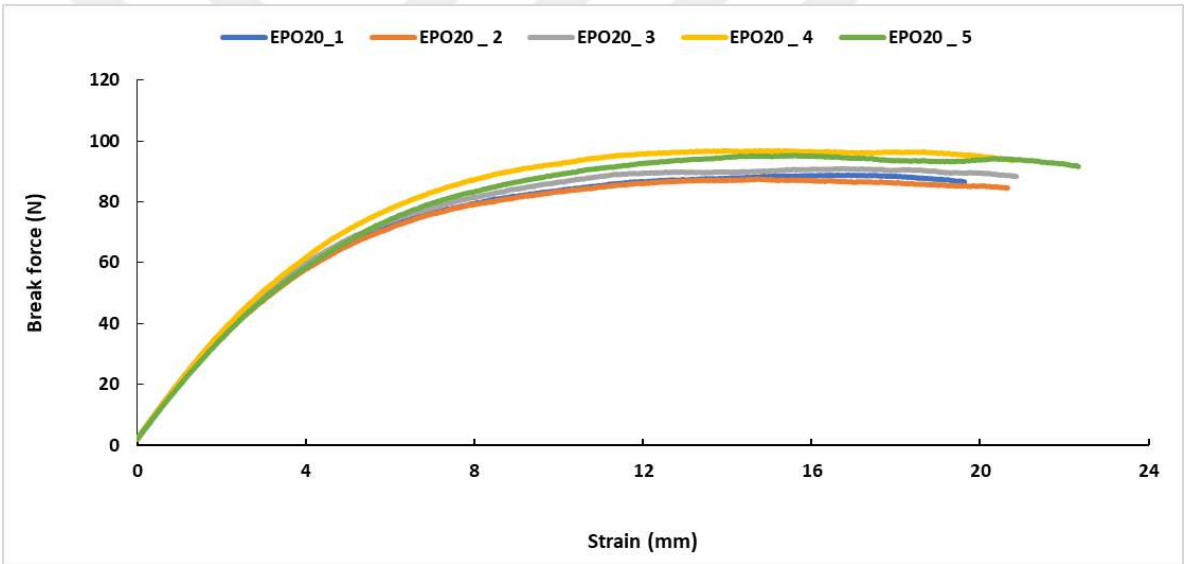

Figure 5.32. Flexural strength results of EPO20 samples

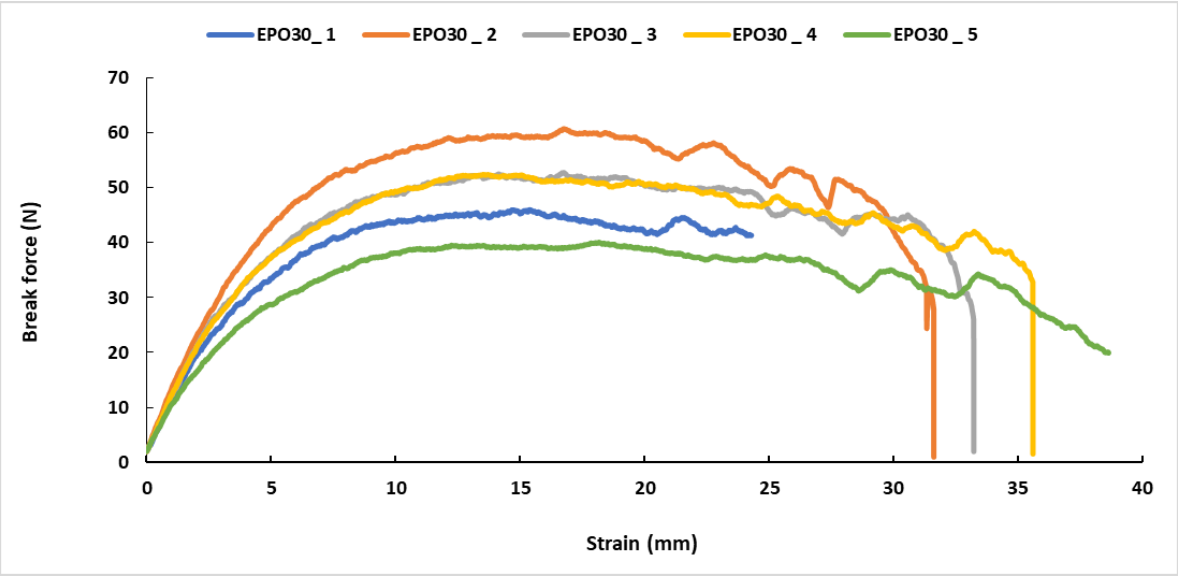

Figure 5.33. Flexural strength results of EPO30 samples

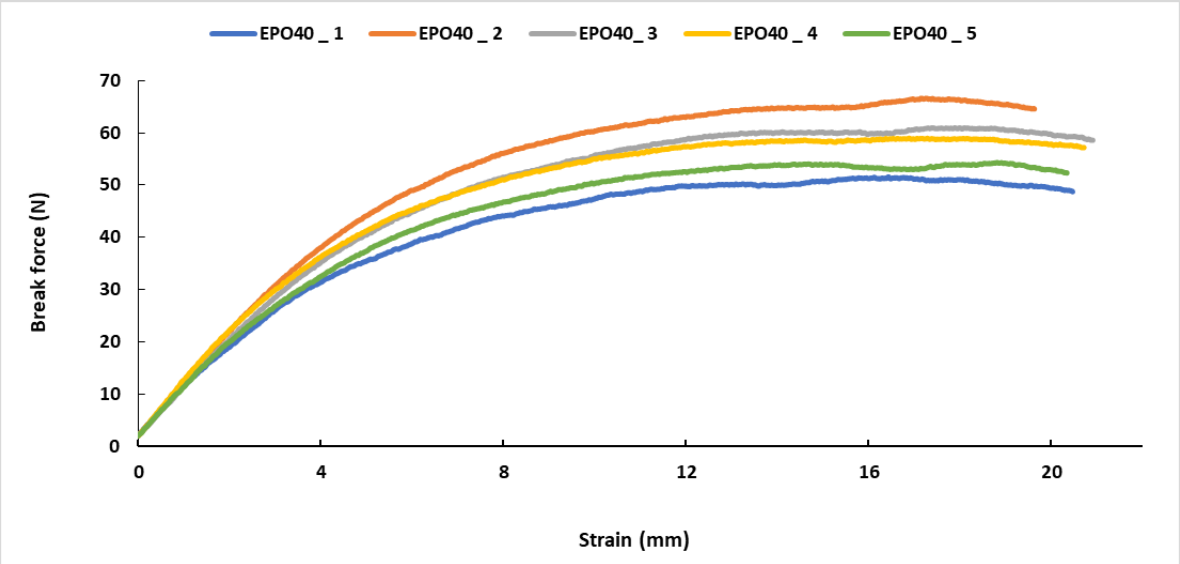

Figure 5.34. Flexural strength results of EPO40 samples

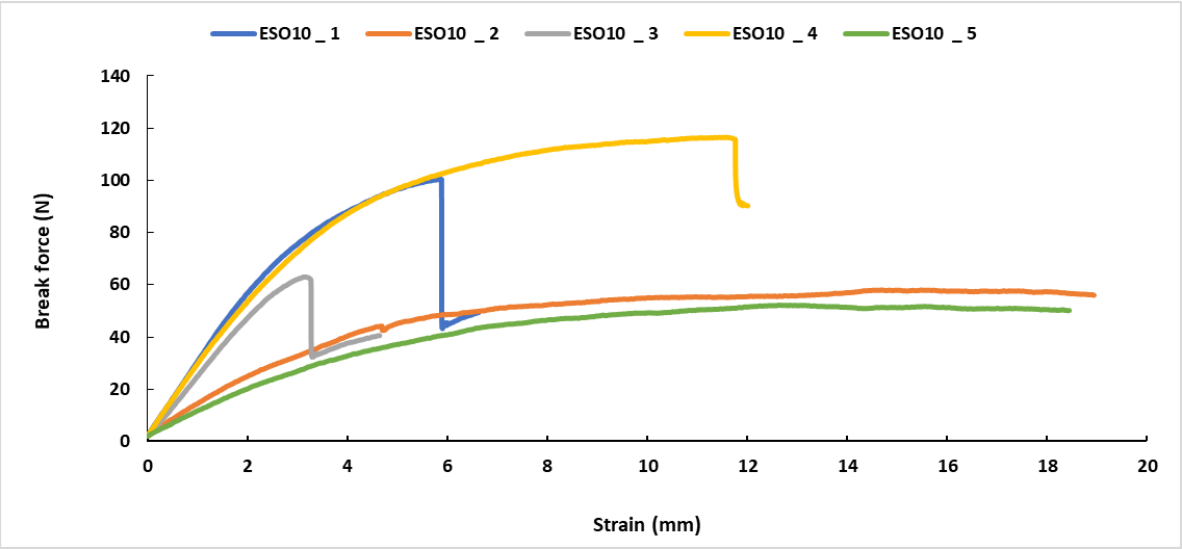

Figure 5.35. Flexural strength results of ESO10 samples

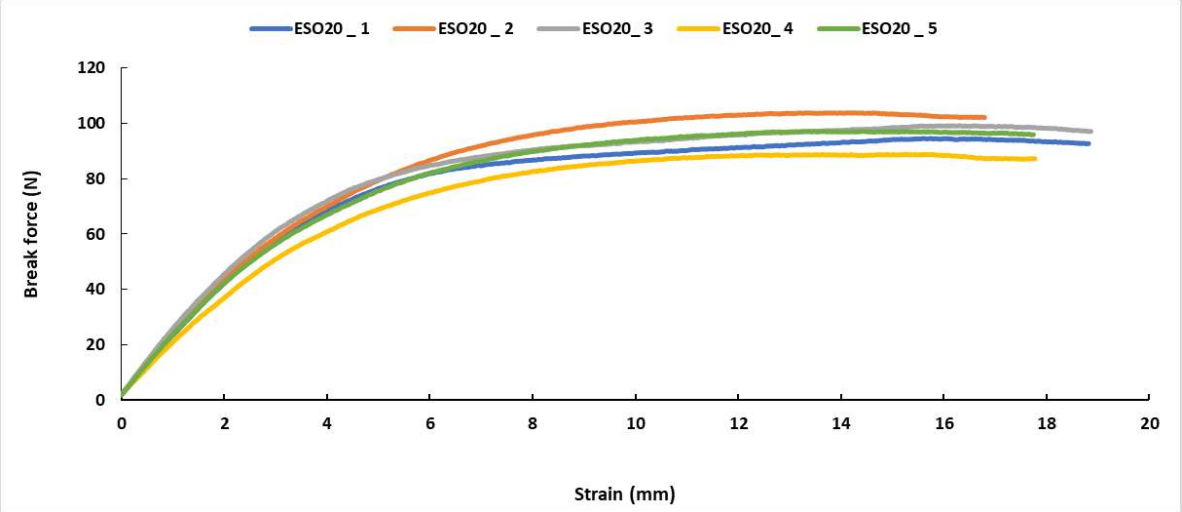

Figure 5.36. Flexural strength results of ESO20 samples

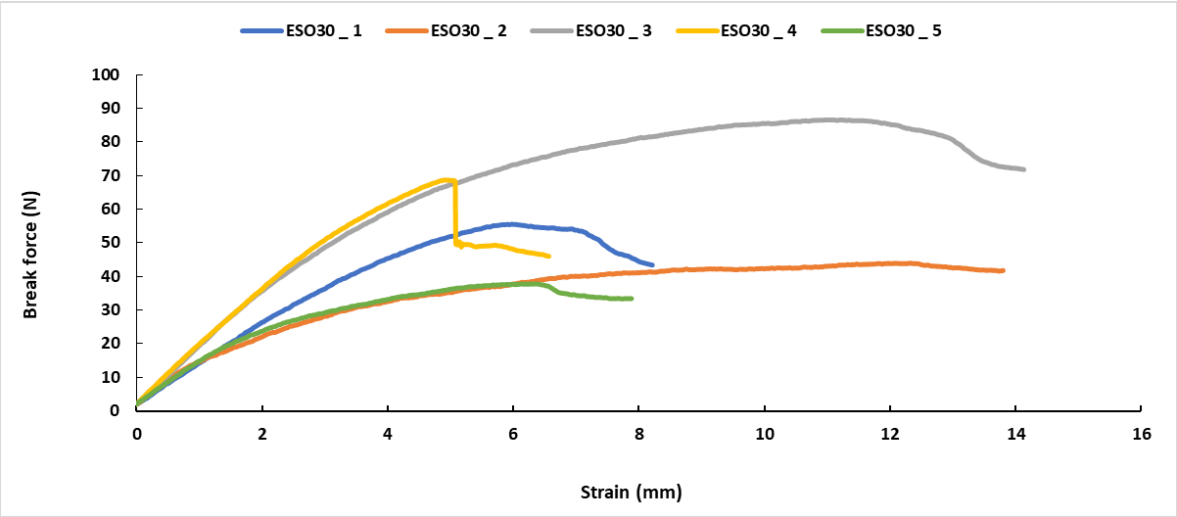

Figure 5.37. Flexural strength results of ESO30 samples

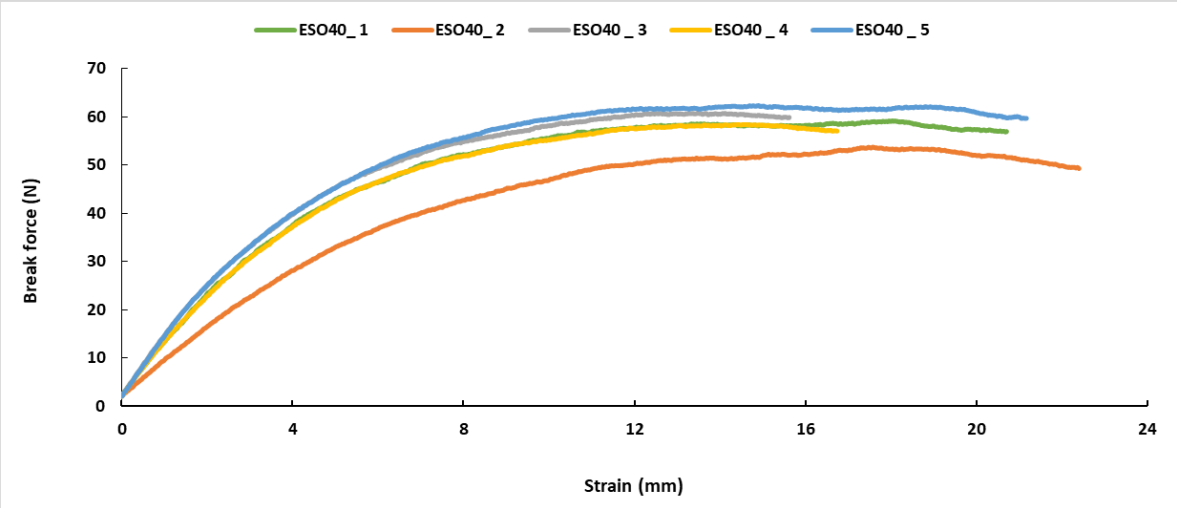

Figure 5.38. Flexural strength results of ESO40 samples

Table 5.6 indicates the differences in flexural strength and maximum force values between EPOXY and other biocomposite samples. While the flexural stress value for EPOXY was 56.33 MPa, the average force required for maximum fracture was 156.21 N. When the table is examined, the bending stress values closest to the EPOXY sample, except for the ESO sample, are seen in the samples with 10% oil added. Bending stress values gradually decrease as the oil ratio in the resin increases from 10% to 40%. This situation is parallel with the tensile test results. Moreover, this behaviour is also reflected in the maximum force values required to break the sample. Among the biocomposites, the sample with the closest bending stress and maximum strength to EPOXY was EFO10. In terms of bending stress, the EPO10 sample comes right after the EFO 10 in terms of value. The EPO30 sample was the sample with the highest bending stress value difference compared to EPOXY. The sample with the second lowest value is the ECO40 sample. The data presented in the studies in the literature also reflect that when the bioresin content exceeds 50%, it leads to a

significant decrement in the flexural characteristics and other mechanical characteristics for the samples (Ozkur et al., 2020; Wu and Li, 2018). In the study by Grishchuk and Karger-Kocsis (Grishchuk and Karger-Kocsis, 2011), 8.2 times lower flexural strength was observed as the AESO ratio increased to 75% compared to the sample using only vinylester resin. In a study using jute fiber (Manthey et al., 2013), it was stated that weak fiber-matrix interface adhesion also caused a decrease in bending strength. In addition, another study has also indicated that excessive plasticization occurs with a high percentage of commercial glycidyl ether-based diluent, excessive plasticization occurs, resulting in a much lower viscosity, which in turn results in a significant decrease in strength and modulus, which in turn inhibits the crosslinking process (Sahoo et al., 2015b).

Table 5.6. Differences in flexural strength and maximum force values

Biocomposite samples	**Difference of flexural strength compared to EPOXY sample (%)**	**Difference of maximum force compared to EPOXY sample (%)**
ECO10	-14.08	-39.05
ECO20	-23.12	-64.12
ECO30	-27.94	-77.49
ECO40	-33.19	-92.03
ECAO10	-18.69	-51.84
ECAO20	-22.60	-62.69
ECAO30	-27.71	-76.84
ECAO40	-36.05	-99.97
EFO10	-9.92	-27.52
EFO20	-19.35	-53.66
EFO30	-26.87	-74.51
EFO40	-32.94	-91.35
EPO10	-11.82	-32.79
EPO20	-23.20	-64.33
EPO30	-38.14	-105.78
EPO40	-35.23	-97.70
ESO10	-28.20	-78.20
ESO20	-21.45	-59.47
ESO30	-35.23	-97.70
ESO40	-35.09	-97.31

5.4. Charpy Impact Test Results

Figure 5.39 to 5.43 displays the Charpy impact test results of ECO, ECAO, EFO, EPO and ESO samples. The impact energy values for ECO10, ECO20, ECO30, and ECO40 are 9.5±2.38 J, 33.75±10.44 J, 23.75±4.11 J, and 15.5±7.59 J, respectively. The impact energy values for ECAO10, ECAO20, ECAO30, and ECOA40 samples were found to be 11.5±1.29 J, 14.75±3.59 J, 17.25±3.77 J, and 11.75±2.99 J, respectively. The impact energy values for EFO10, EFO20, EFO30, and EFO40 samples were determined as 16±2.0 J, 35.5±5.57 J, 24.5±9.00 J, and 21.5±6.45 J, respectively. The impact energy results for EPO10, EPO20, EPO30, and EPO40 samples were 39±12.91 J, 11.25±4.35 J, 18±2.83 J, and 32.2.5±3.9 J, respectively. Impact energy results revealed that ESO10, ESO20, ESO30, and ESO40 samples had values of 40±6.73 J, 43±8.87 J, 37.75±3.3 J, and 12±1.83 J, respectively. The impact energy value for the EPOXY sample was found to be 12.5+2.89 J.

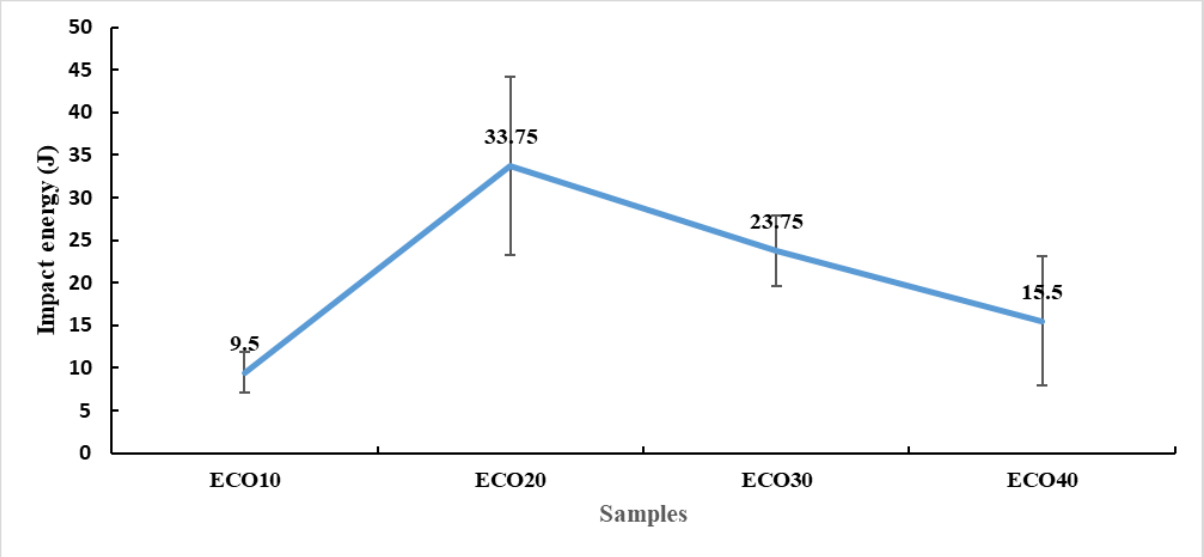

Figure 5.39. Impact test results of ECO samples

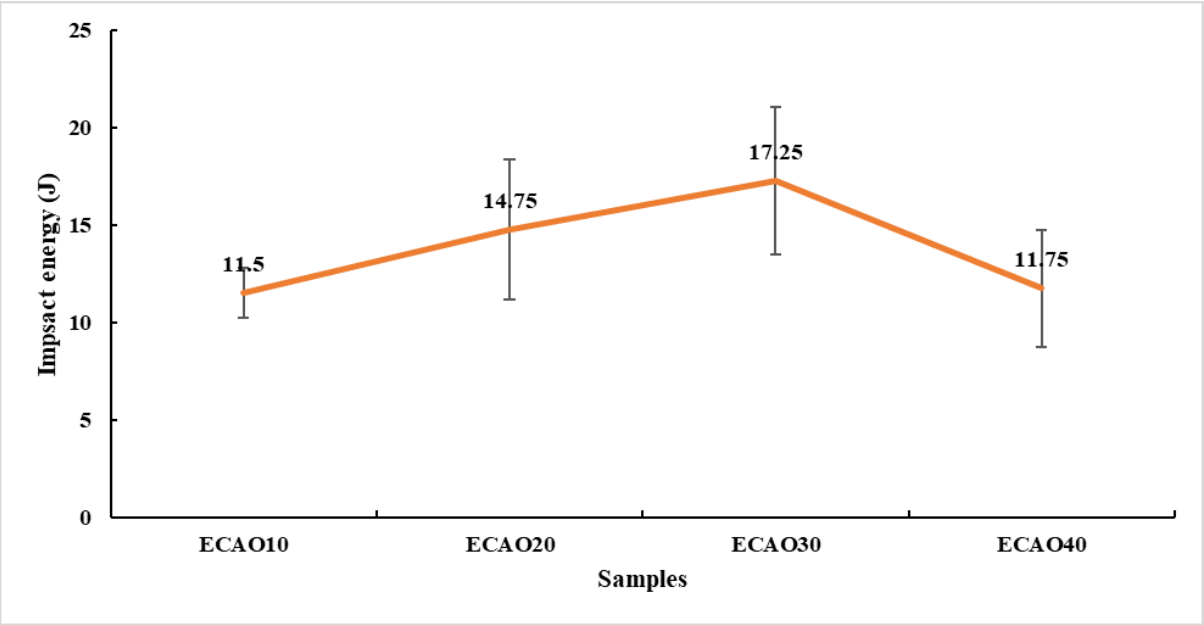

Figure 5.40. Impact test results of ECAO samples

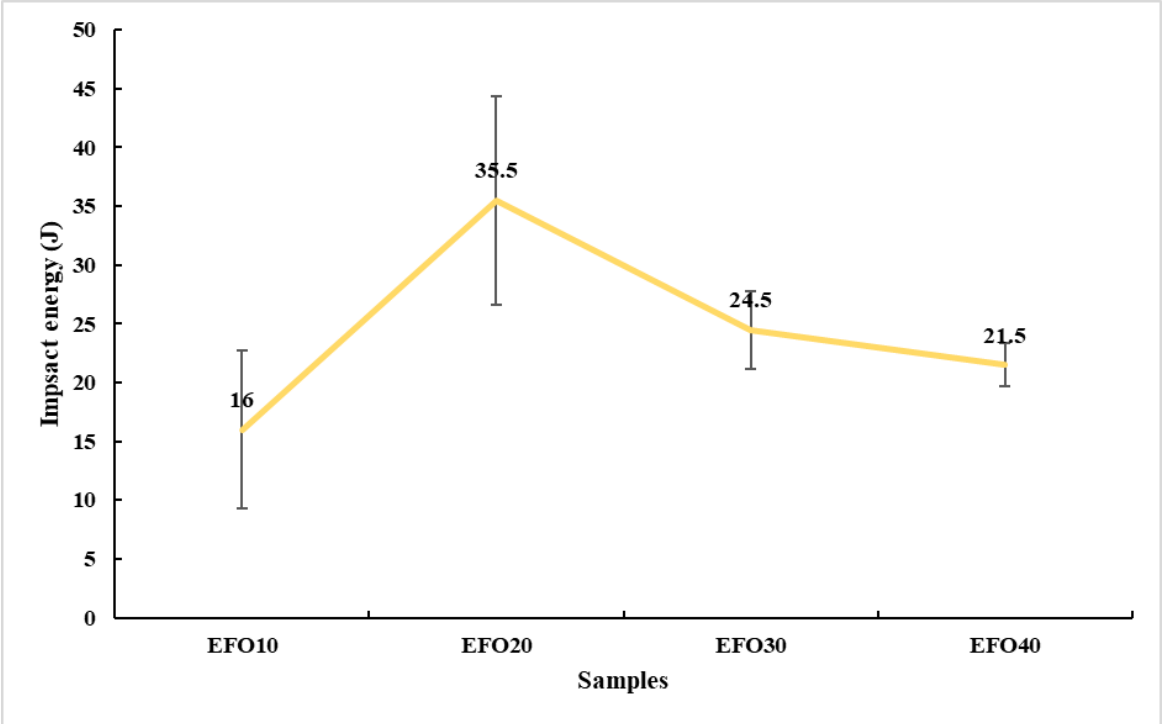

Figure 5.41. Impact test results of EFO samples

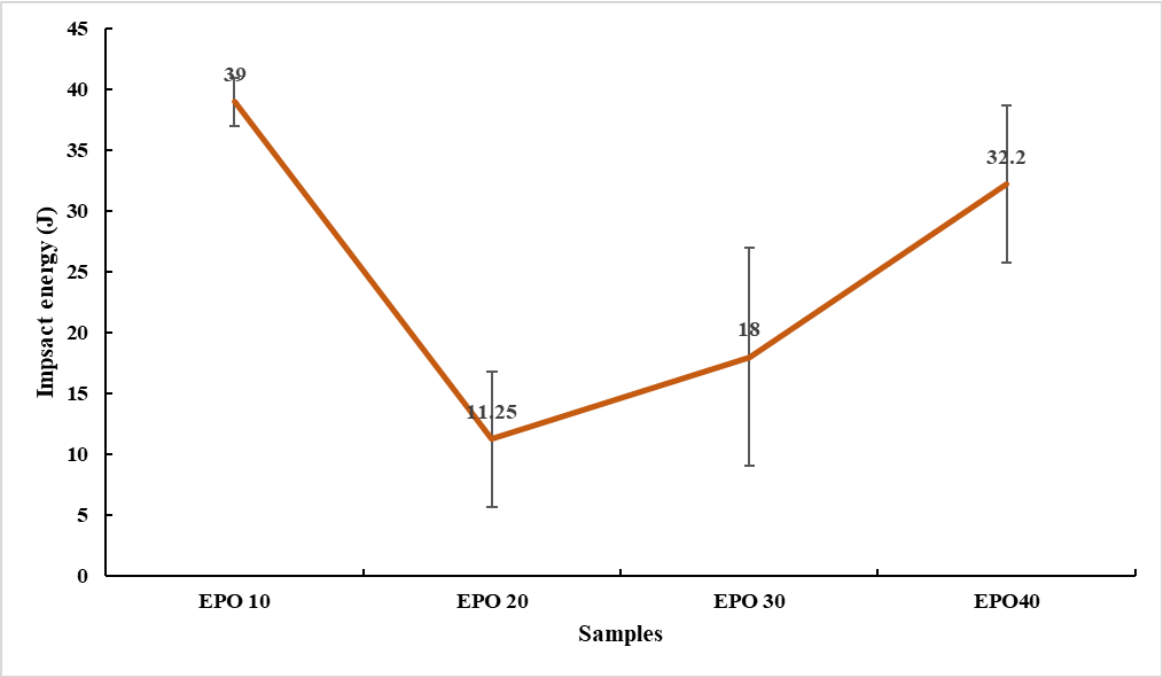

Figure 5.42. Impact test results of EPO samples

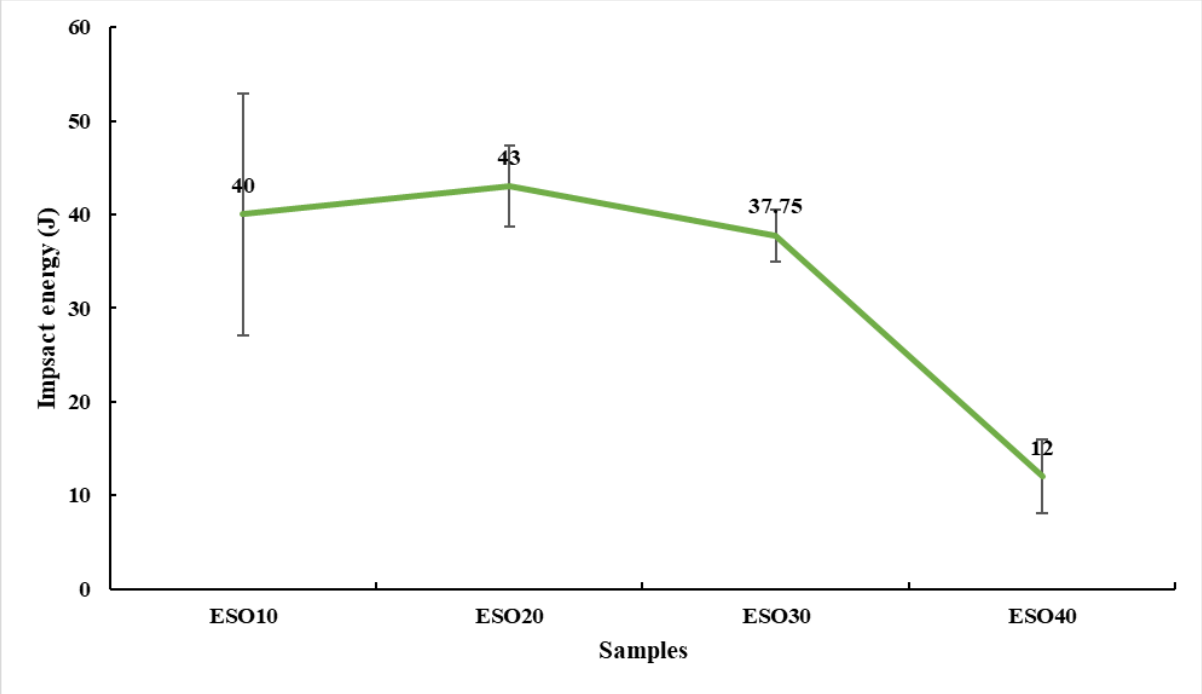

Figure 5.43. Impact test results of ESO samples

Table 5.7 indicates the differences in Charpy impact energy of ECO, ECAO, EFO, EPO and ESO samples to EPOXY sample. When the change values in the table are observed, the biggest difference in the impact energy value compared to EPOXY is seen in the EFO samples. In ESO samples, except for the ESO40 sample, the impact energy value is at a competitive level with the EFO samples with a 200% increase. The least increase among biocomposites is observed in ECAO samples. The sample with the most increased impact energy value compared to the EPOXY sample

is the ESO20 sample with a rate of +244%, while the sample with the most decreased energy value is the ECO10 sample with a rate of -24%.

When the impact energy values are examined in terms of vegetable oil ratios, it is seen that the impact energy values increase as they increase from 10% to 20% and the values decrease after 20% vegetable oil ratio. ECAO30 and EPO30 samples, which showed an increase compared to 20% vegetable oil content, are exceptions to this situation. When compared at 20% vegetable oil content, the ESO20 sample provided the highest impact energy increase. While the increase in the proportion of vegetable oil has a positive effect on the absorbed energy up to a certain level, when this level is exceeded, the effect factor gradually decreases. Epoxy resin materials generally exhibit brittle material properties. These differences between the absorbed energies are correlated to the fact that the bio-resin is not evenly distributed in the fabric and whether the oils are completely mixed with the resin.

Table 5.7. Differences in impact energy values to EPOXY samples

Biocomposites	Difference of impact energy compared to EPOXY sample (%)
ECO10	-24
ECO20	+170
ECO30	+90
ECO40	+24
ECAO10	-8
ECAO20	+18
ECAO30	+38
ECAO40	-6
EFO10	+28
EFO20	+184
EFO30	+96
EFO40	+72
EPO10	+212
EPO20	-10
EPO30	+44
EPO40	+157.6
ESO10	+220
ESO20	+244
ESO30	+202
ESO40	-4

Figure 5.44 presents the impact strength results of samples. In parallel with the results in Table 5.7, the highest impact strength values were obtained in the ESO20 sample. The lowest impact strength value occurred in the ECO10 sample, as expected. ECO samples, except ECO10, have 2.7 times, 1.9 times, and 1.24 times higher impact strength values than EPOXY for ECO20, ECO30, and ECO40 samples, respectively. ECAO samples reached 1.18 times and 1.38 times higher impact strength values than EPOXY in ECAO20 and ECAO30 samples, respectively, except for ECA10 and ECAO40. EFO samples had 1.28 times, 2.84 times, 1.96 times and 1.72 times higher impact strength values in EFO10, EFO20, EFO30 and EFO40 samples, respectively, compared to EPOXY. Compared to EPOXY, EPO samples had 3.12 times, 1.44 times and 2.576 times higher impact strength values in EPO10, EPO30 and EPO40 samples, respectively, except for EPO20. Compared to EPOXY, ESO samples had 3.2 times, 3.44 times and 3.02 times higher impact strength values in ESO10, ESO20 and ESO30 samples, except ESO40, respectively.

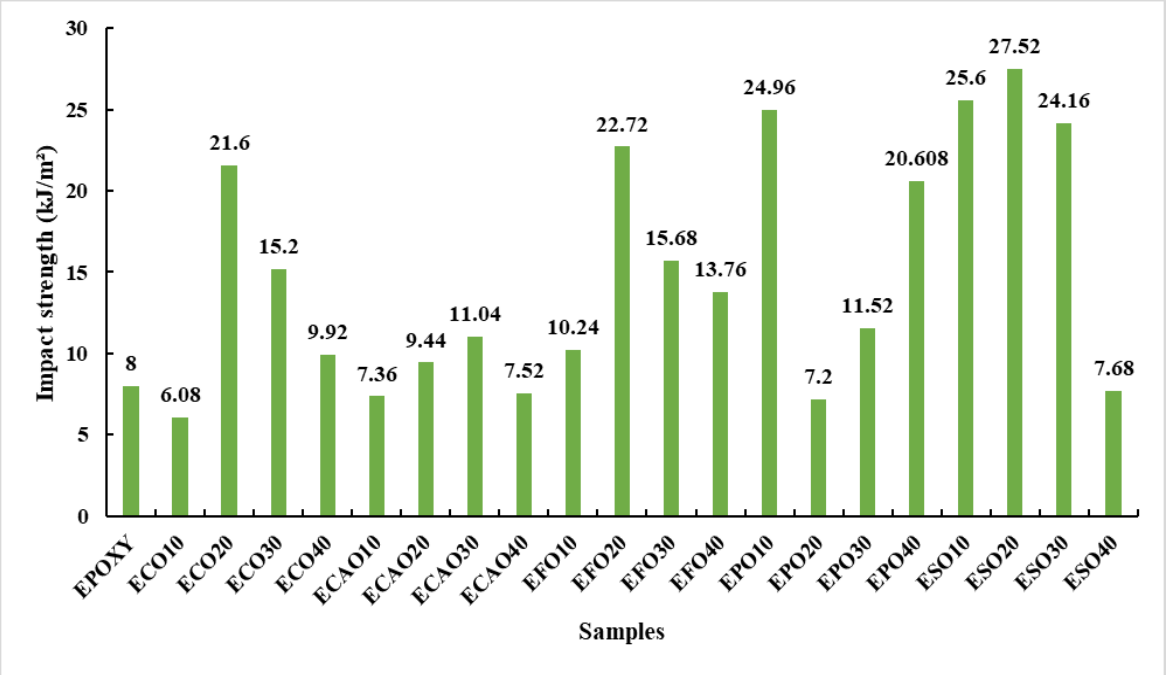

Figure 5.44. Impact strength results of samples

Impact test results show that adding soybean oil to the resin significantly affected the amount of energy absorbed by the bio resin compared to epoxy resin, while adding canola oil to the resin had a smaller effect on the energy absorbed by the bio resin compared to epoxy compared to other oils.

Figure 5.45 to Figure 5.65 indicate the tensile graphs after the test. The toughness of the samples will be calculated according to these graphs. While the toughness of materials can be determined by impact tests, the area under the stress-strain curve reflects the total energy of the material before it breaks. When calculating the area under the stress-strain curve, polynomial equations of the seventh degree were defined on the graphs and calculations were carried out with

the limits of the graphs. In addition, these graphs are graphs that reflect the highest average values of 5 samples tested in each combination. Figure 5.66 to Figure 5.86 indicate the toughness graphs. The toughness value was calculated to equation 5.1.

$$\text{Toughness}(J/m^3) = \int_0^{\varepsilon} y dx \quad (5.1)$$

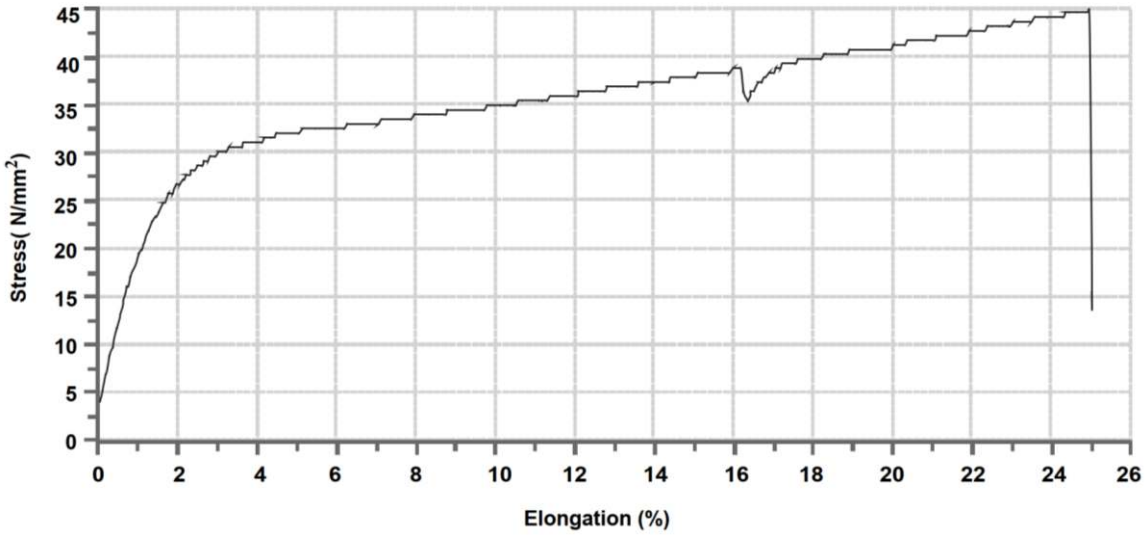

Figure 5.45. Tensile graph of EPOXY

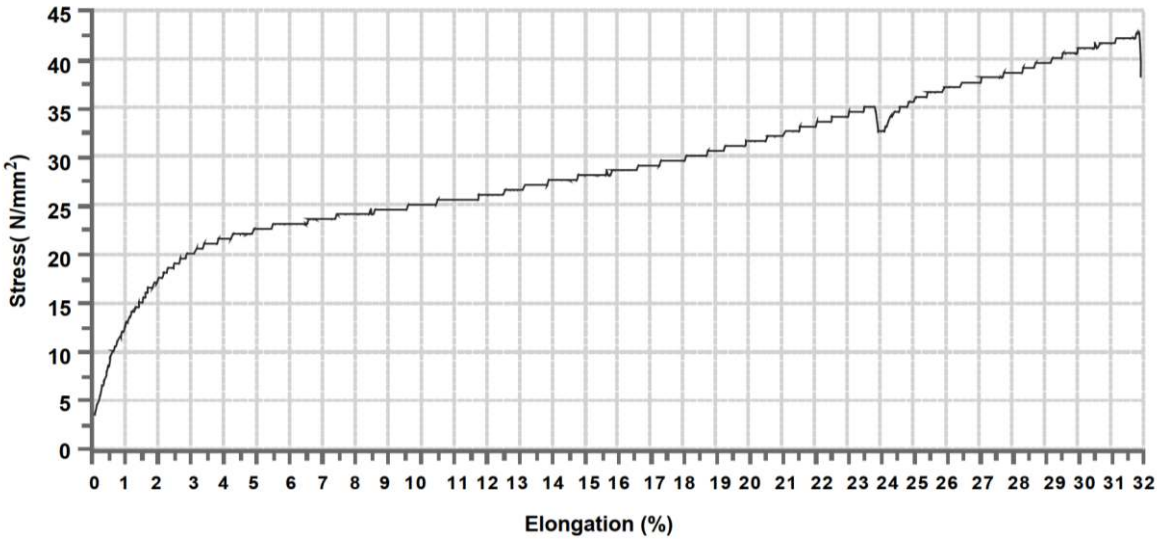

Figure 5.46. Tensile graph of ECO10 samples

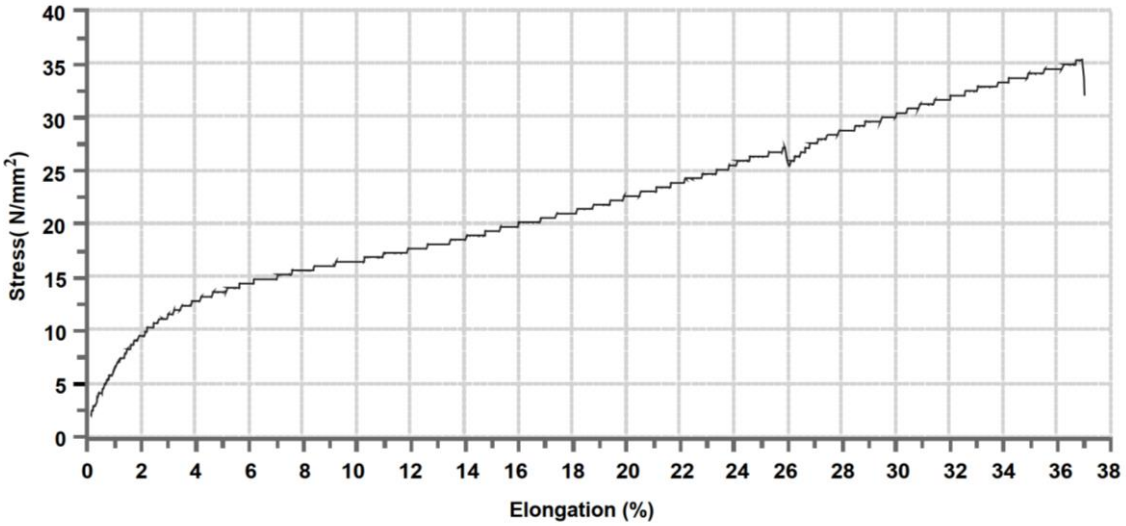

Figure 5.47. Tensile graph of ECO20 samples

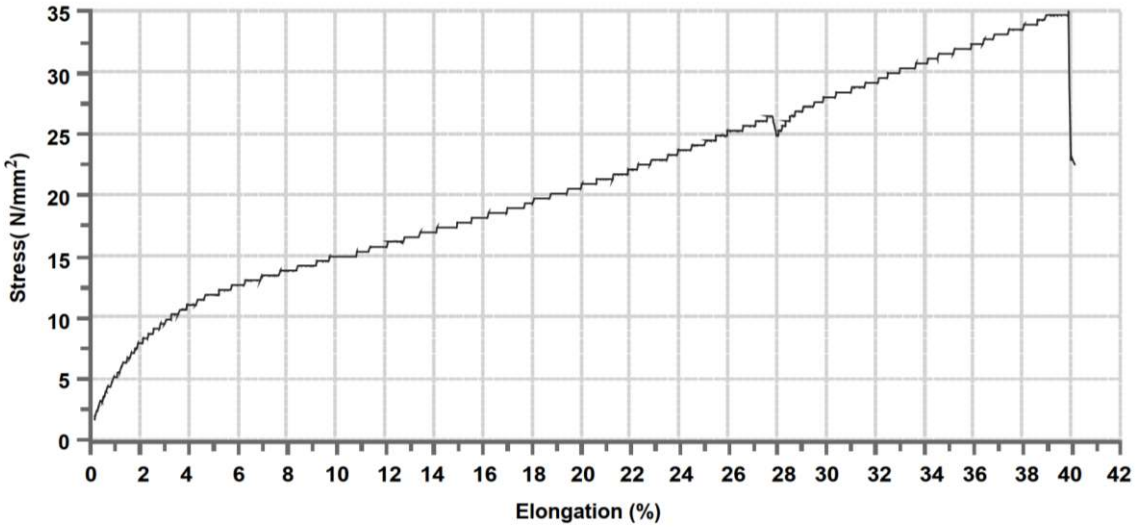

Figure 5.48. Tensile graph of ECO30 samples

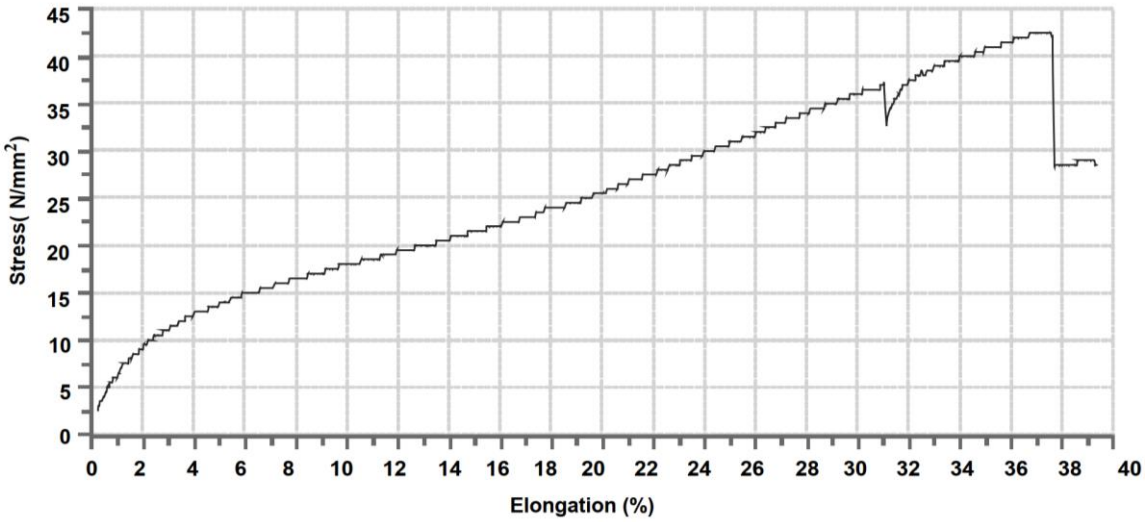

Figure 5.49. Tensile graph of ECO40 samples

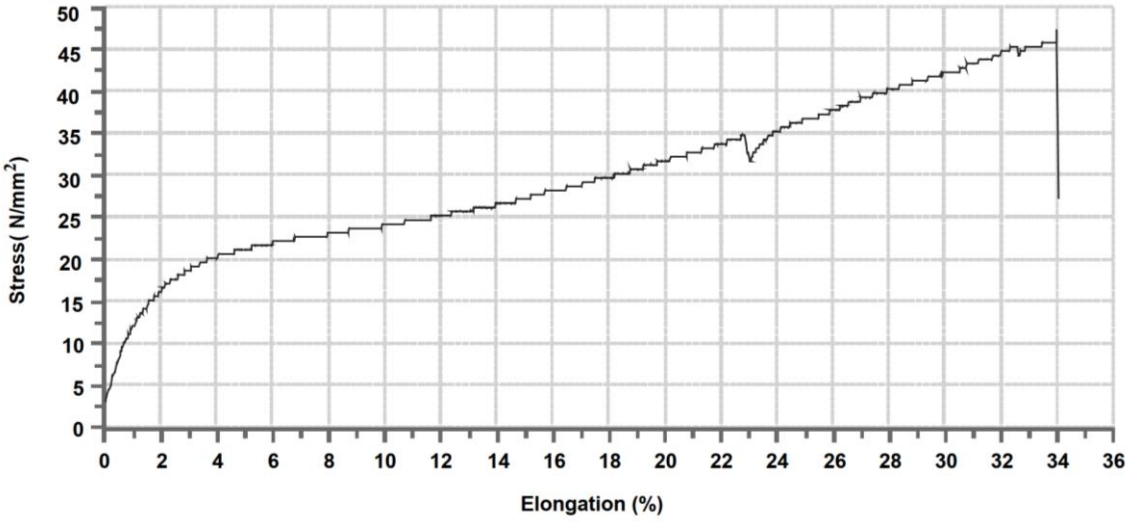

Figure 5.50. Tensile graph of ECAO10 samples

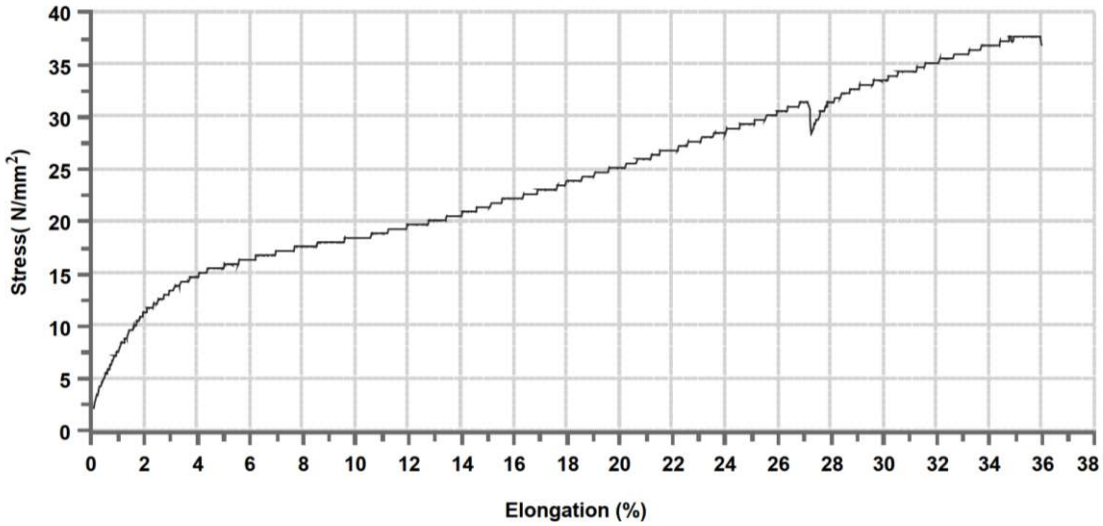

Figure 5.51. Tensile graph of ECAO20 samples

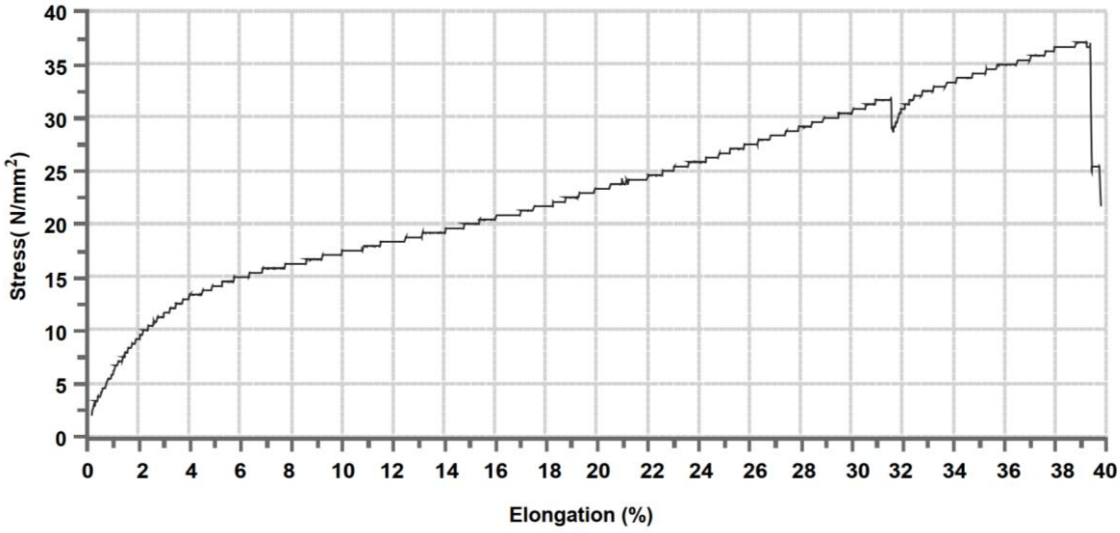

Figure 5.52. Tensile graph of ECAO30 samples

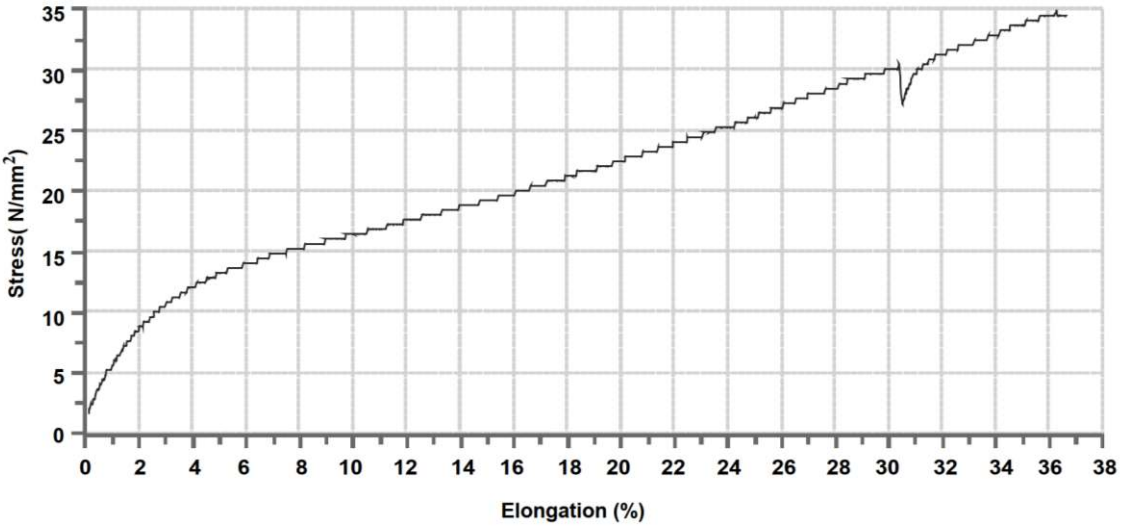

Figure 5.53. Tensile graph of ECAO40 samples

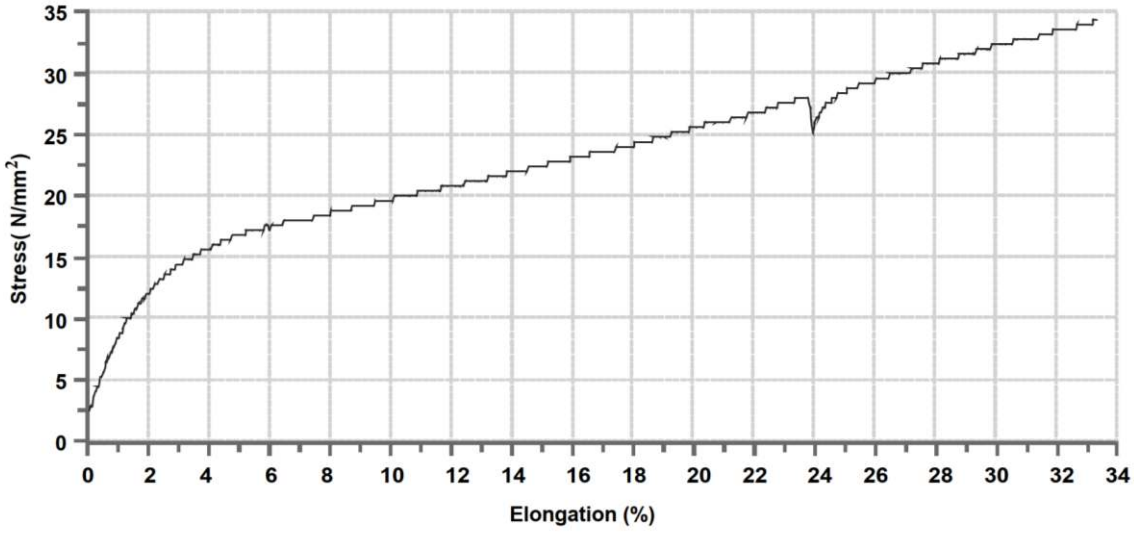

Figure 5.54. Tensile graph of EFO10 samples

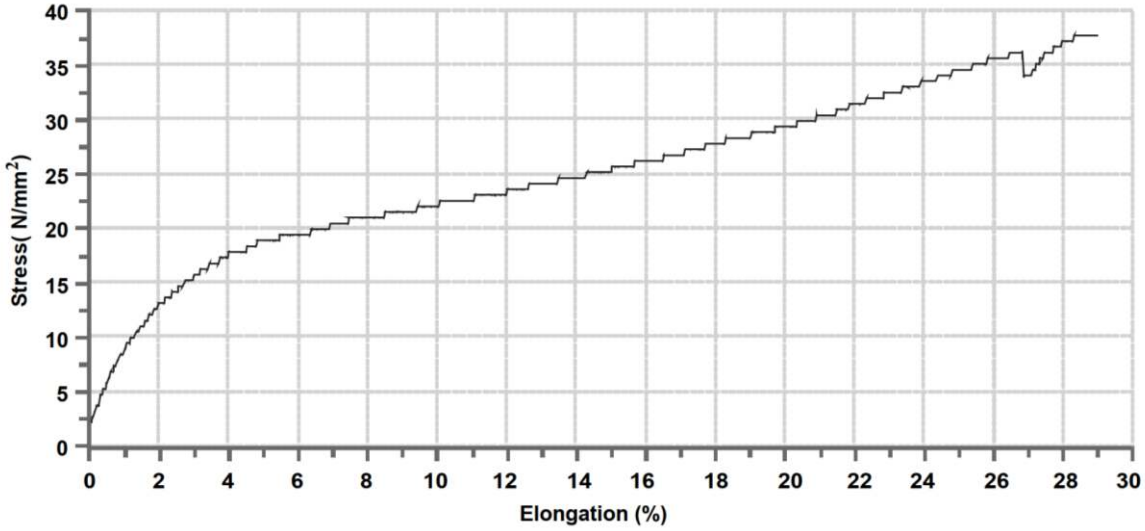

Figure 5.55. Tensile graph of EFO20 samples

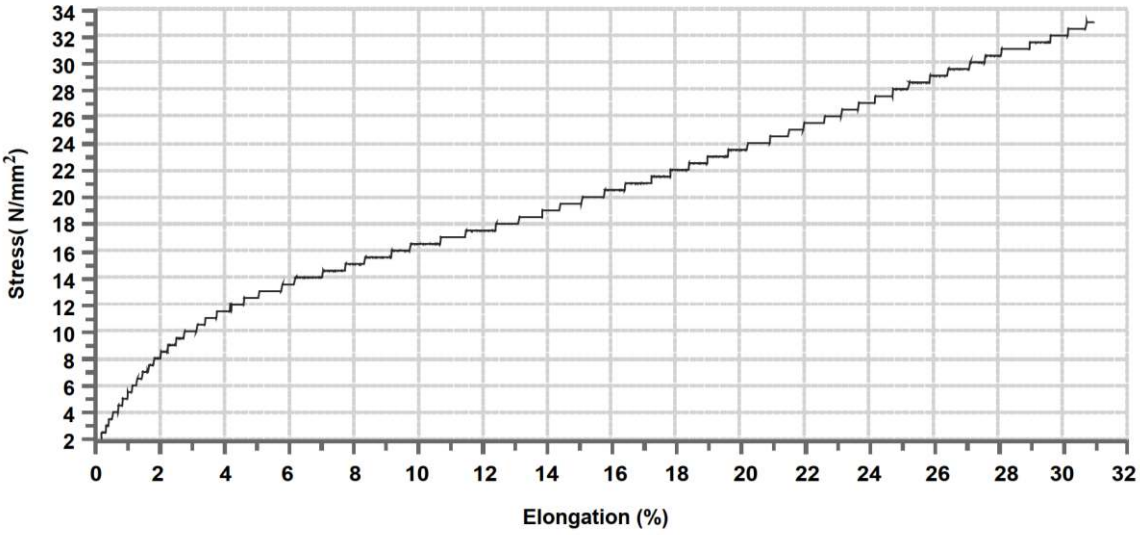

Figure 5.56. Tensile graph of EFO30 samples

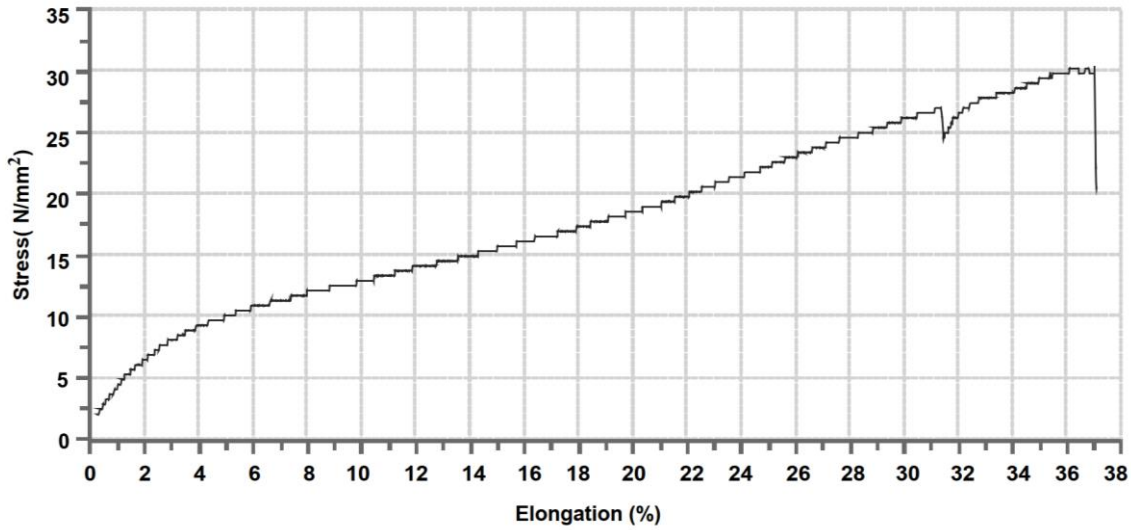

Figure 5.57. Tensile graph of EFO40 samples

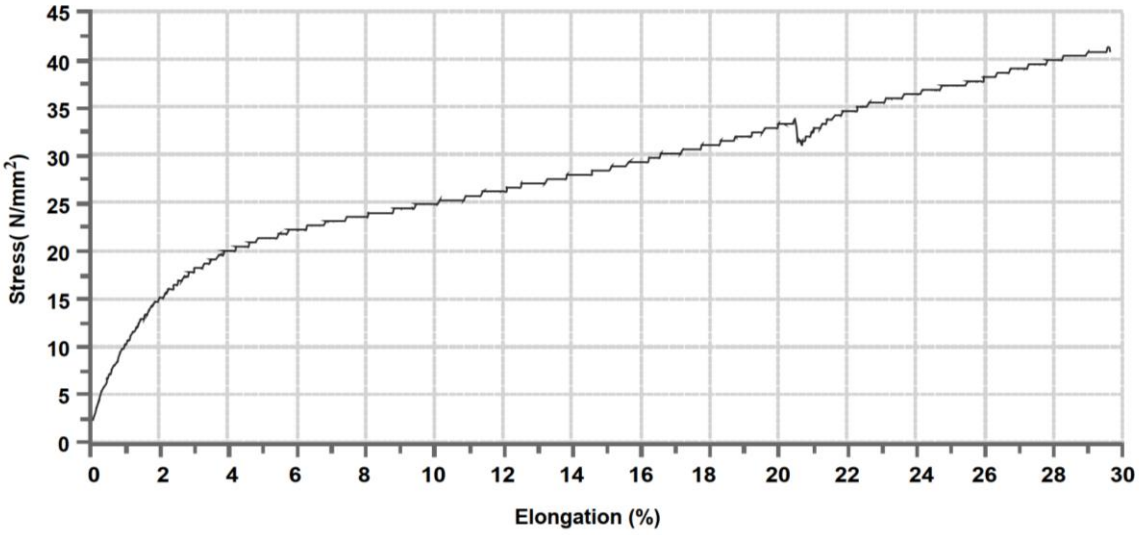

Figure 5.58. Tensile graph of EPO10 samples

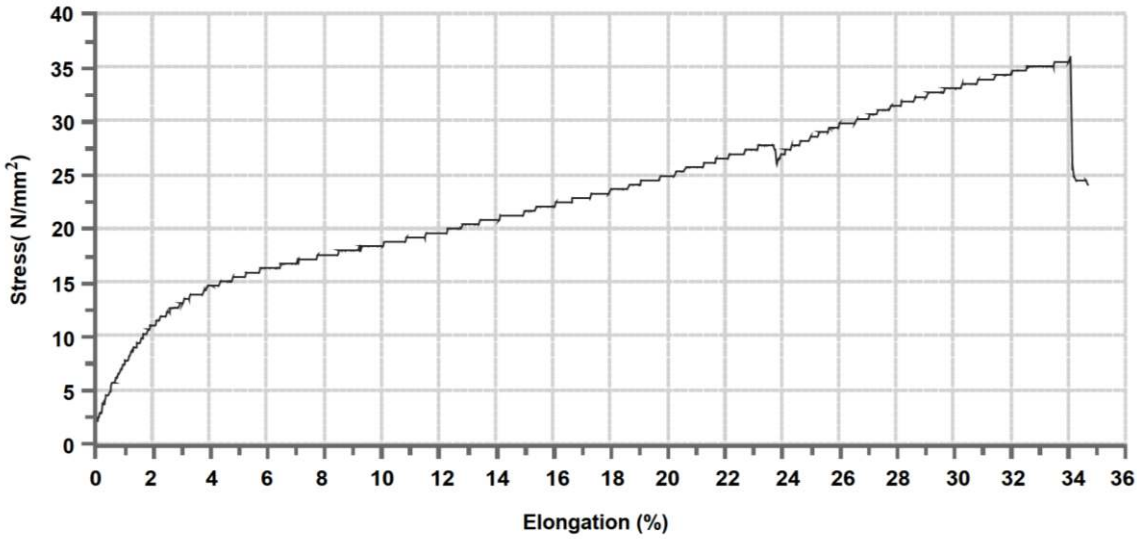

Figure 5.59. Tensile graph of EPO20 samples

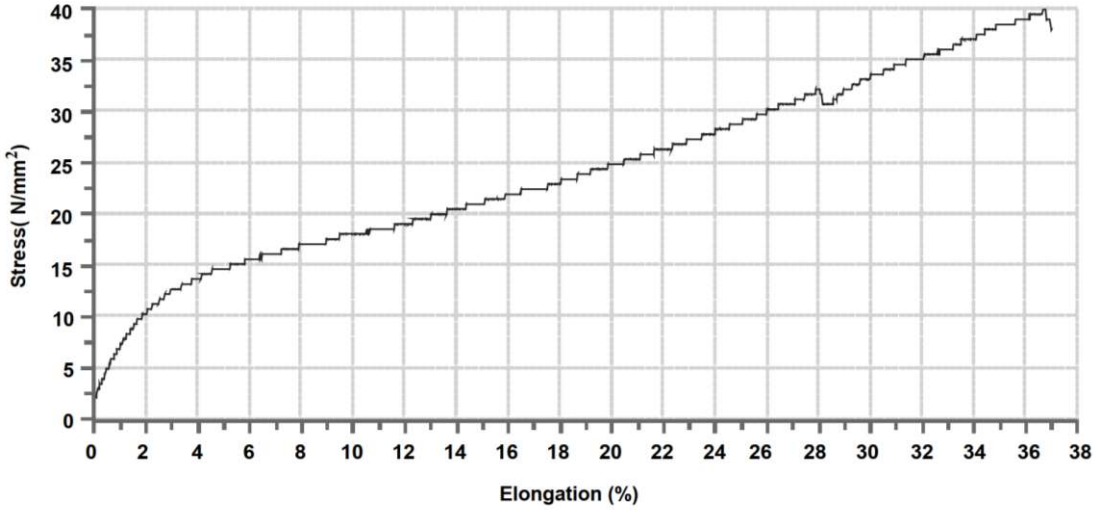

Figure 5.60. Tensile graph of EPO30 samples

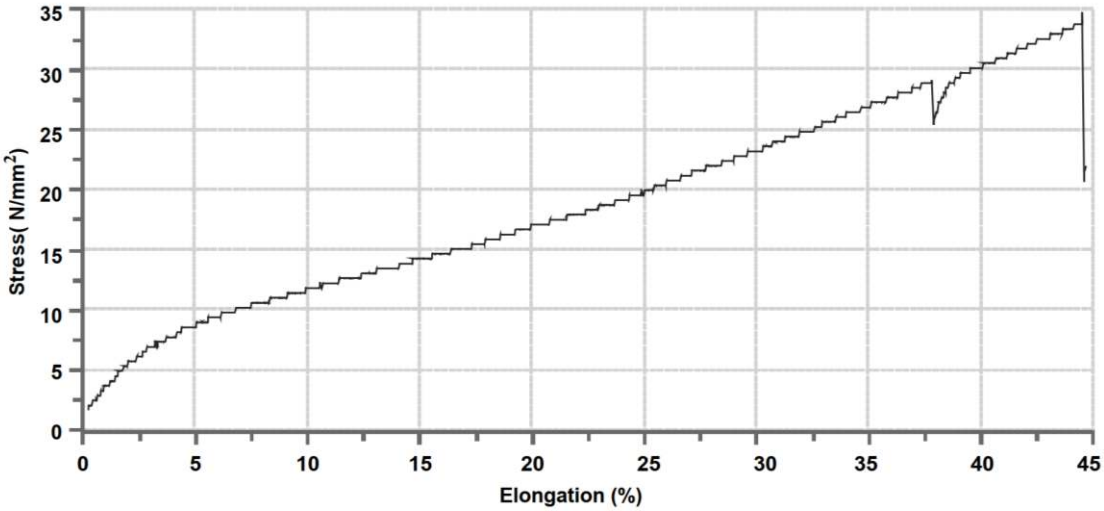

Figure 5.61. Tensile graph of EPO40 samples

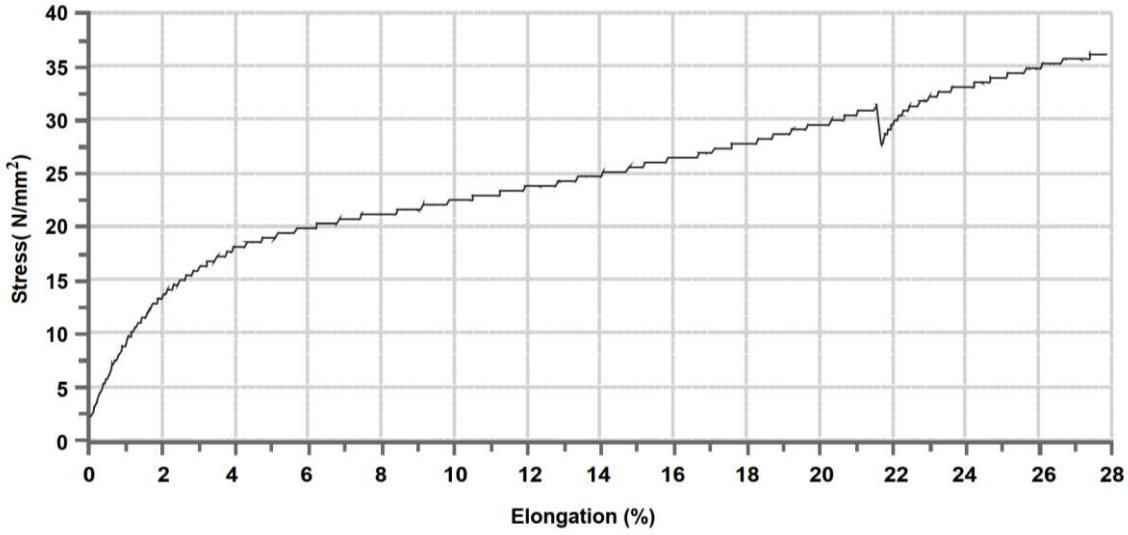

Figure 5.62. Tensile graph of ESO10 samples

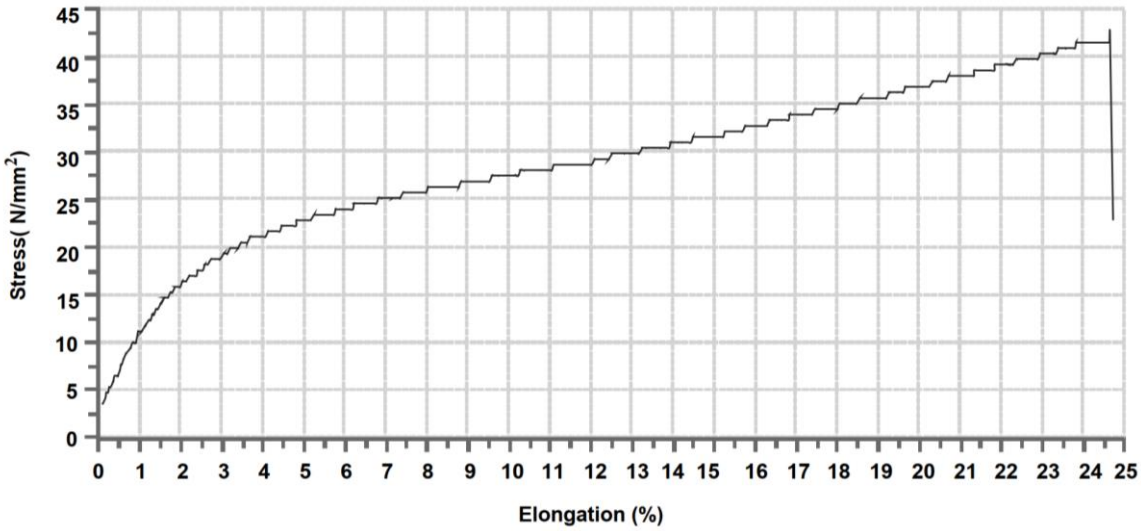

Figure 5.63. Tensile graph of ESO20 samples

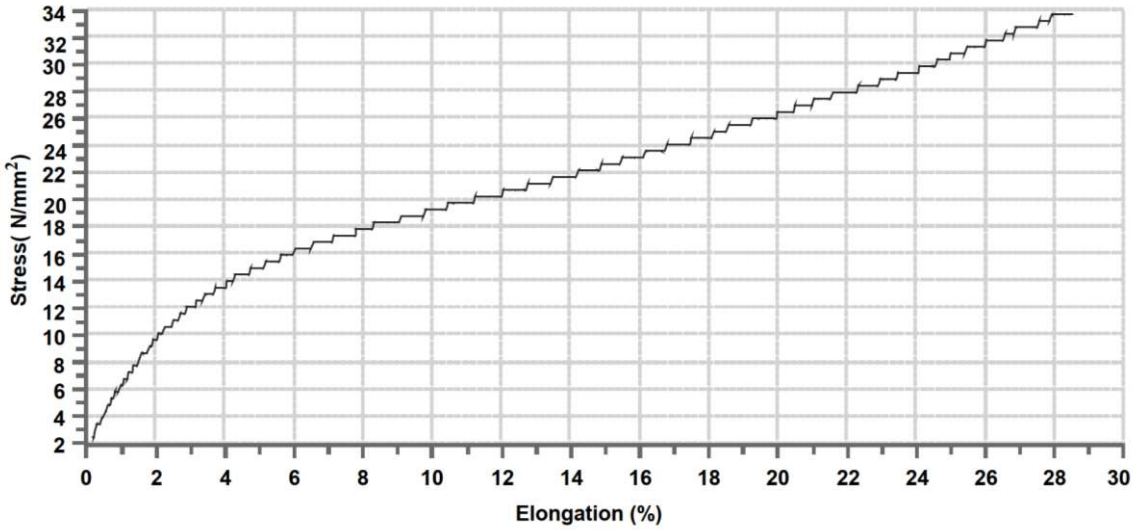

Figure 5.64. Tensile graph of ESO30 samples

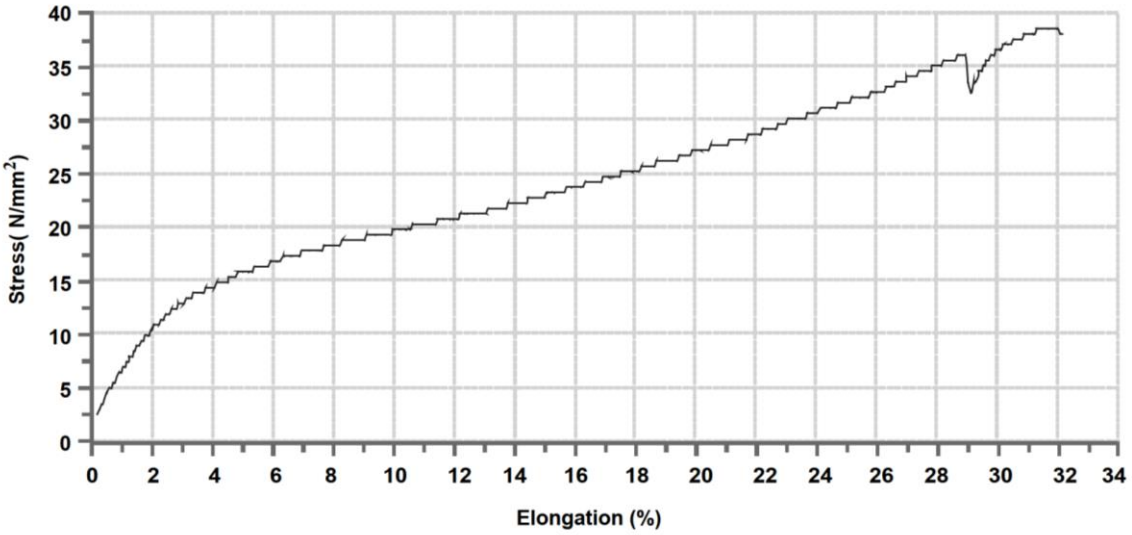

Figure 5.65. Tensile graph of ESO40 sample

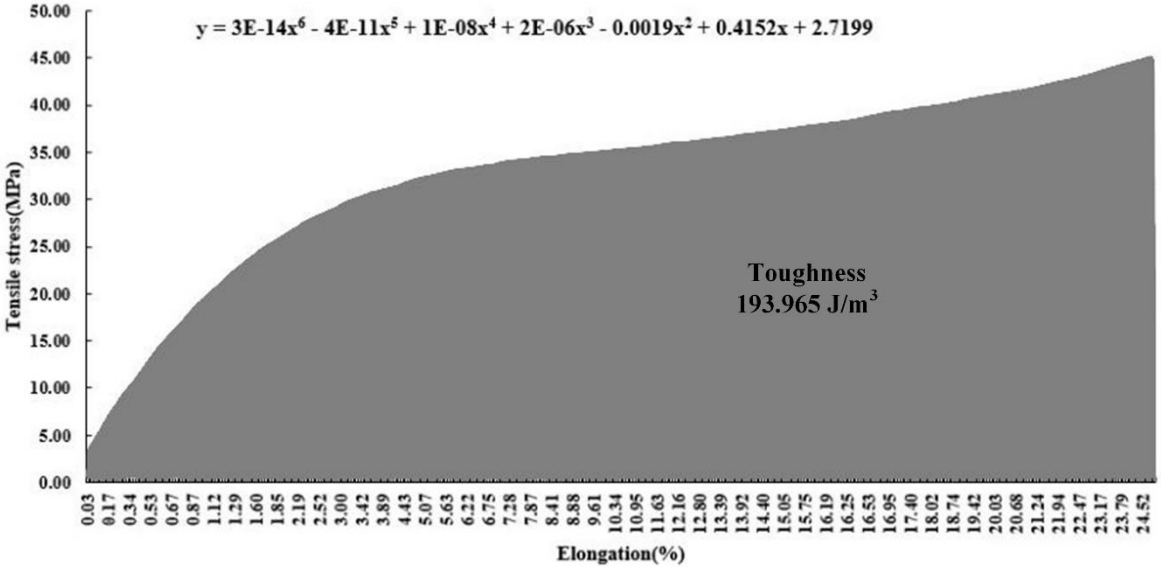

Figure 5.66. Toughness graph of EPOXY sample

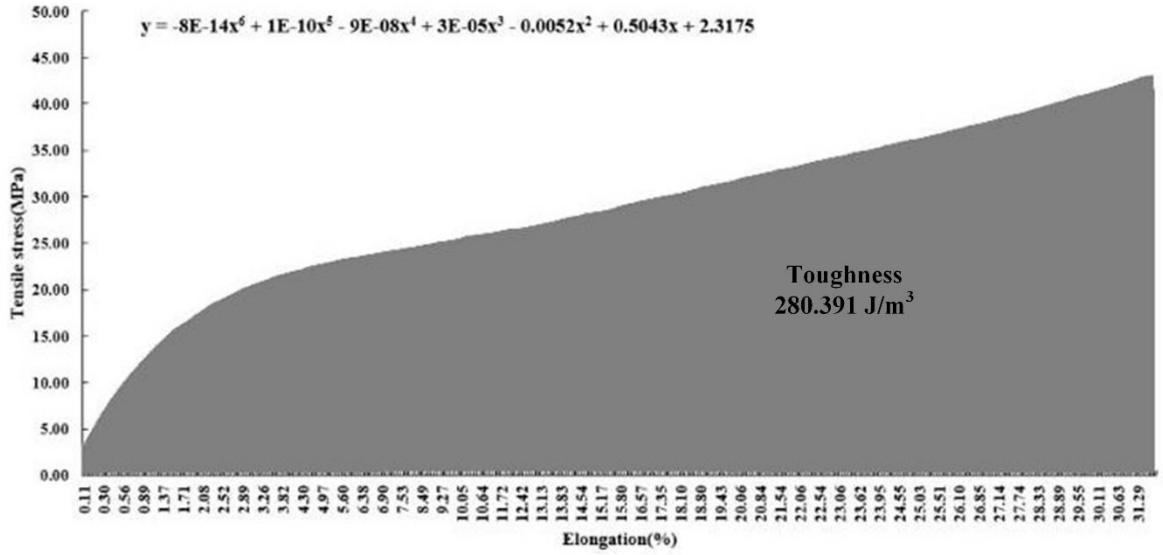

Figure 5.67. Toughness graph of ECO10 sample

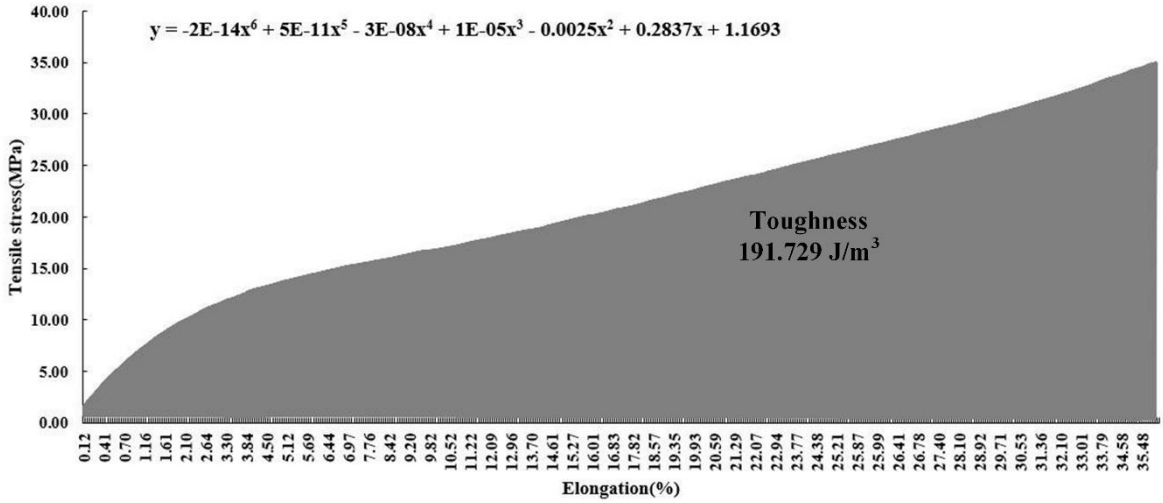

Figure 5.68. Toughness graph of ECO20 sample.

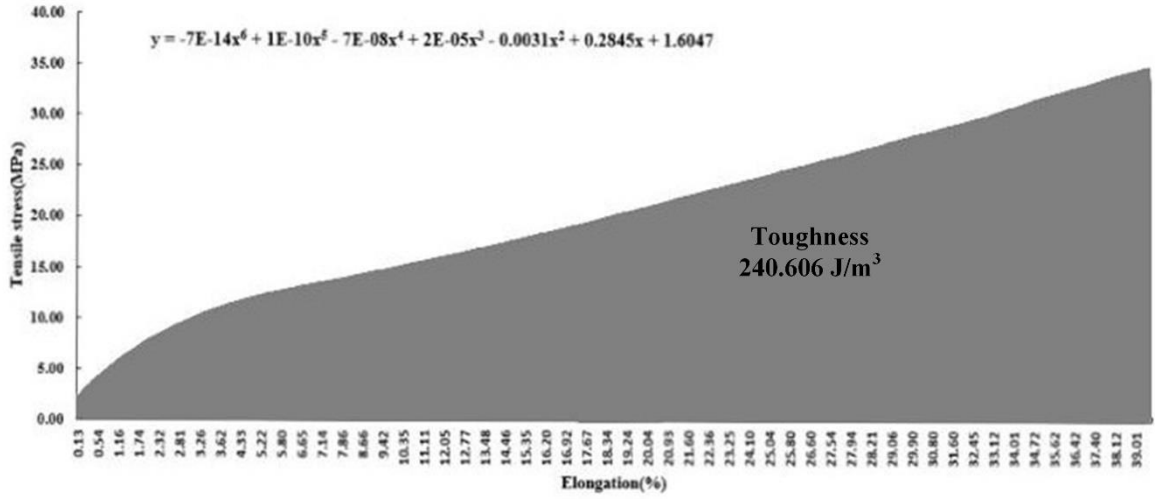

Figure 5.69. Toughness graph of ECO30 sample

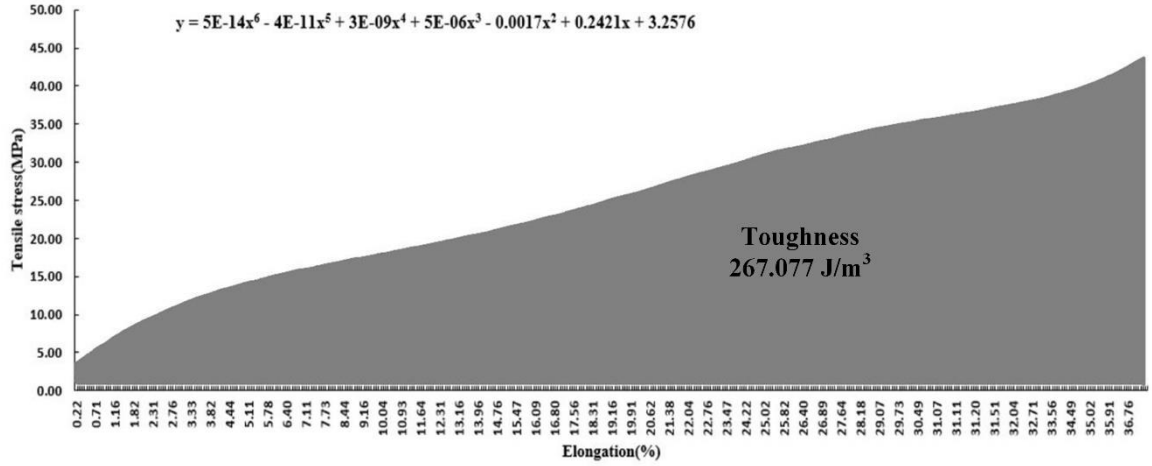

Figure 5.70. Toughness graph of ECO40 sample

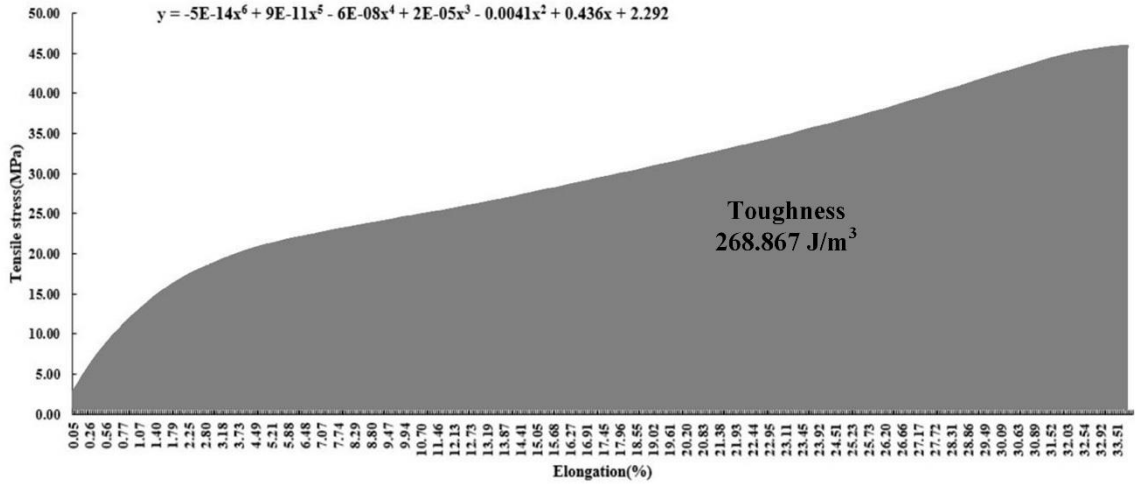

Figure 5.71. Toughness graph of ECAO10 sample

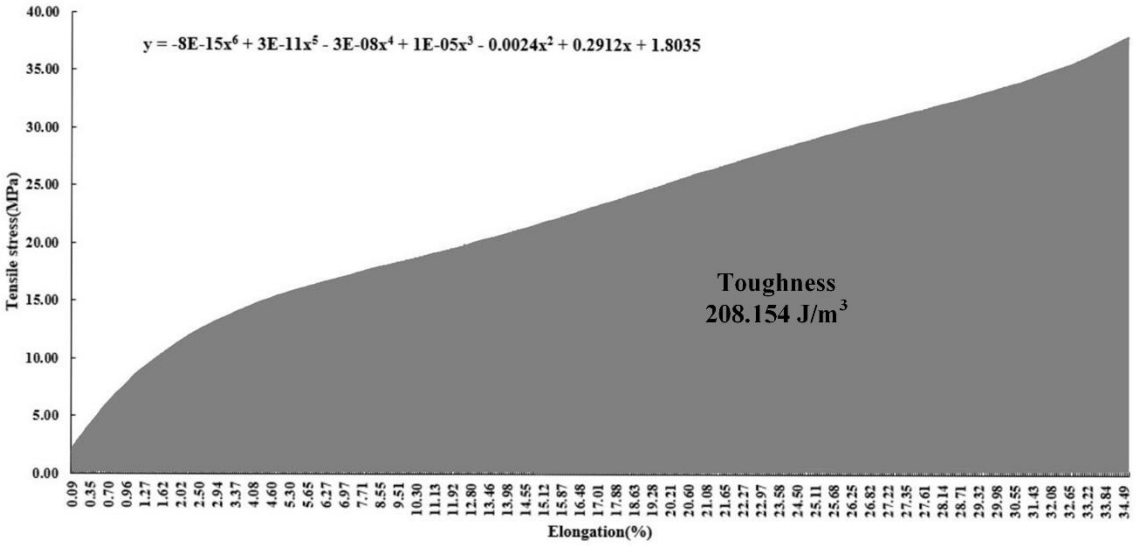

Figure 5.72. Toughness graph of ECAO20 sample

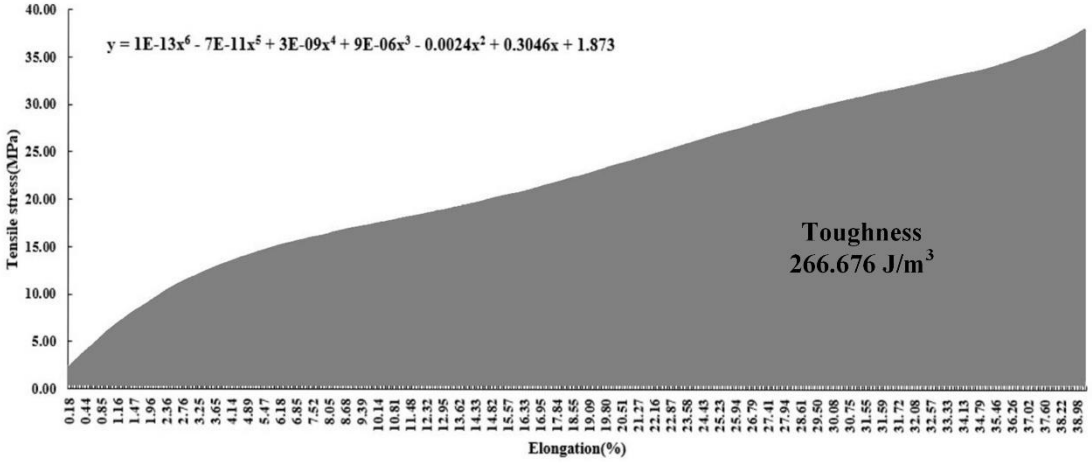

Figure 5.73. Toughness graph of ECAO30 sample

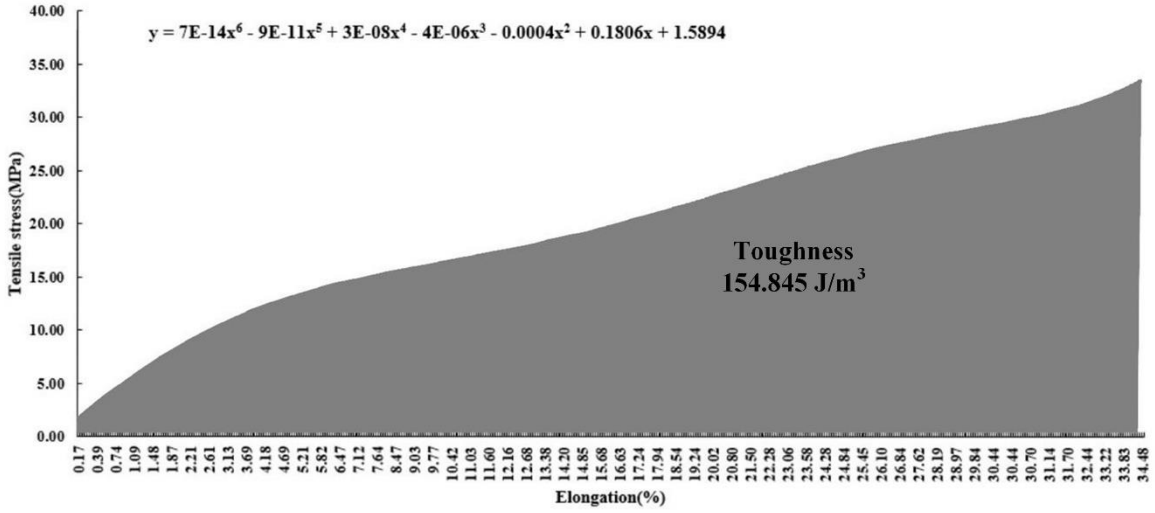

Figure 5.74. Toughness graph of ECAO40 sample

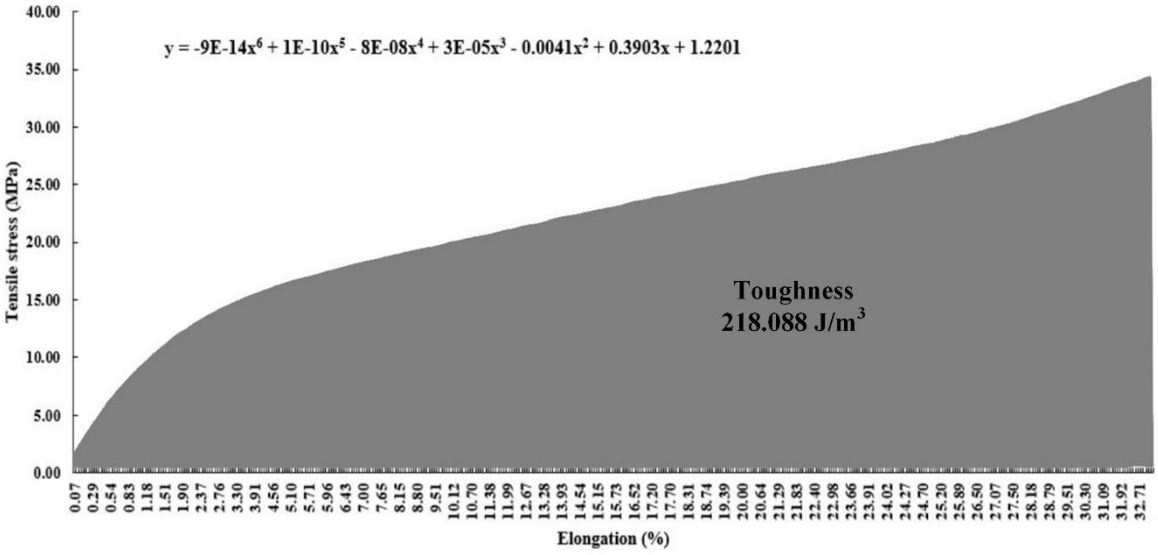

Figure 5.75. Toughness graph of EFO10 sample

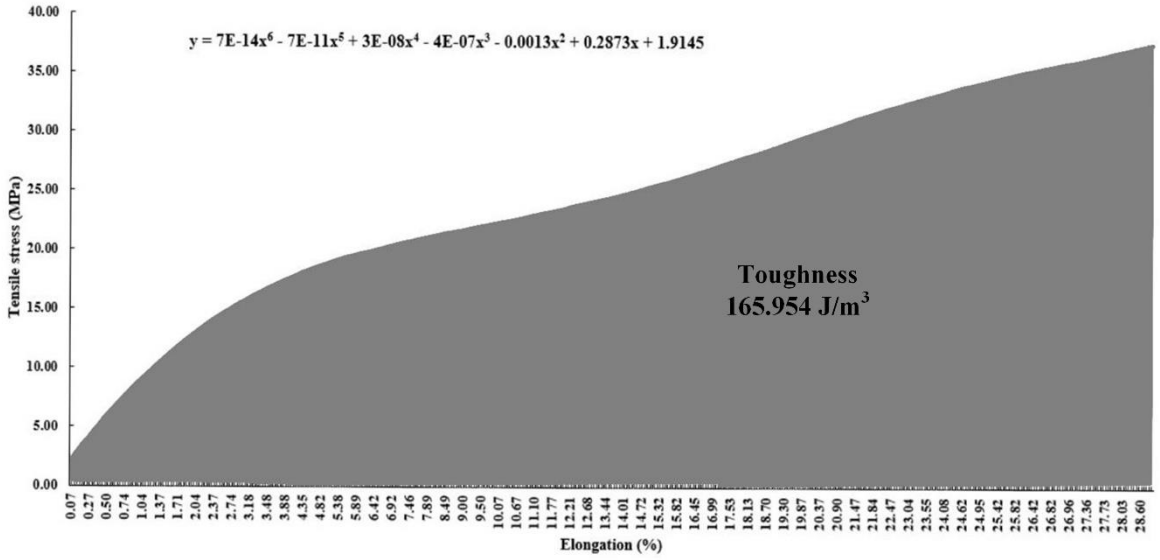

Figure 5.76. Toughness graph of EFO20 sample

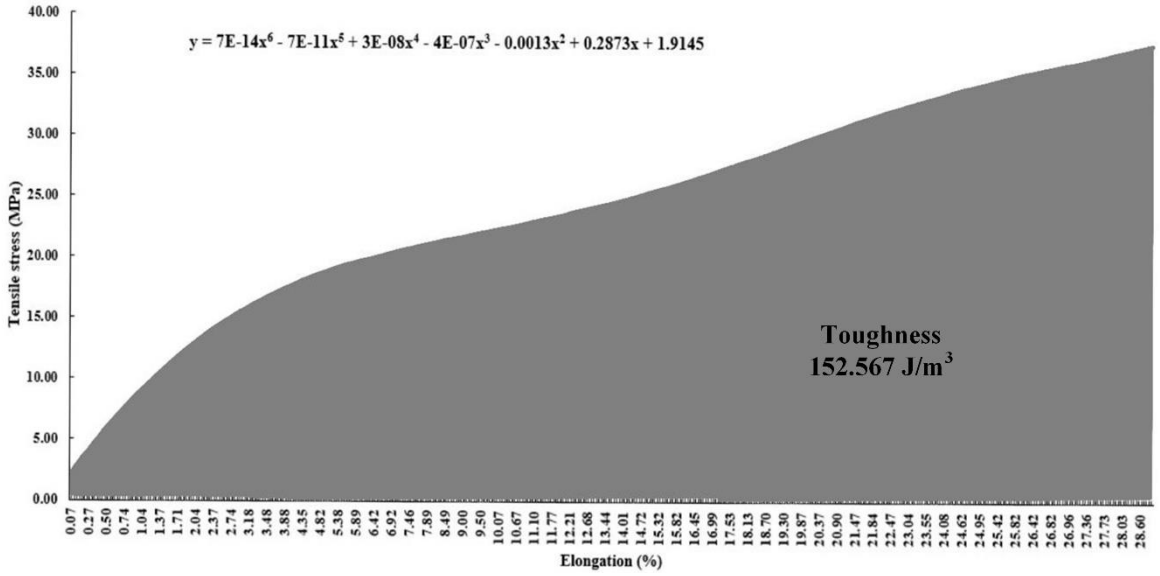

Figure 5.77. Toughness graph of EFO30 sample

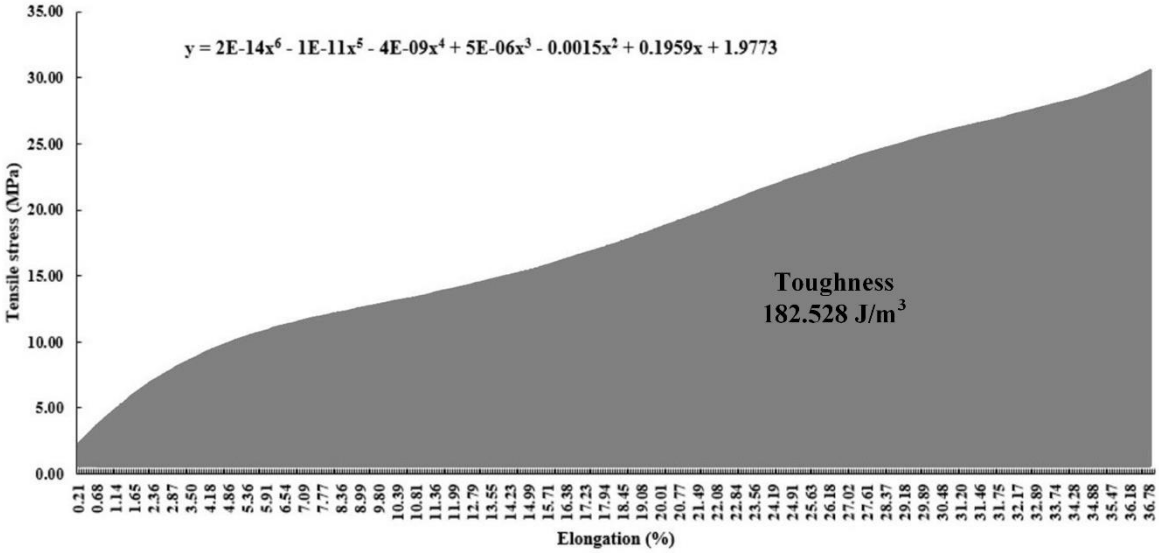

Figure 5.78. Toughness graph of EFO40 sample

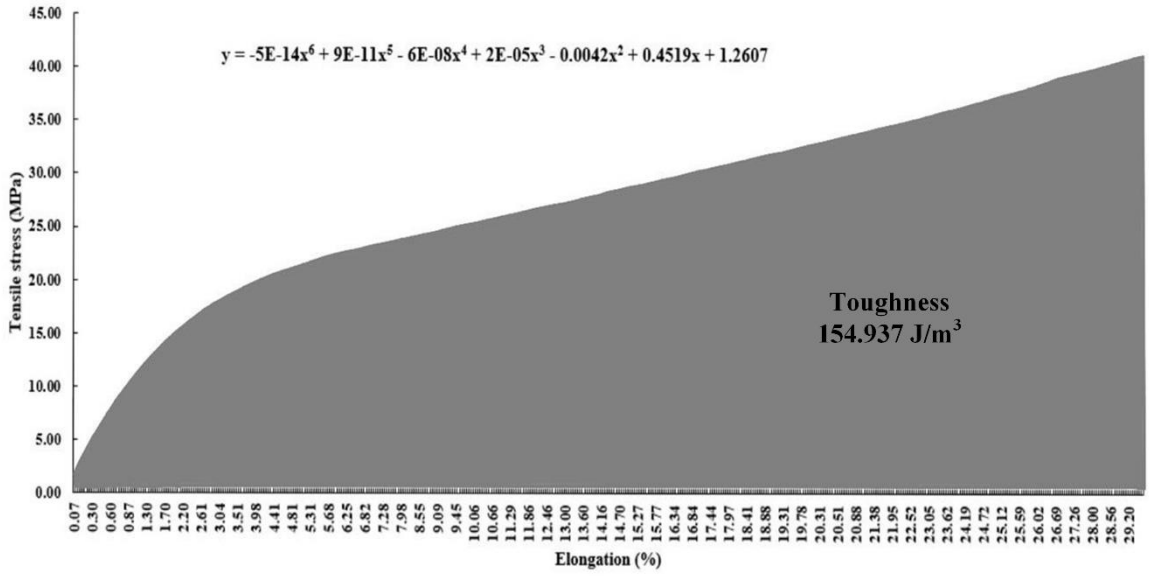

Figure 5.79. Toughness graph of EPO10 sample

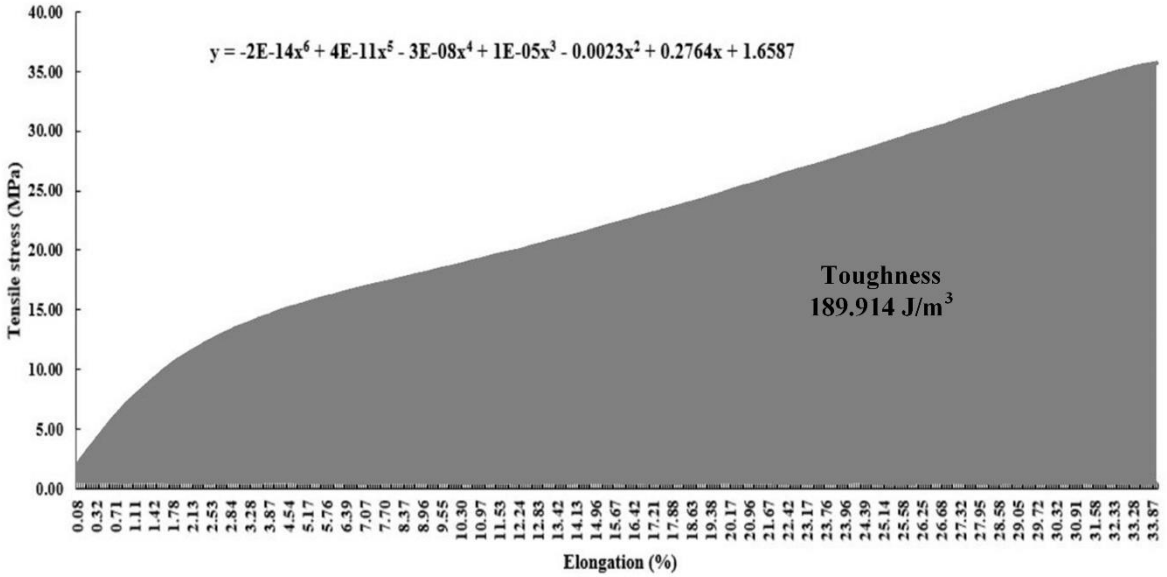

Figure 5.80. Toughness graph of EPO20 sample

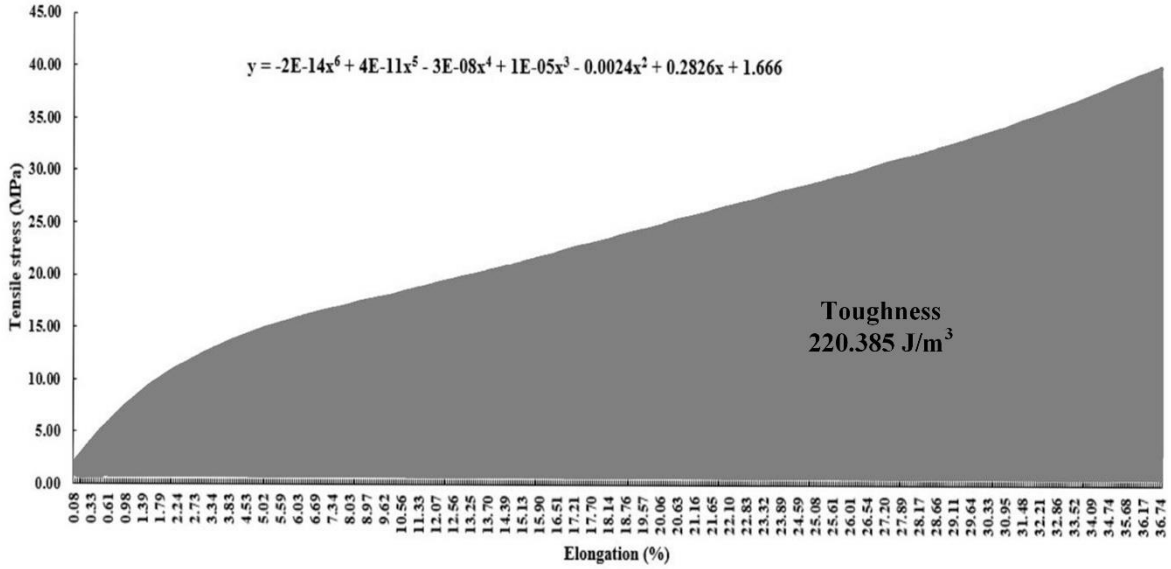

Figure 5.81. Toughness graph of EPO30 sample

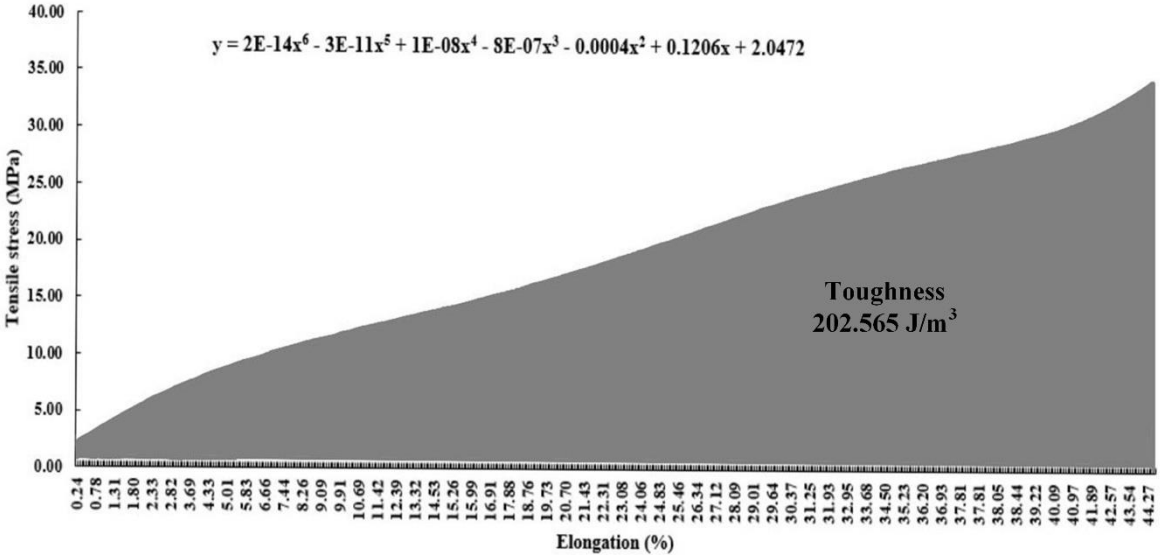

Figure 5.82. Toughness graph of EPO40 sample

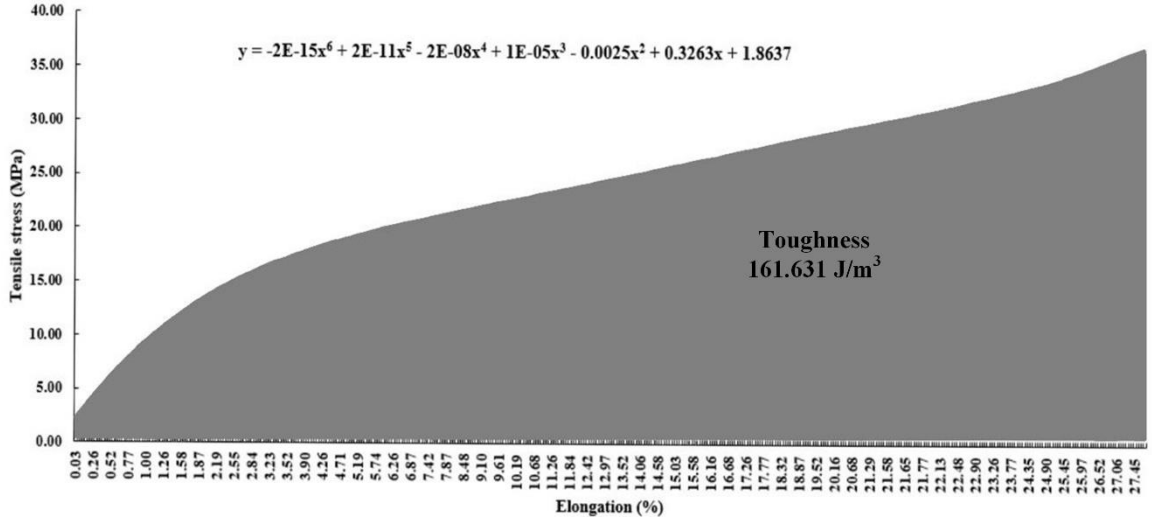

Figure 5.83. Toughness graph of ESO10 sample

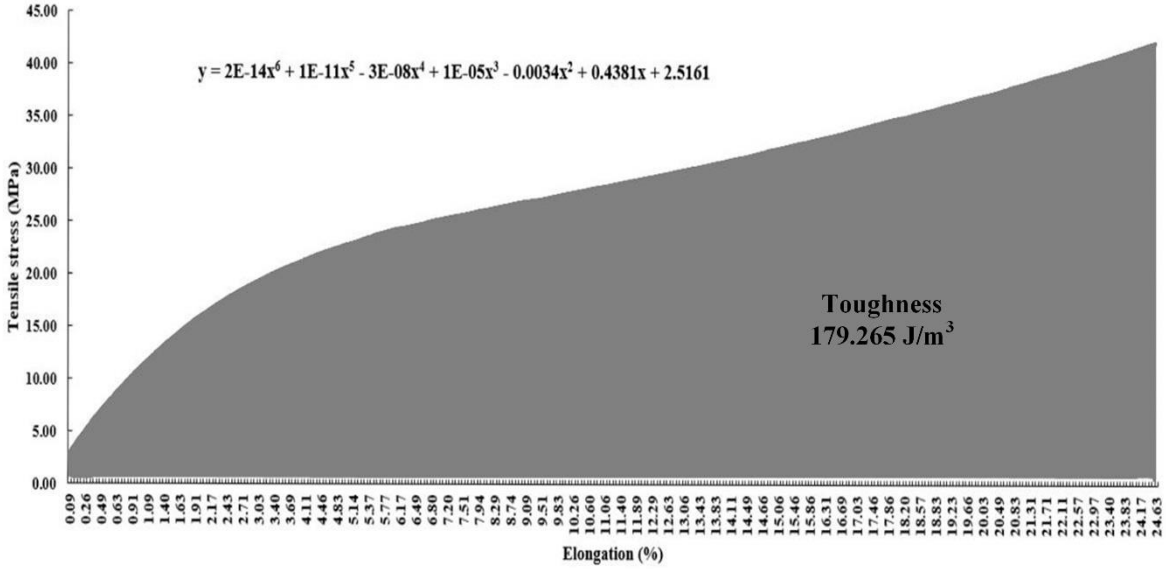

Figure 5.84. Toughness graph of ESO20 sample

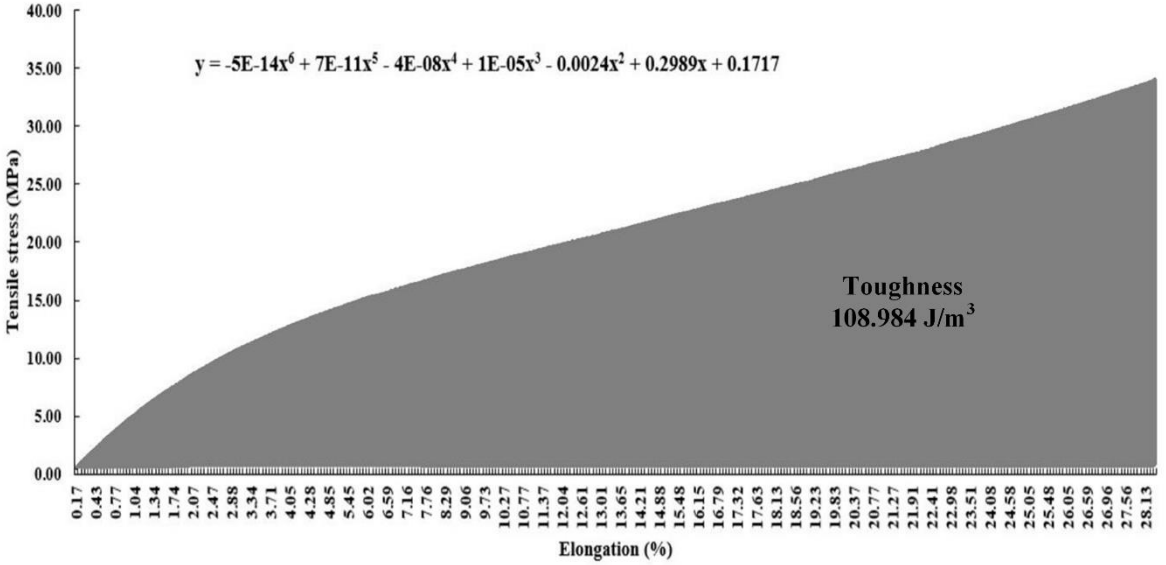

Figure 5.85. Toughness graph of ESO30 sample

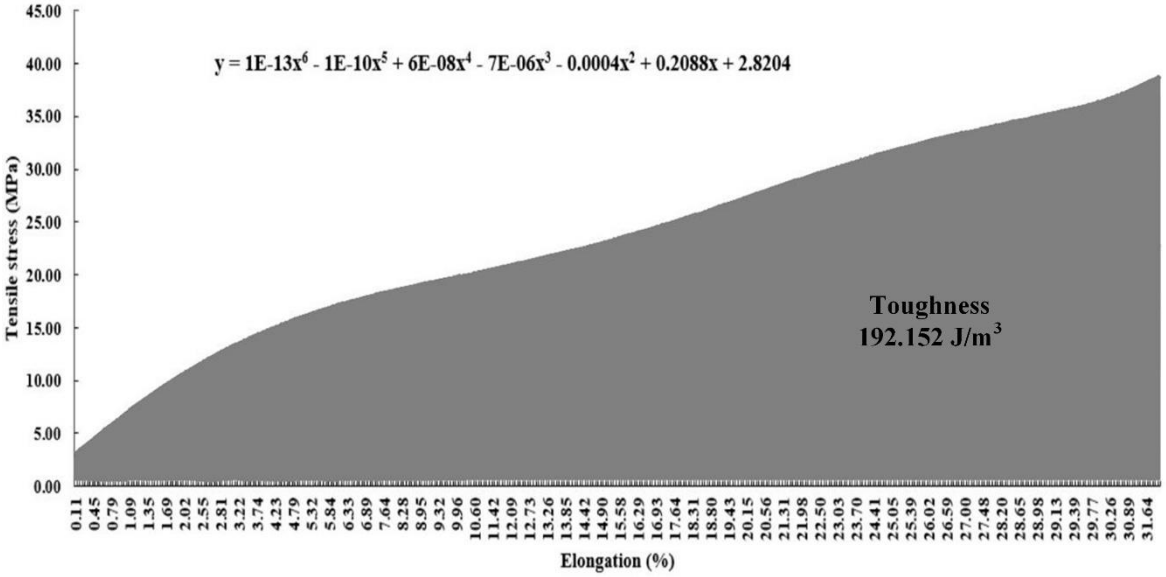

Figure 5.86. Toughness graph of ESO40 sample

In the toughness values calculated based on the stress-strain curves, the graphic area of the samples with higher percentage elongation values was found to be greater, parallel to the percentage elongation values in the tensile test. This reflects the direct relationship between toughness values and the percentage elongation of the material.

5.5. Hardness Test Results

Hardness measurements of the produced biocomposite samples were carried out using the Vickers hardness method by applying a force of 0.2 kg-f. The results are given in graphics between Figures 5.87 and 5.91. While the standard deviations in ECO samples are ±32.33, ±21.88, ±43.18 and ±42.15 for ECO10, ECO20, ECO30 and ECO40, respectively, in ECAO samples these values are ±47.02, ±65.74, ±49.23 and ±51.11 for ECAO10, ECAO20, ECAO30 and ECAO40, respectively. In EFO samples, standard deviations were found ±38.52, ±49.27, ±62.38 and ±56.66 for EFO10, EFO20, EFO30 and EFO40, seriatim, while in EPO samples, these values were calculated as ±50.05, ±41.34, ±64.08 and ±31.93 for EPO10, EPO20, EPO30 and EPO40, seriatim. These values were determined as ±61.49, ±56.28, ±68.40, and ±41.56 for ESO10, ESO20, ESO30, and ESO40 samples, respectively. This standard deviation value was ±64.5 in the sample prepared with pure epoxy resin. The hardness value of the composite sample made with pure epoxy sample was found to be 119.93. When compared to the sample results to which 5 different oils were added, it is seen that the hardness value is generally higher than the hardness value of the epoxy sample. Comparing ECO samples, a decrease in the hardness value was observed as the cotton oil ratio in the epoxy increased from 10% to 30%, while the addition of 40% cotton oil showed a higher hardness value than the other three samples. While the hardness value of the ECO20 specimen decreased by 16.05% compared to ECO

10, and the hardness value of the ECO30 specimen decreased by 17.61% compared to ECO20, the ECO40 specimen had a 57.28% higher value than the hardness value of the ECO 30 sample.

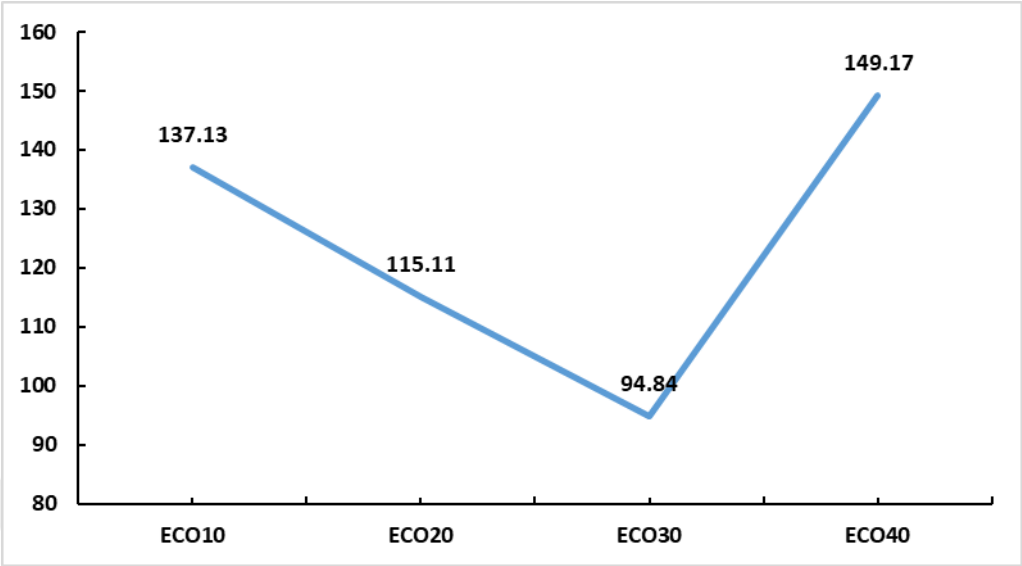

Figure 5.87. ECO sample hardness test results

In the comparison of ECAO samples, a decrease in the hardness value was discovered as the addition of canola oil to the epoxy increased from 10% to 40%. While the hardness value of the ECAO10 sample is 168.52, the hardness value of the ECAO20 sample is 160.61. This is equivalent to a hardness value decrease of 4.69%. The hardness value of the ECAO30 sample was found to be 152.62, which corresponds to a 4.97% decrease in the hardness value compared to the ECAO20 sample. In the ECAO40 sample, the hardness value was measured as 151.21, and there was a 0.92% decrease in the hardness value compared to the ECAO30 sample.

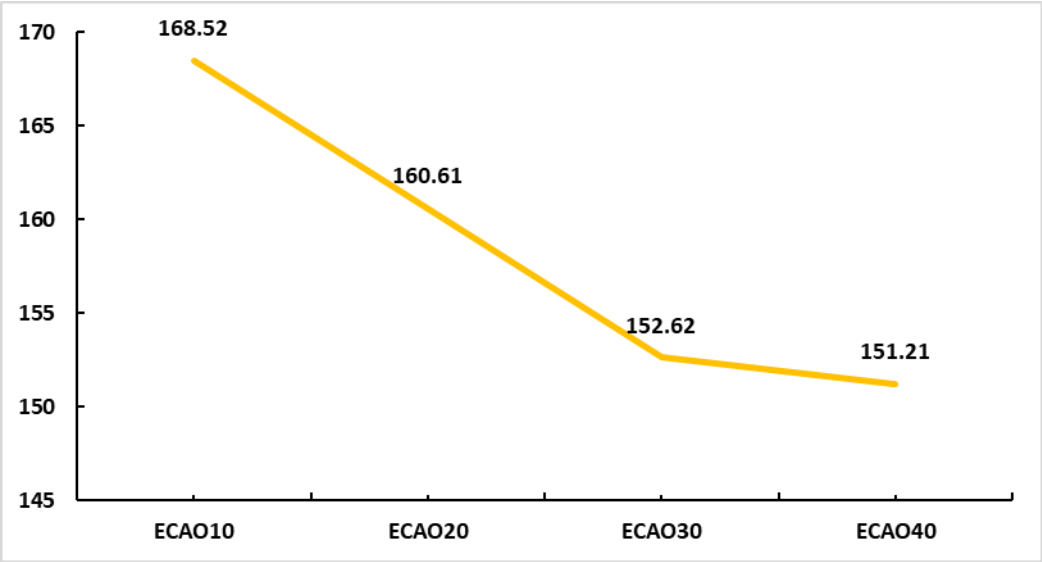

Figure 5.88. ECAO sample hardness test results

In the EFO samples, when the oil ratio added to the epoxy increased from 10% linseed oil to 20% linseed oil, the hardness values increased, but 30% and 40% linseed oil additions decreased the hardness values compared to the 20% oil ratio addition. While the hardness value of the EFO20 sample augmented by 23.95% compared to the EFO10 specimen, the hardness value of the EFO30 specimen was found to be 0.14% lower than the EFO20 sample. The hardness value of the EFO40 specimen decreased by 1.81% compared to the EFO30 specimen.

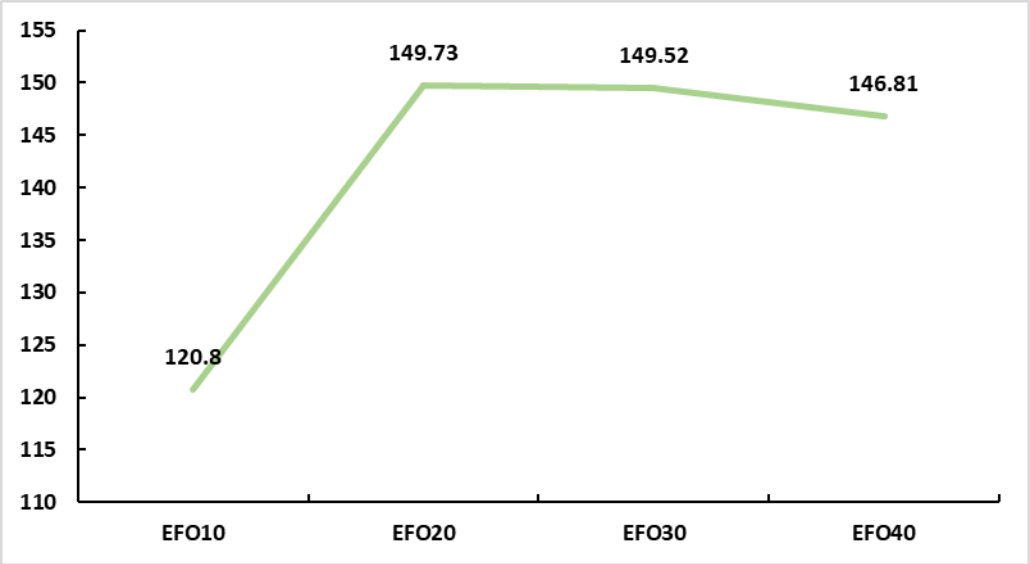

Figure 5.89. EFO sample hardness test results

In EPO samples, as in EFO samples, 20% palm oil addition gave the highest value. Although the hardness value increased from the 10% oil addition to the 20% oil ratio addition to the epoxy, a decrease in the hardness value was observed in the 30% oil ratio and 40% oil ratio addition compared to the 20% oil ratio addition. The hardness value of the EPO20 specimen raised by 2.22% compared to the EPO10 specimen. However, the hardness values of EPO30 and EPO40 samples decreased by 16.8% and 28.36%, respectively, compared to the EPO20 sample.

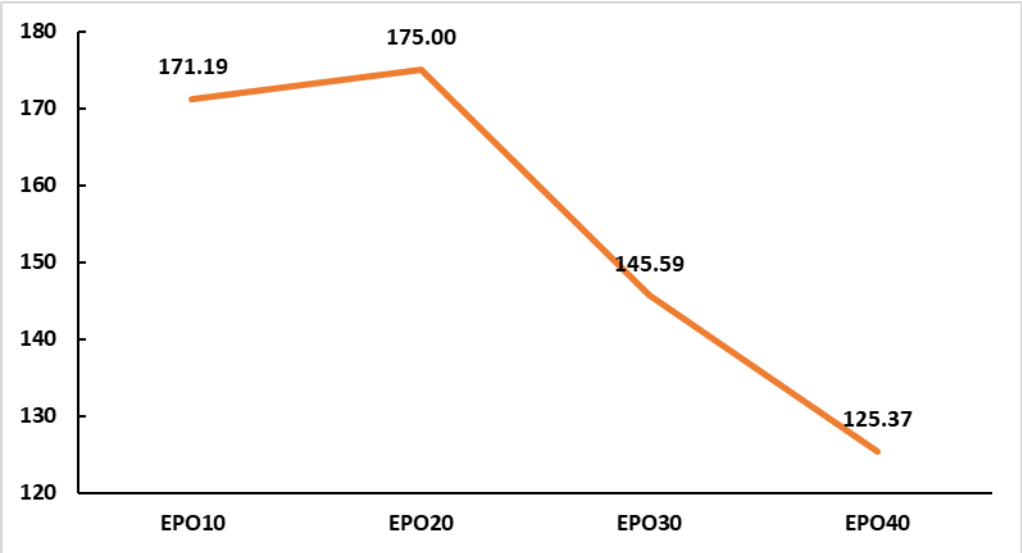

Figure 5.90. EPO sample hardness test results

In ESO samples, as in the results of EFO and EPO, the highest value was observed at 20% oil addition. 30% and 40% oil additions to epoxy caused a decrease in hardness value compared to 20% oil addition. While the hardness value of the ESO20 specimen increased by 3.52% compared to the ESO10 specimen, a decrease of 1.76% and 3.89% was observed in the ESO30 and ESO40 samples, respectively, compared to the ESO20 sample.

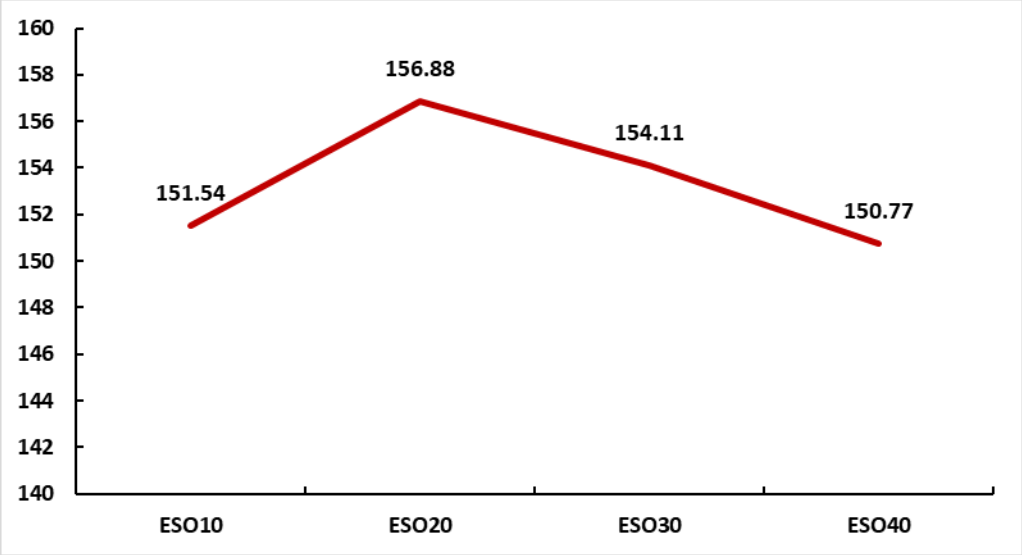

Figure 5.91. ESO sample hardness test results

When 10% and 20% palm oil is added to the epoxy resin in five different oils, the maximum hardness values are 171.19 HV and 175 HV in EPO10 and EPO20. These values are 1.43 times and 1.46 times higher, respectively, than the hardness value of the sample prepared using pure epoxy resin. Among the 30% oil addition ratios, the ESO30 sample to which soybean oil was added reached the highest hardness value with a value of 154.11 HV, which is 1.28 times higher than the pure epoxy

sample composite. Even though, the hardness values of the samples with 40% oil added are close to each other, the ECAO40 sample stands out with its value of 151.21. This value is 1.26 times higher than the composite sample prepared with pure epoxy resin. Examining at the hardness results of 21 samples, the lowest hardness value was observed in the ECO30 specimen with a value of 94.84HV, followed by the EC020 sample with a value of 115.11 HV. The lowest hardness value in the samples with 10% oil addition was determined as 120.8 HV in EFO10, and the lowest hardness value in the samples with 40% oil addition was determined as 125.37 HV in EPO40.

5.6. Water Absorption Test Results

The water absorption amounts of the samples produced are given in the graphs from Figure 5.92 to Figure 5.97. The water absorption amount of the epoxy sample is given in Figure 5.92. While the dry weight of the epoxy sample was 22.0754 g, at the end of the test period this weight became 24.5104 g. The weight increase rate for the epoxy sample was 11.03%.

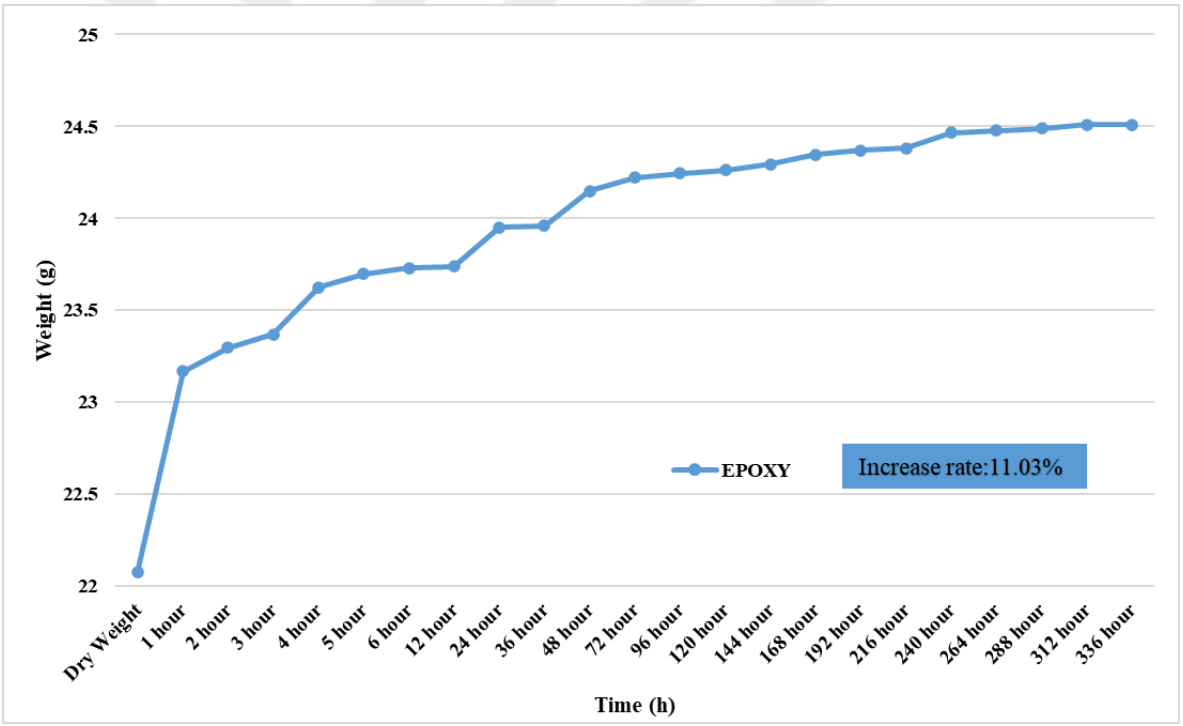

Figure 5.92. EPOXY water absorption test results

Figure 5.93 represents the water absorption amounts of ECO samples. The dry weights of ECO10, ECO20, ECO30 and ECO40 samples were measured as 32.8346 g, 30.5768 g, 31.6702 g and 30.5463 g, respectively. Post-test weights were measured as 36.4625 g, 36.3406 g, 37.9175 g and 33.9497 g for ECO10, ECO20, ECO30 and ECO40 samples, respectively. The percentage weight increase rates were 11.05%, 18.85%, 19.73% and 11.14% for ECO10, ECO20, ECO30 and ECO40 samples, respectively. While the sample with the most water absorption was ECO30, the sample with the least water absorption was ECO40. This situation is parallel to the fact that higher values are

obtained from the ECO40 sample in mechanical results compared to other ECO samples, and the fibers in the ECO40 sample show a better bond with the resin in the SEM analysis images. The condition of the ECO30 sample is also confirmed by other mechanical tests and SEM analyses.

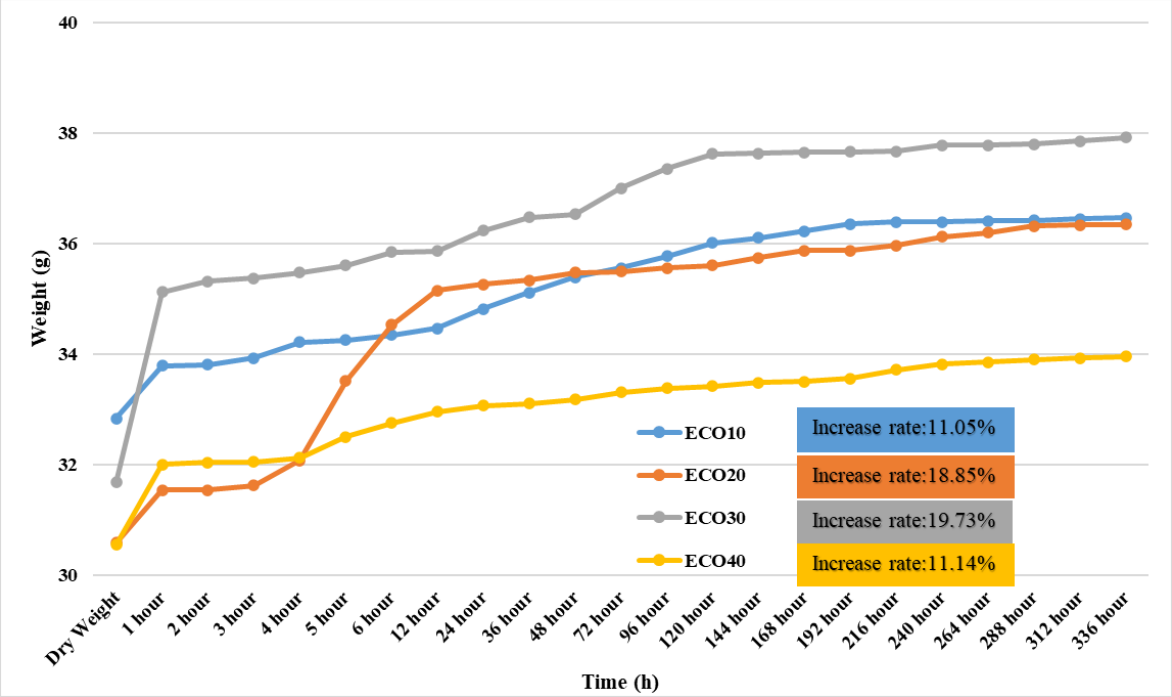

Figure 5.93. ECO water absorption test results

Figure 5.94 shows the water absorption amounts of ECAO samples. While the dry weights for ECAO10, ECAO20, ECAO30 and ECAO40 were 32.052 g, 31.8266 g, 32.7103 g, and 31.2335 g, respectively, their after-test weights were measured as 34.7573 g, 35.084 g, 38.9216 g, and 37.623 g, respectively. Percentage weight rising rates were 8.44%, 9.28%, 15.96% and 16.98% for ECAO10, ECAO20, ECOA30 and ECAO40 samples, respectively. It was determined that as the oil content in ECAO samples increased from 10% to 40%, the amount of water absorption also increased.

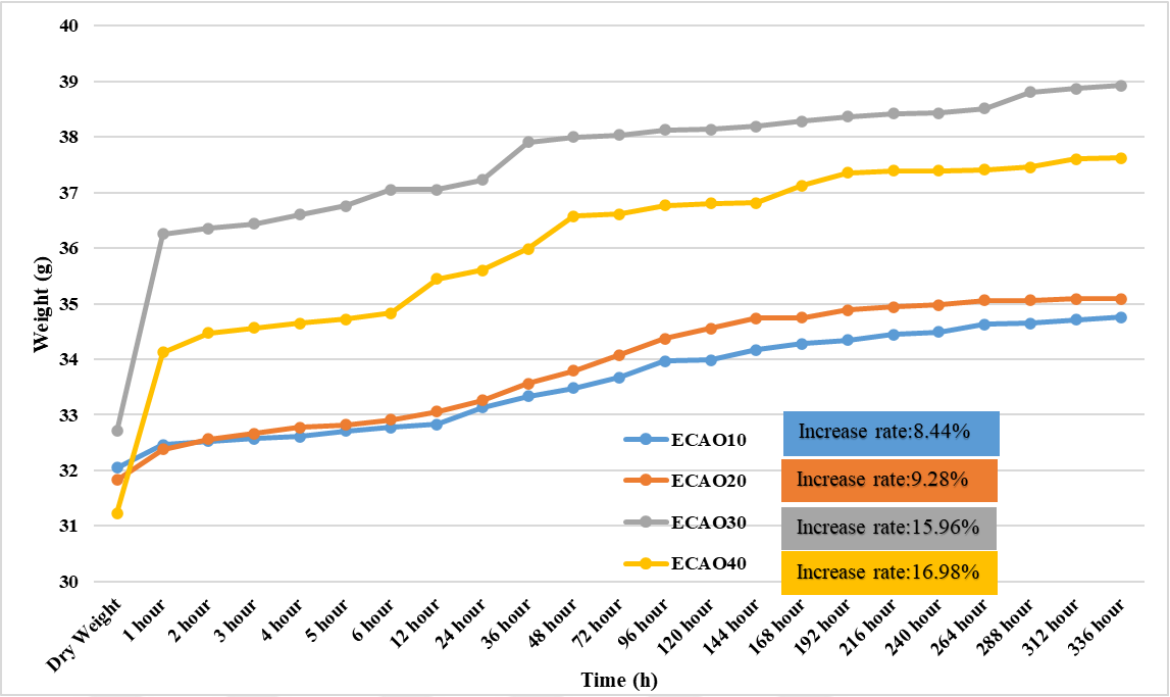

Figure 5.94. ECAO water absorption test results

Figure 5.95 reflects the change in water absorption amounts of EFO samples in the water test applied for 2 weeks. The pre-test dry weights for EFO10, EFO20, EFO30 and EFO40 samples were measured on a precision scale as 32.0565 g, 33.4388 g, 32.4534 g, and 34.6936 g, respectively. The weights measured at the end of 336 hours were 38.2005 g, 37.7671 g, 38.5621 g, and 40.5456 g for EFO10, EFO20, EFO30 and EFO40 samples, respectively. According to these values, the percentage increases were calculated as 19.17%, 12.94%, 18.82% and 16.87% for the EFO10, EFO20, EFO30 and EFO40 samples, respectively. While the EFO20 sample had the least water absorption, the EFO10 sample had the highest water absorption.

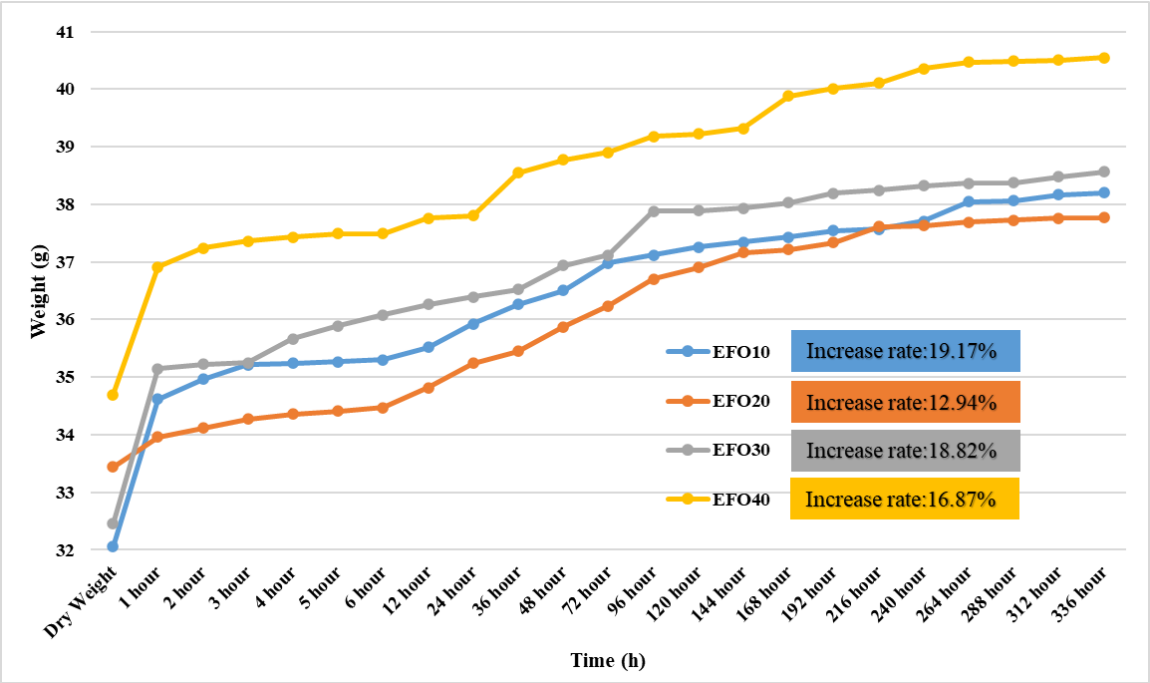

Figure 5.95. EFO water absorption test results

Water absorption amounts of EPO samples are shown in Figure 5.96. While the dry weights for EPO10, EPO20, EPO30 and EPO40 samples were measured as 20.8093 g, 24.9993 g, 22.4239 g, and 21.7308 g, respectively, the weights after the test were measured as 24.1499 g, 27.5841 g, 26.9448 g, and 27.0498 g, respectively. Percentage weight increase rates were found to be 16.05%, 9.37%, 20.16% and 24.48% for EPO10, EPO20, EPO30 and EPO40 samples, respectively. While the EPO20 sample was seen as the sample with the lowest amount of water absorption, the fiber and resin showed good bonding and the water penetration was relatively less than other EPO samples, which was similarly reflected in the results of other tests. Meanwhile, the fact that the EPO40 sample was the sample that showed the highest water absorption affected the mechanical test results similarly for the EPO40 sample.

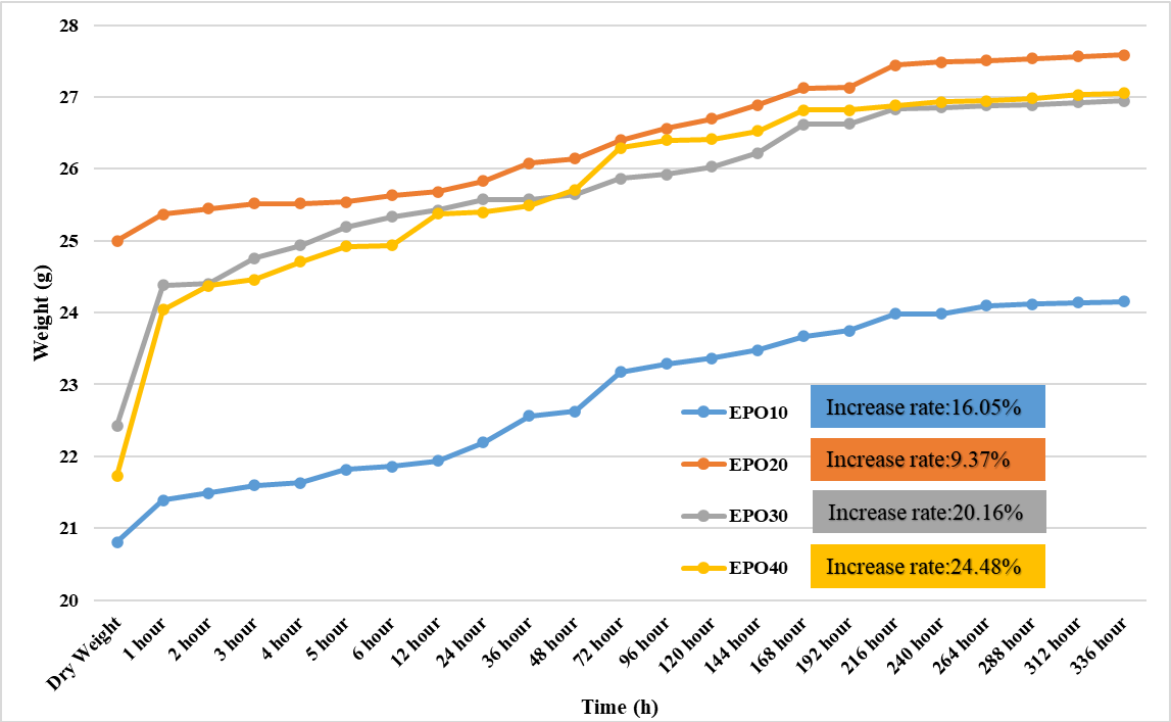

Figure 5.96. EPO water absorption test results

The water absorption amounts in the samples subjected to water testing in ESO samples are shown in Figure 5.97. In the measurements made while the samples were dry before the test, the weights for the ESO10, ESO20, ESO30 and ESO40 samples were 30.6226 g, 34.9686 g, 32.102 g and 32.0159 g, respectively. At the end of the test, the weights of the samples were 36.3192 g, 37.211 g, 36.2261 g and 38.6716 g for the ESO10, ESO20, ESO30 and ESO40 samples, respectively, in the measurements made while the samples were absorbed with water. Percentage weight increase rates are 18.6%, 6.41%, 12.85%, and 20.79% for ESO10, ESO20, ESO30 and ESO40 samples, respectively. As in the other 4 types of composite combinations, the highest amount of water absorption was seen in the ESO40 sample containing 40% oil. The least amount of water absorption was found in the ESO20 sample.

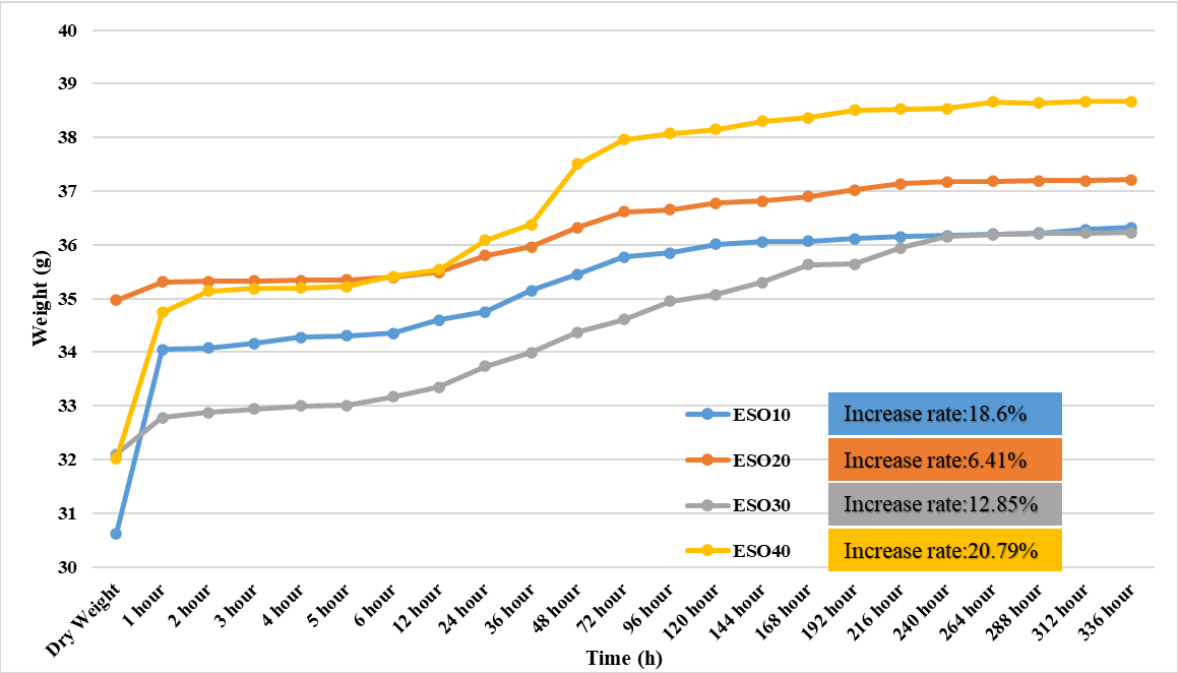

Figure 5.97. ESO water absorption test results

Considering the water absorption test of 21 samples in general, the lowest water absorption rate was encountered in the ESO20 sample with 6.41% in percentage weight increase rates. In the initial and final weight comparison, the ESO20 sample had a weight increase of 0.1926 g less than the sample made with pure epoxy resin. Although it is generally found that the amount of water absorption in the sample augments with the rise in the oil content from 10% to 40%, in the ECO and EFO samples, the samples containing 30% oil absorbed more water than the samples containing 40% oil. The specimen with the highest water absorption percentage is the EPO40 sample. The reason for this situation may be that the fiber and resin do not adhere well and the bonds between them show weak character as the oil content has increased to 40%. In addition, it was determined that samples containing 10% and 20% oil showed less water absorption than samples containing 30% and 40% oil, and as the oil content increased above 20%, the amount of water absorption generally increased. It is seen in almost all samples that the increase in water absorption is especially high in the first 6 hours. It is understood from the graphs that the highest amount of water absorption in the first 6 hours is in the first hour.

5.7. TGA Results

Figure 5.98 to 5.118 displays the TGA graph of EPOXY and biocomposite samples. TGA analysis presents the temperature at which the samples first began to decompose and the amount of loss in their weight before the test.

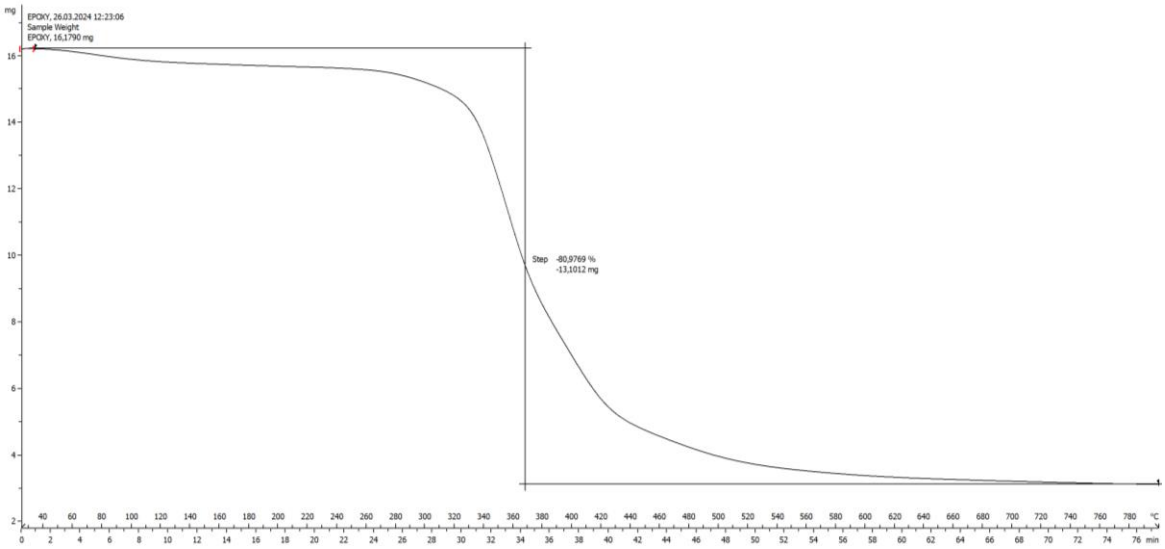

Figure 5.98. EPOXY TGA results

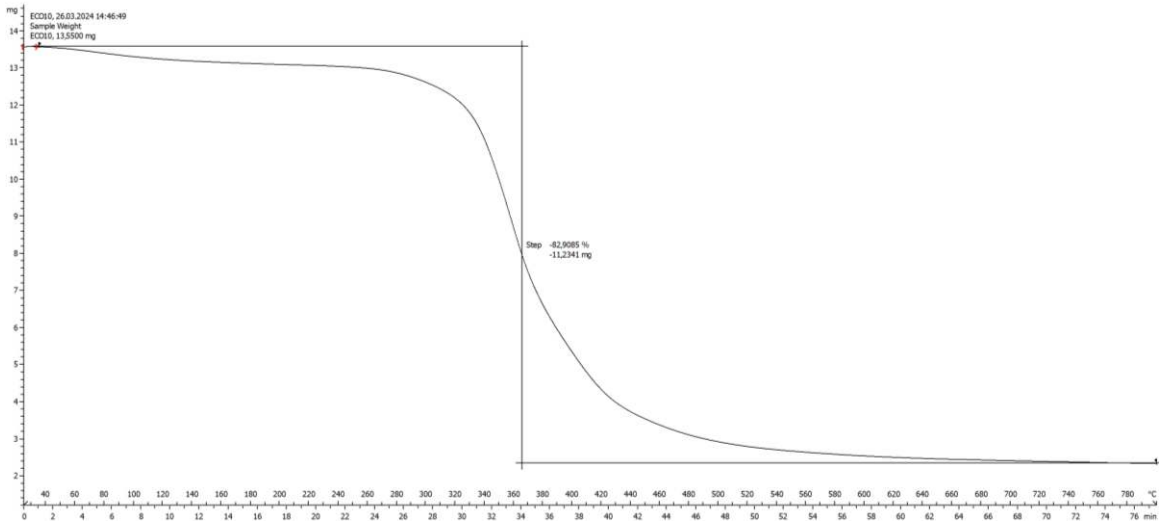

Figure 5.99. ECO10 TGA test results

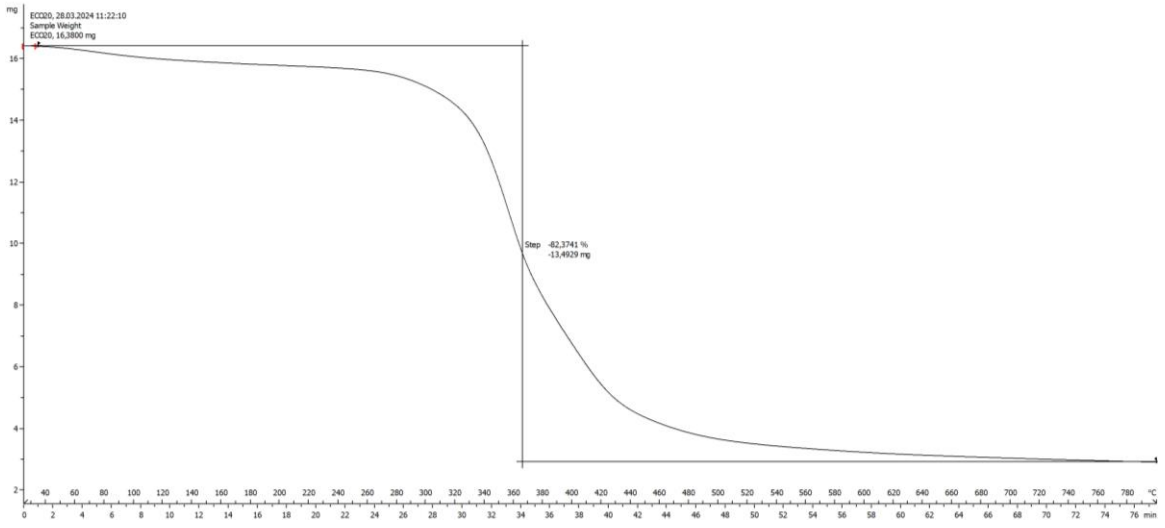

Figure 5.100. ECO20 TGA results

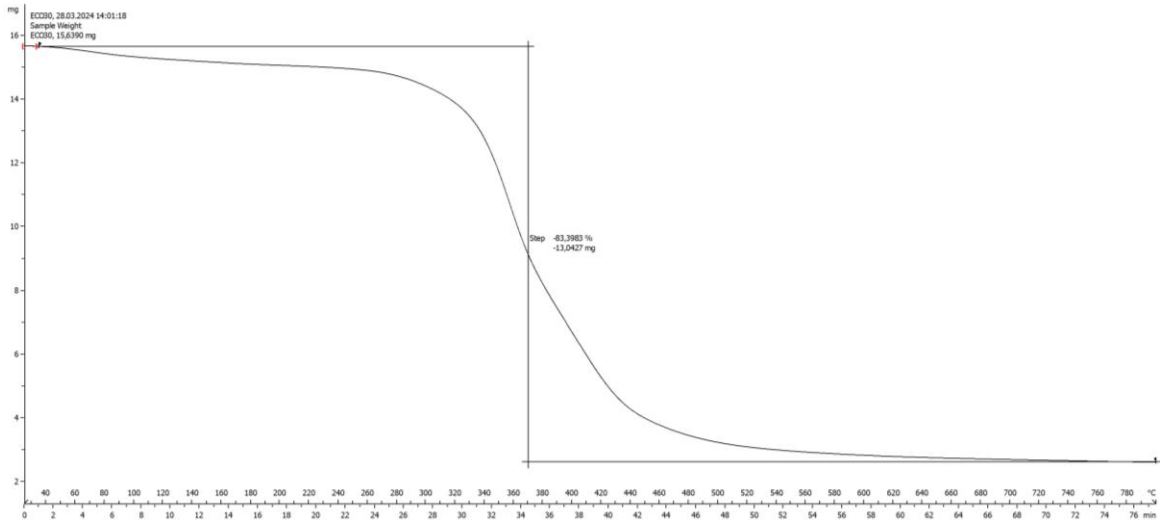

Figure 5.101. ECO30 TGA results

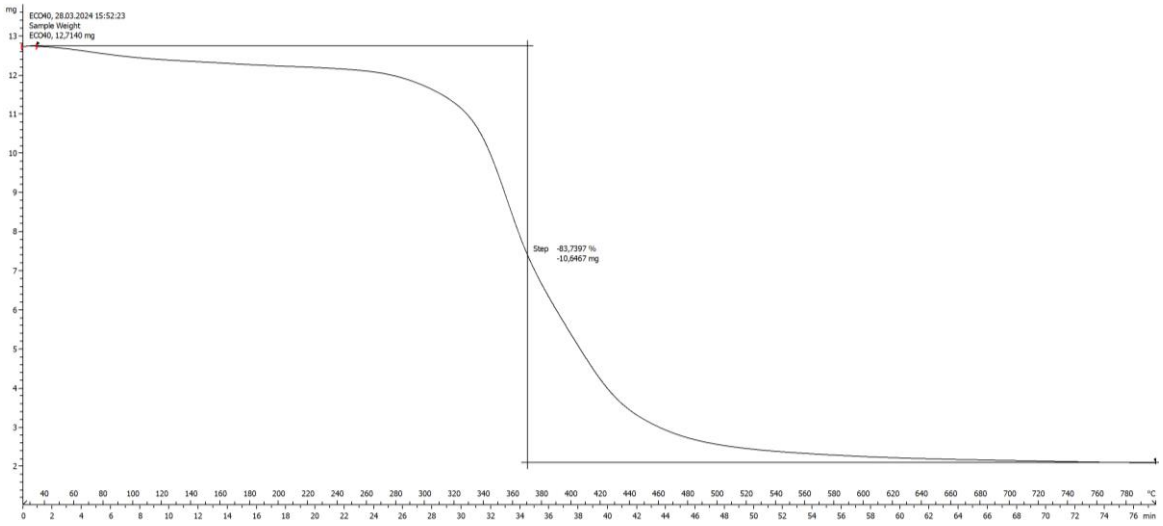

Figure 5.102. ECO40 TGA results

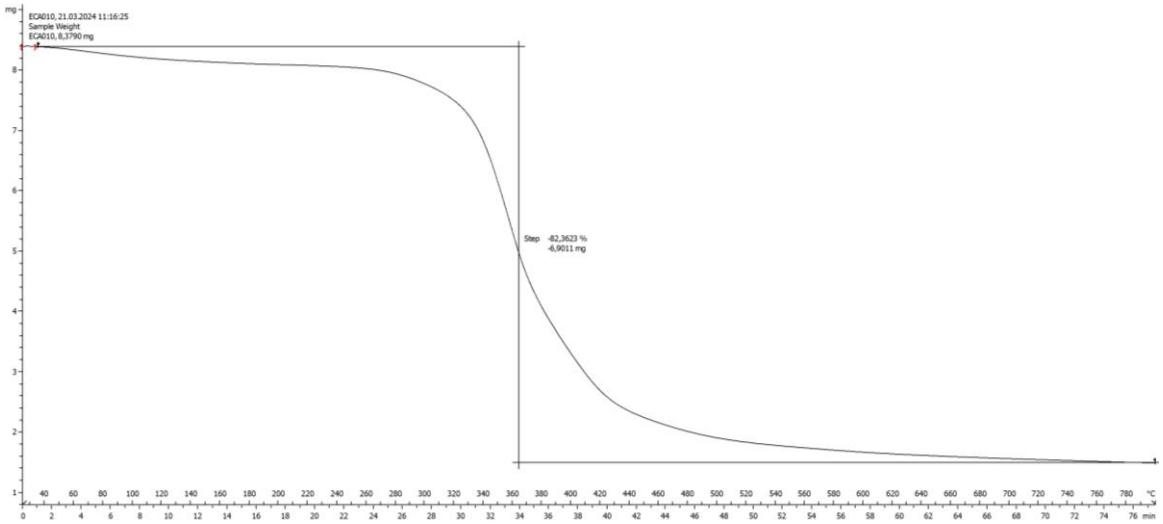

Figure 5.103. ECAO10 TGA results

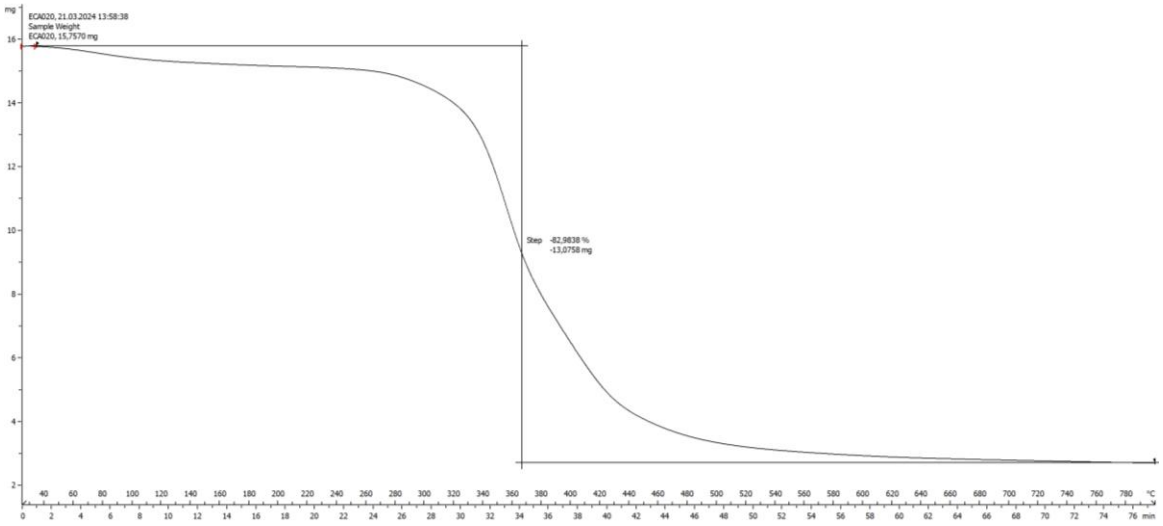

Figure 5.104. ECAO20 TGA results

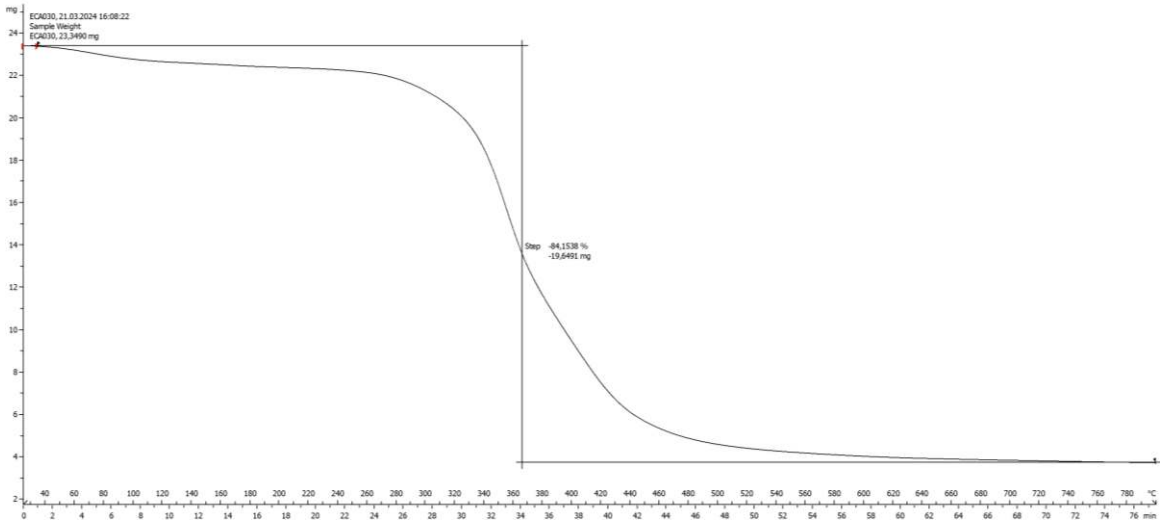

Figure 5.105. ECAO30 TGA results

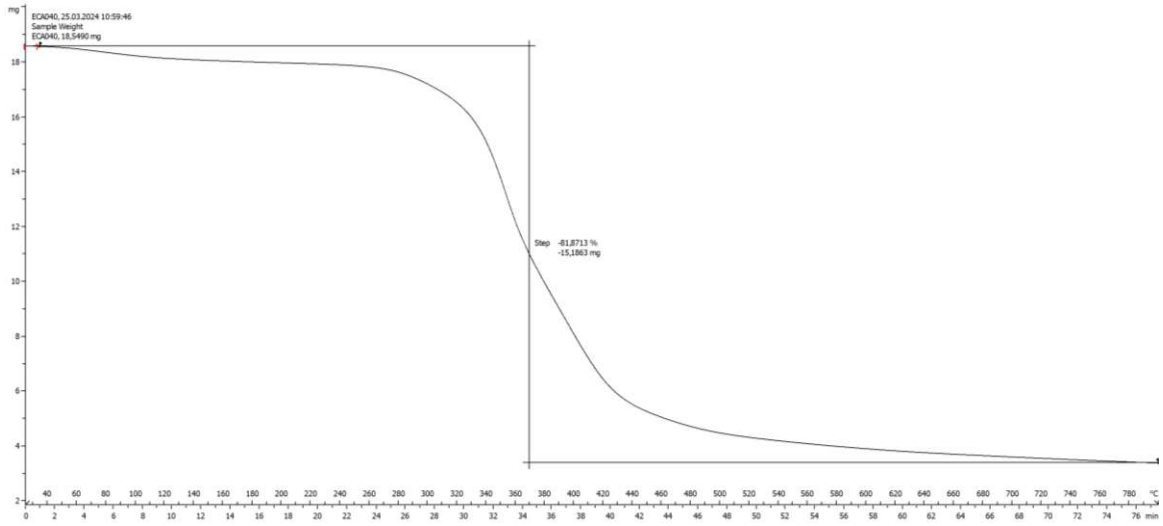

Figure 5.106. ECAO40 TGA results

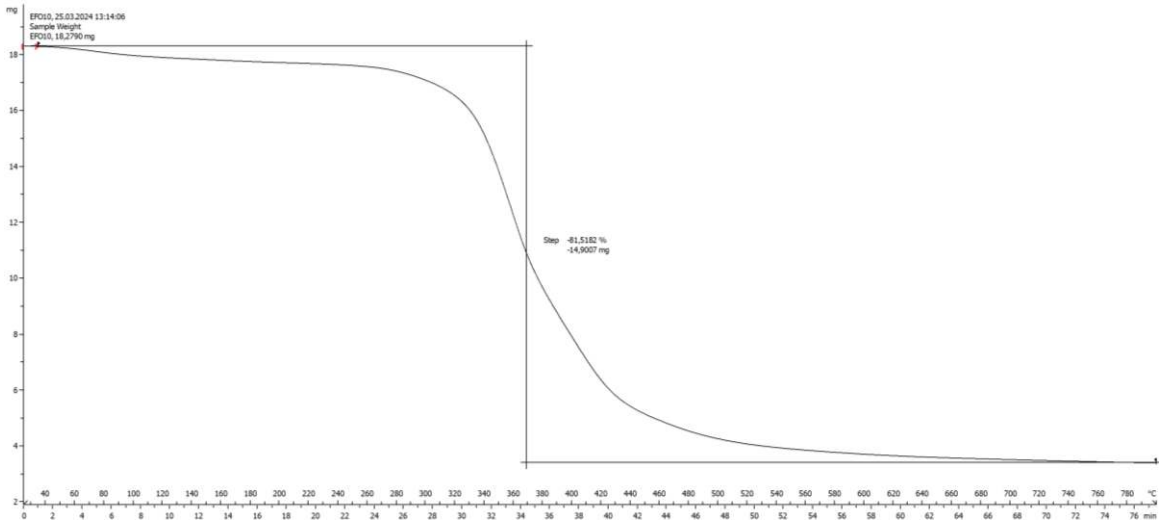

Figure 5.107. EFO10 TGA results

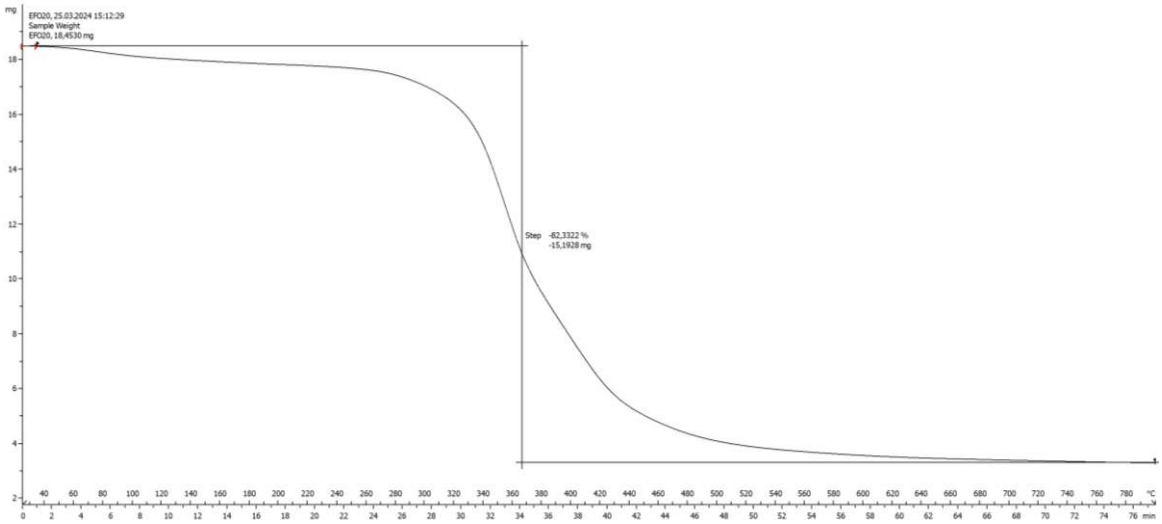

Figure 5.108. EFO20 TGA results

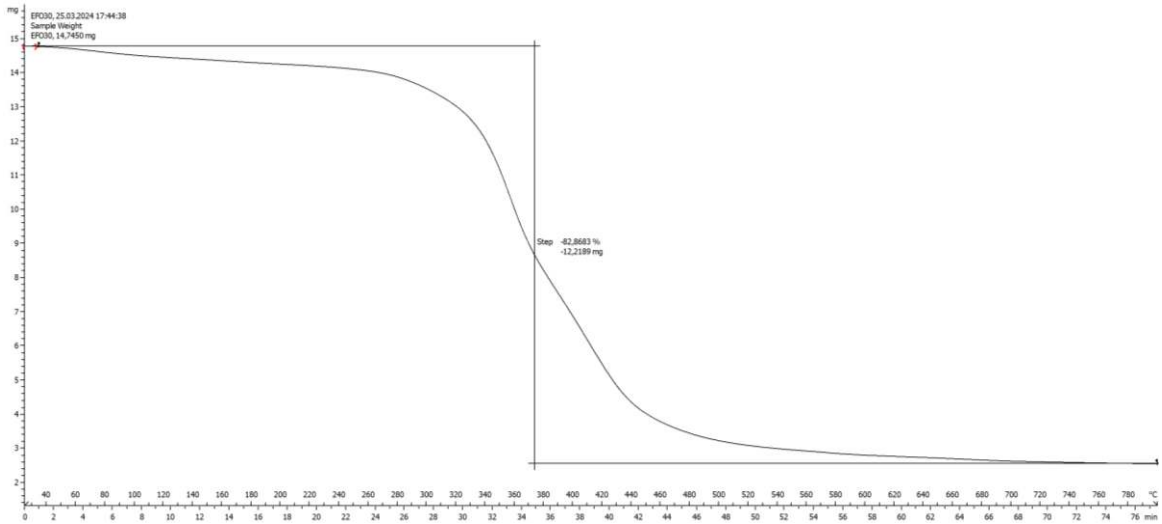

Figure 5.109. EFO30 TGA results

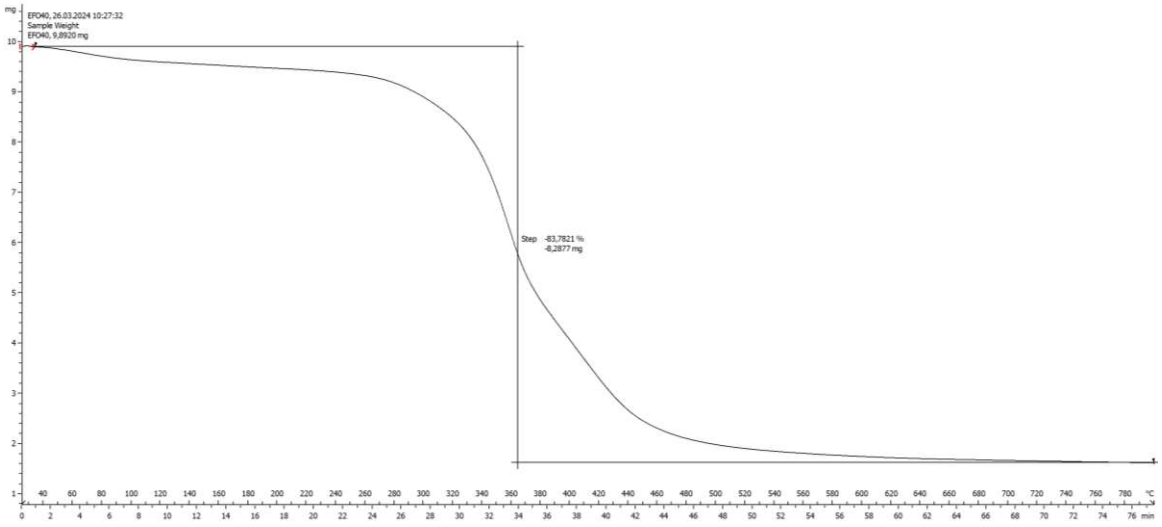

Figure 5.110. EFO40 TGA results

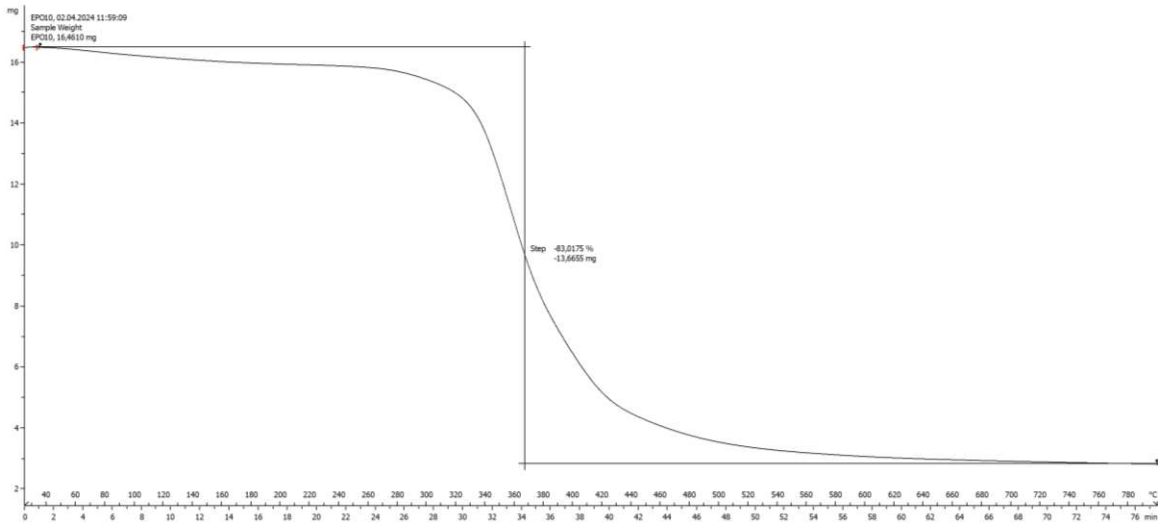

Figure 5.111. EPO10 TGA results

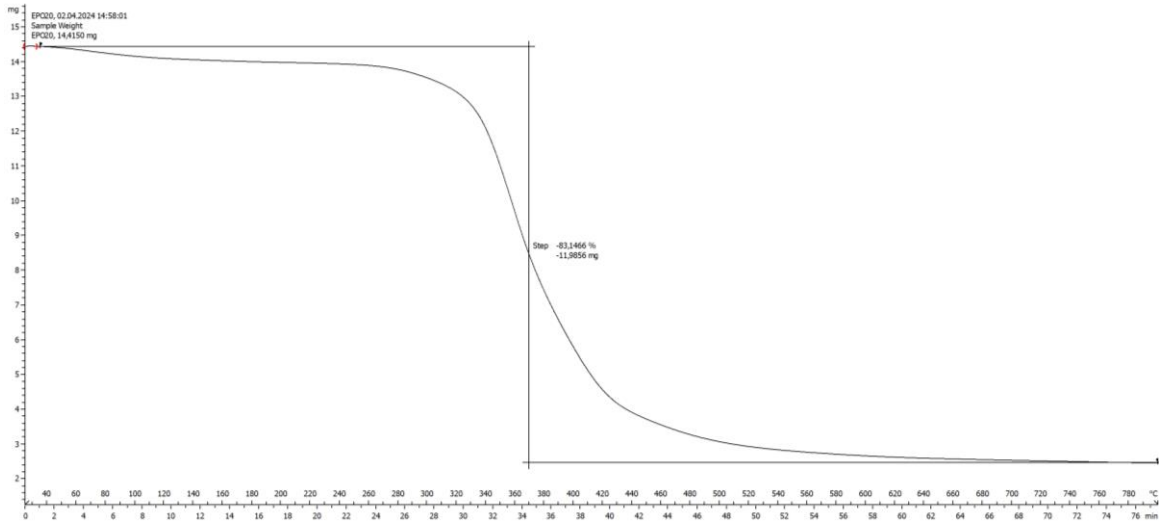

Figure 5.112. EPO20 TGA results

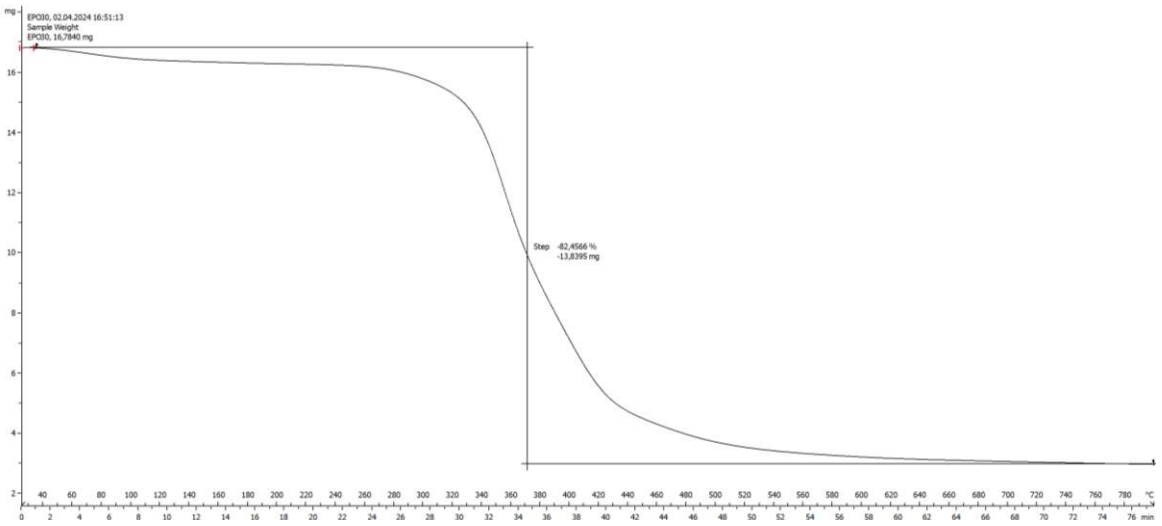

Figure 5.113. EPO30 TGA results

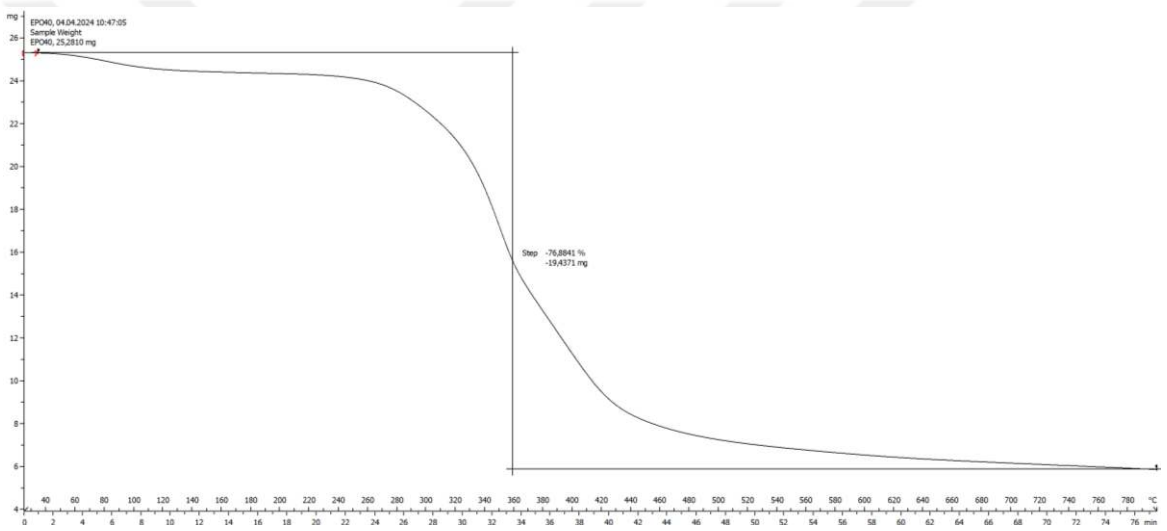

Figure 5.114. EPO40 TGA results

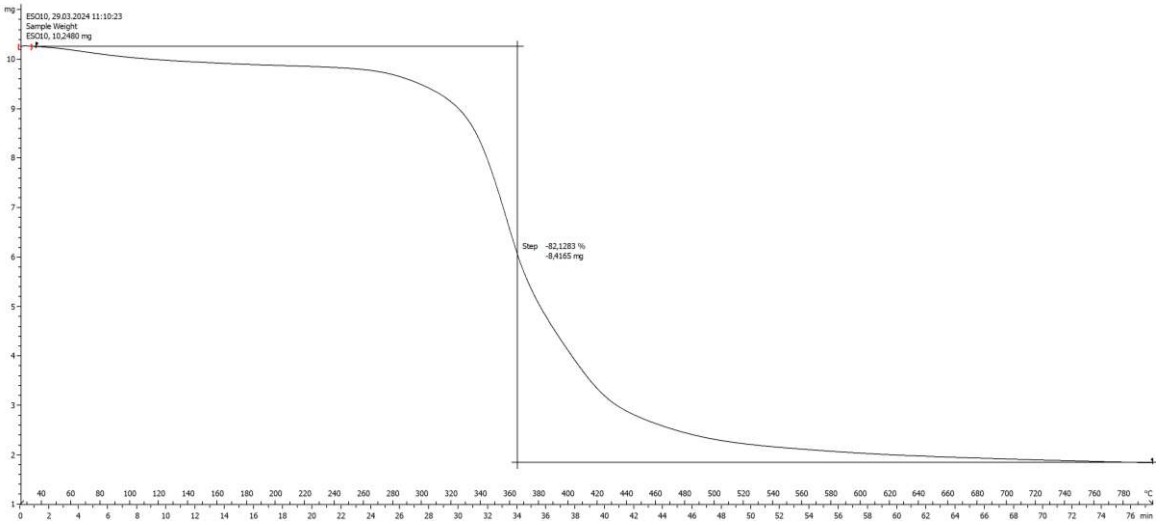

Figure 5.115. ESO10 TGA results

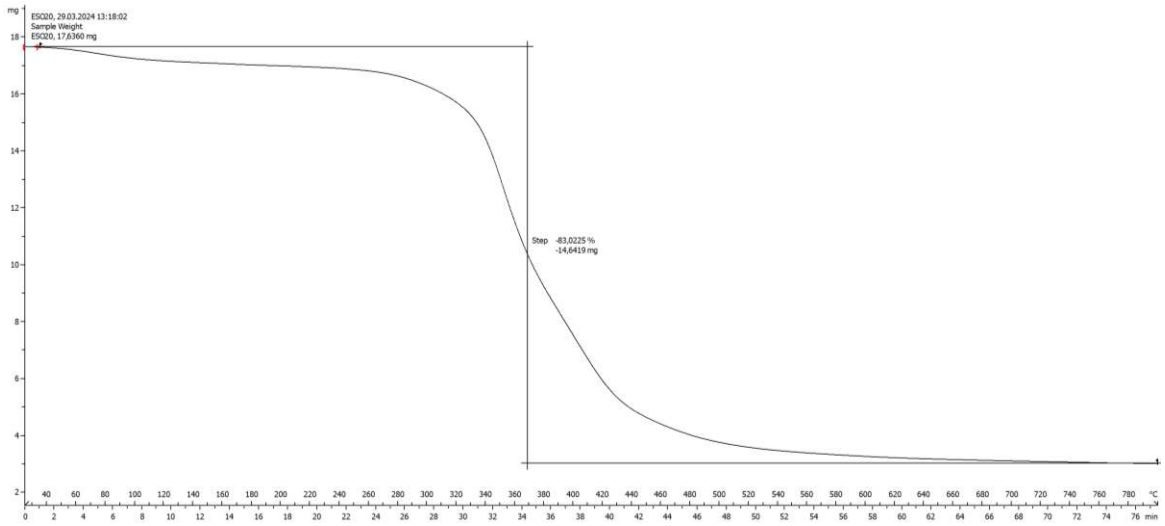

Figure 5.116. ESO20 TGA results

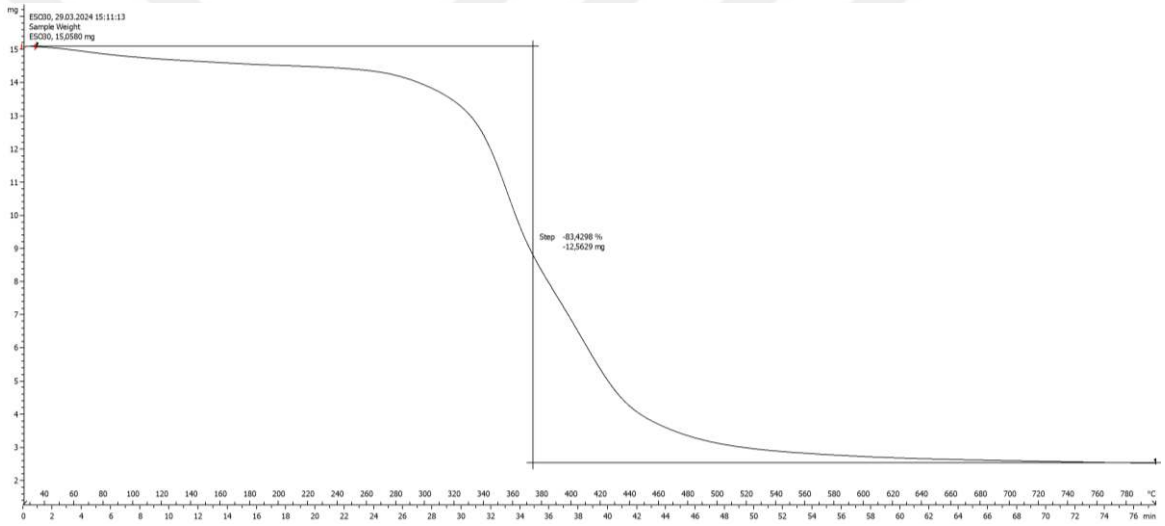

Figure 5.117. ESO30 TGA results

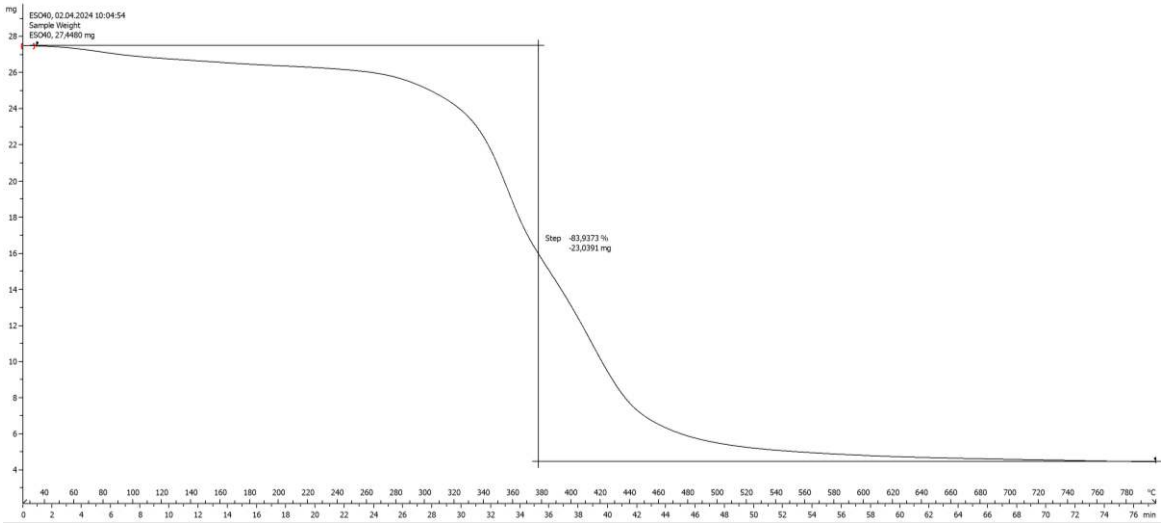

Figure 5.118. ESO40 TGA results

Table 5.8 indicates the weights of the samples before and after TGA analysis and the percentage loss in weight. The sample with the lowest percentage degradation rate compared to EPOXY is the EPO40 sample with 76.9%. The sample with the highest degradation rate compared to EPOXY is the ECO10 sample with 85%. At this point, it is seen that the thermal stability of EPO40 is higher than the other samples between 25-800 °C, while that of ECO10 is lower. The EFO10 sample is listed as the most stable sample after EPO40 with 81.5%. The high thermal stability of EPO40 and EFO10 samples may be due to the fact that the bonds formed by the oils in the samples with the epoxy resin do not break easily. Therefore, the additives can provide superior thermal stability to biocomposite materials in high temperature applications (Karacor and Ozcanli, 2022c). Degradation rates gradually increase with increasing vegetable oil ratios from 10% to 40% in ESO and EFO samples. In ECAO samples, except ECAO40, degradation rates also increase with increasing vegetable oil content from 10% to 30%.

Table 5.8. Initial, final and changes in weight of samples

Biocomposites	Post-test weight (g)	Pre-test weight (g)	Change between initial and final weight (%)
EPOXY	3.0777	16.179	81
ECO10	2.3157	13.55	85
ECO20	2.8871	16.38	82
ECO30	2.5963	15.639	83.4
ECO40	2.0673	12.714	83.7
ECAO10	1.4779	8.379	82.4
ECAO20	2.6812	15.757	83
ECAO30	3.6999	23.349	84.1
ECAO40	3.3627	18.549	81.9
EFO10	3.3783	18.279	81.5
EFO20	3.2602	18.453	82.3
EFO30	2.5261	14.745	82.9
EFO40	1.6043	9.892	83.8
EPO10	2.7955	16.461	83
EPO20	2.4294	14.415	83.1
EPO30	2.9445	16.784	82.5
EPO40	5.8439	25.281	76.9
ESO10	1.8315	10.248	82.1
ESO20	2.9941	17.636	83.0
ESO30	2.4951	15.058	83.4
ESO40	4.4089	27.448	83.9

Table 5.9 shows the temperature differences between the temperatures at which the samples first started to decompose and the temperatures at which the decomposition ended in the TGA analysis compared to the EPOXY sample. The temperature at which EPOXY begins to burn was found to be 302 °C. As the vegetable oil ratio increases from 10% to 40%, the difference in initial decomposition temperatures compared to EPOXY increases in all sample combinations. ECAO samples are the samples with the least difference in decomposition temperatures compared to EPOXY. The highest difference in decomposition temperature was found in EFO samples compared to EPOXY samples. The EFO40 sample was the sample that showed the earliest decomposition with a difference of -26 °C degrees in decomposition temperature compared to the EPOXY samples. The ECAO10 sample is the sample that decomposes the latest, with a difference of -11 °C in decomposition temperature compared to the EPOXY sample. The outcomes display that the incorporation of vegetable oil to EPOXY delays the degradation to a certain extent at earlier temperatures. This situation is caused by the deterioration of the ester-based chain structure in the structure of the oils. It is stated that the absence of a second decomposition temperature in the tested samples is an indication of smooth and slow combustion (Karacor and Ozcanli, in press).

Table 5.9. Comparison of decomposition temperatures

Biocomposites	Difference of decomposition temperature compared to EPOXY sample (°C)
ECO10	-15
ECO20	-17
ECO30	-18
ECO40	-20
ECAO10	-11
ECAO20	-13
ECAO30	-19
ECAO40	-20
EFO10	-23
EFO20	-24
EFO30	-25
EFO40	-26
EPO10	-19
EPO20	-20
EPO30	-21

EPO40	-23
ESO10	-16
ESO20	-19
ESO30	-21
ESO40	-24

5.8. DSC Results

Figure 5.119 to 5.139 indicates the DSC graph of EPOXY and biocomposite samples. With DSC analysis, the glass transition temperature, crystallization temperature, melting point, and the amount of energy in the exothermic and endothermic reactions that occur during the phase change at these points can be determined in the samples.

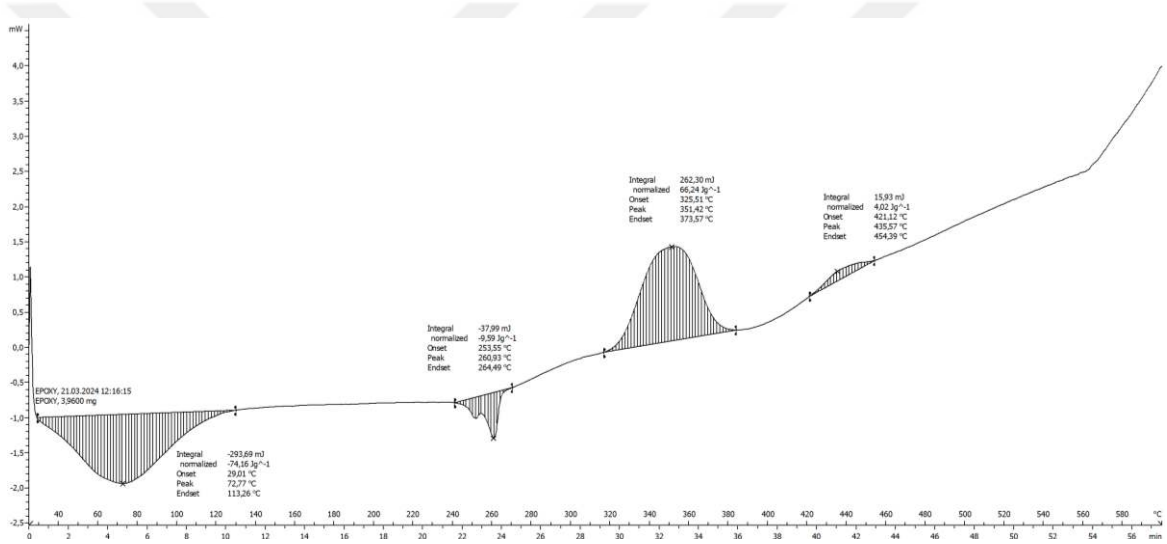

Figure 5.119. EPOXY DSC results

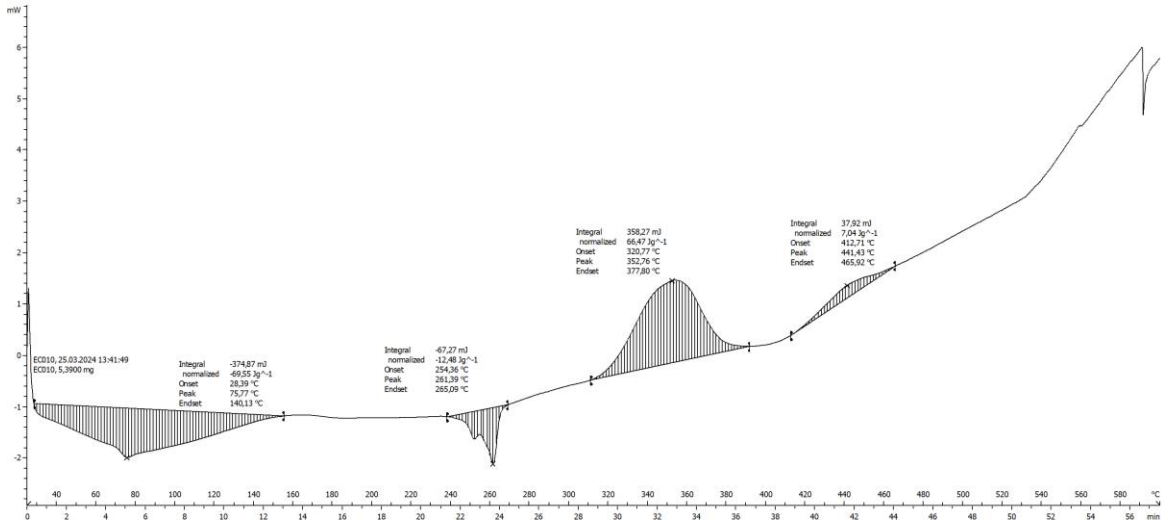

Figure 5.120. . ECO10 DSC test results

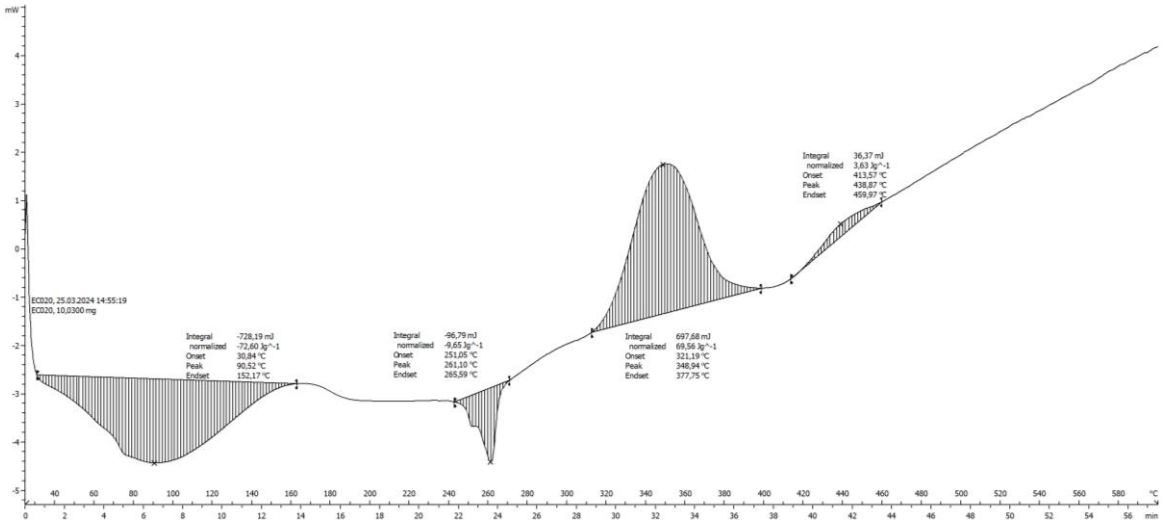

Figure 5.121. ECO20 DSC results

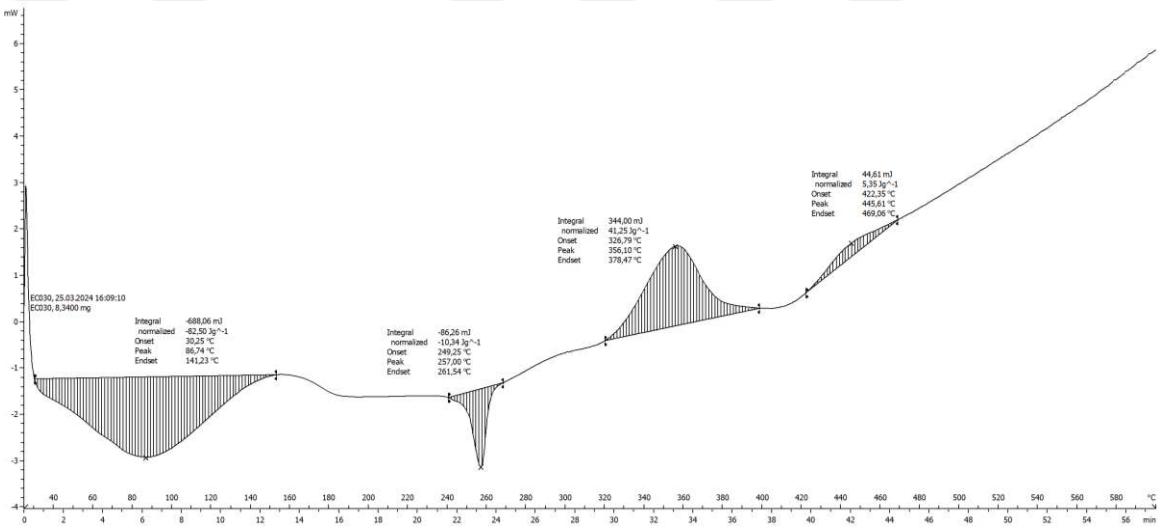

Figure 5.122. ECO30 DSC results

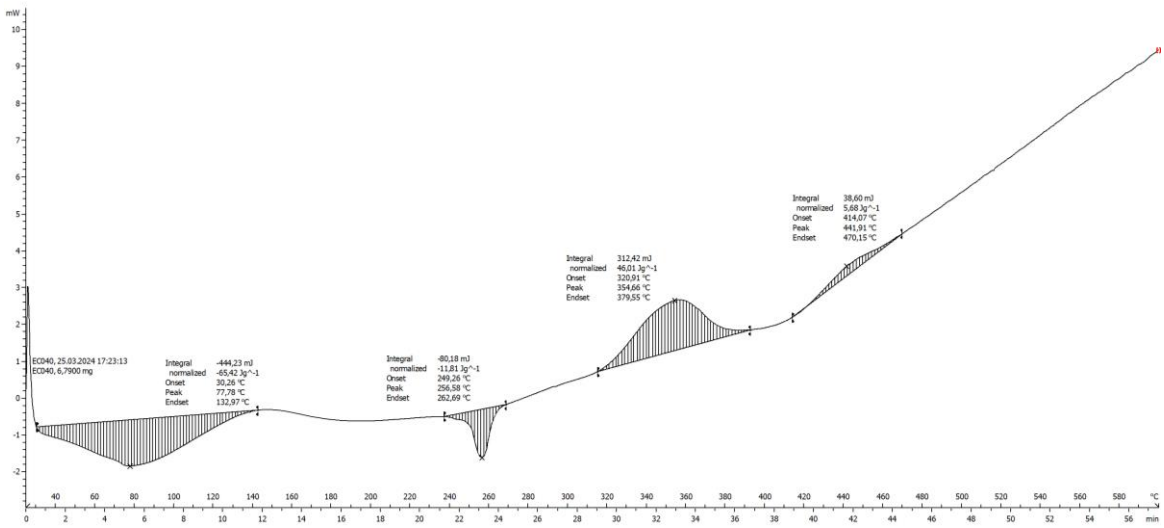

Figure 5.123. ECO40 DSC results

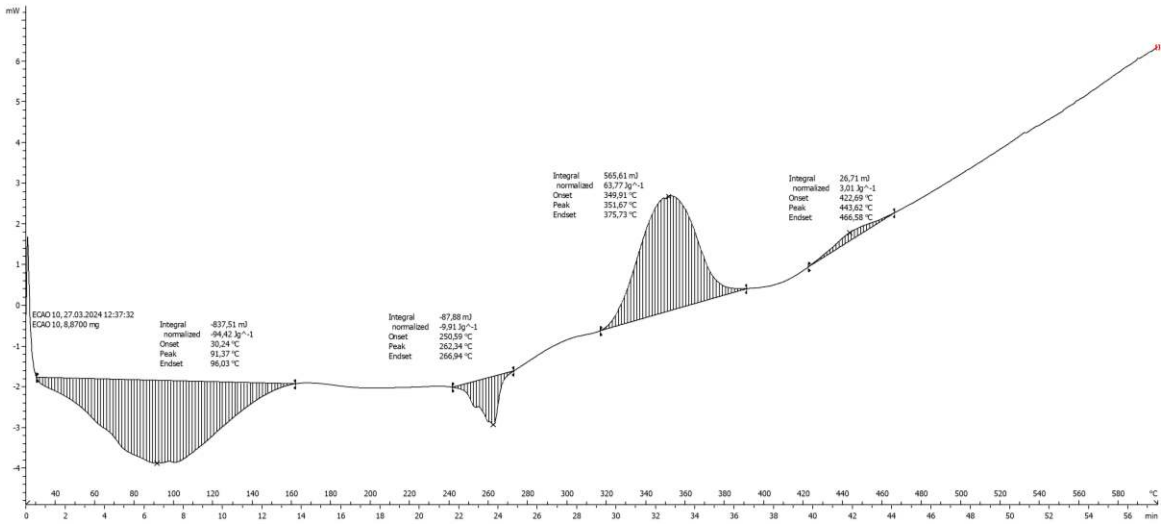

Figure 5.124. ECAO10 DSC results

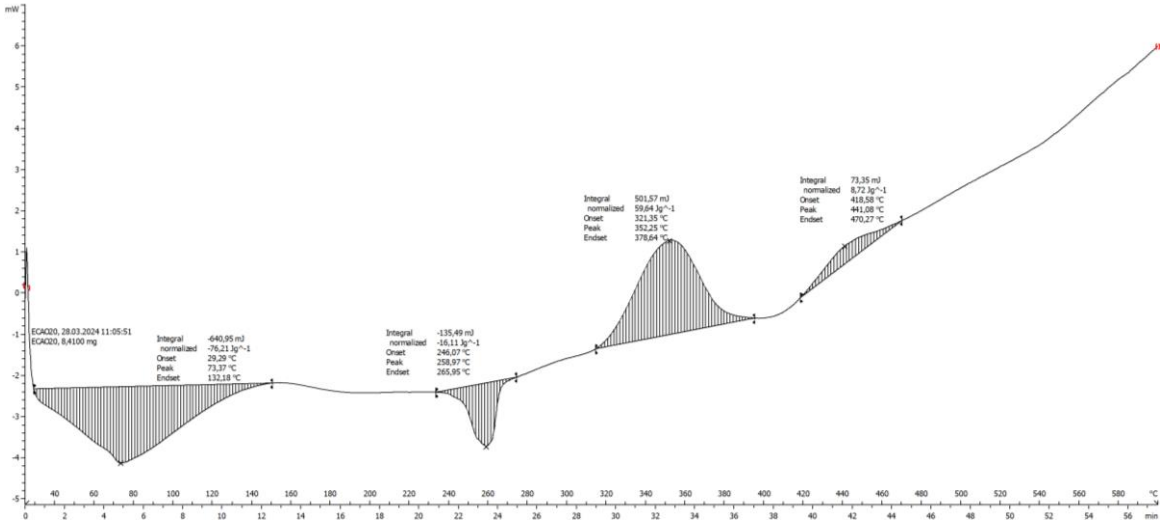

Figure 5.125. ECAO20 DSC results

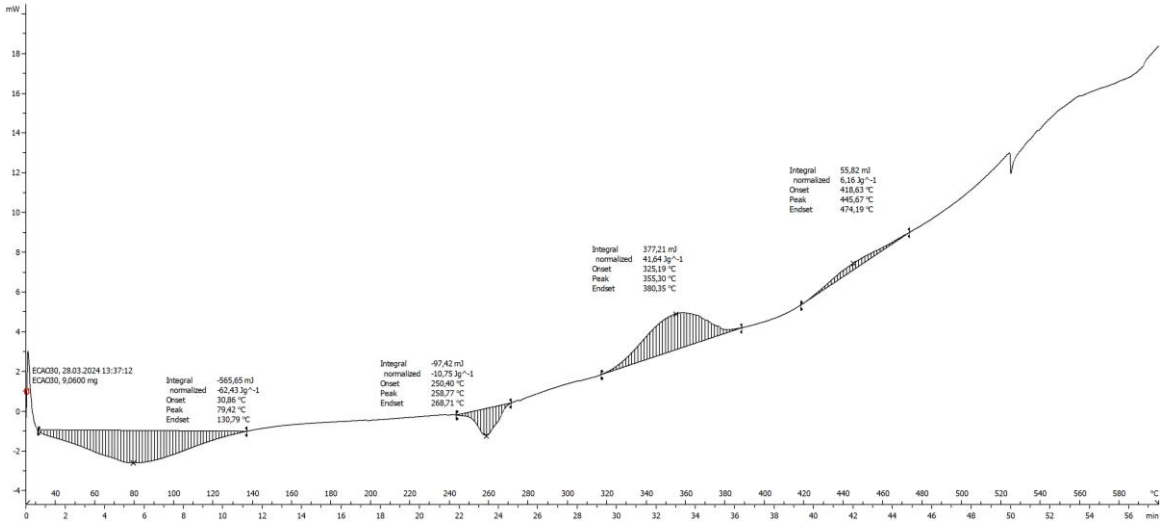

Figure 5.126. ECAO30 DSC results

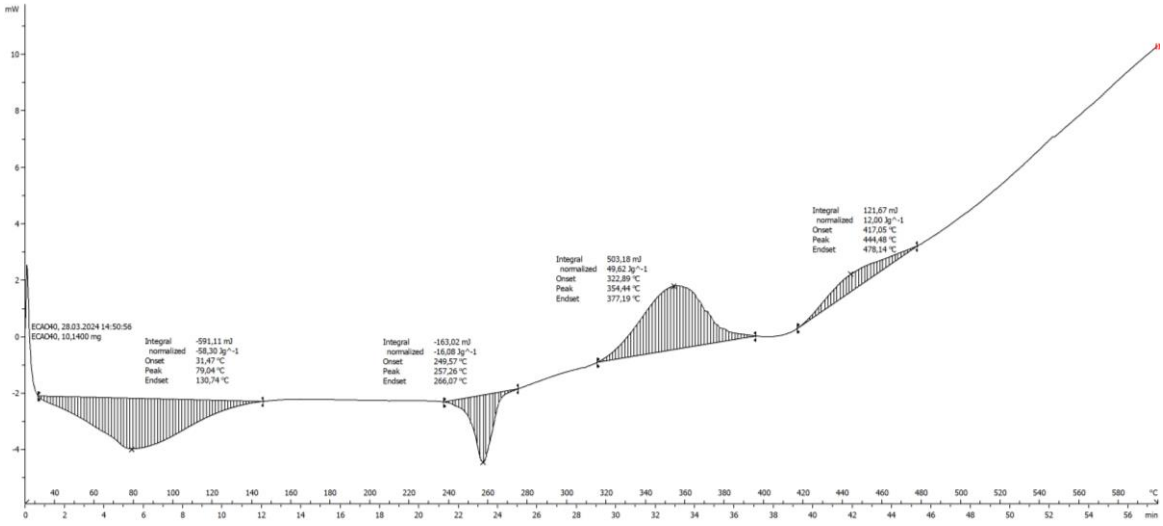

Figure 5.127. ECAO40 DSC results

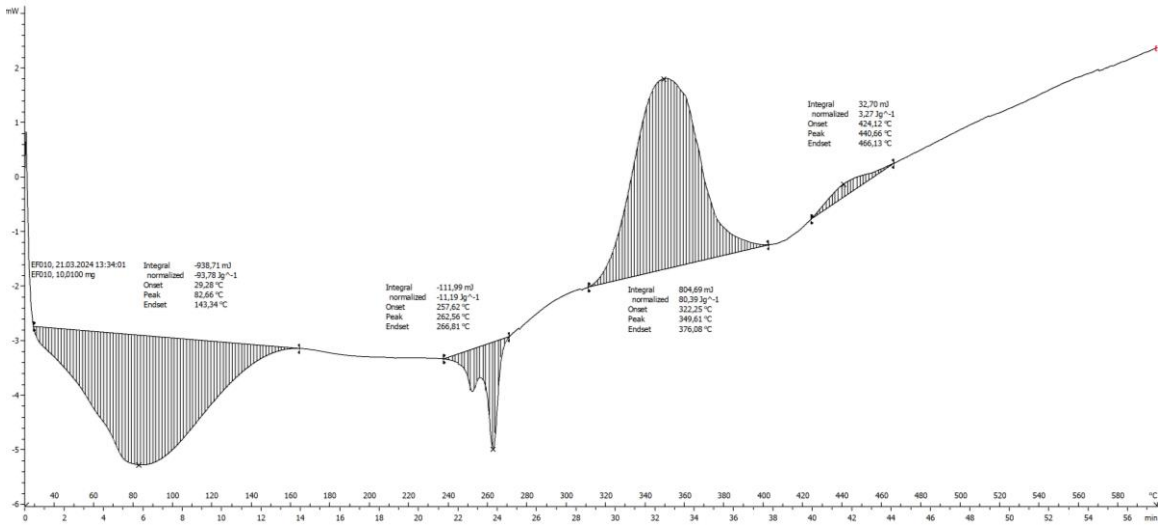

Figure 5.128. EFO10 DSC results

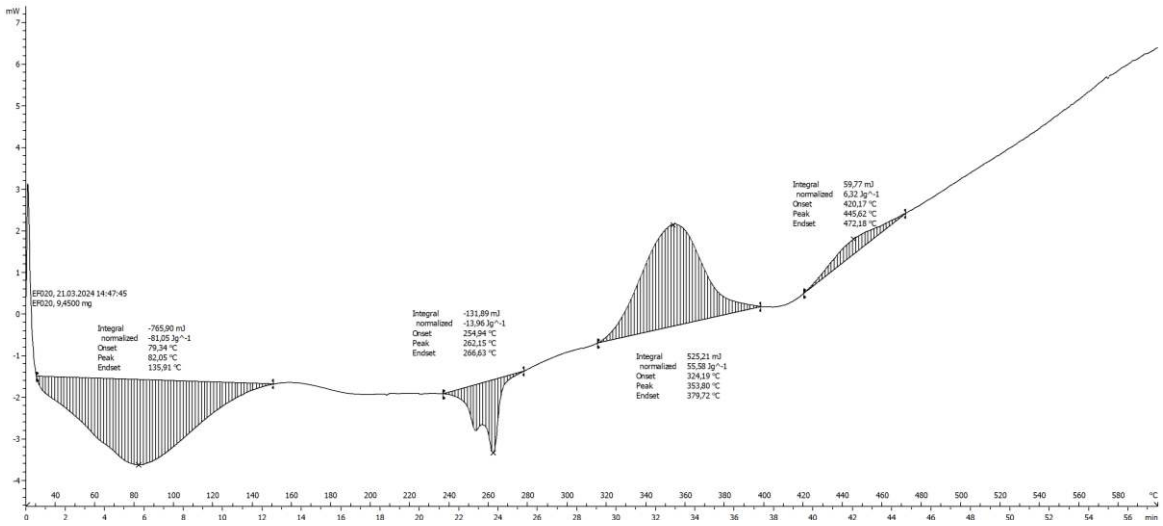

Figure 5.129. EFO20 DSC results

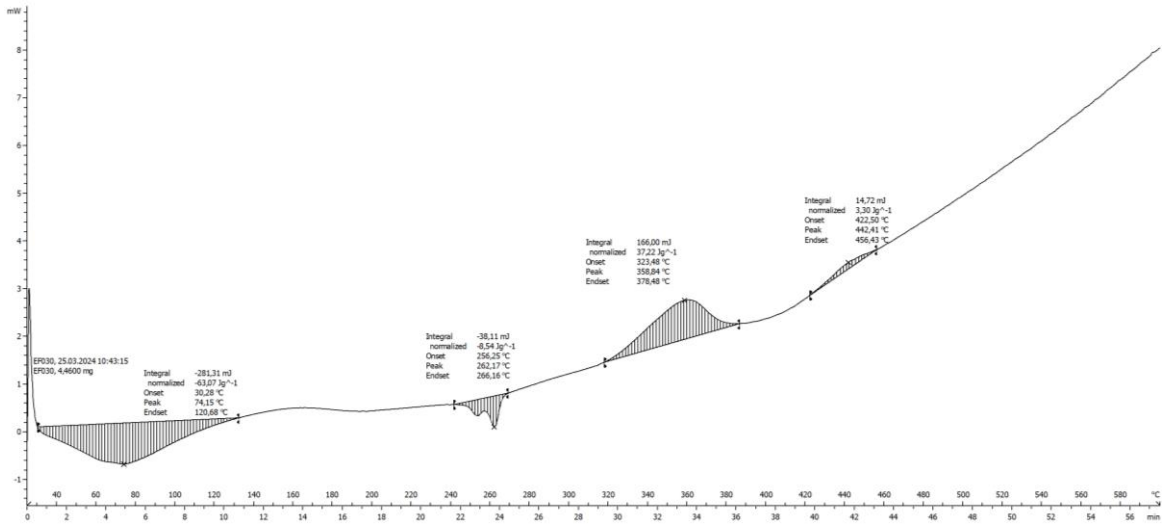

Figure 5.130. EFO30 DSC results

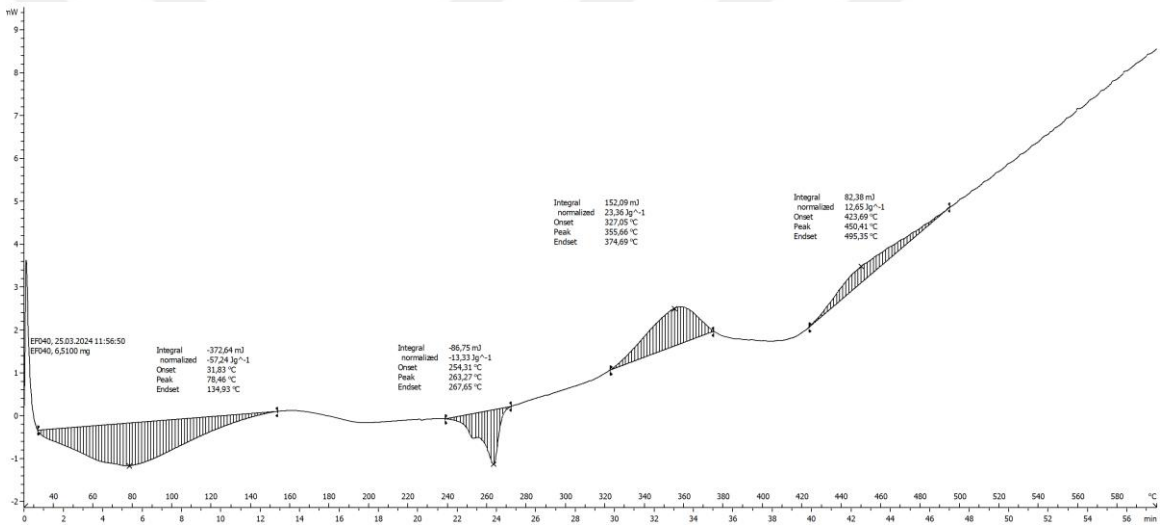

Figure 5.131. EFO40 DSC results

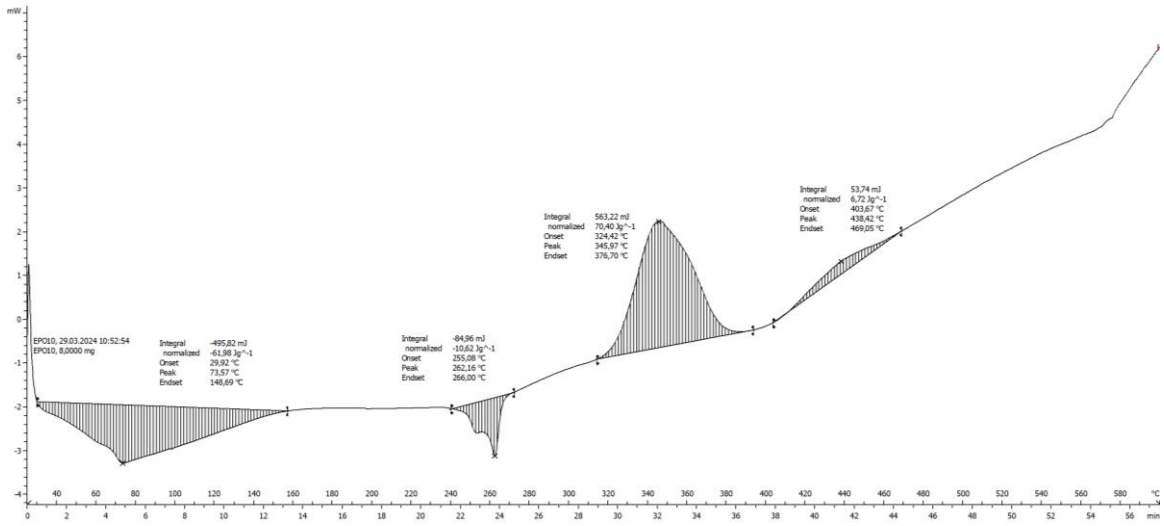

Figure 5.132. EPO10 DSC results

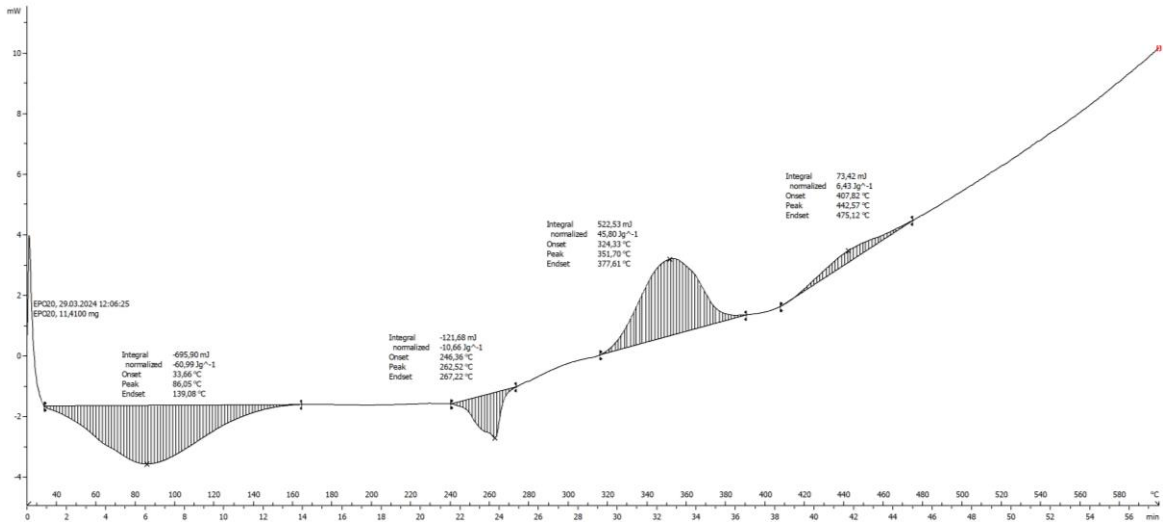

Figure 5.133. EPO20 DSC results

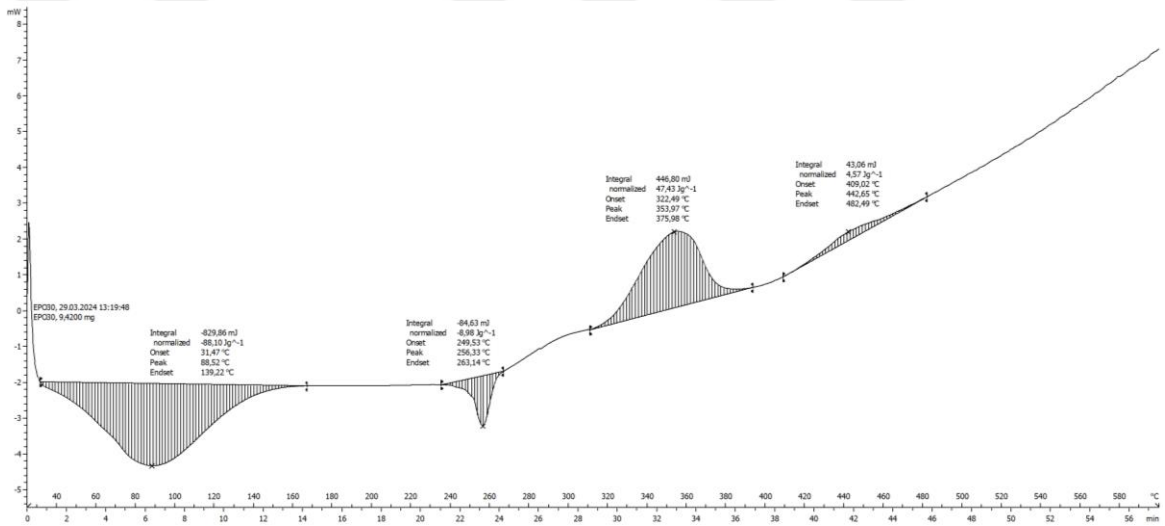

Figure 5.134. EPO30 DSC results

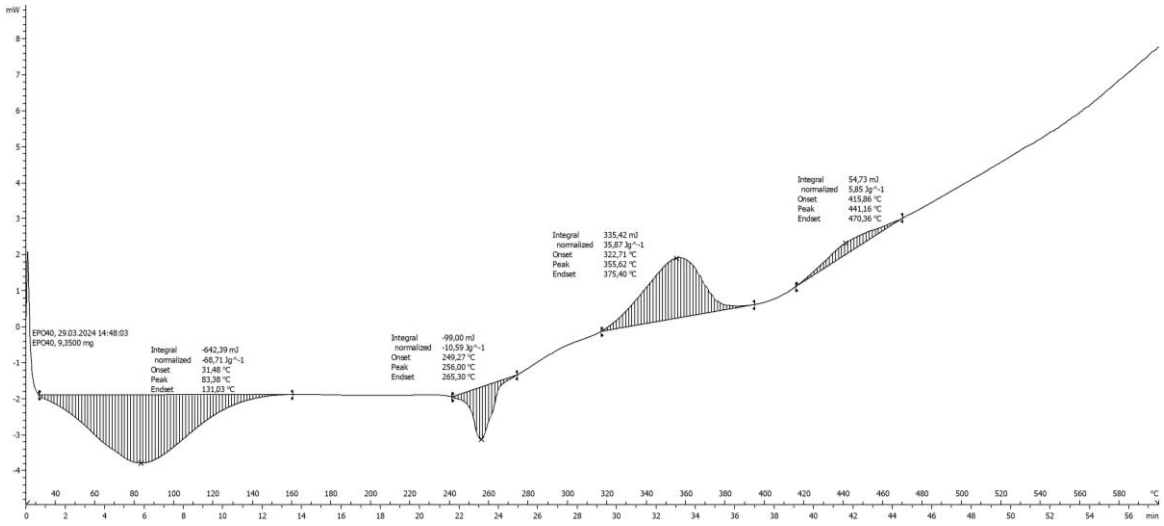

Figure 5.135. EPO40 DSC results

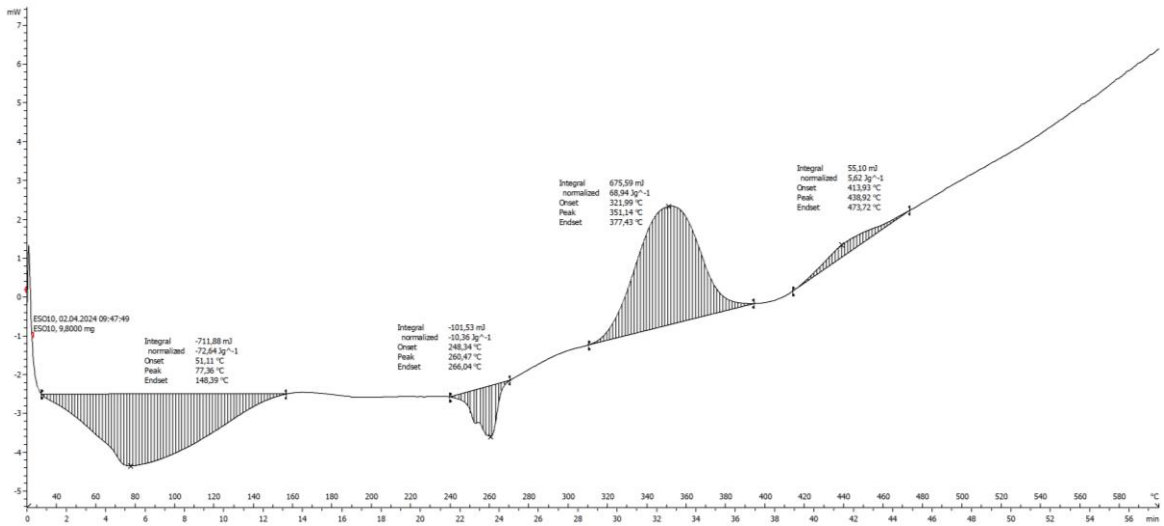

Figure 5.136. ESO10 DSC results

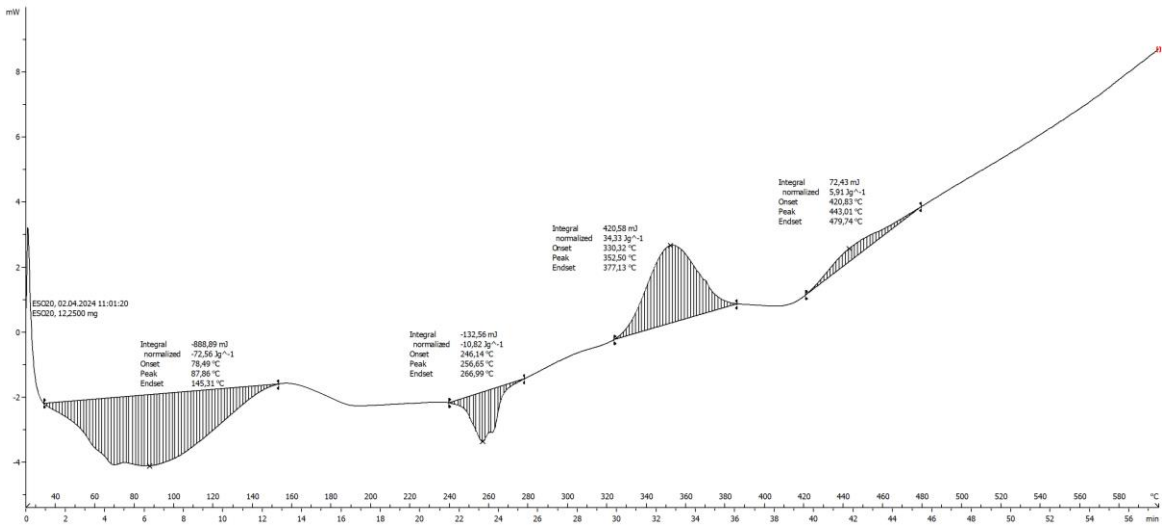

Figure 5.137. ESO20 DSC results

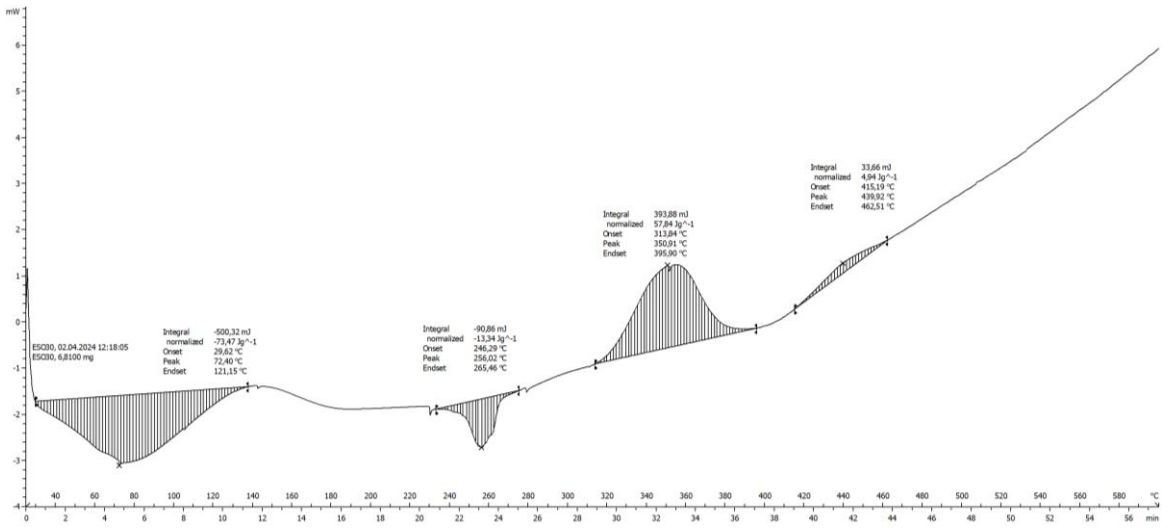

Figure 5.138. ESO30 DSC results

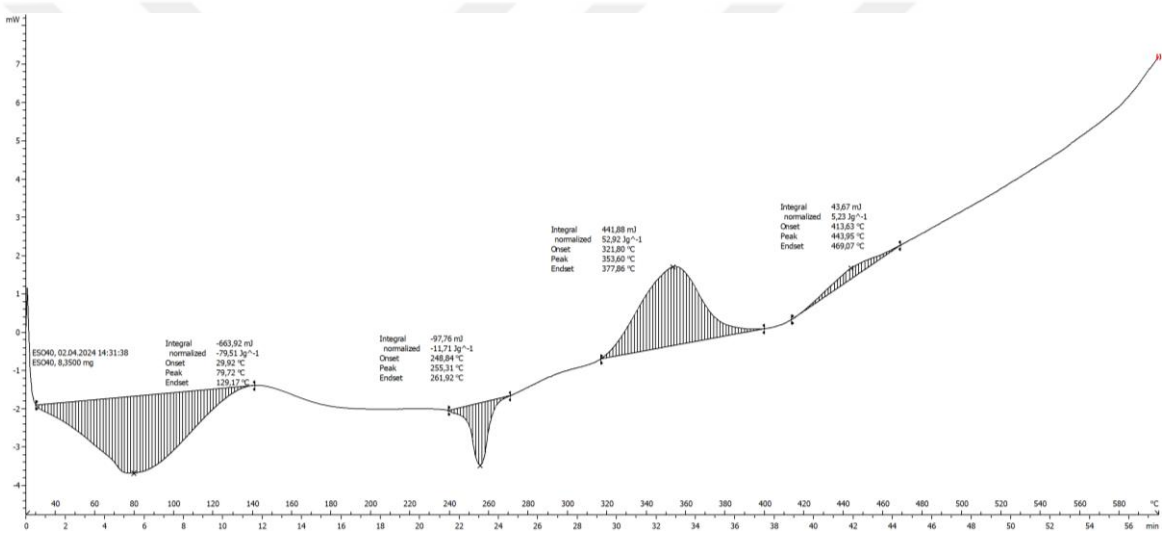

Figure 5.139. ESO40 DSC results

Table 5.10 presents the comparison of T_g and major peak temperatures of EPOXY and biocomposite samples. While the T_g temperature of EPOXY is 72.77 °C, the major peak temperature value is 351.42 °C. According to datas in Table 5.9, there is no sample with a T_g lower than the EPOXY sample except the ESO30 sample. The sample with the highest difference in T_g compared to EPOXY is the ECAO10 sample. The ECO10 sample is listed immediately afterwards. Samples with higher T_g such as ECAO10 and ECO10 exhibited better thermal stabilization, showing much higher initial degradation compared to EPOXY (Karacor and Ozcanli, 2022a). When considered in terms of increasing vegetable oil ratios, as the oil ratio increases from 10% to 40%, the temperature difference in the T_g decreases compared to the EPOXY sample. In other words, as the oil ratio increases towards 40%, the T_g of the sample approach the EPOXY sample. The low oil content increases the T_g value, indicating that the low oil content has a positive effect.

In the major peak temperature comparison, the EFO40 sample is the sample that creates the largest temperature difference compared to EPOXY. The ECO40 sample is also listed with a difference of 4.68 °C behind the EFO40 sample. The EPO10 sample has a lower major peak temperature than EPOXY, -5.42 °C lower. As the vegetable oil ratio increases from 10% to 40%, the major peak temperature difference of biocomposites samples compared to EPOXY also increases. This situation reflects that the major peak temperatures of the samples with 10% oil content are close to EPOXY. An increase in the oil content has a positive effect on the major peak temperature value. In the literature, in the comparison of the large peak temperature, it was stated that the increment in the peak temperature of the specimens containing vegetable oil compared to the EPOXY sample was caused by the reaction of structures with different chain chemical structures such as -OH group and the restriction of the molecular mobility of the resin by the oils (W. Liu et al., 2018). In another study (Sahoo et al., 2018b), it was discovered that long chain triglycerides were added to the epoxy to delay the curing, thus causing the main peak temperature to be higher. It was also stated that the increase in the bio-resin content significantly increased the enthalpy, resulting in a positive effect on the curing reaction temperature by replacing the epoxy with epoxidized linseed oil.

Table 5.10. Comparison of T_g and major peak temperatures of samples

Biocomposites	Difference of T_g temperature compared to EPOXY sample (°C)	Difference of major peak temperature compared to EPOXY sample (°C)
ECO10	+17.75	-2.48
ECO20	+13.97	+1.34
ECO30	+5.01	+3.24
ECO40	+3	+4.68
ECAO10	+18.6	+0.25
ECAO20	+6.65	+0.83
ECAO30	+6.27	+3.02
ECAO40	+0.6	+3.88
EFO10	+9.89	-1.81
EFO20	+9.28	+2.38
EFO30	+5.69	+4.24
EFO40	+1.38	+7.42
EPO10	+15.75	-5.45
EPO20	+10.61	+0.28
EPO30	+13.28	+2.55
EPO40	+0.8	+4.2

ESO10	+15.09	-0.51
ESO20	+6.95	-0.28
ESO30	-0.37	+1.08
ESO40	+4.59	+2.18

Table 5.11 indicates the comparisons of heat reaction values of EPOXY and biocomposite samples. Heat reaction value of EPOXY was 74.16 J/g. There are ECO10, ECAO10, ECAO20, EFO10, EFO20, EPO10, and ESO10 samples with higher heat of reaction values compared to the EPOXY sample. The highest difference in heat of reaction values compared to the EPOXY sample was detected in the ECAO10 sample with +20.26 J/g. The EFO40 sample is the sample with the lowest heat of reaction value compared to the EPOXY sample with a difference of -16.92 J/g. As the oil ratio increases from 10% to 40% in the produced biocomposites, there is a decrease in the heat of reaction value difference according to the EPOXY sample. This indicates that increasing the amount of oil will not have a positive effect on the heat of reaction value. The reason why the reaction heat values are lower than the EPOXY sample with the increase in the amount of vegetable oil is that petroleum-based epoxy resins contain terminal epoxy groups suitable for reaction and the presence of long fatty acids in vegetable oil-based epoxy groups makes it difficult for curing agents to penetrate (Karaçor and Ozcanli, in press). In a study using soybean oil, they found that increasing the amount of soybean-based resin from 10% to 30% resulted in a decrease in the heat of reaction. This indicated that the reactivity in soybean-based epoxy resins increased by adding more epoxide functional groups to short-chain esters via the transesterification process of large-molecule ESO (Zhu et al., 2004).

Table 5.11. Comparison of heat of reaction of samples

Biocomposites	Difference of heat reaction compared to EPOXY sample (J/g)
ECO10	+8.34
ECO20	-1.56
ECO30	-4.61
ECO40	-8.74
ECAO10	+20.26
ECAO20	+2.05
ECAO30	-11.73
ECAO40	-15.86
EFO10	+19.62
EFO20	+6.89
EFO30	-11.09

EFO40	-16.92
EPO10	+13.94
EPO20	-12.18
EPO30	-5.45
EPO40	-13.17
ESO10	+5.35
ESO20	-0.69
ESO30	-1.6
ESO40	-1.52

5.9. SEM Analysis Results

Figure 5.140 to Figure 5.144 indicate the SEM images broken parts after tensile testing. Figure 5.140 displays the SEM images of the broken specimens after the tensile test of EPOXY and ECO samples. While a less brittle structure is observed in the EPOXY sample, the adhesion of the fiber and matrix in the ECO10 sample appears to be good and forms a solid structure. The matrix structure with fiber shows an example of a tougher structure without the addition of oil. In ECO20 and ECO30 samples, it is observed that the formation of porous structures in the samples increases as oil is added. In the ECO40 sample, it is seen that a better adhesion is provided between the fiber and the matrix compared to ECO30 and ECO20. In the literature (Sudha et al., 2017), these situations were encountered in the analysis of bioresins with 30% and 50% oil added, where crack formation and voids are common in bioresins with oil added. These morphological structures were also confirmed in the tensile test results. Considering the void content data in Table 5.2, the void content for EPOXY was calculated as 32.06%, while the void content value for ECO10, ECO20, ECO30 and ECO40 was calculated as 30.7%, 32.47%, 33.71%, and 29.88%, respectively.

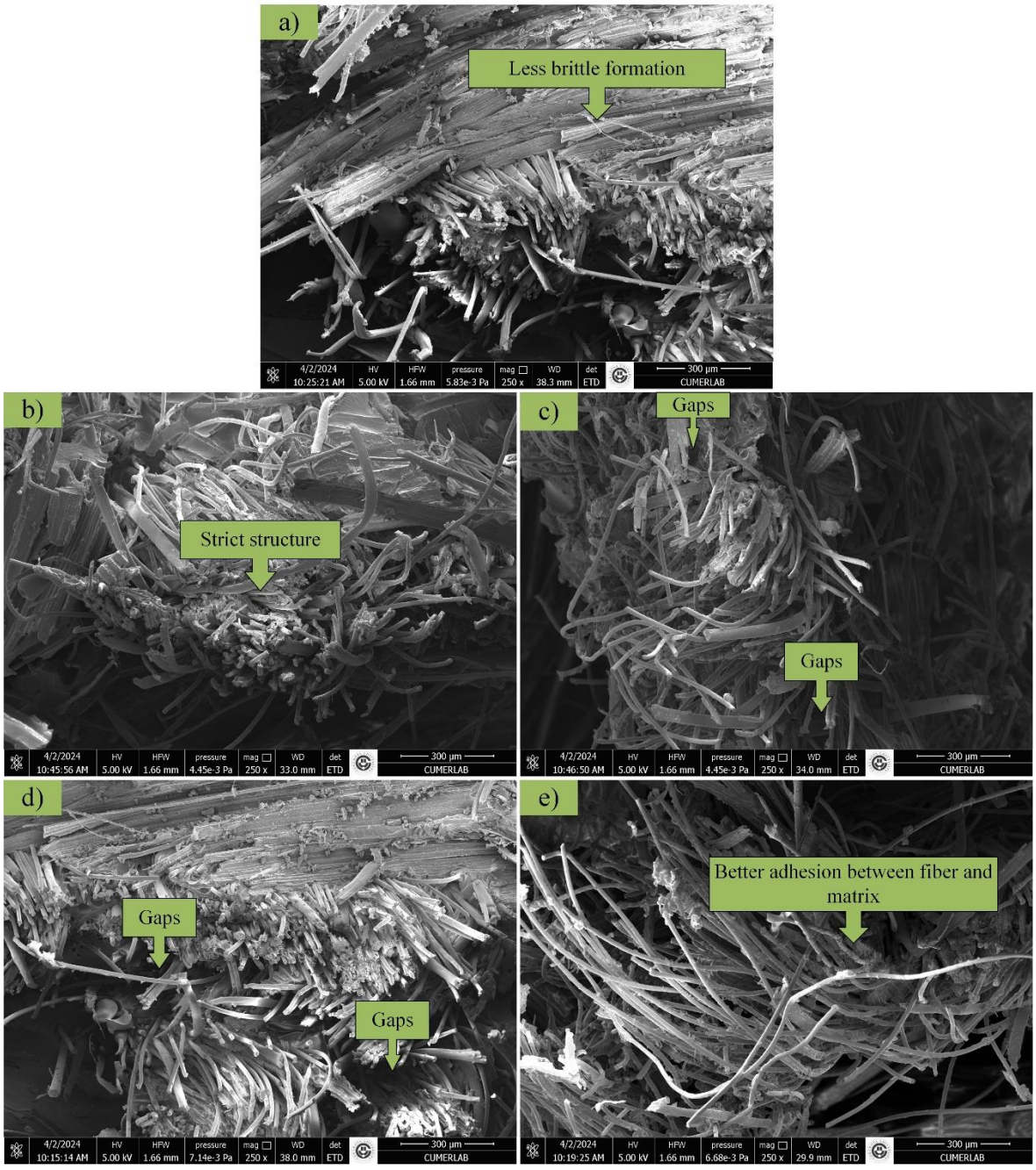

Figure 5.140. SEM images of a) EPOXY b) ECO10 c) ECO20 d) ECO30 and e) ECO40 samples

Figure 5.141 presents SEM images of ECAO samples. In the ECAO10 sample, it is seen that the fibers break radically. This damages the bioresin structure. As the amount of canola oil increases, void formation increases, bubble formation occurs, and direct breakage of the fibers is observed as in micrograph of ECO20, ECO30 and ECO40 samples. This affects the mechanical characteristics and in the tensile test results, this causes the strength to decline as the amount of oil increases. Similarly, in the study conducted by Ozkur et al. (Ozkur et al., 2020), as the amount of bio resin increases, lower strength values are obtained and the percentage elongation increases. The data in

Table 5.2 show that the void ratios are 27.1% for ECAO10, 27.32% for ECAO20, 28.2% for ECAO30 and 32.05% for ECAO40, and these ratios also support the SEM images.

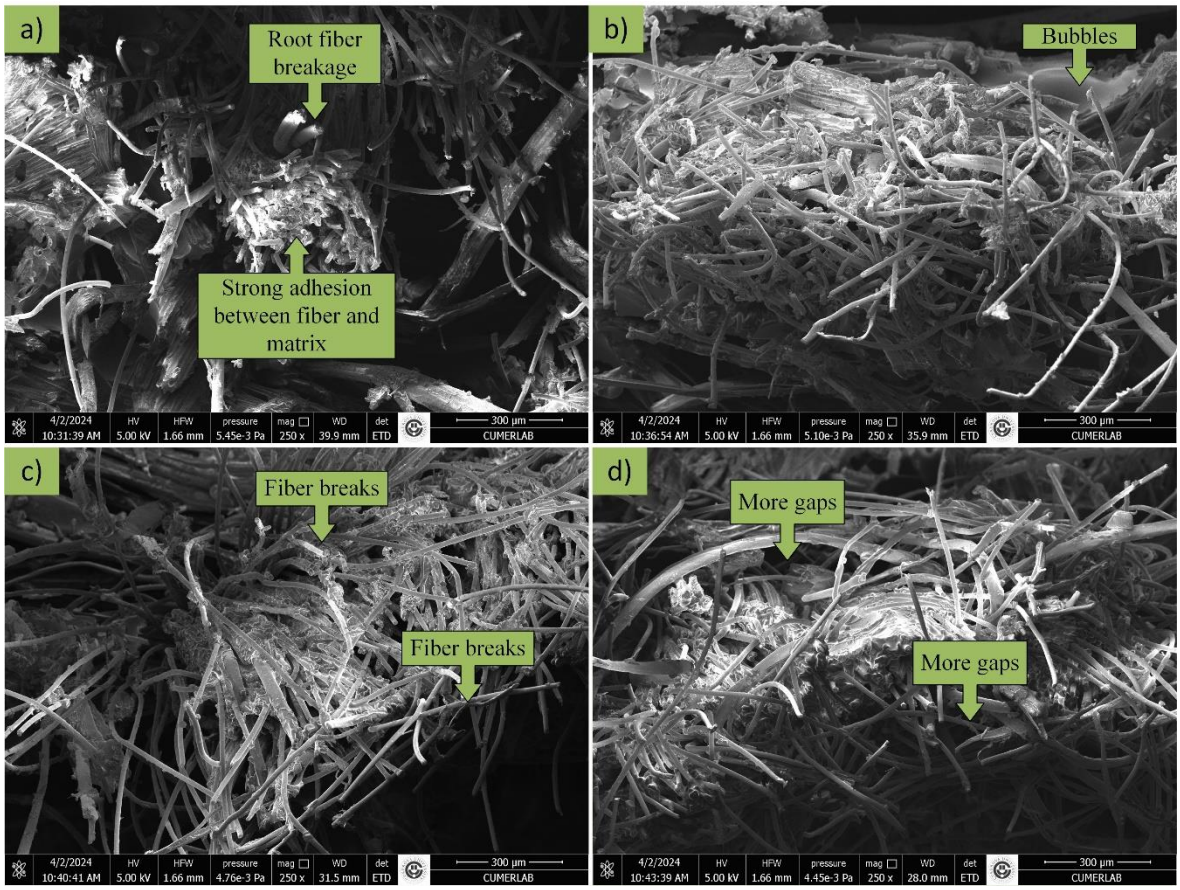

Figure 5.141. SEM images of a) ECAO10 b) ECAO20 c) ECAO30 and d) ECAO40 samples

Figure 5.142 displays the SEM image of EFO samples. The EFO20 sample shows a structure with less porosity and better adhesion of the fibers and matrix to each other compared to the EFO10 sample. In the Sahoo et al. (Sahoo et al., 2018a), increasing the amount of linseed oil in the epoxy resin reduces the potential for breakage and deformation of the bioresin. This situation is consistent with the micrograph results in the current study. In EFO30 and EFO40 samples, porous structures and weak bonds between resin and fiber are observed. This explains why the tensile strength of the sample decreases. It also reflects that the increase in the amount of flaxseed oil results in lower fiber and bioresin adhesion. Void ratio calculations were found to be 29.02%, 27.57%, 32.69% and 33.33% for EFO10, EFO20, EFO30 and EFO40, respectively, and it is theoretically observed that the void amount in EFO30 and EFO40 is higher than the other samples.

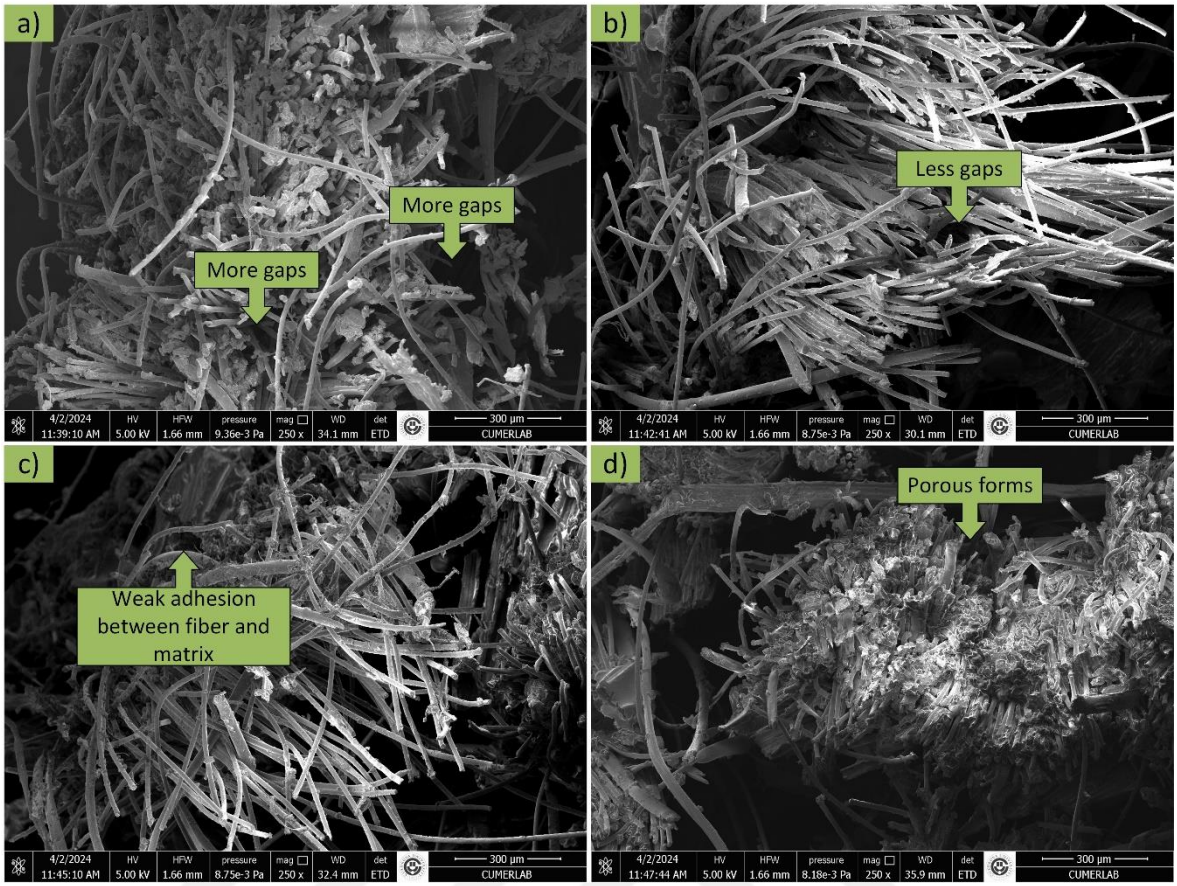

Figure 5.142. SEM images of a) EFO10 b) EFO20 c) EFO30 and d) EFO40 samples

Figure 5.143 displays the SEM images of EPO samples. Increasing palm oil content reduces the formation of interlayer between fiber and matrix and causes more porous structure. However, EPO20 and EPO10 samples show similar micrograph structures, while fiber shrinkage and breakage of strong fiber bundles are present in both micro images. It was determined that more voids were formed in EPO30 and EPO40 and fiber shrinkages were seen in these samples. In the literature, fiber shrinkages in other vegetable oils such as palm oil, hemp oil and soybean oil are also observed in SEM images of samples made with these oils (Manthey et al., 2013). The void rate was calculated as 31.07% for EPO10, 28.29% for EPO20, 31.56% for EPO30 and 36.97% for EPO40.

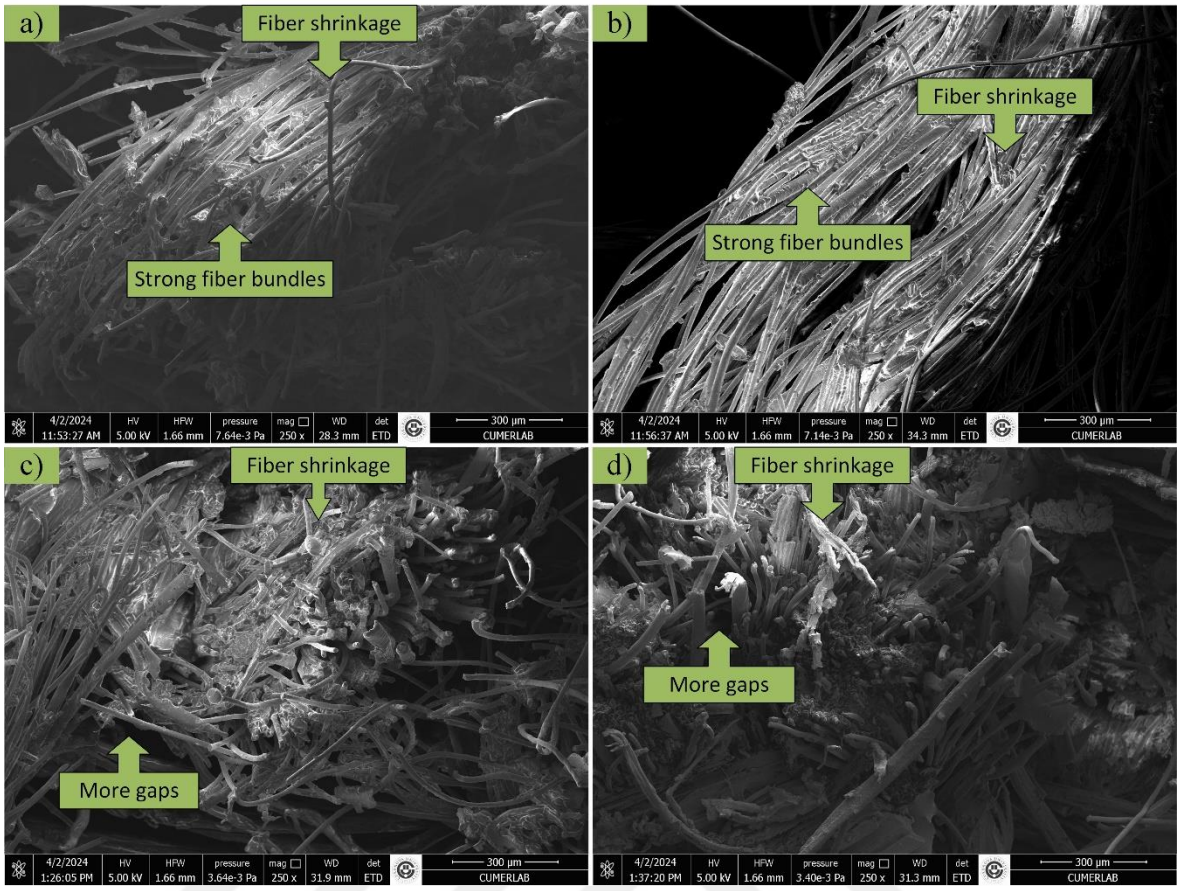

Figure 5.143. SEM images of a) EPO10 b) EPO20 c) EPO30 and d) EPO40 samples

SEM images of ESO specimens are presented in Figure 5.144. While the formation of a hollow structure is observed in the ESO10, ESO30, and ESO40 samples, except for the ESO20 sample, the ESO 20 sample shows a stricter structure with stronger adhesion. The strength of this microstructure shows itself in the tensile strength values. In the study of Sahoo et al. (Sahoo et al., 2015a), uniform distribution of epoxy resin containing soybean oil in the matrix phase increases toughness, while higher oil content leads to heterogeneous particle size distribution and difficulty in bonding resin and fiber. In another study (Sahoo et al., 2017) using soybean oil, increasing the amount of biocomposite soybean oil resin resulted in a good adhesion between the fiber and the matrix. After 30% oil content, the distribution of voids and their lack of uniformity resulted in lower mechanical characteristics. The void contents in ESO10, ESO20, ESO30 and ESO40 samples were found to be 34.91%, 24.36%, 29.35% and 37.35%, respectively.

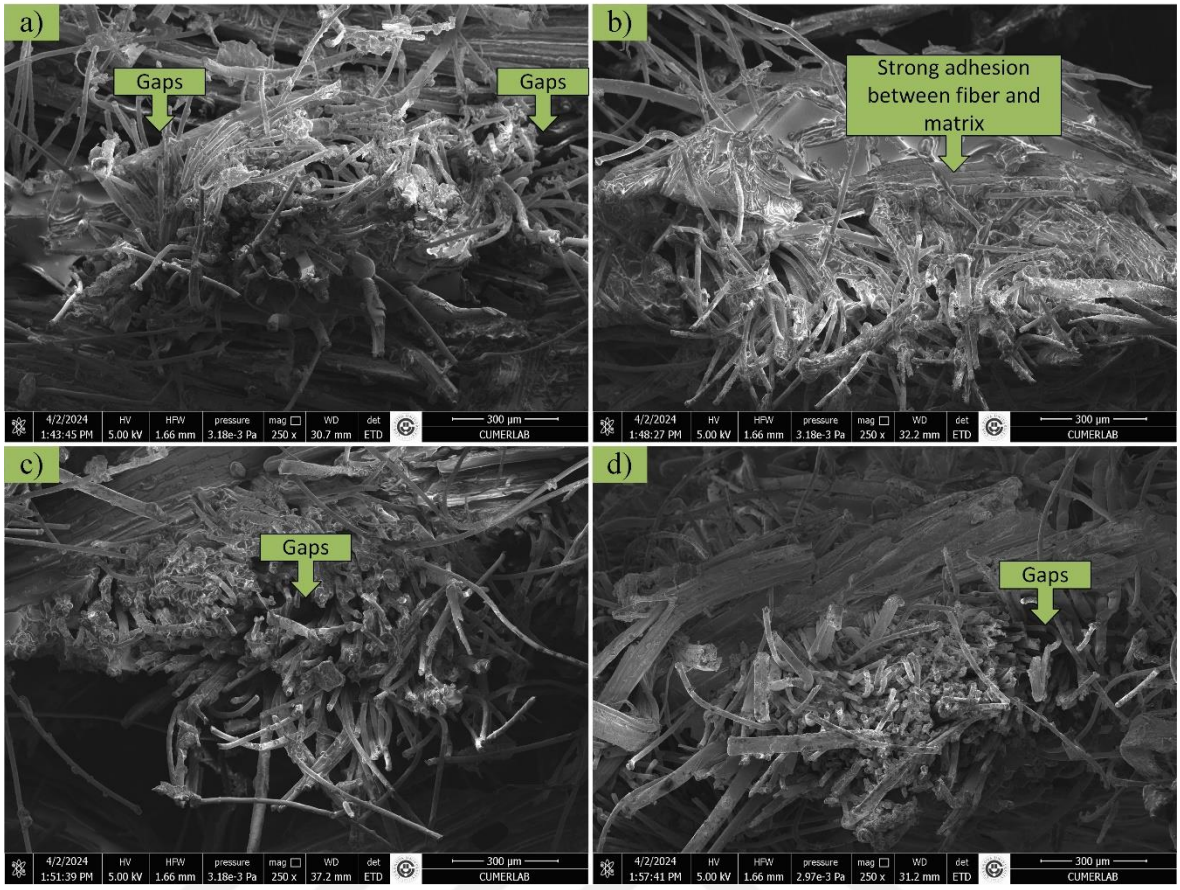

Figure 5.144. SEM images of a) ESO10 b) ESO20 c) ESO30 and d) ESO40 samples

5.10. Cost Analysis Comparisons

The costs of flax/jute fabric, vegetable oils, epoxy and hardener are given in Table 5.12 and Table 5.13. In addition, a comparison of cost calculations per unit weight and unit volume was made in these tables. This cost calculation was made without including laboratory and labor costs. Cost values are obtained from the supplying companies.

Table 5.12. Cost of used matrix and fabrics with unit weight

Biocomposites	Cost of fabric ($)	Cost of vegetable oil ($)	Cost of matrix ($)	Total cost ($)	Unit weight cost ($/kg)
EPOXY	0.05	-	1.87	1.92	165.52
ECO10	0.05	0.026	2.14	2.216	196.106
ECO20	0.05	0.049	1.978	2.077	188.82
ECO30	0.05	0.067	1.82	1.937	176.091
ECO40	0.05	0.085	1.72	1.855	181.863
ECAO10	0.05	0.081	2.14	2.271	216.286
ECAO20	0.05	0.149	1.962	2.161	207.79
ECAO30	0.05	0.207	1.82	2.077	195.943
ECAO40	0.05	0.255	1.68	1.985	190.865
EFO10	0.05	0.086	2.14	2.276	197.913
EFO20	0.05	0.157	1.96	2.167	215.194
EFO30	0.05	0.225	1.87	2.145	196.79
EFO40	0.05	0.276	1.718	2.044	194.67
EPO10	0.05	0.025	2.204	2.279	194.79
EPO20	0.05	0.048	2.09	2.188	206.415
EPO30	0.05	0.062	1.82	1.932	189.412
EPO40	0.05	0.08	1.753	1.883	184.61
ESO10	0.05	0.177	2.14	2.367	232.059
ESO20	0.05	0.327	1.96	2.337	194.750
ESO30	0.05	0.451	1.82	2.321	209.099
ESO40	0.05	0.555	1.68	2.285	209.633

Table 5.13. Cost of used matrix and fabrics with unit volume

Biocomposites	Cost of fabric ($)	Cost of vegetable oil ($)	Cost of matrix ($)	Total cost ($)	Unit volume cost ($/m^3)
EPOXY	0.05	-	1.87	1.92	151181.1024
ECO10	0.05	0.026	2.14	2.216	174763.4069
ECO20	0.05	0.049	1.978	2.077	175422.2973
ECO30	0.05	0.067	1.82	1.937	160613.5987
ECO40	0.05	0.085	1.72	1.855	157738.0952
ECAO10	0.05	0.081	2.14	2.271	197306.6898
ECAO20	0.05	0.149	1.962	2.161	205613.7012
ECAO30	0.05	0.207	1.82	2.077	205643.5644
ECAO40	0.05	0.255	1.68	1.985	181113.1387
EFO10	0.05	0.086	2.14	2.276	174406.1303
EFO20	0.05	0.157	1.96	2.167	193828.2648
EFO30	0.05	0.225	1.87	2.145	172427.6527
EFO40	0.05	0.276	1.718	2.044	188387.0968
EPO10	0.05	0.025	2.204	2.279	185134.0374
EPO20	0.05	0.048	2.09	2.188	169481.0225
EPO30	0.05	0.062	1.82	1.932	170070.4225
EPO40	0.05	0.08	1.753	1.883	167675.8682
ESO10	0.05	0.177	2.14	2.367	196921.797
ESO20	0.05	0.327	1.96	2.337	163655.4622
ESO30	0.05	0.451	1.82	2.321	175037.7074
ESO40	0.05	0.555	1.68	2.285	192340.0673

As the vegetable oil ratio increases from 10% to 40%, the unit cost generally decreases when the unit weight cost is taken into account. This can be associated with the decrease in the amount of epoxy resin used. The ECO30 sample appears to be the most suitable sample in terms of difference with EPOXY in terms of unit weight cost. The most optimum sample in terms of unit volume cost is the ECO40 sample. In determining the cost-property efficiency, the calculation and comparison of specific strength and specific modulus values divided by unit cost are also presented in Tables 5.14 and 5.15. The cost-property tables are also shown graphically in Figures 5.145-148.

Table 5.14. Efficiency of cost property (per unit weight)

Biocomposites	Specific strength/Unit weight cost ($MPa.m^3/\$$)	Specific modulus/Unit weight cost ($GPa.m^3/\$$)
EPOXY	0.000264892	2.45381E-06
ECO10	0.000223235	6.65061E-07
ECO20	0.000196328	4.74977E-07
ECO30	0.000202281	4.64243E-07
ECO40	0.000257972	5.84082E-07
ECAO10	0.000208397	5.91556E-07
ECAO20	0.000171028	4.42891E-07
ECAO30	0.000177354	4.32158E-07
ECAO40	0.000173698	4.50017E-07
EFO10	0.000185633	6.21265E-07
EFO20	0.000172496	5.46541E-07
EFO30	0.000169258	5.64232E-07
EFO40	0.000149215	3.76209E-07
EPO10	0.000207439	6.5074E-07
EPO20	0.000227951	5.11626E-07
EPO30	0.000198012	5.12737E-07
EPO40	0.000196394	3.79477E-07
ESO10	0.000138168	5.51002E-07
ESO20	0.000243725	8.51866E-07
ESO30	0.000202046	5.84832E-07
ESO40	0.000158455	5.58778E-07

Table 5.15. Efficiency of cost property (per unit volume)

Biocomposites	Specific strength/Unit volume cost ($MPa.m^3/\$$)	Specific modulus/Unit volume cost ($GPa.m^{3/}\$$)
EPOXY	2.900106E-07	2.68649E-09
ECO10	2.50502E-07	7.46295E-10
ECO20	2.11322E-07	5.11253E-10
ECO30	2.21772E-07	5.08977E-10
ECO40	2.97422E-07	6.73402E-10
ECAO10	2.28448E-07	6.48471E-10
ECAO20	1.72838E-07	4.47578E-10
ECAO30	1.6864E-07	4.10925E-10
ECAO40	1.83055E-07	4.7426E-10
EFO10	2.1065E-07	7.0499E-10
EFO20	1.91507E-07	6.06775E-10
EFO30	1.93173E-07	6.43953E-10
EFO40	1.54192E-07	3.88755E-10
EPO10	2.18259E-07	6.8468E-10
EPO20	2.77634E-07	6.23136E-10
EPO30	2.20529E-07	5.71043E-10
EPO40	2.16229E-07	4.17802E-10
ESO10	1.62822E-07	6.49322E-10
ESO20	2.90033E-07	1.01372E-09
ESO30	2.41365E-07	6.98641E-10
ESO40	1.72699E-07	6.09008E-10

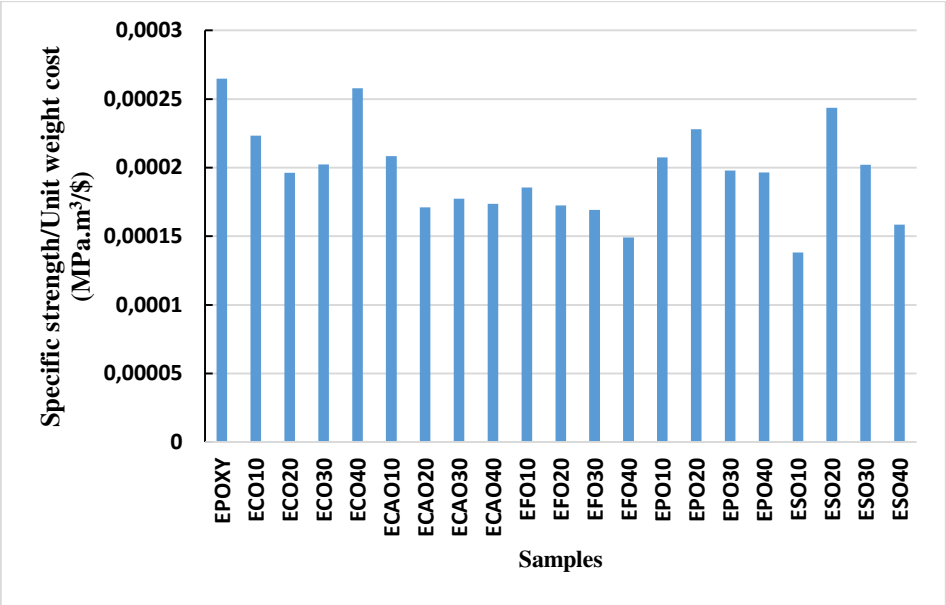

Figure 5.145. Specific strength/Unit weight cost

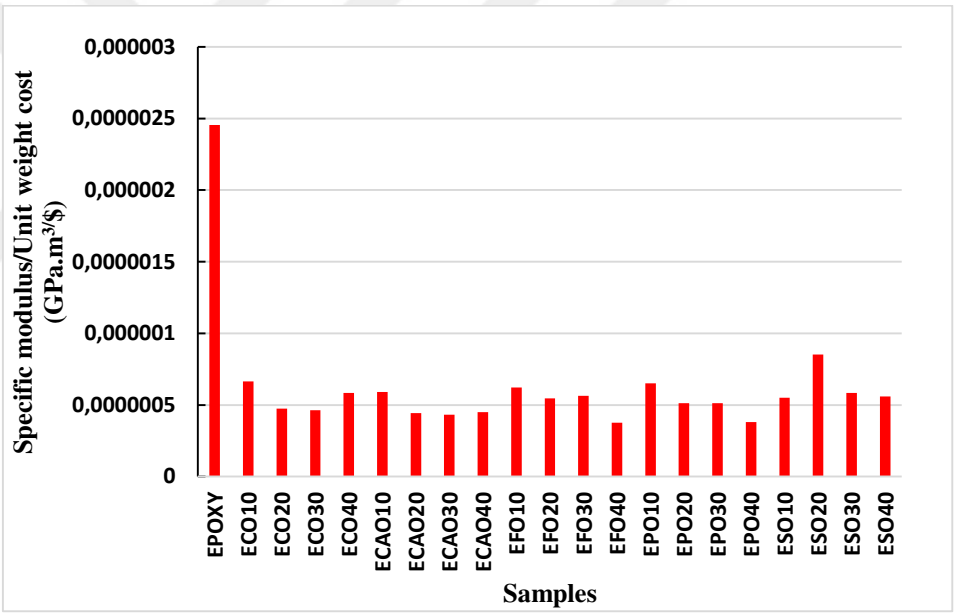

Figure 5.146. Specific modulus/Unit weight cost

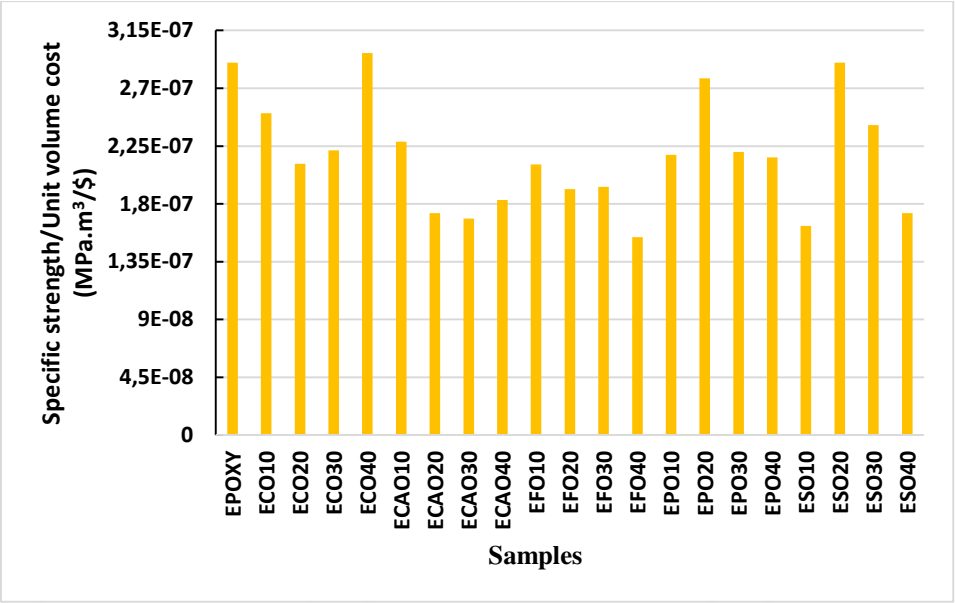

Figure 5.147. Specific strength/Unit volume cost

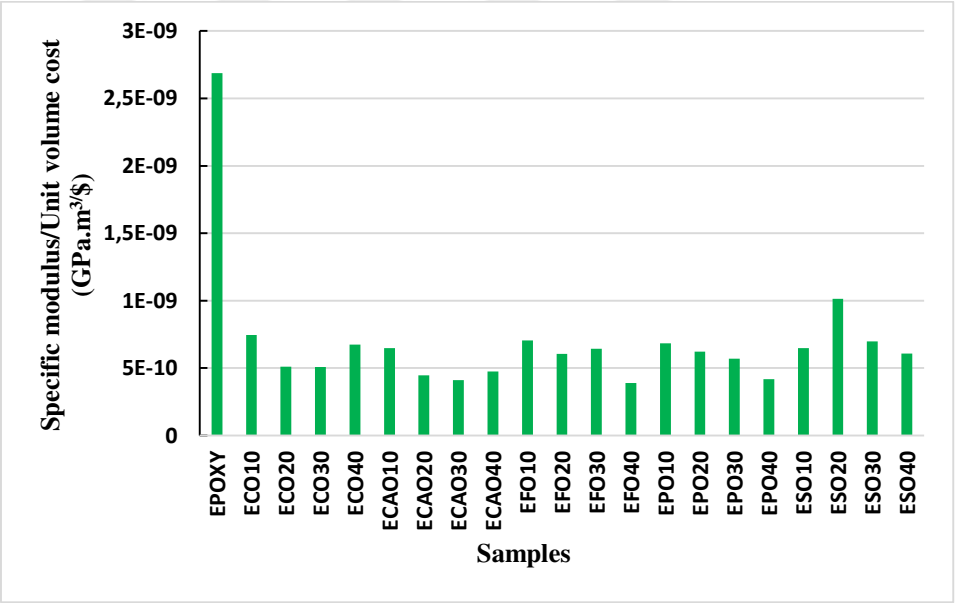

Figure 5.148. Specific modulus/Unit volume cost

Cost analysis calculations for comparison with other commonly used vegetable oils and fibers are given in Table 5.16, Table 5.17, Table 5.18 and Table 5.19. In order to provide comparison with commonly used metals, cost-property analysis was performed in Table 5.20.

Table 5.16. Other vegetable oils property (Baskar et al,2024; Esteban et al.,2012; Mohammed et al.,2020; Karabas,2013; Stanciu,2020)

Other vegetable oil	Density (g/cm^3)	Viscosity (mm^2/s)	Cost ($/L)
Safflower seed oil (ESSO)	0.819	16.5	9
Hemp seed oil (EHO)	0.928	27.28	24
Coconut oil (ECOCO)	0.926	27.6	16.25
Fig seed oil (EFSO)	0.9	38.2	25
Grapeseed oil (EGSO)	0.926	30.19	18

Table 5.17. Other vegetable oils with used natural fiber (Tosmagaza.com, 2024a, 2024b, 2024c; Talyabitkisel.com, 2024a, 2024b)

Biocomposites	Cost of J/F fabric ($)	Cost of other vegetable oil ($)	Total cost ($)
EPOXY	0.05	-	0.05
ESSO10	0.05	0.083	0.133
ESSO20	0.05	0.1548	0.2048
ESSO30	0.05	0.2106	0.2606
ESSO40	0.05	0.2664	0.3164
EHO10	0.05	0.2208	0.2708
EHO20	0.05	0.4128	0.4628
EHO30	0.05	0.5616	0.6116
EHO40	0.05	0.7104	0.7604
ECOCO10	0.05	3.7375	3.7875
ECOCO20	0.05	6.9875	7.0375
ECOCO30	0.05	9.5062	9.5562
ECOCO40	0.05	12.025	12.075
EFSO10	0.05	5.75	5.8
EFSO20	0.05	10.75	10.8
EFSO30	0.05	14.625	14.675
EFSO40	0.05	18.5	18.55
EGSO10	0.05	0.1656	0.2156
EGSO20	0.05	0.3096	0.3596
EGSO30	0.05	0.4212	0.4712
EGSO40	0.05	0.5328	0.5828

Table 5.18. Characteristics of other natural fibers (Karacor and Ozcanli, 2023a)

Fabrics	Density (g/cm^3)	Tensile strength (MPa)	Elongation (%)	Elastic modulus (GPa)	Specific modulus (GPa cm^3/g)
Jute	1.3-1.49	320-800	1-1.8	30	30
Flax	1.4-1.5	343-2000	1.2-3.3	27.6-103	45
Cotton	1.5-1.6	287-800	3-10	5.5-12.6	6
Hemp	1.4-1.5	270-900	1-3.5	23.5-90	40

Table 5.19. Used vegetable oils with other natural fibers (Kumascı.com, 2024b, 2024c, 2024a)

Biocomposites	Cost of vegetable oil ($)	Cost of matrix ($)	Cost of flax fiber ($)	Cost of jute fiber ($)	Cost of cotton fiber ($)	Total cost ($)		
						For flax fiber	For jute fiber	For cotton fiber
EPOXY	-	1.87	0.0615	0.018	0.021	1.931	1.888	1.891
ECO10	0.026	2.14	0.0615	0.018	0.021	2.227	2.184	2.187
ECO20	0.049	1.978	0.0615	0.018	0.021	2.088	2.045	2.048
ECO30	0.067	1.82	0.0615	0.018	0.021	1.948	1.905	1.908
ECO40	0.085	1.72	0.0615	0.018	0.021	1.866	1.823	1.826
ECAO10	0.081	2.14	0.0615	0.018	0.021	2.282	2.239	2.242
ECAO20	0.149	1.962	0.0615	0.018	0.021	2.172	2.129	2.132
ECAO30	0.207	1.82	0.0615	0.018	0.021	2.088	2.045	2.048
ECAO40	0.255	1.68	0.0615	0.018	0.021	1.996	1.953	1.956
EFO10	0.086	2.14	0.0615	0.018	0.021	2.287	2.244	2.247
EFO20	0.157	1.96	0.0615	0.018	0.021	2.178	2.135	2.138
EFO30	0.225	1.51	0.0615	0.018	0.021	1.796	1.753	1.756
EFO40	0.276	1.718	0.0615	0.018	0.021	2.055	2.012	2.015
EPO10	0.025	2.204	0.0615	0.018	0.021	2.29	2.247	2.25
EPO20	0.048	2.09	0.0615	0.018	0.021	2.199	2.156	2.159
EPO30	0.062	1.82	0.0615	0.018	0.021	1.943	1.9	1.903
EPO40	0.08	1.753	0.0615	0.018	0.021	1.894	1.851	1.854
ESO10	0.177	2.14	0.0615	0.018	0.021	2.378	2.335	2.338
ESO20	0.327	1.96	0.0615	0.018	0.021	2.348	2.305	2.308
ESO30	0.451	1.82	0.0615	0.018	0.021	2.332	2.289	2.292
ESO40	0.555	1.68	0.0615	0.018	0.021	2.296	2.253	2.256

Table 5.20. Comparison to common other materials

Materials	Density (kg/m³)	Elastic modulus (GPa)	Specific modulus (GPa.m³ / kg)	Unit cost ($/kg)	Cost property efficiency (Specific modulus/Unit cost) (Gpa.m³ /$)
Al 6061 (Liu et al., 2013)	2700	68.9	0.0255	3.5	0.00729
St-37 (Liu et al., 2013)	7850	200	0.0254	0.72	0.03528
CFRP (Kaw, 2006)	1800	18.96	0.0105	95	0.00011
GFRP (Kaw, 2006)	17101	23.752	0.0014	5	0.00028
LDPE (Ozerpolimer, 2024)	910-925	0.07-0.3	0.0001-0.0003	0.5	0.0002-0.0006
HDPE (Plastem, 2024)	950	1	0.0011	4	0.00027
PET (Metapanel, 2024)	1490-1800	6-14.6	0.0040-0.0081	1.01	0.00396-0.00801
ABS (plasticextrusiontech.net, 2024)	1010-1200	1-2.65	0.0009-0.0022	1.45	0.00062-0.00152

6. CONCLUSIONS

In this study, the biocomposite production and testing of bioresin formed by mixing five different vegetable oils with epoxy resin in certain proportions and intraply flax/jute woven fabric, which has not been tested together in the literature before, was investigated. Five different vegetable oils, cottonseed oil, canola oil, linseed oil, palm oil and soybean oil, were selected and added to the epoxy resin at rates of 10%, 20%, 30% and 40% to form bioresin. Although soybean oil is widely used in the literature with the epoxidation process, it has not been mixed into epoxy resin without any chemical treatment like the other four different oils used. The main goal of the study was to reduce the use of petroleum-based epoxy and to create a new generation bio resin using vegetable oils obtained from natural plants. A bio-composite product was created by selecting intraply flax /jute fabric as the reinforcement element, and the usability of this product in the automotive sector was investigated. In this investigation, mechanical tests such as tensile test, three-point bending test, Charpy impact test and Vickers hardness test, physical analyzes such as water test and density calculation, and thermal analyzes with thermogravimetric and differential scanning calorimetry were performed. In addition, morphological analysis of the samples after mechanical testing was performed to investigate fiber and bioresin interactions. It was determined after these analyses which ratio among four different oil ratios would be the optimum oil level and which vegetable oil would exhibit the closest characteristics to the pure epoxy resin sample. Finally, cost analysis was performed to examine whether the produced biocomposites were at a competitive level in the sector. The results obtained are listed as follows:

- Vegetable oils are materials with lower density values than epoxy resin. In the produced biocomposites, the calculated experimental densities of ECO20, ECO30, EFO30, EFO40, EPO10, EPO30, EPO40, ESO10 and ESO40 samples are lower than the sample produced with pure epoxy resin.
- Their low density naturally affects the weights, and the lighter material position expected from biocomposite materials has been reached. This will provide a great performance/weight advantage, especially in areas such as the automotive industry, where these parts are used directly.
- When considered in terms of tensile strength values, 40% oil addition in ECO sample and 10% oil addition in ECAO sample gave higher values than EPOXY sample. While vegetable oil addition to resin did not have a positive effect on elastic modulus, it had a positive effect on all samples in terms of percentage elongation.
- As the vegetable oil content in the samples increases from 10% to 40% in percent elongation, the elongation amounts increase more compared to EPOXY. In this case, it

is seen that adding vegetable oil to the resin directs the samples to a more elastic behavior.

- When examined in terms of specific strength, ECO40, ECAO10, EPO20 and ESO20 samples reached higher values than EPOXY samples, while when examined in terms of specific modulus, no sample reached the value of the EPOXY sample. One of the utilization advantages could be that the addition of 10 % and 20 % vegetable oil to the resin leads to a relatively higher specific strength compared to the EPOXY sample.
- In the three-point bending test results, the EPOXY sample has the highest bending stress with 56.33 MPa, while the EFO10 sample has the closest bending stress value, with a value of 1.21 times less.
- The sample with the lowest bending stress is the EPO30 sample with 18.19 MPa, followed by the ECAO40 sample, reaching a value 1.11 times higher than EPO30.
- As the oil content increases (except from ESO 10 to ESO 20), the bending stress value decreases. Compared to oil additives, bioresins with 10% oil additive reach the highest bending stress.
- In the evaluation of Charpy impact test results, it was determined that the 20% oil addition was generally the sample that gave the highest values compared to EPOXY in all produced biocomposites.
- Among the vegetable oils used, the highest difference values in terms of impact energy compared to EPOXY were found in ESO samples. EFO was ranked after ESO samples, and the lowest difference compared to EPOXY samples was seen in ECAO samples.
- In the examination of impact strength, it was determined that the samples with 20% and 30% vegetable oil added had an average of 1.38 times and 3.44 times higher values than the EPOXY sample.
- Among the vegetable oil samples, ESO samples, except ESO40, have 3.02 to 3.44 times higher impact strength values than EPOXY. ECAO samples, except ECAO10 and ECAO40, have the lowest difference compared to EPOXY with an impact strength of 1.18-1.38 times.
- In terms of Vickers hardness results, compared to the other three oil ratios, 10% vegetable oil addition increases the hardness value by an average of 0.27%-35.97% compared to the EPOXY sample except EFO10.
- The highest hardness value among the samples is found in the EPO20 sample, followed by EPO10. The lowest hardness values are found in the ECO20 and ECO30 samples.
- The results of the water test indicated that the addition of 20% oil to the resin generally reduced the water absorption of the samples by increasing the hydrophobic structure.

- The ESO20 sample was the sample that displayed the least water absorption compared to other produced samples and EPOXY. According to the test, it showed 7.91% less water absorption compared to EPOXY. Following ESO20, EPO20 and ECAO10 samples are also listed.
- TGA analysis results showed that EPO40 sample lost less weight than EPOXY in terms of weight loss. Increasing the vegetable oil percentage from 10% to 40% generally increases the weight loss. This reflects that adding more than a certain amount of vegetable oil has a negative effect on thermal stability.
- In TGA analysis, the increase in the amount of vegetable oil in the decomposition temperature significantly decreases the temperature compared to EPOXY. The ECAO10 sample is the sample with the least decomposition temperature difference of -11 °C compared to EPOXY.
- In DSC analysis, ECAO10 sample has the highest positive glass transition temperature difference compared to EPOXY. ESO30 sample has a glass transition temperature lower than EPOXY with -0.37 °C.
- As the vegetable oil content increases from 10 % to 40 %, the difference in glass transition temperature compared to EPOXY gradually decreases. The highest temperature difference is in samples with 10% vegetable oil content.
- The largest difference in major peak temperature compared to EPOXY is in the EFO40 sample with +7.42 C, while the EPO10 sample has a major peak temperature of -5.45 C lower than EPOXY.
- As the vegetable oil addition increases from 10% to 40%, the major peak temperature difference of the samples compared to EPOXY also increases.
- The ECAO10 sample is the sample with the highest positive difference compared to EPOXY in heat of reaction value, while the EFO40 sample is the sample with the highest negative difference.
- Increasing the vegetable oil content from 10% to 40% reduces the heat of reaction value by negatively affecting the value difference.
- SEM results show that, in parallel with the void fraction calculations, the ESO20 sample is the sample with the least void structure. The highest void structure was found in the ESO40 sample with 37.35%.
- Although increasing the vegetable oil content generally leads to an increase in the void ratio values, the samples with a combination of 10% and 20% vegetable oil addition are the samples with the lowest calculated void ratio.

- When comparing the fiber weight ratio, the samples ECAO40 and ESO40 have the highest values, while the sample EPO20 has the highest values for the matrix weight ratios.
- In the fiber volume fraction value comparison, the highest value in terms of fiber volume fraction value was calculated for the ECO10 sample, while in the matrix volume comparison, the highest value in terms of matrix volume fraction value was calculated for the EPO20 sample.
- In the unit weight cost comparison, as the vegetable oil content increases from 10% to 40%, the cost per unit weight decreases, and in the unit volume cost comparison, lower values were reached at 30% and 40% vegetable oil content.
- The sample with the closest unit weight cost to EPOXY is ECO30, with a difference of 1.063 times compared to EPOXY. The ESO10 sample is the sample with the highest difference of 1.4 times compared to EPOXY.
- In the unit volume cost comparison, the sample closest to EPOXY is ECO40, which has a value 1.043 times higher than EPOXY. The ECAO30 sample is the sample with the highest difference from EPOXY, with a value of 1.36 times.
- In the Specific strength/Unit weight cost comparison, the ECO40 sample has the closest value to EPOXY, while in the Specific modulus/Unit weight cost comparison, the ESO20 sample has the closest value to EPOXY.
- In the Specific strength/Unit volume cost comparison, the closest value to EPOXY was obtained in the ECO40 sample, while in the Specific modulus/Unit volume cost comparison, the ESO20 sample was the sample with the closest value to EPOXY.

When all the results are considered in their entirety, it was aimed and achieved to create a bio resin by adding vegetable oil to the epoxy resin at different rates due to the high cost of epoxy and its being a petroleum derivative. The order of the most ideal vegetable oil types for this study is cottonseed oil, soybean oil, canola oil, flaxseed oil and palm oil. The optimum oil rate was found to be between 10% and 20% for this study. While it is seen that the biocomposite material produced with these oil ratios and ideal oil type has gained a more ductile structure compared to the sample produced with epoxy resin, it has become possible to evaluate these produced parts in different sectors, especially in automotive parts, vehicle bumpers, where energy absorption is required and flexibility in the material is important. Suggestions for future studies can be listed as follows:

- Using another natural fiber instead of flax/jute fabric
- Determining the most optimum ratio for vegetable oils
- Trying a different production method
- Mixing different vegetable oils into the resin in binary or triple combinations.

REFERENCES

Abbasov, V. M., Nasirov, F. A., Rzayeva, N. S., Nasirova, L. I., and Musayeva, K. Z., 2020. Epoxidated Vegetable Oils : Preparation , Properties and Application. Processes of Petrochemistry and Oil Refining (PPOR), 19(4):427–449.

Acheson, J. A., Simacek, P., and Advani, S. G., 2004. The Implications of Fiber Compaction and Saturation on Fully Coupled VARTM Simulation. Composites Part A: Applied Science and Manufacturing, 35(2):159–169.

Ahn, B.-J. K., 2011. Design and Preparation of Plant Oil-Based Polymers and Their Applications. PhD Thesis, Kansas State University, Manhattan,134p.

Åkesson, D., Skrifvars, M., and Walkenström, P., 2009. Preparation of Thermoset Composites from Natural Fibres and Acrylate Modified Soybean Oil Resins. Journal of Applied Polymer Science, 114(4):2502–2508.

Al-Oqla, F. M., and Sapuan, S. M., 2014. Natural Fiber Reinforced Polymer Composites in Industrial Applications: Feasibility of Date Palm Fibers for Sustainable Automotive Industry. Journal of Cleaner Production, 66 (2014) 347-354.

Almaguer, R., Clark, A., and Odea, N., 2011. Growth opportunities in the global composites industry Society of Plastics Engineers - 11th-Annual Automotive Composites Conference and Exhibition, ACCE 2011, Michigan, USA.

Altuncu, M. S., 2015. Synthesis of Networks and Interpenetrating Networks of Maleated Castor Oil and Epoxy Resins.Msc Thesis, Boğaziçi University,İstanbul,65p.

Anastas, P. T., and Zimmerman, J. B., 2013. Innovations in Green Chemistry and Green Engineering Selected. Springer,New York,333p.

Andjelkovic, D. D., Valverde, M., Henna, P., Li, F., and Larock, R. C., 2005. Novel Thermosets Prepared by Cationic Copolymerization of Various Vegetable Oils—Synthesis and Their Structure–Property Relationships. Polymer, 46(23):9674–9685.

Anonymous,2012.*Biocomposites*.http://yudysi.lecture.ub.ac.id/files/2012/12/MaterialBaru09thBiocomposites.pdf

Asim, M., Abdan, K., Jawaid, M., Nasir, M., Dashtizadeh, Z., Ishak, M. R., … Deng, Y., 2015. A Review on Pineapple Leaves Fibre and Its Composites. International Journal of Polymer Science, 2015(1),1-16.

ASTM D3039/D3039-M, 2000. Standard Test Method for Tensile Properties of Polymer Matrix Composite Material. (www.astm.org)

ASTM D6110-10, 2010. Designation: D6110−10Standard Test Method for Determining the Charpy Impact Resistance of NotchedSpecimens of Plastics ASTM International. https://doi.org/10.1520/D6110-10.

ASTM D790-03, 2003. Standard Test Methods for Flexural Properties of Unreinforced and

Reinforced Plastics and Electrical Insulating Materials. (www.astm.org)

ASTM E92-17, 2017. Standard Test Methods for Vickers Hardness and Knoop Hardness of Metallic Materials. https://doi.org/10.1520/E0092-17.

ASTM International D5229, 2004. Standard test method for moisture absorption properties and equilibrium conditioning of polymer matrix composite materials Annual book of ASTM standards (Vol. 92).

Auvergne, R., Caillol, S., David, G., Boutevin, B., and Pascault, J.-P., 2014. Biobased Thermosetting Epoxy: Present and Future. Chemical Reviews, 114(2):1082–1115.

Bakar, M. B. A., Masri, M. N., Amini, M. H. M., Thirmizir, M. Z. M., and Salim, M. S., 2018. Mechanical, Thermal and Morphological Properties of Epoxy Resin Toughened with Epoxidized Soybean Oil. In AIP Conference Proceedings , 2030, 020277.

Bao, L., Bian, L., Zhao, M., Lei, J., and Wang, J., 2014. Synthesis and Self-Assembly Behavior of a Biodegradable and Sustainable Soybean Oil-Based Copolymer Nanomicelle. Nanoscale Research Letters, 9(1):391.

Basaltex.com, 2023. Basalt Fiber Types. https://www.basaltex.com/products/fibers-and-rovings[Accessed date:23.11.2023]

Baskar, S., Arumugam, S., Krishnamoorthy, S. 2024. Yield enhancement through synergism by ultrasonication assistance in the transesterification of fig seed oil using waste fig leaves catalyst. Journal of Industrial and Engineering Chemistry, 135 (2024): 286–296.

Biermann, U., Friedt, W., Lang, S., Lühs, W., Machmüller, G., Metzger, U. O., … Schneider, M. P., 2005. New Syntheses with Oils and Fats as Renewable Raw Materials for the Chemical Industry. In Biorefineries-Industrial Processes and Products, 2, 253–289.

Bledzki, A. K., Reihmane, S., and Gassan, J., 1996. Properties and Modification Methods for Vegetable Fibers for Natural Fiber Composites. Journal of Applied Polymer Science, 59(8):1329–1336.

Bodaghi, M., Costa, R., Gomes, R., Silva, J., Correia, N., and Silva, F., 2020. Experimental Comparative Study of the Variants of High-Temperature Vacuum-Assisted Resin Transfer Moulding. Composites Part A: Applied Science and Manufacturing, 129 (November 2019):105708.

Boon, Y. Di, Joshi, S. C., and Bhudolia, S. K., 2021. Review: Filament Winding and Automated Fiber Placement with In Situ Consolidation for Fiber Reinforced Thermoplastic Polymer Composites. Polymers, 13(12):1951.

Boquillon, N., 2006. Use of an Epoxidized Oil-Based Resin as Matrix in Vegetable Fibers-Reinforced Composites. Journal of Applied Polymer Science, 101(6):4037–4043.

Campbell, F. C., 2010. Structural Composite Materials Geostatistics. ASM International,Ohio,612p.

Can, E., Küsefoğlu, S., and Wool, R. P., 2001. Rigid, Thermosetting Liquid Molding Resins from Renewable Resources. I. Synthesis and Polymerization of Soy Oil Monoglyceride Maleates.

Journal of Applied Polymer Science, 81(1):69–77.

Çelik, O., Yaşar, A., and Karaçor, B., 2023. Properties of Basalt/Aramid Fiber Reinforced Hybrid Composites Compared to Carbon Fiber Composites. Polymer Composites, 44(6):3509–3521.

Cheong, M. Y., Lye Ooi, T., Ahmad, S., Yunus, W. M. Z. W., and Kuang, D., 2009. Synthesis and Characterization of Palm-Based Resin for UV Coating. Journal of Applied Polymer Science, 111(5):2353–2361.

de Lemos, A. L., Pires, P. G. P., de Albuquerque, M. L., Botaro, V. R., de Paiva, J. M. F., and Domingues Junior, N. S., 2017. Biocomposites Reinforced with Natural Fibers: Thermal, Morphological and Mechanical Characterization. Revista Materia, 22(2):8–10.

Debnath, S., 2017. Sustainable Production of Bast Fibres. In Sustainable Fibres and Textiles (pp. 69–85). Editor: Subramanian Senthilkannan Muthu,Elsevier,1 st Edition.

Dhimole, V. K., Serrao, P., and Cho, C., 2021. Review and Suggestion of Failure Theories in Voids Scenario for VARTM Processed Composite Materials. Polymers, 13(6):969.

Di Mauro, C., Malburet, S., Genua, A., Graillot, A., and Mija, A., 2020. Sustainable Series of New Epoxidized Vegetable Oil-Based Thermosets with Chemical Recycling Properties. Biomacromolecules, 21(9):3923–3935.

Dinda, S., Patwardhan, A. V., Goud, V. V., and Pradhan, N. C., 2008. Epoxidation of Cottonseed Oil by Aqueous Hydrogen Peroxide Catalysed by Liquid Inorganic Acids. Bioresource Technology, 99(9):3737–3744.

Djunaedi, K., 2007. Development of a Sliver Polymer Matrix Composite (SPMC) using Flax Fibers and Epoxy / Acrylated Epoxidized Soybean Oil Resin. Msc Thesis, North Carolina State University, North Carolina ,114p.

Drzal, L. T., Mohanty, A. K., and Misra, M., 2001. Bio-Composite Materials as Alternatives to Glass Fibre Reinforced Composites for Automotive Applications. Magnesium, 40:386–390.

Enis, I. Y., and Sezgin, H., 2021. Full Factorial Experimental Design for Water Absorption and Wettability of Jute Fabric Reinforced Acrylated Epoxidized Soybean Oil/Epoxy Biocomposites. Tekstil ve Mühendis, 28(123):163–170.

Ernault, E., Richaud, E., and Fayolle, B., 2017. Origin of Epoxies Embrittlement during Oxidative Ageing. Polymer Testing, 63:448–454.

Ertekin, M., 2017. Aramid fibers.In Fiber Technology for Fiber-Reinforced Composites(pp.153-167). Editors: M. Özgür Seydibeyoğlu, Amar K. Mohanty,Manjusri Misra, Elsevier,1 st Edition.

Espinoza Pérez J. D., Haagenson D. M., Pryor S. W., Ulven C. A., and Wiesenborn D. P., 2009. Production and Characterization of Epoxidized Canola Oil. Transactions of the ASABE, 52(4):1289–1297.

Espinoza-Perez, Judith D., Nerenz, B. A., Haagenson, D. M., Chen, Z., Ulven, C. A., and

Wiesenborn, D. P., 2011. Comparison of Curing Agents for Epoxidized Vegetable Oils Applied to Composites. Polymer Composites, 32(11):1806–1816.

Espinoza-Perez, Judith Dolores, 2009. Production, Characterization, and Raw Material Cost Analysis of a Canola Oil-Epoxy Resin Applied To Composites. PhD Thesis,North Dakota State University,Fargo,151p.

Esteban B, Riba JR, Baquero G, Rius A, Puig R.,2012. Temperature dependence of density and viscosity of vegetable oils. Biomass and bioenergy, 42(2012):164 -171.

Fahimian, M., Adhikari, D., Raghavan, J., and Wool, R. P., 2008. Biocomposites from Canola Oil Based Resins and Hemp and Flax Fibers. The Thirteenth European Conference on Composite Materials (ECCM 13), (June 2008):1–10.

Faruk, O., Bledzki, A. K., Fink, H.-P., and Sain, M., 2014. Progress Report on Natural Fiber Reinforced Composites. Macromolecular Materials and Engineering, 299(1):9–26.

Flanigan, C., Perry, C., Lee, E., Houston, D., Mielewski, D., and Harris, A., 2006. Use of Agricultural Materials in Flexible Polyurethanes and Composites for Automotive Applications. 6th Annual SPE Automotive Composites Conference 2006, 1270–1287.

Fowler, P. A., Hughes, J. M., and Elias, R. M., 2006. Biocomposites: Technology, Environmental Credentials and Market Forces. Journal of the Science of Food and Agriculture, 86(12):1781–1789.

Fu, L., Yang, L., Dai, C., Zhao, C., and Ma, L., 2010. Thermal and Mechanical Properties of Acrylated Expoxidized-Soybean Oil-Based Thermosets. Journal of Applied Polymer Science, 117(4):2220–2225.

Gandini, A., 2008. Polymers from Renewable Resources: A Challenge for the Future of Macromolecular Materials. Macromolecules, 41(24):9491–9504.

George, J., Sreekala, M. S., and Thomas, S., 2001. A Review on Interface Modification and Characterization of Natural Fiber Reinforced Plastic Composites. Polymer Engineering and Science, 41(9):1471–1485.

Gerbase, A. E., Gregório, J. R., Martinelli, M., Brasil, M. C., and Mendes, A. N. F., 2002. Epoxidation of Soybean Oil by the Methyltrioxorhenium-CH 2 Cl 2 /H 2 O 2 Catalytic Biphasic System. Journal of the American Oil Chemists' Society, 79(2):179–181.

Gerbase, A. E., Petzhold, C. L., and Costa, A. P. O., 2002. Dynamic Mechanical and Thermal Behavior of Thermotropic Polyesters Based On. JAOCS, 79(8):797–802.

Griffith, M. L., and Halloran, J. W., 1996. Freeform Fabrication of Ceramics via Stereolithography. Journal of the American Ceramic Society, 79(10):2601–2608.

Grishchuk, S., and Karger-Kocsis, J., 2011. Hybrid Thermosets from Vinyl Ester Resin and Acrylated Epoxidized Soybean Oil (AESO). Express Polymer Letters, 5(1):2–11.

Haghani, R., and Yang, J., 2016. Application of FRP Materials for Construction of Culvert Road Bridges--Manufacturing and Life-Cycle Cost Analysis., Chalmers University Of

Technology,Göteborg, Sweden.133p.

Haq, M., Burgueño, R., Mohanty, A. K., and Misra, M., 2008. Hybrid Bio-Based Composites from Blends of Unsaturated Polyester and Soybean Oil Reinforced with Nanoclay and Natural Fibers. Composites Science and Technology, 68(15–16):3344–3351.

Hidalgo-Salazar, M. A., and Correa, J. P., 2018. Mechanical and Thermal Properties of Biocomposites from Nonwoven Industrial Fique Fiber Mats with Epoxy Resin and Linear Low Density Polyethylene. Results in Physics, 8 (2018) 461–467.

Holbery, J., and Houston, D., 2006. Natural-Fiber-Reinforced Polymer Composites in Automotive Applications. JOM, 58(11):80–86.

Holmes, M., 2019. Biocomposites Take Natural Step Forward: Applications for Biocomposites and the Use of Natural Fiber Reinforcements Are Increasing. Reinforced Plastics Looks at a Number of Examples. Reinforced Plastics, 63(4):194–201.

Holser, R. A., 2008. Transesterification of Epoxidized Soybean Oil to Prepare Epoxy Methyl Esters. Industrial Crops and Products, 27(1):130–132.

Hong, C. K., and Wool, R. F., 2005. Development of a Bio-Based Composite Material from Soybean Oil and Keratin Fibers. Journal of Applied Polymer Science, 95(6):1524–1538.

International Agency for Research on Cancer (IARC), 2012. Arsenic, metals, fibres, and dusts Iarc Monographs (Vol. 100). https://www.iarc.fr/[Accessed date:20.10.2023]

Izran, K., Mohd Zharif, T., Beyer, G., Mohamad Jani, S., Noor Azrieda, A. R., and Yanti, A. Ka., 2014. Kenaf For Biocomposite: An Overview. Journal of Science and Technology, 6(2):41–66.

J, S., and Satish, D. K. G., 2018. Preparation of Magnesium Metal Matrix Composites by Powder Metallurgy Process. IOP Conf. Series: Materials Science and Engineering, 310: 012130

Jabbar, A., Militký, J., Wiener, J., Kale, B. M., Ali, U., and Rwawiire, S., 2017. Nanocellulose Coated Woven Jute/Green Epoxy Composites: Characterization of Mechanical and Dynamic Mechanical Behavior. Composite Structures, 16:1340–1349.

Jabbar, A., Militký, J., Wiener, J., and Karahan, M., 2016. Static and Dynamic Mechanical Properties of Novel Treated Jute/Green Epoxy Composites. Textile Research Journal, 86(9):960–974.

Jafferjı, K., 2011. Bio-Based Thermoset Nanocomposites From Epoxidized Linseed Oil For Structural Applications.Msc Thesis, University Of Massachusetts Lowell, Massachusetts,66p.

Jakobsen, J., Andreasen, J., and Thomsen, O., 2014. A Comparison of Gel Point for a Glass/Epoxy Composite and a Neat Epoxy Material during Isothermal Curing. Journal of Composite Materials, 48(8):917–929.

Jiang, L., 2015. A new manufacturing process for biocomposite sandwich parts using a myceliated core, natural reinforcement and infused bioresin. PhD Thesis,Rensselaer Polytechnic Institute.New York,189p.

Jin, F.-L., Li, X., and Park, S.-J., 2015. Synthesis and Application of Epoxy Resins: A Review. Journal of Industrial and Engineering Chemistry, 29 (2015) 1–11.

Jin, F.-L., and Park, S.-J., 2008. Thermomechanical Behavior of Epoxy Resins Modified with Epoxidized Vegetable Oils. Polymer International, 57(4):577–583.

John, M. J., and Sabu, T., 2012. Natural Polymers Volume 1: Composites (M. J. John & T. Sabu, Eds.),1st ed., Cambridge: Royal Society of Chemistry,London, 349p.

Johnson, R. D. J., Prabu, V. A., Amuthakkannan, P., and Prasath, K. A., 2017. A Review on Biocomposites and Bioresin Based Composites for Potential Industrial Applications. Reviews on Advanced Materials Science, 49(1):112–121.

Kandar, M. I. M., and Akil, H. M., 2016. Application of Design of Experiment (DoE) for Parameters Optimization in Compression Moulding for Flax Reinforced Biocomposites. Procedia Chemistry, 19 (2016) 433 – 440.

Karabas H., 2013. Safflower Remzibey-05 (Carthamus tinctorius L.) Seed Oil as an Alternative Feedstock for the Production of Biodiesel in Turkey. Journal of Agricultural Faculty of Uludag University,27(1):9-17.

Karacor, B., and Özcanlı, M., 2020. Investigation of Use of Hybrid Composite Materials in Automobile Interior. International Journal of Automotive Engineering and Technologies, 9(4):214–228.

Karacor, B., and Ozcanli, M., 2022.a Thermal and Mechanical Characteristic Investigation of the Hybridization of Basalt Fiber with Aramid Fiber and Carbon Fiber. Polymer Composites, 43(11):8529–8544.

Karacor, B., and Özcanlı, M., 2022.b Characterization Of Jute/Aramid Hybrid Composite Materials with Using Different Resins. Sakarya University Journal of Science, 26(5):915–930.

Karacor, B., and Özcanlı, M., 2022.c Post Curing Temperature Effect on Mechanical Characterization of Jute/Basalt Fiber Reinforced Hybrid Composites. International Advanced Researches and Engineering Journal, 6(2):90–99.

Karacor, B., and Ozcanli, M., 2023.a Examination of Fiber Reinforced Composite Materials. Gazi University Journal of Science, 36(1):301–320.

Karacor, B., and Özcanlı, M., 2023.b Analysis Of Mechanical Properties Of Flax/Carbon Fiber Reinforced Hybrid Composites Produced Using Two Different Production Methods. Mühendislik Bilimleri ve Tasarım Dergisi, 11(2):459–473.

Karaçor, B., Özcanlı, M., and Kumlu, U., 2023. Hybrid Jute/Carbon Fiber Composites: Optimum Post-Curing Time. Iranian Polymer Journal (English Edition), 32(11):1443–1454.

Karacor, B., and Özcanlı, M., 2024. A Short Review: The Use and Application of Matrix Resins Formed with Some Plant-Based Oils in Bio-Composite Materials. Düzce Üniversitesi Bilim ve Teknoloji Dergisi, 12(3):1315–1333.

Karaçor, B., Özcanlı, M., and Serin, H., 2024. The Influence of Hybridization and Different

Manufacturing Methods on the Mechanical Properties of the Composites Reinforced with Basalt, Jute, and Flax Fibers. Iranian Polymer Journal (English Edition), 33(3):289–304.

Karaçor, B., and Özcanlı, M. 2025. The use of bioresin composites created with five different vegetable oils such as soybean oil, palm oil, rapeseed oil, cottonseed oil, linseed oil in the automotive industry. Polymer Composites, doi.org/10.1002/pc.29415.

Karahan, H. A., Öktem, T., and Necdet, S., 2006. Natural Bamboo Fiber. Tekstil Ve Konfeksiyon, 16(4):236–240.

Karak, N., 2012. Vegetable oil-based polymers: Properties, processing and applications Vegetable Oil-Based Polymers: Properties, Processing and Applications.Woodhead Publishing,Sawston,322pL

Kaw, A. K., 2006. Mechanics of composite materials (2nd ed.). Taylor & Francis Group, LLC, Boca Raton,457p.

Kerni, L., Singh, S., Patnaik, A., and Kumar, N., 2020. A Review on Natural Fiber Reinforced Composites. Materials Today: Proceedings, 28 (2020) 1616–1621.

Khandelwal, V., Sahoo, S. K., Kumar, A., and Manik, G., 2018. Electrically Conductive Green Composites Based on Epoxidized Linseed Oil and Polyaniline: An Insight into Electrical, Thermal and Mechanical Properties. Composites Part B: Engineering, 136(July 2017):149–157.

Khot, S. N., Lascala, J. J., Can, E., Morye, S. S., Williams, G. I., Palmese, G. R., … Wool, R. P., 2001. Development and Application of Triglyceride-Based Polymers and Composites. Journal of Applied Polymer Science, 82(3):703–723.

Kim, S.-Y., Shim, C. S., Sturtevant, C., Kim, D. (Dae-W.), and Song, H. C., 2014. Mechanical Properties and Production Quality of Hand-Layup and Vacuum Infusion Processed Hybrid Composite Materials for GFRP Marine Structures. International Journal of Naval Architecture and Ocean Engineering, 6(3):723–736.

Kocaman, S., Ahmetli, G., and Materials, A., 2016. Eco-Friendly Natural Filler Based Epoxy Composites. International Journal of Chemical and Molecular Engineering, 10(4):471–474.

Kompozitshop.com,2024.Epoxy and hardener properties. https://www.kompozitshop.com/mgs-laminasyon-epoksi-recine-l160.[Accessed date:30.05.2024]

Kozlowski, R., Wladyka-Przybylak, M., Helwig, M., and Kurzydloski, K. J., 2004. Composites Based on Lignocellulosic Raw Materials. Molecular Crystals and Liquid Crystals, 418:1, 131-151

Kumar, V. M., and Venkatesh, C. V., 2019. A Comprehensive Review on Material Selection, Processing, Characterization and Applications of Aluminium Metal Matrix Composites. Materials Research Express, 6 (2019) 072001.

Kumascı.com, 2024.a Cotton Fabric. https://www.kumasci.com/urun/amerikan-bezi-kumas-beyaz-220-cm/1240[Accessed date:29.05.2024]

Kumascı.com, 2024.b Flax Fabric. https://www.kumasci.com/urun/keten-acik-gri-kanvas-kumas/6746[Accessed date:29.05.2024]

Kumascı.com, 2024.c Jute Fabric (250 Gr/M2). https://www.kumasci.com/urun/jut-telis-cuval-kumasi-ham-en-sik-jut-10-onz-100-cm-en/8490. [Accessed date:29.05.2024]

La Mantia, F. P., and Morreale, M., 2011. Green Composites: A Brief Review. Composites Part A: Applied Science and Manufacturing, 42(6):579–588.

Lalit, R., Mayank, P., and Ankur, K., 2018. Natural Fibers and Biopolymers Characterization: A Future Potential Composite Material. Strojnícky Casopis – Journal of Mechanical Engineering, 68(1):33–50.

Learn.genetics.utah.edu, 2023. Cotton Fibers. https://learn.genetics.utah.edu/content/cotton/what. [Accessed date:29.09.2023]

Lee, T. S., Choi, H. Y., Choi, H. N., Lee, K. Y., Kim, S. H., Lee, S. G., and Yong, D. K., 2013. Effect of Surface Treatment of Ramie Fiber on the Interfacial Adhesion of Ramie/Acetylated Epoxidized Soybean Oil (AESO) Green Composite. Journal of Adhesion Science and Technology, 27(12):1335–1347.

Liu, B., Villavicencio, R., and Soares, C. G., 2013. Failure characteristics of strength-equivalent aluminium and steel plates in impact conditions. Analysis and Design of Marine Structures, Marstruct 2013: 167-174

Liu, K., 2014. Novel plant oil-based thermosets and polymer composites.Msc Thesis, Iowa State University,Iowa,83p.

Liu, W., Chen, T., Fei, M. en, Qiu, R., Yu, D., Fu, T., and Qiu, J., 2019. Properties of Natural Fiber-Reinforced Biobased Thermoset Biocomposites: Effects of Fiber Type and Resin Composition. Composites Part B: Engineering, 171(November 2018):87–95.

Liu, W., Fei, M. en, Ban, Y., Jia, A., Qiu, R., and Qiu, J., 2018. Concurrent Improvements in Crosslinking Degree and Interfacial Adhesion of Hemp Fibers Reinforced Acrylated Epoxidized Soybean Oil Composites. Composites Science and Technology, 160 (2018) 60-68.

Liu, Z., Erhan, S. Z., Akin, D. E., and Barton, F. E., 2006. “Green” Composites from Renewable Resources: Preparation of Epoxidized Soybean Oil and Flax Fiber Composites. Journal of Agricultural and Food Chemistry, 54(6):2134–2137.

Lligadas, G., Ronda, J. C., Galià, M., and Cádiz, V., 2013. Renewable Polymeric Materials from Vegetable Oils: A Perspective. Materials Today, 16(9):337–343.

Lu, Y., and Larock, R. C., 2009. Novel Polymeric Materials from Vegetable Oils and Vinyl Monomers: Preparation, Properties, and Applications. ChemSusChem, 2(2):136–147.

Lu, Z., Cao, J., Song, Z., Li, D., and Lu, B., 2019. Research Progress of Ceramic Matrix Composite Parts Based on Additive Manufacturing Technology. Virtual and Physical Prototyping, 14(4):333–348.

Lutton, R. E. M., Taylor, S. E., and Sonebi, M., 2017. Commercial Potential of Bioresins and Their Success in Thermosetting Composites: An Overview. 2nd International Conference on Bio-Based Building Materials & 1st Conference on Ecological Valorisation of Granular and FIbrous Materials, (June):1–10.

Madbouly, S. A., Zhang, C., and Kessler, M. R., 2016. Bio-Based Plant Oil Polymers And Composites. Elsevier, New York, 218p.

Manthey, N. W., Cardona, F., Francucci, G., and Aravinthan, T., 2013. Thermo-Mechanical Properties of Epoxidized Hemp Oil-Based Bioresins and Biocomposites. Journal of Reinforced Plastics and Composites, 32(19):1444–1456.

Marrot, L., Bourmaud, A., Bono, P., and Baley, C., 2014. Multi-Scale Study of the Adhesion between Flax Fibers and Biobased Thermoset Matrices. Materials & Design, 62 (2014): 47–56.

Marsh, G., 2003. Next Step for Automotive Materials. Materials Today, 6(4):36–43.

Mazumdar, S., 2002. Composites Manufacturing Materials,Product and Process Engineering. CRC Press, Boca Raton.396p.

Meier, M. A. R., Metzger, J. O., and Schubert, U. S., 2007. Plant Oil Renewable Resources as Green Alternatives in Polymer Science. Chemical Society Reviews, 36(11):1788.

Melelli, A., Jamme, F., Beaugrand, J., and Bourmaud, A., 2022. Evolution of the Ultrastructure and Polysaccharide Composition of Flax Fibres over Time: When History Meets Science. Carbohydrate Polymers, 291 (2022) 119584.

Mercangöz, M., Küsefoğlu, S., Akman, U., and Hortaçsu, Ö., 2004. Polymerization of Soybean Oil via Permanganate Oxidation with Sub/Supercritical CO2. Chemical Engineering and Processing: Process Intensification, 43(8):1015–1027.

Metapanel.com., 2024. PET properties. https://www.metapanel.com.tr/PET-en.[Accessed date:25.09.2024]

Miyagawa, H., Misra, M., Drzal, L. T., and Mohanty, A. K., 2005. Fracture Toughness and Impact Strength of Anhydride-Cured Biobased Epoxy. Polymer Engineering & Science, 45(4):487–495.

Miyagawa, H., Mohanty, A. K., Burgueño, R., Drzal, L. T., and Misra, M., 2007. Novel Biobased Resins from Blends of Functionalized Soybean Oil and Unsaturated Polyester Resin. Journal of Polymer Science Part B: Polymer Physics, 45(6):698–704.

Miyagawa, H., Mohanty, A. K., Misra, M., and Drzal, L. T., 2004.a Thermo-Physical and Impact Properties of Epoxy Containing Epoxidized Linseed Oil, 1. Macromolecular Materials and Engineering, 289(7):629–635.

Miyagawa, H., Mohanty, A. K., Misra, M., and Drzal, L. T., 2004.b Thermo-Physical and Impact Properties of Epoxy Containing Epoxidized Linseed Oil, 2. Macromolecular Materials and Engineering, 289(7):636–641.

Mohammed M. N., Atabani A. E.,Uguz G.,Lay C-H.,Kumar G., Al-Samaraae R. R.,2020.

Characterization of Hemp (Cannabis sativa L.) Biodiesel Blends with Euro Diesel, Butanol and Diethyl Ether Using FT-IR, UV–Vis, TGA and DSC Techniques.Waste and Biomass Valorization,11:1097–1113.

Mohan Kumar, S., Srinivas, S., Ramachandra, M., and Mahendra, K. V., 2018. Characterization of Aluminium Metal Matrix Composite Produced by Squeeze Casting Technique. Materials Today: Proceedings, 5(10):22718–22726.

Mohanty, A. K., Misra, M., and Hinrichsen, G., 2000. Biofibres, Biodegradable Polymers and Biocomposites: An Overview. Macromolecular Materials and Engineering, 276/277, 1–24.

Mohanty, Amar K., Misra, M., and Drzal, L. T., 2005. Natural Fibers, Biopolymers, and Biocomposites.Taylor & Francis Group, LLC, Boca Raton.896p.

Monteiro, S., Terrones, L. H., Lopes, F., and Almeida, J., 2005. Mechanical Strength of Polyester Matrix Composites Reinforced with Coconut Fiber Wastes. Revista Matéria, 10(4):571–576.

Montero de Espinosa, L., and Meier, M. A. R., 2011. Plant Oils: The Perfect Renewable Resource for Polymer Science?! European Polymer Journal, 47(5):837–852.

Morye, S. S., and Wool, R. P., 2005. Mechanical Properties of Glass/Flax Hybrid Composites Based on a Novel Modified Soybean Oil Matrix Material. Polymer Composites, 26(4):407–416.

Mosiewicki, M. A., and Aranguren, M. I., 2013. A Short Review on Novel Biocomposites Based on Plant Oil Precursors. European Polymer Journal, 49(6):1243–1256.

Muthu, S. S., 2019. Green Composites Processing, Characterisation and Applications for Textiles (S. S. Muthu, Ed.). Springer, Gateway East.102p.

Narewska, J., Lassila, L., and Fardim, P., 2014. Preparation and Characterization of New Mouldable Cellulose-AESO Biocomposites. Cellulose, 21(3):1769–1780.

Naslain, R., 2004. Recent Advances in the Field of Ceramic Fibers and Ceramic Matrix Composites. Journal De Physique. IV, 123 (2005) 3–17.

Neg.co.jp, 2023. Glass Fiber. https://www.neg.co.jp/en/product/fiber/[Accessed date:15.08.2023]

Nickel, J., and Riedel, U., 2003. Activities in Biocomposites. Materials Today, 6(4):44–48.

Nickels, L., 2019. New Innovations in Automotive Thermoplastics. Reinforced Plastics, 63(4):185–188.

Niedermann, P., Szebenyi, G., and Toldy, A., 2014. Effect of Epoxidized Soybean Oil on Curing, Rheological , Mechanical and Thermal Properties of Aromatic and Aliphatic Epoxy Resins, J Polym Environ, 22:525–536.

Niedermann, P., Szebényi, G., and Toldy, A., 2017. Effect of Epoxidized Soybean Oil on Mechanical Properties of Woven Jute Fabric Reinforced Aromatic and Aliphatic Epoxy Resin Composites. Polymer Composites, 38(5):884–892.

O'Donnell, A., Dweib, M. A., and Wool, R. P., 2004. Natural Fiber Composites with Plant Oil-Based Resin. Composites Science and Technology, 64(9):1135–1145.

Omonov, T. S., and Curtis, J. M., 2016. Plant Oil-Based Epoxy Intermediates for Polymers. In Bio-

Based Plant Oil Polymers and Composites (pp. 99–125). Editors:Samy A. Madbouly,Chaoqun Zhang, Michael R. Kessler,Elsevier.1 st ed.

Onlineclothingstudy, 2020. Banana Fiber. https://www.onlineclothingstudy.com/2020/10/banana-fibre-for-sustainable-fashion.html.[Accessed date:20.10.2020]

Ozerpolimer.com.2024. LDPE properties. https://ozerpolimer.com/?page_id=260. [Accessed date:20.09.2024]

Ozkur, S., 2021. Investigation Of Performance Characteristics Of Bio- Resin Based Textile Composites.Msc Thesis, İstanbul Technical University,İstanbul,100p.

Ozkur, S., Sezgin, H., and Yalcin-Enis, I., 2019. The Effect of Increaseed Bioresin Ratio on Impact Behaviour of Jute Reinforce Epoxy Composites. National Cukurova Textile Congress-UÇTEK'2019. 26-27 September 2019, Adana, Türkiye.

Ozkur, S., Leskovšek, M., Golja, B., Demsar, A., Sezgin, H., and Yalcin-Enis, I., 2021. Characterization of Thermo-Mechanical and Morphological Properties of Jute Fabric Reinforced Epoxy/AESO Bio-Composites. Fibers and Polymers, 22(12):3414–3424.

Ozkur, S., Sezgin, H., Akay, E., and Yalcin-Enis, I., 2020. Hybrid Bio-Based Composites from Blends of Epoxy and Soybean Oil Resins Reinforced with Jute Woven Fabrics. Materials Research Express, 7(1):015335.

Ozkur, S., Sezgin, H., and Yalcin-Enis, I., 2022. The Effect of Curing and Post-Curing Processes on Physical and Mechanical Behaviors of Jute Fabric Reinforced AESO/Epoxy Based Bio-Composites. Fibers and Polymers, 23(5):1410–1421.

Oztemur, J., Sezgin, H., and Yalcin-Enis, I., 2022. Design of an Impact Absorbing Green Composite. Materials Today: Proceedings, 60 (2022) 97–99.

Oztemur, J., Sezgin, H., and Yalçin-Enis, I., 2021. Design of an Impact Absorbing Composite Panel from Denim Wastes and Acrylated Epoxidized Soybean Oil Based Epoxy Resins. Tekstil ve Konfeksiyon, 31(3):228–234.

Paramarta,A. A., 2016. High Performance Bio-based Thermosets for Composites and Coatings North Dakota State University Plant Sciences.PhD Thesis, North Dakota State University of Agriculture and Applied Science, Fargo,169p.

Patil, H., and Waghmare, J., 2013. Catalyst for Epoxidation of Oils: A Review. Discovery, 3(7):10–14.

Pawar, M., Kadam, A., Yemul, O., Thamke, V., and Kodam, K., 2016. Biodegradable Bioepoxy Resins Based on Epoxidized Natural Oil (Cottonseed & Algae) Cured with Citric and Tartaric Acids through Solution Polymerization: A Renewable Approach. Industrial Crops and Products, 89 (2016) 434–447.

Pearce, N. R. L., Summerscales, J., and Guild, F. J., 2000. Improving the Resin Transfer Moulding Process for Fabric-Reinforced Composites by Modification of the Fabric Architecture. Composites Part A: Applied Science and Manufacturing, 31(12):1433–1441.

Peças, P., Carvalho, H., Salman, H., and Leite, M., 2018. Natural Fibre Composites and Their Applications: A Review. Journal of Composites Science, 2(4):1–20.

Peters, S.T., 1998. Handbook of Composites Chapman & Hal*l* (2nd ed.). Chapman & Hall,London,1118p.

Petrović, Z. S., 2010. Polymers From Biological Oils. Contemporary Materials, 1(1):39–50.

Petrović, Z. S., Zlatanić, A., Lava, C. C., and Sinadinović-Fišer, S., 2002. Epoxidation of Soybean Oil in Toluene with Peroxoacetic and Peroxoformic Acids— Kinetics and Side Reactions. European Journal of Lipid Science and Technology, 104(5):293–299.

Pilla, S., 2011. Handbook of Bioplastics and Biocomposites Engineering Applications. Scrivener Publishing, Beverly, 587p.

PinettePei Engineering and Machinery, 2023. Automotive Composite Parts. https://pinetteemidecau.eu/en/solutions-by-industry/automotive-composites.[Accessed date:28.12.2023]

Plastem, 2024. HDPE Properties. https://plastem.co.za/plastic-technical-data/[Accessed date:27.10.2024]

Plasticextrusion.net., 2024. ABS Properties. https://plasticextrusiontech.net/what-is-abs-material/.[Accessed date:27.10.2024]

Prededence research, 2023. Global Market Size from 2023 to 2032. https://www.precedenceresearch.com/composites-market. [Accessed date:28.12.2023]

Puttegowda, M., Rangappa, S. M., Jawaid, M., Shivanna, P., Basavegowda, Y., and Saba, N., 2018. Potential of natural/synthetic hybrid composites for aerospace applications (pp.315-351). In Sustainable Composites for Aerospace Applications.Editors: Mohammad Jawaid, Mohamed Thariq, Elsevier Ltd.1 st ed.

Quirino, R. L., 2011. Natural oil-based composites reinforced with natural fillers , and conjugation / isomerization of carbon-carbon double bonds.PhD Thesis, Iowa State University Ames, Iowa, 207p.

Radojčić, D., Hong, J., and Petrović, Z. S., 2022. From Natural Oils to Epoxy Resins: A New Paradigm in Renewable Performance Materials. Journal of Polymers and the Environment, 30(2):765–775.

Ramamoorthy, S. K., 2015. Properties and Performance of Regenerated Cellulose Thermoset BioComposites.PhD Thesis, University of Borås, Borås,50p.

Ramamoorthy, S. K., Di, Q., Adekunle, K., and Skrifvars, M., 2012. Effect of Water Absorption on Mechanical Properties of Soybean Oil Thermosets Reinforced with Natural Fibers. Journal of Reinforced Plastics and Composites, 31(18):1191–1200.

Rana, A., and Evitts, R. W., 2015. Development and Characterization of Flax Fiber Reinforced Biocomposite Using Flaxseed Oil-Based Bio-Resin. Journal of Applied Polymer Science, 132(15):41807.

Raquez, J.-M., Deléglise, M., Lacrampe, M.-F., and Krawczak, P., 2010. Thermosetting (Bio)Materials Derived from Renewable Resources: A Critical Review. Progress in Polymer Science, 35(4):487–509.

Reddy, N., and Yang, Y., 2011.a Biocomposites Developed Using Water-Plasticized Wheat Gluten as Matrix and Jute Fibers as Reinforcement. Polymer International, 60(4):711–716.

Reddy, N., and Yang, Y., 2011.b Completely Biodegradable Soyprotein–Jute Biocomposites Developed Using Water without Any Chemicals as Plasticizer. Industrial Crops and Products, 33(1):35–41.

Ronda, Juan C., Lligadas, G., Galià, M., and Cádiz, V., 2013. A Renewable Approach to Thermosetting Resins. Reactive and Functional Polymers, 73(2):381–395.

Ronda, Juan Carlos, Lligadas, G., Galià, M., and Cádiz, V., 2011. Vegetable Oils as Platform Chemicals for Polymer Synthesis. European Journal of Lipid Science and Technology, 113(1):46–58.

Roy, P., Defersha, F., Rodriguez-Uribe, A., Misra, M., and Mohanty, A. K., 2020. Evaluation of the Life Cycle of an Automotive Component Produced from Biocomposite. Journal of Cleaner Production, 273 (2020) 123051.

Ru, S., Zhao, C., and Yang, S., 2022. Multi-Objective Optimization and Analysis of Mechanical Properties of Coir Fiber from Coconut Forest Waste. Forests, 13, 2033.

Saba, N., Jawaid, M., Alothman, O. Y., Paridah, M., and Hassan, A., 2016. Recent Advances in Epoxy Resin, Natural Fiber-Reinforced Epoxy Composites and Their Applications. Journal of Reinforced Plastics and Composites, 35(6):447–470.

Saheb, D. N., and Jog, J. P., 1999. Natural Fiber Polymer Composites: A Review. Advances in Polymer Technology, 18(4):351–363.

Sahoo, S. K., Khandelwal, V., and Manik, G., 2018.a Development of Completely Bio-Based Epoxy Networks Derived from Epoxidized Linseed and Castor Oil Cured with Citric Acid. Polymers for Advanced Technologies, 29(7):2080–2090.

Sahoo, S. K., Khandelwal, V., and Manik, G., 2018.b Development of Toughened Bio-Based Epoxy with Epoxidized Linseed Oil as Reactive Diluent and Cured with Bio-Renewable Crosslinker. Polymers for Advanced Technologies, 29(1):565–574.

Sahoo, S. K., Khandelwal, V., and Manik, G., 2018.c Influence of Epoxidized Linseed Oil and Sisal Fibers on Structure-Property Relationship of Epoxy Biocomposite. Polymer Composites, 39(S4):E2595–E2605.

Sahoo, S. K., Khandelwal, V., and Manik, G., 2019. Sisal Fibers Reinforced Epoxidized Nonedible Oils Based Epoxy Green Composites and Its Potential Applications (pp. 73–102). In S. S. Muthu (Ed.), Green Composites Processing, Characterisation and Applications for Textiles. Springer Singapore.1 st ed.

Sahoo, S. K., Mohanty, S., and Nayak, S. K., 2015.a Synthesis and Characterization of Bio-Based

Epoxy Blends from Renewable Resource Based Epoxidized Soybean Oil as Reactive Diluent. Chinese Journal of Polymer Science (English Edition), 33(1):137–152.

Sahoo, S. K., Mohanty, S., and Nayak, S. K., 2015.b Toughened Bio-Based Epoxy Blend Network Modified with Transesterified Epoxidized Soybean Oil: Synthesis and Characterization. RSC Advances, 5(18):13674–13691.

Sahoo, S. K., Mohanty, S., and Nayak, S. K., 2017. Mechanical, Thermal, and Interfacial Characterization of Randomly Oriented Short Sisal Fibers Reinforced Epoxy Composite Modified with Epoxidized Soybean Oil. Journal of Natural Fibers, 14(3):357–367.

Sahoo, S. K., Mohanty, S., and Nayak, S. K., 2018. Mechanical, Dynamic Mechanical, and Interfacial Properties of Sisal Fiber-Reinforced Composite with Epoxidized Soybean Oil-Based Epoxy Matrix. Polymer Composites, 39(6):2065–2072.

Sarasini, F., Tirillò, J., Ferrante, L., Valente, M., Valente, T., Lampani, L., … Sorrentino, L., 2014. Drop-Weight Impact Behaviour of Woven Hybrid Basalt–Carbon/Epoxy Composites. Composites Part B: Engineering, 59 (2014) 204–220.

Sarikaya, E., Çallioğlu, H., and Demirel, H., 2019. Production of Epoxy Composites Reinforced by Different Natural Fibers and Their Mechanical Properties. Composites Part B: Engineering, 167(15):461–466.

Sas, H. S., Šimáček, P., and Advani, S. G., 2015. A Methodology to Reduce Variability during Vacuum Infusion with Optimized Design of Distribution Media. Composites Part A: Applied Science and Manufacturing, 78 (2015) 223–233.

Seabra, C. P., Sousa, A. C., Bragancą, I. M. F., Silva, C. M. A., Robalo, M. P., Loja, M. A. R., and Martins, P. A. F., 2020. On the Performance and Recyclability of a Green Composite Based on AESO Resin. Journal of Manufacturing and Materials Processing, 4(3), 65.

Seniha Güner, F., Yağcı, Y., and Tuncer Erciyes, A., 2006. Polymers from Triglyceride Oils. Progress in Polymer Science, 31(7):633–670.

Sevkat, E., and Brahimi, M., 2011. The Bearing Strength of Pin Loaded Woven Composites Manufactured by Vacuum Assisted Resin Transfer Moulding and Hand Lay-up Techniques. Procedia Engineering, 10(January 2012):153–158.

Sezgin, H., Mishra, R., Militky, J., and Berk Berkalp, O., 2020. Mechanical, Thermo-Mechanical and Thermal Characteristics of Multi-Walled Carbon Nanotubes-Added Textile-Reinforced Composites. Journal of Industrial Textiles, 50(5):692–715.

Sezgin, H., Mishra, R., Militky, J., and Berkalp, O. B., 2022. Thermal and Thermo-Mechanical Characterization of MWCNTs Integrated E-Glass/Carbon Fabric Reinforced Composites. Journal of Industrial Textiles, 51(5_suppl):8845S-8864S.

Shah, D. U., 2013. Developing Plant Fibre Composites for Structural Applications by Optimising Composite Parameters: A Critical Review. Journal of Materials Science, 48(18):6083–6107.

Shah, M., and Chaudhary, V., 2020. Flow Modeling and Simulation Study of Vacuum Assisted Resin

Transfer Molding (VARTM) Process: A Review. IOP Conference Series: Materials Science and Engineering, 872(1):012087.

Shebaz Ahmed, J. P., Sudarsan, S., Parthiban, E., Trofimov, E., and Sridhar, B., 2023. Exploration of Mechanical Properties of Hemp Fiber/Flax Fiber Reinforced Composites Based on Biopolymer and Epoxy Resin. Materials Today: Proceedings, (Article in press)

Shukla, U., and Garg, K., 2023. Journey of Smart Material from Composite to Shape Memory Alloy (SMA), Characterization and Their Applications-A Review. Smart Materials in Medicine, 4(August 2022):227–242.

Simbaña, E. A., Ordóñez, P. E., Ordóñez, Y. F., Guerrero, V. H., Mera, M. C., and Carvajal, E. A., 2020. Abaca: Cultivation, Obtaining Fibre and Potential Uses. Handbook of Natural Fibres: Second Edition, 1197–1218.

Sivasubramanian, S., 2010. Novel Bio-Based Thermoset Resins Based On Epoxidized Vegetable Oils For Structural Adhesives. Msc Thesis,University Of Massachusetts Lowell,Lowell,116p.

Somani, N., Tyagi, Y. K., Kumar, P., Srivastava, V., and Bhowmick, H., 2019. Enhanced Tribological Properties of SiC Reinforced Copper Metal Matrix Composites. Materials Research Express, 6 (2019) 016549.

Stanciu I., 2020. Viscosity Index for Oil Used as Biodegradable Lubricant.Indian Journal of Science and Technology, January 2020, 13(03): 352 – 359.

Suardana, N. P. G., Lokantara, I. P., and Lim, J. K., 2011. Influence of Water Absorption on Mechanical Properties of Coconut Coir Fiber/Poly-Lactic Acid Biocomposites. Materials Physics and Mechanics, 12(2):113–125.

Sudha, G. S., Kalita, H., Mohanty, S., and Nayak, S. K., 2017. Biobased Epoxy Blends from Epoxidized Castor Oil: Effect on Mechanical, Thermal, and Morphological Properties. Macromolecular Research, 25(5):420–430.

talyabitkisel.com, 2024a. Coconut oil. https://talyabitkisel.com/-hindistan-cevizi-yagi-20ml-soguk-pres.[Accessed date:23.10.2024]

talyabitkisel.com, 2024b. Figseed oil. https://talyabitkisel.com/-incir-cekirdegi-yagi-20ml. [Accessed date:23.10.2024]

Tan, S. G., and Chow, W. S., 2010.a Biobased Epoxidized Vegetable Oils and Its Greener Epoxy Blends: A Review. Polymer-Plastics Technology and Engineering, 49(15):1581–1590.

Tan, S. G., and Chow, W. S., 2010.b Thermal Properties, Fracture Toughness and Water Absorption of Epoxy-Palm Oil Blends. Polymer-Plastics Technology and Engineering, 49(9):900–907.

Taub, A. I., 2006. Automotive Materials: Technology Trends and Challenges in the 21st Century. MRS Bulletin, 31(4):336–343.

Temmink, R., Baghaei, B., and Skrifvars, M., 2018. Development of Biocomposites from Denim Waste and Thermoset Bio-Resins for Structural Applications. Composites Part A: Applied

Science and Manufacturing, 106 (2018) 59–69.

textileblog.com, 2021. Asbestos Fibre. https://www.textileblog.com/asbestos-fibre-properties-and-uses/.[Accessed date:20.10.2021]

Thakur, V. K., and Thakur, M. K., 2018. Functional Biopolymers Journal of Synthetic Organic Chemistry. Springer, Gewerbestrasse ,371p.

Thakur, V. K., Thakur, M. K., and Kessler, M. R., 2017. Handbook of Composites from Renewable Materials (V. K. Thakur, M. K. Thakur, & M. R. Kessler, Eds.), *Wiley* (Vol. 1). Scrivener Publishing, Beverly, 550p.

Torres, F. G., Rodriguez, S., and Saavedra, A. C., 2019. Green Composite Materials from Biopolymers Reinforced with Agroforestry Waste. Journal of Polymers and the Environment, 27(12):2651–2673.

tosmagaza.com, 2024a. Safflower seed oil. https://www.tosmagaza.com/aspir-tohumu-yagi-500-ml. [Accessed date:20.10.2024]

tosmagaza.com, 2024b. Hempseed oil. https://www.tosmagaza.com/kenevir-tohumu-yagi-500-ml. [Accessed date:20.10.2024]

tosmagaza.com, 2024c. Grapeseed oil. https://www.tosmagaza.com/uzum-cekirdegi-yagi-500-ml. [Accessed date:20.10.2024]

Tran, P., Graiver, D., and Narayan, R., 2006. Biocomposites Synthesized from Chemically Modified Soy Oil and Biofibers. Journal of Applied Polymer Science, 102(1):69–75.

Trofimov, A., Ravey, C., Droz, N., Therriault, D., and Lévesque, M., 2023. A Review on the Representative Volume Element-Based Multi-Scale Simulation of 3D Woven High Performance Thermoset Composites Manufactured Using Resin Transfer Molding Process. Composites Part A: Applied Science and Manufacturing, 169(November 2022):107499.

Tsujimoto, T., Takeshita, K., and Uyama, H., 2016. Bio-based Epoxy Resins from Epoxidized Plant Oils and Their Shape Memory Behaviors. Journal of the American Oil Chemists' Society, 93(12):1663–1669.

Unnikrishnan, K. P., and Thachil, E. T., 2006. Toughening of Epoxy Resins. Designed Monomers and Polymers, 9(2):129–152.

Uosukainen, E., Linko, Y., Lämsä, M., Tervakangas, T., and Linko, P., 1998. Transesterification of Trimethylolpropane and Rapeseed Oil Methyl Ester. Journal of the American Oil Chemists' Society, 75(11):1557–1563.

Väisänen, T., Das, O., and Tomppo, L., 2017. A Review on New Bio-Based Constituents for Natural Fiber-Polymer Composites. Journal of Cleaner Production, 149 (2017) 582-596.

Wang, C., Ding, L., He, M., Wei, J., Li, J., Lu, R., … Cheng, R., 2016. Facile One-Step Synthesis of Bio-Based AESO Resins. European Journal of Lipid Science and Technology, 118(10):1463–1469.

Wen, X., Xiao, Z., Jiang, T., Li, J., Zhang, W., Zhang, L., and Shao, H., 2013. Constructing Novel

Fiber Reinforced Plastic (FRP) Composites through a Biomimetic Approach: Connecting Glass Fiber with Nanosized Boron Nitride by Polydopamine Coating. Journal of Nanomaterials, 13, Article ID 470583, doi.org/10.1155/2013/470583:.

Wiedmer, S., and Manolesos, M., 2006. An Experimental Study of the Pultrusion of Carbon Fiber-Polyamide 12 Yarn. Journal of Thermoplastic Composite Materials, 19(1):97–112.

Williams, G. I., and Wool, R. P., 2000. Composites from Natural Fibers and Soy Oil Resins. Applied Composite Materials, 7(5–6):421–432.

Wilzer, J., Windmann, M., Weber, S., Hill, H., Bennekom, A. Van, and Theisen, W., 2015. Thermal Conductivity of Advanced TiC Reinforced Metal Matrix Composites for Polymer Processing Applications. Journal of Composite Materials, 49(2):243–250.

Windhorst, T., and Blount, G., 1997. Carbon-Carbon Composites: A Summary of Recent Developments and Applications. Materials & Design, 18(1):11–15.

Woo, Y. J., and Kim, D. S., 2021. Cure and Thermal Decomposition Kinetics of a DGEBA/Amine System Modified with Epoxidized Soybean Oil. Journal of Thermal Analysis and Calorimetry, 144(1):119–126.

Wu, Y., and Li, K., 2016. Replacement of Styrene with Acrylated Epoxidized Soybean Oil in an Unsaturated Polyester Resin from Propylene Glycol, Isophthalic Acid, and Maleic Anhydride. Journal of Applied Polymer Science, 133(8):1–6.

Wu, Y., and Li, K., 2018. Acrylated Epoxidized Soybean Oil as a Styrene Replacement in a Dicyclopentadiene-Modified Unsaturated Polyester Resin. Journal of Applied Polymer Science, 135(19):1–8.

Xia, Y., and Larock, R. C., 2010. Vegetable Oil-Based Polymeric Materials: Synthesis, Properties, and Applications. Green Chemistry, 12(11):1893.

Yang, H. M., 2017. Aramid fibers(pp.187-217).In Comprehensive Composite Materials II (Vol. 1).Editors: Peter W.R. Beaumont,Carl H. Zweben.Elsevier,1 st ed.

Yildizhan, Ş., 2020. Fabrication and Characterization of Expanded Polystyrene / Chopped Glass Fiber / Epoxy Novel Composite. PhD Thesis,Çukurova University,Adana,130p.

Yim, Y.-J., Rhee, K. Y., and Park, S.-J., 2017. Fracture Toughness and Ductile Characteristics of Diglycidyl Ether of Bisphenol-A Resins Modified with Biodegradable Epoxidized Linseed Oil. Composites Part B: Engineering, 131 (2017) 144-152.

Yıldızhan, Ş., Çalık, A., Özcanlı, M., and Serin, H., 2018. Bio-Composite Materials: A Short Review of Recent Trends, Mechanical and Chemical Properties, and Applications. European Mechanical Science, 2(3):83–91.

Zhan, M., 2010. Bio-Based Composites From Soybean Oil Resins And Feather Fibers For Electronic Applications. PhD Thesis,University of Delaware,Newark,223p.

Zhu, J., Chandrashekhara, K., Flanigan, V., and Kapila, S., 2004. Curing and Mechanical Characterization of a Soy-Based Epoxy Resin System. Journal of Applied Polymer Science,

91(6):3513–3518.

Zin, M. H., Razzi, M. F., Othman, S., Liew, K., Abdan, K., and Mazlan, N., 2016. A Review on the Fabrication Method of Bio-Sourced Hybrid Composites for Aerospace and Automotive Applications. IOP Conference Series: Materials Science and Engineering, 152 (2016) 012041.

Zoltek.com, 2023. Different Type of Carbon Fiber. https://zoltek.com/carbon-fiber/what-is-carbon-fiber/.[Accessed date:25.11.2023]

CURRICULUM VITAE

Berkay KARAÇOR graduated from Adana Ticaret Odası Anatolian High School in 2012. Then, he started his undergraduate education at Çukurova University Automotive Engineering Department in 2012 and graduated in 2017. He started his master's degree in the same department of Çukurova University in 2017 and graduated in 2020. Then, he started his doctorate in the same department in 2020. He has been working as a Research Assistant in Çukurova University Automotive Engineering Department since 2018.